Wiadomości Lekarskie
Medical Advances

VOLUME LXXVII, ISSUE 8, AUGUST 2024
Official journal of Polish Medical Association has been published since 1928

ISSN 0043-5147
E-ISSN 2719-342X

INDEXED IN PUBMED/MEDLINE, SCOPUS, EMBASE, EBSCO, INDEX COPERNICUS,
POLISH MINISTRY OF EDUCATION AND SCIENCE, POLISH MEDICAL BIBLIOGRAPHY

Wiadomości Lekarskie
Medical Advances

VOLUME LXXVII, ISSUE 8, AUGUST 2024
Official journal of Polish Medical Association has been published since 1928

ISSN 0043-5147
E-ISSN 2719-342X

ALUNA Publishing

Memory of
dr Władysław
Biegański

Wiadomości Lekarskie is abstracted and indexed in: PUBMED/MEDLINE, SCOPUS, EMBASE, INDEX COPERNICUS, MINISTRY OF SCIENCE AND HIGHER EDUCATION, POLISH MEDICAL BIBLIOGRAPHY

Distribution and Subscriptions:
Bartosz Guterman prenumerata@wydawnictwo-aluna.pl

Graphic design / production:
Grzegorz Sztank fajne.work

Publisher:
ALUNA Publishing
29 Przesmyckiego st.,
05-510 Konstancin – Jeziorna, Poland
www.wydawnictwo-aluna.pl
www.wiadomoscilekarskie.pl
www.wiadlek.pl

Wiadomości Lekarskie
Medical Advances

CONTENTS

ORIGINAL ARTICLES

REVIEW ARTICLES

CASE STUDIES

ORIGINAL ARTICLE

CONTENTS

Initial experience with 3T breast MRI in Ukraine

Andrii V. Gurando[1,2], Tetiana M. Kozarenko[2,3], Viacheslav R. Gurando[4]

[1]SI, "INSTITUTE OF NUCLEAR MEDICINE AND DIAGNOSTIC RADIOLOGY OF NATIONAL ACADEMY OF MEDICAL SCIENCE OF UKRAINE", KYIV, UKRAINE

[2]MEDICAL CENTRE NEUROMED, KYIV, UKRAINE

[3]SHUPYK NATIONAL HEALTHCARE UNIVERSITY OF UKRAINE, KYIV, UKRAINE

[4]UZHHOROD NATIONAL UNIVERSITY, UZHHOROD, UKRAINE

ABSTRACT

Aim: To assess the initial results of using 3 Tesla contrast-enhanced breast magnetic resonance imaging in Ukraine.

Materials and Methods: Our study included 498 diagnostic breast magnetic resonance imaging performed in Neuromed medical center in Kyiv, between March 2020 and December 2022. Patients were positioned prone, with breasts suspended in a dedicated 7-channel bilateral breast coil. MR-images were acquired with the PHILIPS Achieva 3.0Tesla x-series scanner. All studies were made by standard protocol: localizer, morphological and dynamic studies were performed.

Results: Our study revealed a statistically significant increase in problem-solving contrast-enhanced breast magnetic resonance examinations compared to other indications. Additionally, we observed a higher incidence of women with a greater amount of fibroglandular tissue (p-value<0.05).

Conclusions: The utilization of 3Tesla contrast-enhanced breast magnetic resonance imaging has become prevalent in Ukraine as a problem-solving tool for inconclusive findings in ultrasound (US) or/and mammography (MG). It is particularly useful in preoperative local breast cancer staging for women with a significant amount of fibroglandular breast tissue. However, the implementation of breast magnetic resonance imaging in Ukraine is in its nascent stages and requires further investigation, especially in middle-income country settings.

KEY WORDS: magnetic resonance imaging, breast cancer, problem-solving tool

Wiad Lek. 2024;77(8):1525-1532. doi: 10.36740/WLek202408101 DOI

INTRODUCTION

Mammography (MG), ultrasound (US), and magnetic resonance imaging (MRI) constitute the primary methods for detecting breast cancer (BC) [1]. While MG and US are widely utilized imaging modalities in Ukraine, they may yield inconclusive results in certain cases, necessitating further examination [2]. Contrast-enhanced (CE) breast MRI, owing to its high sensitivity, serves as a valuable problem-solving tool in diagnostically challenging scenarios where conventional imaging falls short [2-6]. Furthermore, CE breast MRI complements MG screening for women at high risk of breast cancer [7-10].

Apart from its role as a problem-solving and high-risk screening tool, primary indications for breast MRI include preoperative staging of newly diagnosed BC (for excluding additional ipsilateral and contralateral cancer), assessing the effects of neoadjuvant chemotherapy, evaluating breast implants, investigating cancer of unknown primary localization, examining suspicious nipple discharge, and screening following breast-conserving surgery [11, 12].

AIM

Our study aimed to evaluate the initial outcomes of implementing 3T CE breast MRI in Ukraine.

MATERIALS AND METHODS

Our study encompassed 498 diagnostic breast MRIs conducted at Neuromed Medical Center in Kyiv from March 2020 to December 2022. Adhering to the principles of the Helsinki Declaration, this retrospective study posed no risks to patient safety or privacy. All examinations were conducted subsequent to patients' informed consent. To reduce background parenchymal enhancement (BPE), contrast-enhanced (CE) breast MRIs were specifically scheduled during the second week of the menstrual cycle for premenopausal women.

Patients assumed a prone position, with their breasts positioned in a dedicated 7-channel bilateral breast coil. MR images were acquired using a PHILIPS Achieva 3.0Tesla x-series scanner, employing standard protocol for localizer, morphological, and dynamic studies. Prior to scanning, a venous catheter was inserted into the patient's cubital

Table 1. Assessment of Contrast-Enhanced Breast Magnetic Resonance Findings According to BI-RADS Fifth Edition

	Mass	Non-mass enhancement	Focus	Total, № 487
BI-RADS-1	0 (0,0%)	0 (0,0%)	0 (0,0%)	48 (9,9%)
BI-RADS-2	246 (50,5%)	18 (3,7%)	0 (0,0%)	264 (54,2%)
BI-RADS-3	21 (4,3%)	36 (7,4%)	8 (1,6%)	65 (13,3%)
BI-RADS-4	47 (9,7%)	28 (5,7%)	0 (0,0%)	75 (15,4%)
BI-RADS-5	17 (3,5%)	3 (0,6%)	0 (0,0%)	20 (4,1%)
BI-RADS-6	11 (2,3%)	4 (0,8%)	0 (0,0%)	15 (3,1%)

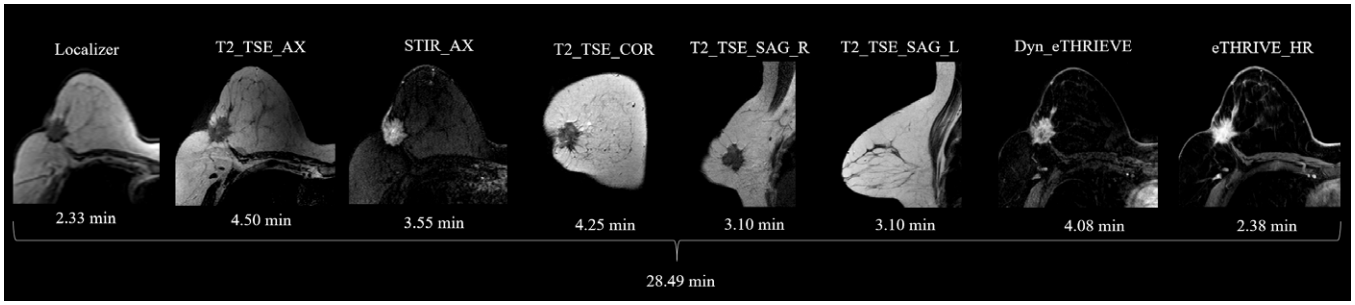

Fig. 1. Contrast-Enhanced Breast MRI Protocol. The scanning sequence started with Localizer and morphological sequences, followed by 6 series of THRIVE dynamic scanning, concluding with a delayed high-resolution THRIVE series. The default overall scanning duration was 28.49 minutes; however, for larger breasts, the scanning duration could extend by up to 10 minutes.

vein for the administration of the contrast agent (Gadovist) during dynamic CE. The contrast agent was injected as a bolus at a rate of 3 ml/s, followed by a 15ml saline flush via an automated MEDRAD injection system.

After conducting a localizer scan, we performed the following sequences:

- A morphological axial T2-weighted sequence with a slice thickness of 2mm and an acquisition time of 4.50 minutes. Parameters included a field of view (FOV) of 337x210mm, a repetition time (TR) of 4405 ms, an echo time (TE) of 120, a flip angle (FA) of 90, and a scan matrix (SM) of 264x285.

- An axial short-tau inversion recovery (STIR) sequence with a slice thickness of 4mm and an acquisition time of 3.55 minutes. Parameters comprised an FOV of 337x210mm, a TR of 11024 ms, a TE of 60, an FA of 120, and an inversion time (TI) of 230 ms.

- Coronal T2-weighted images with a slice thickness of 2.5mm and an acquisition time of 4.25 minutes. Parameters involved an FOV of 300x303mm, a TR of 4405 ms, a TE of 120, an FA of 90, and an SM of 376x285.

- Sagittal right and left T2-weighted images with a slice thickness of 3mm and an acquisition time of 3.10 minutes each. Parameters included an FOV of 240x240mm, a TR of 4757 ms, a TE of 120, an FA of 90, and an SM of 300x227.

The dynamic imaging utilized 3D T1-weighted low-angle shot [T1 High Resolution Isotropic Volume Excitation (THRIVE)] with the following parameters: TR/TE 3.8 /2.0 ms, flip angle 12, acceleration factor SENSE 3; matrix, 336x342 (reconstruction – 640x640); field of view, 330mm x 330mm; slice thickness, 1mm; and voxel size, 0.5 x 0.5 x 0.1mm. Depending on the breast volume and field of view, we obtained temporal acquisitions lasting less than 1 minute.

Following 1 series of pre-contrast THRIEVE and 6 series of THRIVE dynamic scanning lasting 4.08 minutes, we conducted a delayed high-resolution THRIVE with a slice thickness of 4.0mm and an acquisition time of 2.38 minutes. The default overall scanning time was 28.49 minutes; however, for larger breasts, the scan duration could extend up to 10 minutes longer (Fig 1).

Post-processing of the acquired images included subtraction series, MIP reconstruction, and construction of dynamic curves based on the Kuhl classification. These post-processed images were analyzed utilizing the Extended MR Workspace R3.2.3 workstation [13]. Lesions were categorized based on the pattern of the time-signal intensity curve and morphological appearance utilizing the Atlas BI-RADS fifth edition [1]. Data analysis was performed using Microsoft® Excel®

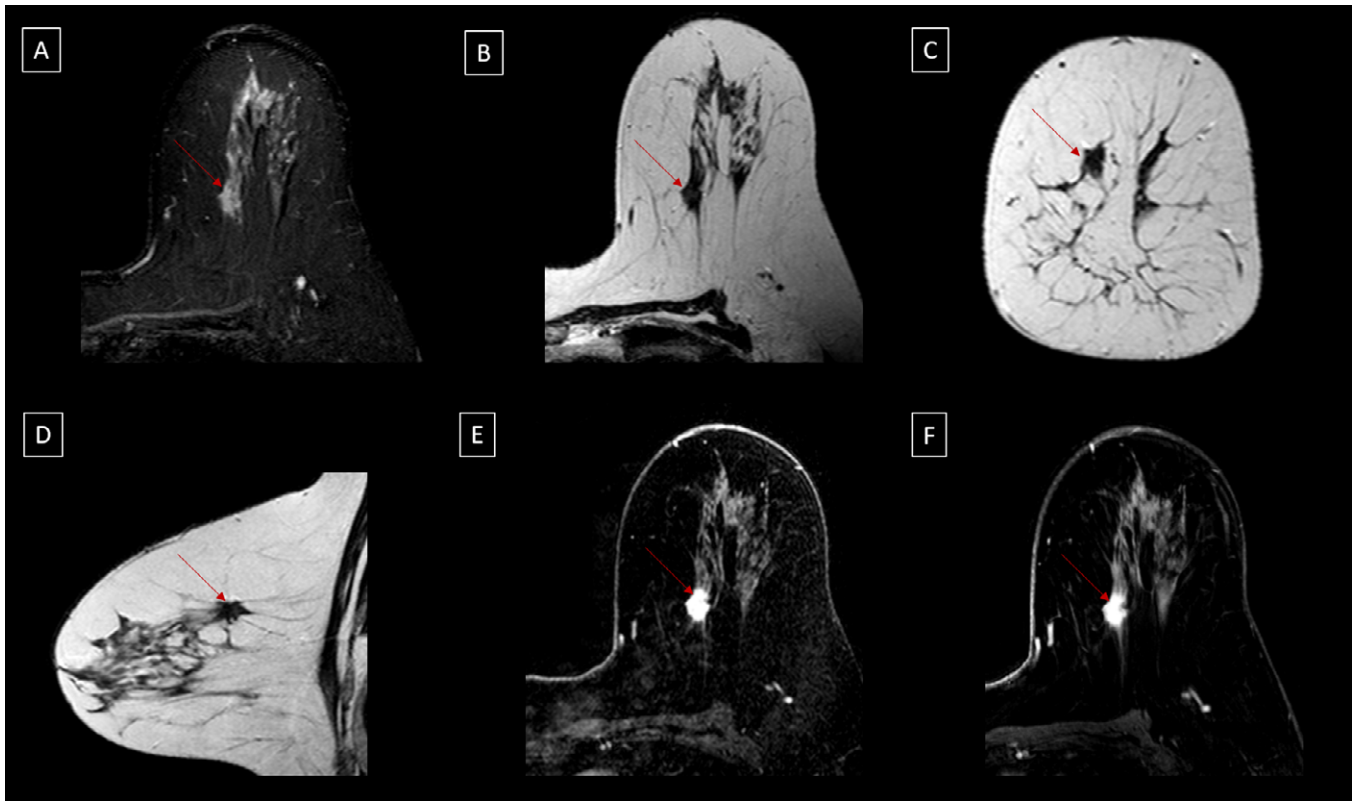

Fig. 2. A female patient diagnosed with histologically confirmed invasive breast carcinoma G1 (NST) who underwent diagnostic contrast-enhanced breast MRI to evaluate the local extent of the disease. The diagnostic MRI reveals a noncircumscribed, spiculated mass with washout and heterogeneous internal enhancement situated in the upper-inner quadrant of the left breast. The images include an axial short-tau inversion recovery image (A), axial T-2 image (B), coronal T-2 image (C), sagittal T-2 image (D), axial contrast-enhanced T-1fs THRIVE image (E), and axial T-1fs delayed high-resolution THRIVE image (F). The malignant mass is consistently marked with a red arrow across all images.

LTSC MSO, and correlations between the groups were assessed using the $\chi 2$ test.

RESULTS

Our study included data from 498 breast MRI examinations, consisting of 487 (97.8%) with contrast enhancement (CE) and 11 (2.2%) without CE, solely for assessing breast implants. The mean age of patients was 42.3 years (ranging from 19 to 78 years). CE breast MRIs were categorized into six BI-RADS (Breast Imaging Reporting and Data System) categories and eight examination indication categories [1, 11, 12]. Among these, biopsy-proven breast cancer (BI-RADS-6) accounted for 15 (3.0%) examinations, while those showing high suspicion for malignancy (BI-RADS-5) were 20 (4.0%). Cases indicating suspicion for malignancy (BI-RADS-4) totaled 75 (15.1%), probably benign findings (BI-RADS-3) were observed in 65 (13.1%) patients, benign findings (BI-RADS-2) in 264 (53.0%) examinations, and no pathological changes (BI-RADS-1) in 48 (9.6%) examinations. As mentioned earlier, 11 (2.2%) examinations focused solely on implant evaluation, thus BI-RADS assessment was not performed (Table 1).

The identified findings were categorized into three main groups: mass, non-mass enhancement (NME), and focus. The majority of CE breast MRIs exhibited solid and cystic masses (246; 50.5%), predominantly displaying benign characteristics and categorized as BI-RADS-2. However, those with suspicious morphology or kinetic curve were classified as suspicious for malignancy (BI-RADS-4; 47 cases) or highly suspicious with suspicions morphology and kinetic curve (BI-RADS-5; 17 cases). Additionally, 11 cases were histologically confirmed as breast cancer and were classified as BI-RADS-6 (Fig. 2). Solitary breast masses displaying benign morphology but with type II kinetic curve (plateau) in patients with a family history of breast cancer were categorized as BI-RADS-3 (21 cases) (Table 1).

We classified non-mass enhancement (NME) based on pattern and distribution within the breast parenchyma. Linear and segmental NME distributions with heterogeneous, clumped, or clustered ring internal enhancements were categorized as suspicious (BI-RADS-4 or BI-RADS-5) (Fig. 3). Focal NME without corresponding findings on other modalities or breast clinical examinations were considered probably benign, with recommendations for a follow-up CE breast MRI in 6 months. Multiple regions and diffuse distributions with homogeneous internal enhancements were categorized as benign NME (Table 1).

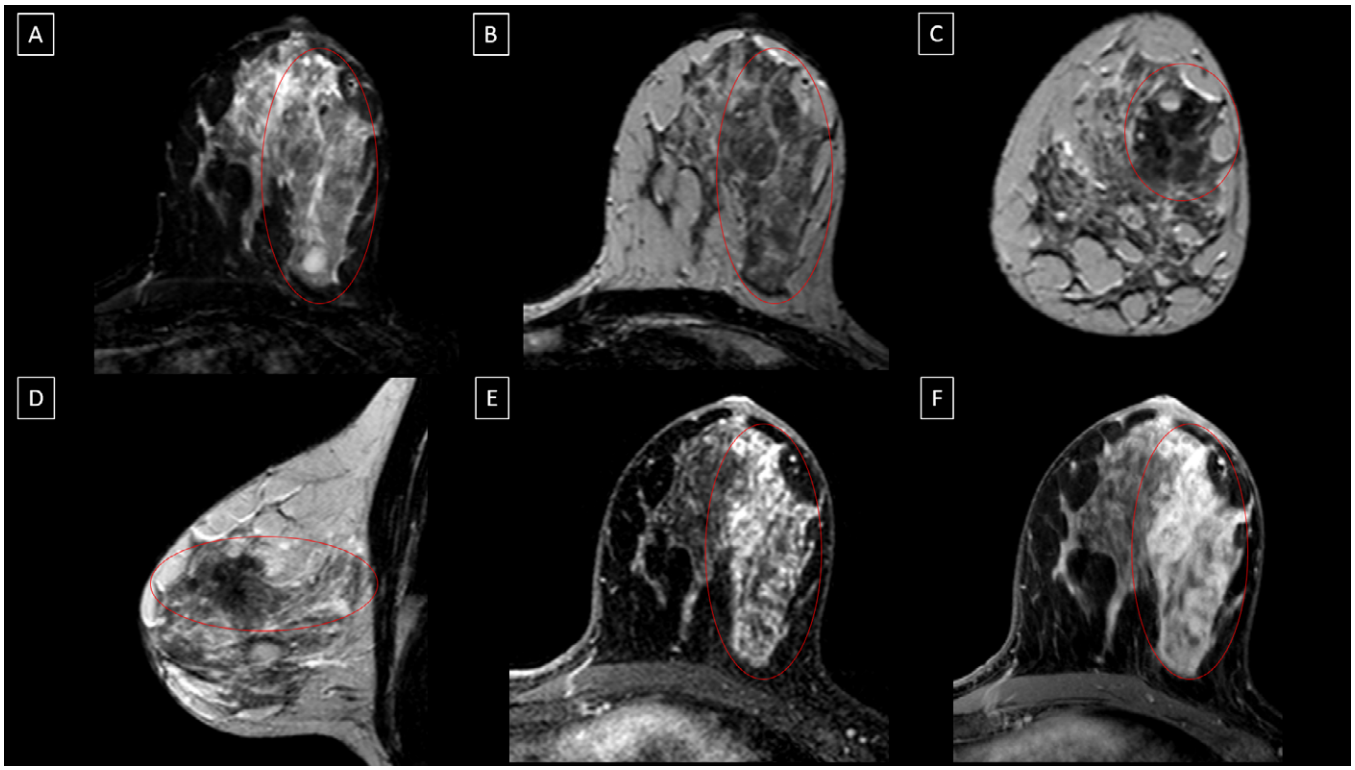

Fig. 3. A female patient presenting with bloody nipple discharge from the left breast underwent diagnostic contrast-enhanced breast MRI. The diagnostic MRI revealed suspicious heterogeneous segmental non-mass enhancement with a plateau dynamic curve in the upper-outer quadrant of the left breast. Subsequent core-needle biopsy under ultrasound guidance confirmed ductal carcinoma in situ. The imaging series comprised an axial short-tau inversion recovery image (A), axial T-2 image (B), coronal T-2 image (C), sagittal T-2 image (D), axial contrast-enhanced T-1fs THRIVE image (E), and axial T-1fs delayed high-resolution THRIVE image (F). The segmental non-mass enhancement was consistently demarcated with a red oval across all images.

Solitary focuses (<5 mm) without corresponding findings in morphological sequences and type II (plateau) and III (washout) kinetic curves were assessed as BI-RADS-3, with recommendations for a short interval (6 months) follow-up examination. Multiple bilateral focuses were categorized as background parenchymal enhancement (BPE) with BI-RADS-1 (Table 1).

All examinations adhered to structured reporting in accordance with BI-RADS Atlas recommendations. This involved comprehensive documentation encompassing the indication for examination, details of the MRI technique, a concise depiction of overall breast composition including the extent of fibroglandular tissue (FGT) and background parenchymal enhancement (BPE), a thorough description of important findings, a comparative analysis with previous examinations, and a comprehensive assessment guiding subsequent management decisions [1].

In most cases, the amount of fibroglandular tissue (FGT) on T1W fat-saturated images was heterogeneous (278; 57.2%) (Fig. 4), and the level of background parenchymal enhancement (BPE) was predominantly mild (Fig. 5). A statistically significant number of CE breast MRIs were performed for women with heterogeneous and extreme FGT compared to women with almost entirely fat breasts and scattered FGT (p-value <0.05). Additionally, a significant proportion of BPE was observed to be minimal and mild in comparison with moderate and marked BPE, indicative of the appropriate timing of the study (second week of the menstrual cycle) (p-value <0.05).

The most common indication for CE breast MRI was problem-solving (352; 70.8%) for inconclusive findings on breast ultrasound or mammography, followed by preoperative breast MRI (68; 13.7%) for local breast cancer staging. The least number of breast MRIs were performed for detecting cancer of unknown primary localization (8; 1.6%) and non-contrast studies for breast implant evaluation only (11; 2.2%) (Table 2). A statistically significant higher number of problem-solving CE breast MRIs were noted compared to all other indications for examination (p-value <0.05).

DISCUSSION

The introduction of 3T CE breast MRI in Ukrainian breast imaging represents a novel diagnostic approach. Notably, we didn't discover any prior publications from Ukraine documenting the utilization of such technology in breast imaging. Given that breast MRI stands as the most sensitive diagnostic tool for detecting breast

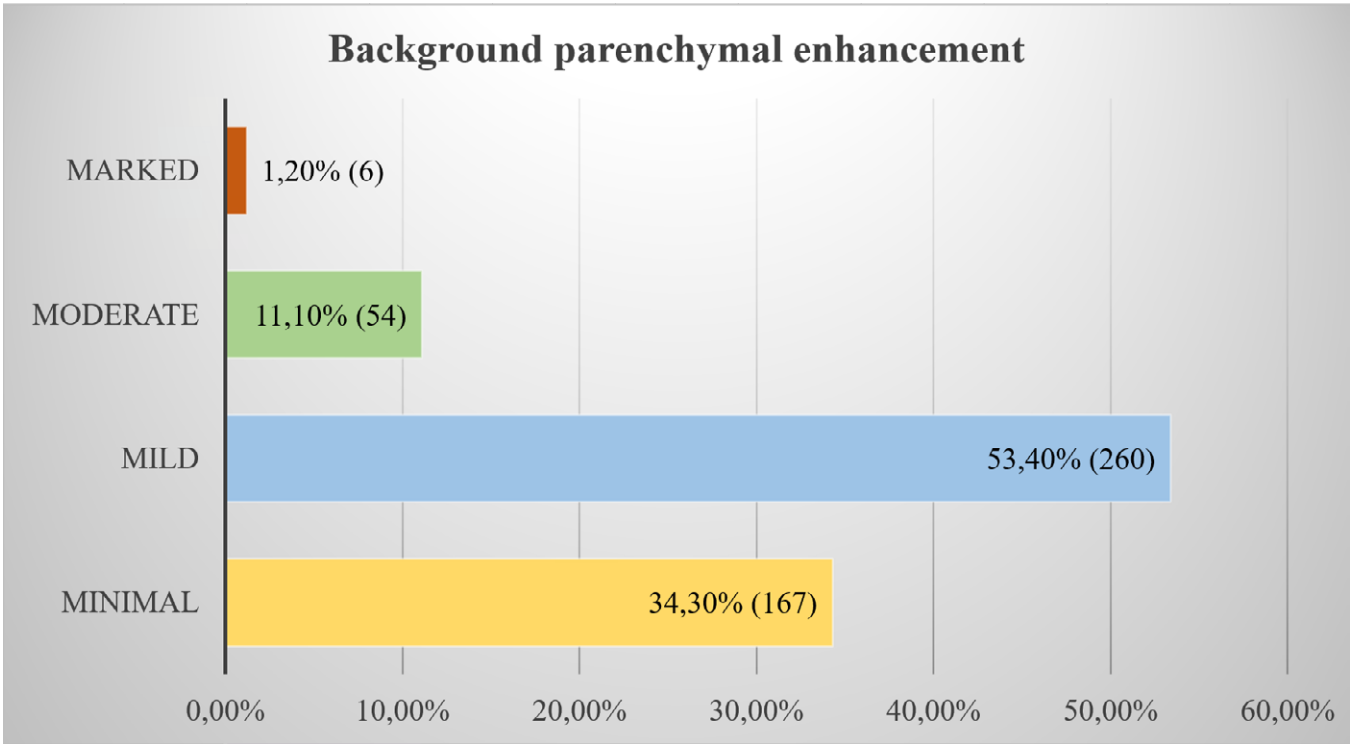

Fig. 4. Amount of fibroglandular tissue in patients which underwent contrast-enhanced breast magnetic resonance imaging according to BI-RADS fifth edition.

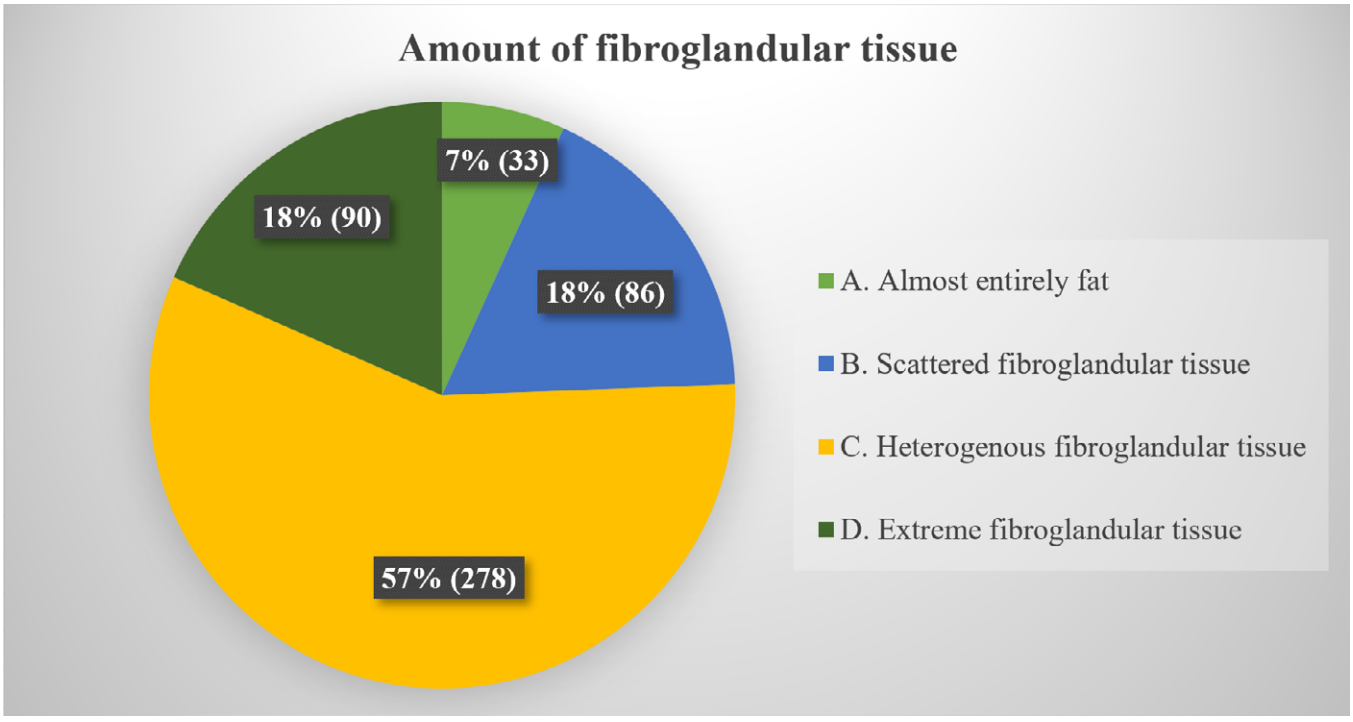

Fig. 5. Level of background enhancement of fibroglandular breast parenchyma in patients which underwent contrast-enhanced breast MRI according to BI-RADS fifth edition.

cancer, we embarked on analyzing our initial experience employing this imaging modality [14-18].

Our study unveiled that the primary indication for CE breast MRI was problem-solving, aligning with existing research demonstrating the efficacy of breast MRI in excluding malignancy when conventional breast imaging results are inconclusive [19-21]. Subsequently, the second most frequent indication was preoperative BC local staging. This finding resonates with studies indicating that preoperative breast MRI can identify additional disease in the ipsilateral breast in 20.0% of cases and in the contralateral breast in 5.5%, potentially reducing

Table 2. Indications for Breast MR Examinations in Our Study

Indications for breast MRI, № 487 (100%)	
Problem-solving	352 (70,8%)
Preoperative	68 (13,7%)
Screening after breast conserving surgery	17 (3,4%)
Monitoring of neoadjuvant chemotherapy	16 (3,2%)
Evaluation of nipple discharge	14 (2,8%)
High-risk screening	12 (2,4%)
Implant evaluation (non-contrast)	11 (2,2%)
Cancer of unknown primary localization	8 (1,6%)

reoperation rates by 3.0% while possibly increasing mastectomy rates by 11.0% [22-23].

Presently, MRI assumes a critical role in breast cancer screening among high-risk women, as well as mammography [24-26]. Despite the absence of a National BC screening program in Ukraine, conventional breast imaging methods, as previously mentioned in our studies, are widely utilized [27-30]. Consequently, one of the indications for CE breast MRI in our study involved high-risk screening for patients with BRCA1/2 mutations or a lifetime risk of BC development exceeding 20% based on genetic predisposition or family history, accounting for 2.4% of all our examinations.

Consistent with prior research and international recommendations, our utilization of CE breast MRI extended to detecting cancer of unknown primary localization, screening post-breast-conserving surgery, monitoring neoadjuvant chemotherapy effectiveness, evaluating patients with nipple discharge following conventional imaging, and conducting non-contrast studies for implant evaluation [31-35]. Notably, both 3T and 1.5T breast MRI systems exhibit comparable high diagnostic performance for breast cancer detection, with sensitivity and specificity values reflecting similar trends between the two systems [36].

However, a notable limitation in our setting, both at the national level and within our medical center, pertained to the unavailability of technical resources and requisite software for MR-guided biopsies. Furthermore, our study's limitations included its retrospective, single-institution design, interpretation of images by a single radiologist, and the absence of ongoing patient monitoring, although this was not the study's intended focus.

CONCLUSIONS

In summary, we can conclude that 3T CE breast MRI is widely used in Ukraine as a problem-solving tool for inconclusive findings in ultrasound or mammography, followed by preoperative local BC staging in women with a significant amount of fibroglandular breast tissue.

REFERENCES

1. D'Orsi CJ, Sickles EA, Mendelson EB et al. ACR BI-RADS® Atlas, Breast Imaging Reporting and Data System. Reston, VA, American College of Radiology. 2013.
2. Spick C, Szolar DHM, Preidler KW et al. 3 Tesla breast MR imaging as a problem-solving tool: Diagnostic performance and incidental lesions. PLoS One. 2018;13(1):e0190287. doi:10.1371/journal.pone.0190287. DOI
3. Gommers JJ, Voogd AC, Broeders MJ et al. Breast magnetic resonance imaging as a problem solving tool in women recalled at biennial screening mammography: A population-based study in the Netherlands. Breast. 2021;60:279-286. doi:10.1016/j.breast.2021.11.014. DOI
4. Taşkın F, Polat Y, Erdoğdu İH et al. Problem-solving breast MRI: useful or a source of new problems?. Diagn Interv Radiol. 2018;24(5):255-261. doi:10.5152/dir.2018.17504. DOI
5. Locke, R., Rubin, G. Role of MRI as a problem-solving tool in screening assessment. Breast Cancer Res. 2011;13(1):31. doi:10.1186/bcr2983. DOI
6. Pötsch N, Korajac A, Stelzer P et al. Breast MRI: does a clinical decision algorithm outweigh reader experience?. Eur Radiol. 2022;32(10):6557-6564. doi:10.1007/s00330-022-09015-8. DOI
7. Ren W, Chen M, Qiao Y, Zhao F. Global guidelines for breast cancer screening: A systematic review. Breast. 2022;64:85-99. doi:10.1016/j.breast.2022.04.003. DOI
8. Mann RM, Kuhl CK, Moy L. Contrast-enhanced MRI for breast cancer screening. J Magn Reson Imaging. 2019;50(2):377-390. doi:10.1002/jmri.26654. DOI
9. Lowry KP, Geuzinge HA, Stout NK et al. Breast Cancer Screening Strategies for Women With ATM, CHEK2, and PALB2 Pathogenic Variants: A Comparative Modeling Analysis. JAMA Oncol. 2022;8(4):587-596. doi:10.1001/jamaoncol.2021.6204. DOI
10. Ding W, Fan Z, Xu Y et al. Magnetic resonance imaging in screening women at high risk of breast cancer: A meta-analysis. Medicine (Baltimore). 2023;102(10):e33146. doi:10.1097/MD.0000000000033146. DOI
11. Clauser P, Mann R, Athanasiou A et al. A survey by the European Society of Breast Imaging on the utilisation of breast MRI in clinical practice. Eur Radiol. 2018;28(5):1909-1918. doi:10.1007/s00330-017-5121-4. DOI
12. Mann RM, Balleyguier C, Baltzer PA et al. Breast MRI: EUSOBI recommendations for women's information. Eur Radiol. 2015;25(12):3669-3678. doi:10.1007/s00330-015-3807-z. DOI

13. Kuhl CK, Mielcareck P, Klaschik S et al. Dynamic breast MR imaging: are signal intensity time course data useful for differential diagnosis of enhancing lesions?. Radiology. 1999;211(1):101-110. doi:10.1148/radiology.211.1.r99ap38101. DOI
14. Chen HL, Zhou JQ, Chen Q, Deng YC. Comparison of the sensitivity of mammography, ultrasound, magnetic resonance imaging and combinations of these imaging modalities for the detection of small (≤2cm) breast cancer. Medicine (Baltimore). 2021;100(26):e26531. doi:10.1097/MD.0000000000026531. DOI
15. Berg WA, Gutierrez L, NessAiver MS et al. Diagnostic accuracy of mammography, clinical examination, US, and MR imaging in preoperative assessment of breast cancer. Radiology. 2004;233(3):830-849. doi:10.1148/radiol.2333031484. DOI
16. Aristokli N, Polycarpou I, Themistocleous SC et al. Comparison of the diagnostic performance of Magnetic Resonance Imaging (MRI), ultrasound and mammography for detection of breast cancer based on tumor type, breast density and patient's history: A review. Radiography (Lond). 2022;28(3):848-856. doi:10.1016/j.radi.2022.01.006. DOI
17. Vourtsis A, Berg WA. Breast density implications and supplemental screening. Eur Radiol. 2019;29(4):1762-1777. doi:10.1007/s00330-018-5668-8. DOI
18. Houser M, Barreto D, Mehta A, Brem RF. Current and Future Directions of Breast MRI. J Clin Med. 2021;10(23):5668. doi:10.3390/jcm10235668. DOI
19. Taşkın F, Polat Y, Erdoğdu İH et al. Problem-solving breast MRI: useful or a source of new problems?. Diagn Interv Radiol. 2018;24(5):255-261. doi:10.5152/dir.2018.17504. DOI
20. Mann RM, Cho N, Moy L. Breast MRI: State of the Art. Radiology. 2019;292(3):520-536. doi:10.1148/radiol.2019182947. DOI
21. Shimauchi A, Machida Y, Maeda I et al. Breast MRI as a Problem-solving Study in the Evaluation of BI-RADS Categories 3 and 4 Microcalcifications: Is it Worth Performing?. Acad Radiol. 2018;25(3):288-296. doi:10.1016/j.acra.2017.10.003. DOI
22. Plana MN, Carreira C, Muriel A et al. Magnetic resonance imaging in the preoperative assessment of patients with primary breast cancer: systematic review of diagnostic accuracy and meta-analysis. Eur Radiol. 2012;22(1):26-38. doi:10.1007/s00330-011-2238-8. DOI
23. Sardanelli F, Trimboli RM, Houssami N et al. Magnetic resonance imaging before breast cancer surgery: results of an observational multicenter international prospective analysis (MIPA). Eur Radiol. 2022;32(3):1611-1623. doi:10.1007/s00330-021-08240-x. DOI
24. Mann RM, Kuhl CK, Moy L. Contrast-enhanced MRI for breast cancer screening. J Magn Reson Imaging. 2019;50(2):377-390. doi:10.1002/jmri.26654. DOI
25. Vreemann S, Gubern-Mérida A, Schlooz-Vries MS et al. Influence of Risk Category and Screening Round on the Performance of an MR Imaging and Mammography Screening Program in Carriers of the BRCA Mutation and Other Women at Increased Risk. Radiology. 2018;286(2):443-451. doi:10.1148/radiol.2017170458. DOI
26. Saadatmand S, Obdeijn IM, Rutgers EJ et al. Survival benefit in women with BRCA1 mutation or familial risk in the MRI screening study (MRISC). Int J Cancer. 2015;137(7):1729-1738. doi:10.1002/ijc.29534. DOI
27. Babkina TM, Gurando AV, Kozarenko TM et al. Detection Of Breast Cancers Represented As Architectural Distortion: A Comparison Of Full-Field Digital Mammography And Digital Breast Tomosynthesis. Wiad Lek. 2021;74(7):1674-1679. doi: 10.18370/2309-4117.2021.62.86-91. DOI
28. Kovtun AY, Hurando AV, Telnyi VV et al. Clinical Case: Pregnancy-Associated Breast Cancer. Reproductive Endocrinology. 2021;62:86-91. doi: 10.18370/2309-4117.2021.62.86-91. DOI
29. Gurando AV, Babkina TM, Dykan IM et al. Digital breast tomosynthesis and full-field digital mammography in breast cancer detection associated with four asymmetry types. Wiad Lek. 2021;74(4):842-848. doi: 10.36740/WLek202107121. DOI
30. Babkina TM, Dykan IM, Gurando AV et al. Detection of breast cancer presenting as a mass in women with dense breasts - digital breast tomosynthesis versus full-field digital mammography. Exp Oncol. 2020;42(3):215-219. doi:10.32471/exp-oncology.2312-8852.vol-42-no-3.14898. DOI
31. de Bresser J, de Vos B, van der Ent F, Hulsewé K. Breast MRI in clinically and mammographically occult breast cancer presenting with an axillary metastasis: a systematic review. Eur J Surg Oncol. 2010;36(2):114-119. doi:10.1016/j.ejso.2009.09.007. DOI
32. Gigli S, Amabile MI, Di Pastena F et al. Magnetic Resonance Imaging after Breast Oncoplastic Surgery: An Update. Breast Care (Basel). 2017;12(4):260-265. doi:10.1159/000477896. DOI
33. Reig B, Lewin AA, Du L et al. Breast MRI for Evaluation of Response to Neoadjuvant Therapy. Radiographics. 2021;41(3):665-679. doi:10.1148/rg.2021200134. DOI
34. de Paula IB, Campos AM. Breast imaging in patients with nipple discharge. Radiol Bras. 2017;50(6):383-388. doi:10.1590/0100-3984.2016.0103. DOI
35. Expert Panel on Breast Imaging:, Lourenco AP, Moy L, et al. ACR Appropriateness Criteria® Breast Implant Evaluation. J Am Coll Radiol. 2018;15(5S):S13-S25. doi:10.1016/j.jacr.2018.03.009. DOI
36. Dietzel M, Wenkel E, Hammon M et al. Does higher field strength translate into better diagnostic accuracy? A prospective comparison of breast MRI at 3 and 1.5 Tesla. Eur J Radiol. 2019;114:51-56. doi:10.1016/j.ejrad.2019.02.033. DOI

CONFLICT OF INTEREST
The Authors declare no conflict of interest

CORRESPONDING AUTHOR
Viacheslav R. Gurando
Uzhhorod National University
3 Narodna Square, 88000 Uzhhorod, Ukraine
e-mail: vhurando@gmail.com

ORCID AND CONTRIBUTIONSHIP
Andrii V. Gurando: 0000-0002-2708-3040 A B C D
Tetiana M. Kozarenko: 0000-0002-0838-9773 A D E F
Viacheslav R. Gurando: 0000-0001-6303-3799 D E F

A – Work concept and design, B – Data collection and analysis, C – Responsibility for statistical analysis, D – Writing the article, E – Critical review, F – Final approval of the article

RECEIVED: 13.01.2024
ACCEPTED: 17.07.2024

ORIGINAL ARTICLE

CONTENTS

Effectiveness of treatment of oropharyngeal carcinoma patients

Ervin V. Lukach[1], Viktor Ya. Dikhtiaruk[1], Oleksandr V. Kovtunenko[2], Anatoliy A. Bakaiev[2]

[1] INSTITUTE OF OTOLARYNGOLOGY NAMED AFTER PROF. O.S. KOLOMIYCHENKO OF NAMS OF UKRAINE, KYIV, UKRAINE

[2] DNIPRO STATE MEDICAL UNIVERSITY, DNIPRO, UKRAINE

ABSTRACT

Aim: To analyze the results of treatment of patients with oropharyngeal carcinoma.

Materials and Methods: 276 patients with oropharyngeal carcinoma were treated in 2008-2021. Neoadjuvant chemotherapy consisted of three to six cycles: paclitaxel 175 mg/m^2 and carboplatin 350 mg/m^2 (or cisplatin 100 mg/m^2) on the first day. The interval between cycles was 21 days. After the cycles, all patients were prescribed a course of radiation therapy in a total focal dose (TFD) of 65 Gy. The outcome of treatment was assessed by the degree of tumor regression according to RECIST criteria one month after the end of combination treatment. Statistical processing was performed using STATISTICA 6.1 software (StatSoftInc).

Results: The three- and five-year survival rates of the examined patients with oropharyngeal carcinoma after treatment were 40.8% respectively (95% CI 33.7 - 47.9) and 27.0%, (95% CI 20.6 - 33, 4) with a median survival of 36 months with 95% CI (35.5 - 40.2). Processing was performed using STATISTICA 6.1 software (StatSoftInc).

Conclusions: Analysis of treatment of patients with oropharyngeal carcinoma with predominance of squamous cell carcinoma (90.6%), localized primarily in the palatine tonsil (73.2%), with the most common stages $T_3N_1M_0$ (30.1%) and $T_3N_1M_0$ %), with regional metastases to the lymph nodes of the neck (89.9%), showed that the effectiveness of treatment of patients is quite high, because in most of the examined in the short term after combined treatment there was complete or partial regression of the tumor (91.7%),
no progression of the oncological process was detected in any of them.

KEY WORDS: oropharyngeal carcinoma, survival rate, treatment of patients with oropharyngeal carcinoma, chemotherapy

Wiad Lek. 2024;77(8):1533-1546. doi: 10.36740/WLek202408102 DOI

INTRODUCTION

According to the National Cancer Registry, the incidence of oropharyngeal carcinoma in Ukraine is 6.5 per 100 thousand population. At the time of diagnosis, more than 75.0% of patients have stage III-IV, and mortality up to one year is 40.1% [1]. In recent decades, approaches to combination therapy of patients with squamous cell carcinoma in most sites of the head and neck have changed significantly. Non-surgical organ-preserving approaches with the use of neoadjuvant chemotherapy and subsequent radiation therapy have demonstrated effectiveness and are widely used in the treatment of patients with squamous cell carcinoma of the oral pharynx [2].

The task of this work was to conduct neoadjuvant chemotherapy for patients with oropharyngeal cancer at the first stage and to determine its effectiveness in different localizations of the tumor in the pharynx and depending on the association with the papilloma virus.

We present the results of such treatment in our study.

AIM

Aim of the work is to analyze effectiveness of treatment of patients with malignant neoplasms of the oral pharynx to improve scientifically substantiated medical technology of treatment.

MATERIALS AND METHODS

The prospective study included 276 treatment-naïve patients with malignant neoplasms of the oral pharynx, who were treated in the Department of Oncopathology of the ENT organs of the State Institution «Institute of Otolaryngology named after prof. O.S. Kolomiychenko of National Academy of Medical Sciences of Ukraine « in 2008-2021. The study included 219 (79.3%) men and 57 (20.7%) women. The age of patients ranged from 26 to 83 years, the mean age was 55.65 years with a 95% confidence interval (CI) 54.46 - 56.84 years. In all cases, the diagnosis was verified histologically. The localization, stage, TNM classification and other characteristics of the tumor were evaluated.

Treatment started with three to six cycles of neoaduvant chemotherapy: paclitaxel 175 mg/m^2 on the first day and carboplatin 350 mg/m^2 (or cisplatin 100 mg/m^2) on the second day. Three weeks later, chemotherapy was repeated. With tumor regression by 50%, up to six courses of chemotherapy were carried out.After three or six cycles of chemotherapy, radiation therapy in a total focal dose (TFD) of 65 Gy was prescribed. It was performed in all patients regardless of tumor regression after chemotherapy. The outcome of treatment was assessed by the degree of tumor regression according to the RECIST criteria one month after combination treatment on the basis of contrast-enhanced CT studies, therapeutic pathomorphosis data and clinical examination of the patient. Subsequently, appropriate treatment was prescribed for residual tumor and existing regional metastases or progression. Statistical processing was performed using STATISTICA 6.1 software (StatSoftInc. ROC analysis was performed in the software package MedCalc Statistical Software trial version 20.015 (MedCalc Software bvba, Ostend, Belgium; https://www.medcalc.org; 2021). Relative values were calculated with a 95% confidence interval (95% CI) by the Wald normal approximation method. The comparison of relative values was performed according to the Pearson Chi-square ($\chi 2$) criterion (including the Yates correction for continuity for low frequencies) [3-5]. To assess the relationships of ordinal and numerical variables, a rank correlation analysis was performed with the calculation of Spearman correlation coefficients (r_s), the association was evaluated by the criterion phi-square (φ). ROC-analysis (Receiver Operating Characteristic) was performed with the calculation of standard operating characteristics: sensitivity, specificity and area under the ROC-curve (area under ROC curve - AUC) with 95% CI [6, 7]. The analysis of patient survival was performed by constructing mortality tables and the Kaplan-Meier method. Differences in the survival of different groups were determined by the log-rank criterion (log-rank test - logarithmic rank test). Comparison of survival rates in more than 2 groups was performed according to Chi-square statistics on the basis of a generalized logarithmically ranked test [8-10] . To analyze the influence of the studied factors on survival rate, we used a regression model of proportional risks (Cox proportional-hazards regression) with the calculation of the hazard ratio (HR hazard ratio) [9,11-13] . The critical value of the level of statistical significance (p) for all types of analysis was taken as <5% ($p < 0.05$).

The study included measures to ensure the safety and health of patients, respect for their rights, human dignity and moral and ethical standards in accordance with the principles of the Helsinki Convention on Human Rights, set out in the document «Bioethics of the Helsinki Declaration on the Moral Regulation of Medical Research». Council of Europe Convention on Human Rights and Biomedicine and relevant laws of Ukraine.

RESULTS

Microscopic examination of tumors showed a significant predominance of squamous cell carcinoma. Thus, 250 (90.6%) patients were histologically diagnosed with squamous cell carcinoma (SCC): keratinized in 118 (42.8%) patients and non-keratinized in 132 (47.8%) patients; in 17 (6.2%) patients - low-grade cancer and in 5 patients (1.8%) - transitional cell carcinoma, in the rest (4 patients - 1.4%) - other forms. (Fig. 1). Most often the tumors were localized in the palatine tonsil - 202 (73.2%) patients, on the lateral and posterior walls of the oropharynx - in 38 (13.8%) patients, on the vallecular sinus and on the lingual surface of the epiglottis - in 28 (10.1%) patients, on the soft palate – in 8 (2.9%) patients. (Fig. 2). According to the classification of the ICD of the 10th revision, the diagnoses of patients according to localization were represented by the codes C05.1-soft palate, C09.9-palatine tonsil, C10.0-vallecular sinus and C10.2-lateral wall of the oropharynx. Stage II was in 16 patients (5.8%), stage III - in 139 patients (50.4%) and stage IV - in 121 patients (43.8%). In 248 patients (89.9%) regional metastases to the lymph nodes of the neck were found, of which 71 (28.6%) patients had bilateral metastases. The most commonly lesions of IIA, IIB and III levels of lymph nodes of the neck according to the classification of K. Robbins were diagnosed.

The distribution of the examined patients with malignant neoplasms of the oral pharynx by stage of the disease and TNM classification is presented in (Table 1).

By the estimates, according to the International TNM classification, patients with a prevalence of T3 tumor prevailed - 180 patients (65.2%), stage T2 was determined in 77 patients (27.9%), stage T4 - in 19 (6.9%)); N0 was determined in 30 patients (10.9%), N1 - in 126 (45.65%), N2 - in 119 (43.1%) and N3 - in one patient (0.35) %). All subjects had no signs of distant metastases (M0). The most common characteristics of the tumor process (Fig. 3) were $T_3N_1M_0$ - 83 (30.1%) and $T_3N_2M_0$ - 66 (23.9%), which were observed mainly in patients with stage III of the disease. $T_2N_0M_0$ was revealed with insignificant frequency - in 9 patients (3.3%), $T_4N_2M_0$ - 5 (1.8%), $T_3N_3M_0$ - 1 (0.4%), $T_4N_0M_0$ - 1 (0.4%).

After completion of chemotherapy and radiation therapy in patients with malignant neoplasms of the oral pharynx, none of the subjects showed tumor

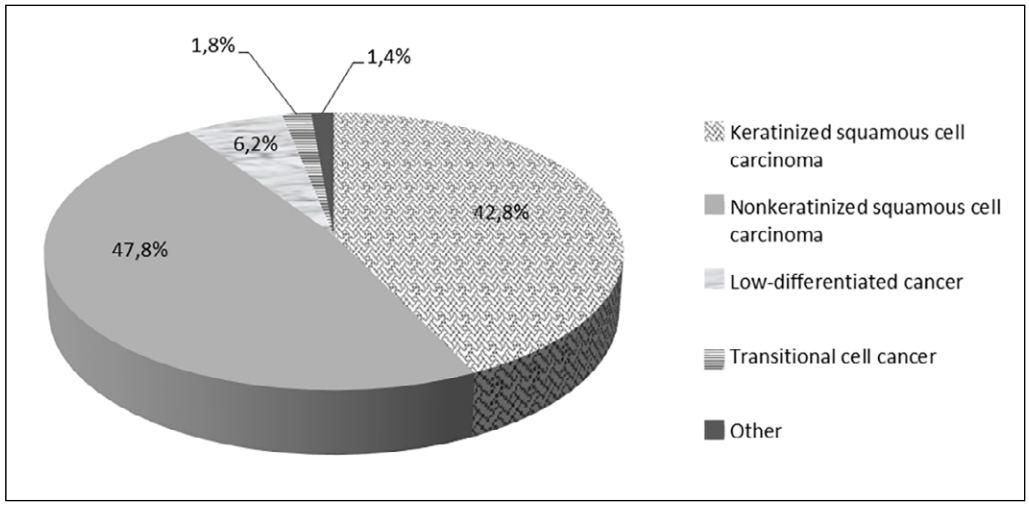

Fig. 1. Distribution of the examined patients by morphological characteristic of the tumor (in % per 100 of the examined).

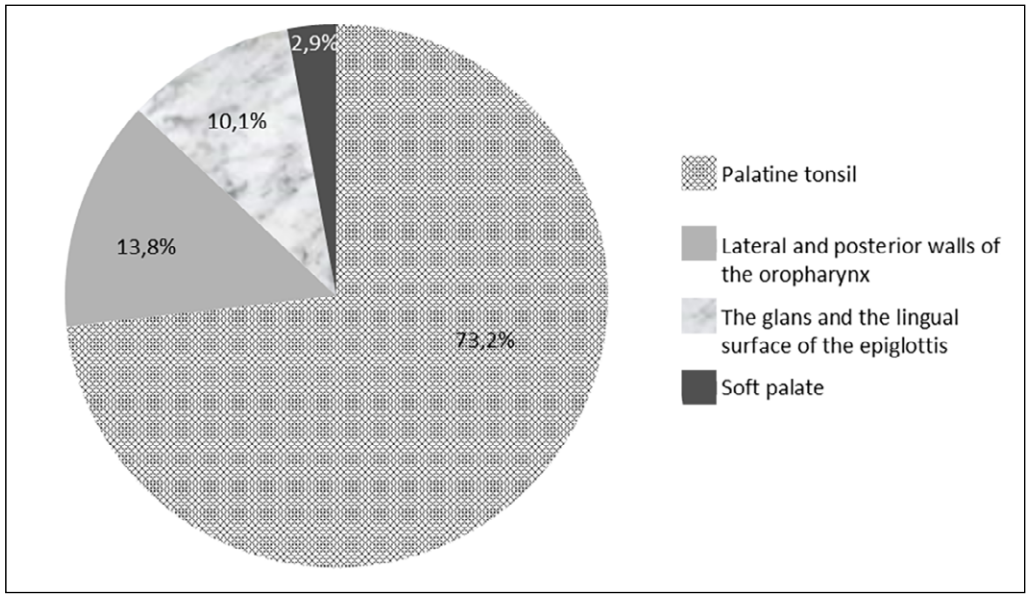

Fig. 2. Distribution of the examined patients by localization of the tumor (in % per 100 of the examined).

progression, 102 (37%) showed complete tumor regression, 151 (54.7%) - partial regression and 23 (8.3%) - stabilization of the disease(Table 2).

The largest proportion of patients with complete tumor regression was determined in patients with stage II - 12 (75.0%), which was statistically significantly higher (*p <0.001*) compared to patients with stage III and IV (46.0% and 21.5% respectively). Between the results of combination therapy and the stage of the disease, a significant rank correlation was determined (Spearman's correlation coefficient $r_s = 0.29$; *p <0.001*), and it was also influenced by the correlation analysis, morphological characteristics of the tumor ($r_s = 0.14$; *p = 0.024*), keratinization of the tumor ($r_s = 0.16$; $p = 0.006$), T stage ($r_s = 0.41$; *p <0.001*) and N stage ($r_s = 0.241$; *p <0.001*).

Of the total number of subjects, 18 patients (6.5%) underwent appropriate surgery. Of those operated on, 4 (22.22%) patients underwent laryngectomy, 13 (72.22%) - cervical dissection, and 1 patient underwent both surgeries.

Almost a quarter of patients - 64 (23.2%) underwent immunohistochemical (IHC) study of $p16^{INK4}$ gene expression. When evaluating the immunohistochemical analysis with the tumor suppressor $p16^{INK4}$, a negative reaction was found in 27 (42.2%) patients, while in 37 patients (57.8%) the presence of a mixed (nuclear-cytoplasmic) reaction of individual cells with the marker was determined. A significant associative and rank correlation ($r_s = 0.33$; *p = 0.007*) was determined between the reaction with the biomarker $p16^{INK4}$ and the direct results of the combined treatment, which is due to the presence of tumor suppressor $p16^{INK4}$ in patients with complete and partial regression of the tumor and its absence in patients. with stabilization. In compete regression the proportion of patients with the present reaction with the tumor suppressor $p16^{INK4}$ makes up 75,9% whereas in partial - 42,9% (*p = 0.029*) (Table 3).

The chances of achieving complete tumor regression increase by 4.2 times in the presence of a reaction with the tumor suppressor $p16^{INK4}$ compared to its absence

Table 1. Distribution of the examined patients by disease stages and classification (absolute number and %)

Stagen (%)	T - tumor n (% of patients of a certain stage)			N – regional lymph nodes n (% of patients of a certain stage)				TNM	Number of patients	
	T_2	T_3	T_4	N_0	N_1	N_2	N_3		abs.	%
II 16 (5,8)	14 (87,5)	2 (12,5)	0 (0)	9 (56,25)	4 (25,0)	4 (18,75)	0 (0)	$T_2N_0M_0$	9	3,3
								$T_2N_1M_0$	4	1,4
								$T_2N_2M_0$	1	0,4
								$T_3N_2M_0$	2	0,7
III 139 (50,4)	29 (20,9)	110 (79,1)	0 (0)	20 (14,4)	108 (77,7)	11 (7,9)	0 (0)	$T_2N_1M_0$	26	9,4
								$T_2N_2M_0$	3	1,1
								$T_3N_0M_0$	20	7,2
								$T_3N_1M_0$	83	30,1
								$T_3N_2M_0$	8	2,9
IV 121 (43,8)	34 (28,1)	68 (56,2)	19 (15,7)	1 (0,8)	14 (11,6)	105 (86,8)	1 (0,8)	$T_2N_2M_0$	34	12,3
								$T_3N_1M_0$	1	0,4
								$T_3N_2M_0$	66	23,9
								$T_3N_3M_0$	1	0,4
								$T_4N_0M_0$	1	0,4
								$T_4N_2M_0$	5	1,8
								$T_4N_1M_0$	13	4,7
In total	77 (27,9)	180 (65,2)	19 (6,9)	30 (10,9)	126 (45,65)	119 (43,1)	1 (0,35)		276	100

Table 2. Short-term results of combination treatment of patients with oropharyngeal carcinoma by diseases stages (absolute number and %)

Result	II stage n=16		III stage n=139		IV stage n=121		In total n=276	
	abs.	%	abs.	%	abs.	%	abs.	%
Full regression	12	75,0	64	46,0	26	21,5	102	37,0
Partial regression	4	25,0	64	46,0	83	68,6	151	54,7
Stabilization	0	0	11	8,0	12	9,9	23	8,3
Differences between groups	χ^2=27,69 (p<0,001)							

(the odds ratio (OR) = 4.2; 95% CI (1.3 - 12.3); *p = 0.010*). Regarding the informativeness of the biomarker for predicting tumor regression, according to ROC-analysis, which shows the dependence of the number of correctly classified results (true positive) on the number of incorrectly classified results (false negative), no convincing evidence of discriminant ability of $p16^{INK4}$ was obtained, it is defined as medium. Operational characteristics according to ROC analysis: sensitivity - Se = 75.86%; specificity Sp = 57.14%, area under the ROC curve - AUC = 0.665 and 95% CI (0.536 - 0.778); *p = 0.005* (Fig. 4).

The area under the ROC curve for the prognostic ability of complete tumor regression reached a statistically significant level (*p = 0.005*), but is not of sufficient clinical significance, because AUC <0.700, being the prognostic characteristic of $p16^{INK4}$ is considered average.

It should be noted that in $p16^{INK4}$ at a low level of specificity - Sp = 57.14%, a fairly high level of sensitivity - Se = 75.86% was noted, which indicates a high proportion of true positive results and a small number of false positive results. This is more appropriate for the initial conclusion on tumor regression.

Indicators of disease-specific (disease-dependent) cumulative survival rate for all examined patients with oropharyngeal cancer over the study period by the median value were 36 months with 95% CI (35.5 - 40.2). The probability of living a year or more was 97.3% (95% CI 94.9 - 99.7); three and more years - 40.8% (95% CI 33.7 - 47.9); five and more years - 27.0% (95% CI 20.6 - 33.4) (Table 4, Fig. 5).

According to the analysis of survival rate, there were no differences in the that of in patients divided into age groups (up to and over 65 years), morphological characteristics of the tumor, reactions with the tumor suppressor $p16^{INK4}$ (*p> 0.05*). The higher level of median survival in women compared to men was determined - 34.0 months (95% CI 30.0 - 60.0) compared to 30.0

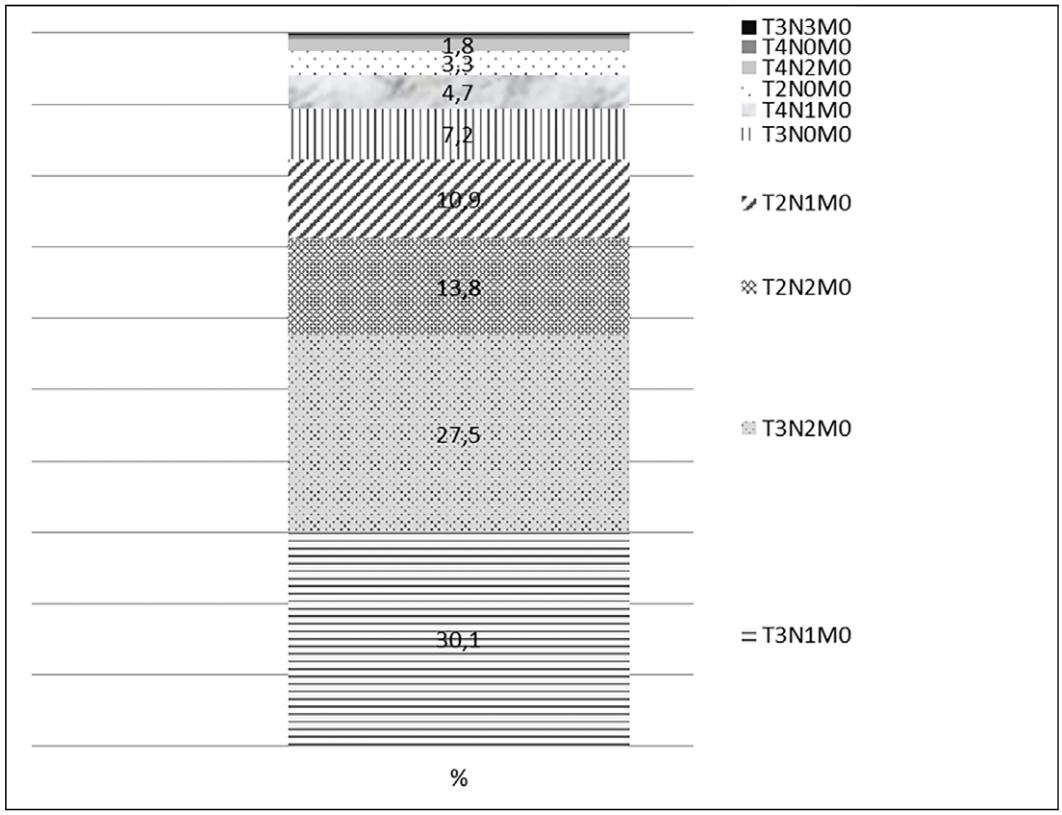

Fig. 3. Distribution of the examined patients by TNM stage (in % per 100 of the examined).

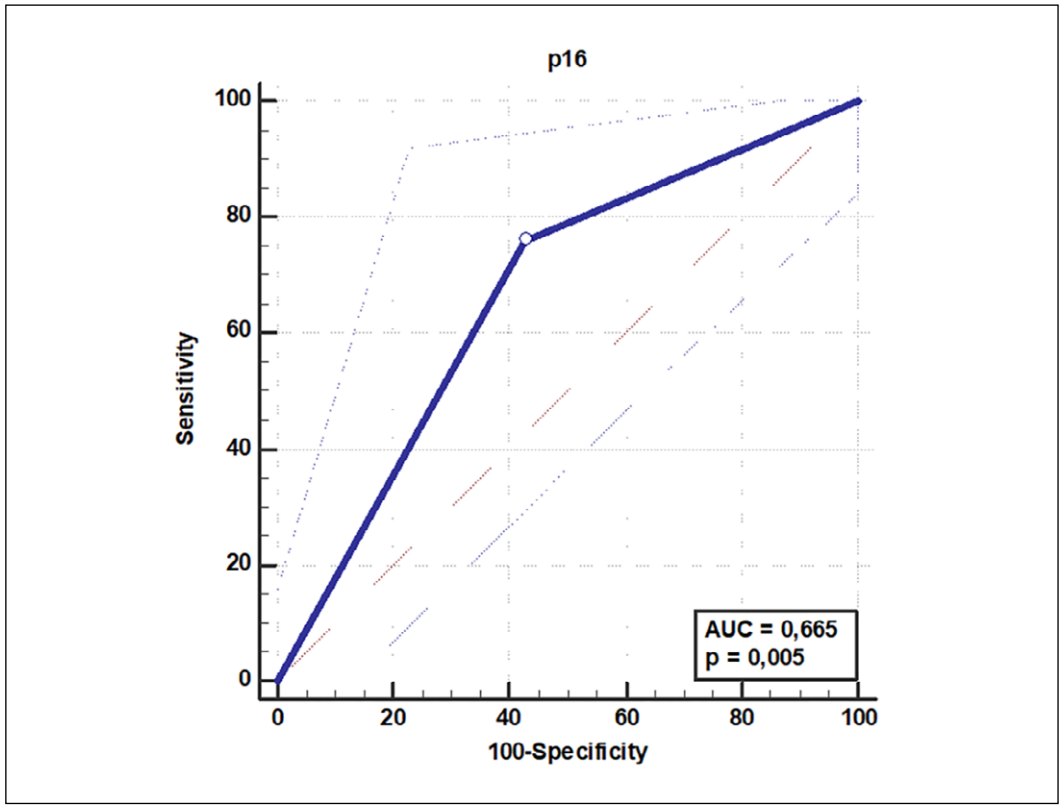

Fig. 4. ROC curve for evaluating prognostic capabilities of complete regression of the tumor by p16INK4 expression in the examined patients.

months (95% CI 20.0 - 36.0)); the one-, three-, and five-year survival rates of the women surveyed were also higher. Differences in survival rate of patients by gender were characterized by the presence of statistically significant differences ($p = 0.013$) (Fig. 6).

When comparing survival rates in different age groups, no statistically significant differences were found ($p = 0.109$), but there is a tendency to decrease with age: in patients under 65 years, three-year and five-year survival rates are 45.5%, respectively (95%

Table 3. Indicators of reaction with tumor suppressor $p16^{INK4}$ in the examined patients depending on results of combination treatment

Result	Reaction with an oncosupressor $p16^{INK4}$, n (%)		Discrepancies and associations *
	Negative	Available	
Full regression (n=29)	7 (24,1)	22 (75,9)	p=0,029* φ=0,33 r_s=0,33 (p=0,007)
Partial regression (n=35)	20 (57,1)	15 (42,9)	
Stabilization (n=0)	0 (0)	0 (0)	
All were examined for tumor markers (n=64)	27 (42,2)	37 (57,8)	-

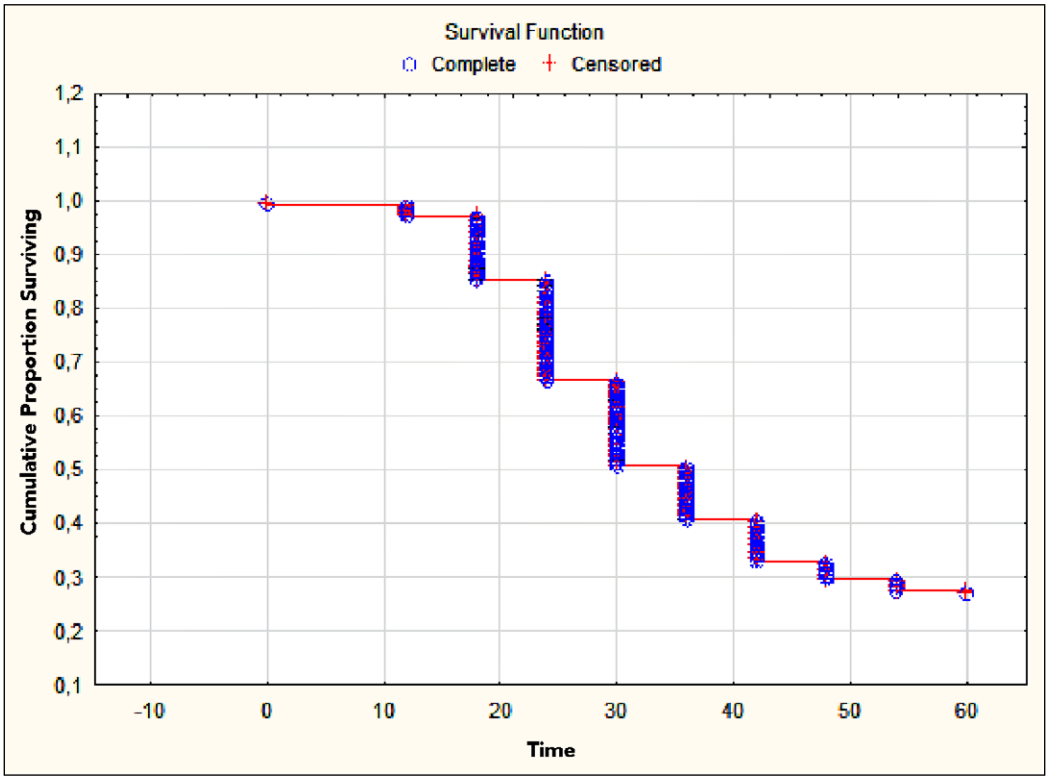

Fig. 5. Cumulative survival rate of the examined patients with oropharyngeal carcinoma (survival period in months).

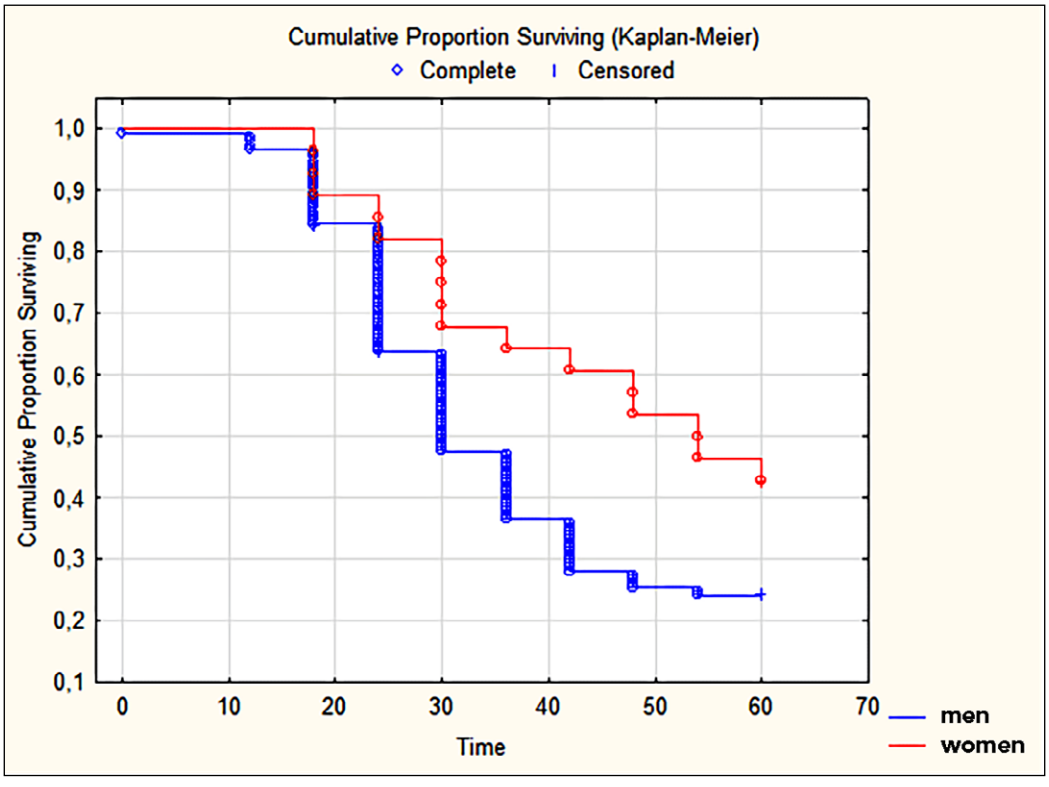

Fig. 6. Cumulative survival rate of the examined patients with oropharyngeal carcinoma depending on gender (survival period in months).

Table 4. Indicators of two-year, three- and five-year survival rate in the examined patients with malignant oropharyngeal neoplasms after treatment

Survival by individual groups	Overall cumulative survival (%)						Median survival		
	1-year-old		3-year-old		5-year-old		Mon-ths	25 %; 75 %	95 % CI
	%	95 % CI	%	95 % CI	%	95 % CI			
Overall survival	97,3	94,9 - 99,7	40,8	33,7 - 47,9	27,0	20,6 - 33,4	36,0	24,0; n/d	35,5 - 40,2
Gender									
men	96,8	94 - 99,6	36,5	28,9 - 44,1	30,9	17,3 – 32,9	30,0	24,0; 52,2	30,0 - 36,0
women	100,0	77,8 – 100,0	64,3	46,5 - 82,1	42,9	24,6 - 61,2	54,0	30,0; n/d	30,0 - 60,0
p *the level of disagreement by the log-rank test*									*0,013*
Age									
up to 65 years old	96,7	93,5 - 99,9	45,5	36,6 - 54,4	31,2	22,9 - 39,5	36,0	24,0; n/d	30,0 - 42,0
65 years of age and older	89,1	81,5 - 96,7	31,8	20,3 - 43,3	9,1	-0,6 - 18,8	30,0	24,0; 42,0	24,0 - 36,0
p *the level of disagreement by the log-rank test*									*0,109*
Morphological characteristics of the tumor									
keratinized squamous cell cancer	98,8	96,4 - 99,2	32,3	22,1 - 42,5	22,4	13,3 - 31,5	30,0	24,0; 47,3	30,0 - 36,0
non-keratinized squamous cell carcinoma	96,2	92 - 98,4	45,6	34,6 - 56,6	30,4	20,3 - 40,5	36,0	24,0; n/d	30,0 - 42,0
others	95,7	87,4 – 100,0	55,2	34,4 - 76	32,2	12,6 - 51,8	42,0	24,0; n/d	24,0 - 54,0
p the level of differences according to χ2 based on the generalized log-rank test									*0,336*
Diagnosis according to the international classification of diseases									
C05.1	n/d	n/d	n/d	n/d	n/d	n/d	24,0	18,0; 37,5	18,0 - 42,0
C09.9	98,4	96,2 - 100,0	51,4	42,6 - 60,2	33,5	25,2 - 41,8	42,0	24,5; n/d	36,0 - 48,0
C10.0	96,0	88,3 - 99,7	24,0	7,3 - 40,7	n/d	n/d	30,0	18,0; 36,0	24,0 - 36,0
C10.2	93,1	83,9 - 99,3	10,3	-0,8 - 21,4	n/d	n/d	24,0	24,0; 30,0	24,0 - 30,0
p the level of differences according to χ2 based on the generalized log-rank test									*<0,001*
Stage of the disease									
II	87,5	64,6 - 95,4	62,5	29,0 – 96,0	n/d	n/d	42,0	30,0; n/d	0,0 - 42,0
III	98,9	96,8 – 100,0	55,7	45,4 - 66	39	28,9 - 49,1	42,0	30,0; n/d	36,0 - 60,0
IV	96,5	92,6 - 100,0	22,7	13,7 - 31,7	11,9	5,0 - 18,8	24,9	24,0; 36,0	n/d
p the level of differences according to χ2 based on the generalized log-rank test									*<0,001*
The stage of the tumor process according to the TNM classification (tumor – T)									
T_2	96,8	90,6 – 100,0	58,1	40,7 - 75,5	41,9	24,5 - 59,3	48,0	28,5; n/d	30,0 - 60,0
T_3	98,5	96,4 - 99,6	42,6	34,2 - 51	27,4	19,8 - 35	36,0	24,0; n/d	30,0 - 42,0
T_4	89,5	75,7 - 96,3	n/d	n/d	n/d	n/d	24,0	18,0; 24,0	18,0 - 30,0
p the level of differences according to χ2 based on the generalized log-rank test									*<0,001*
Tumor stage according to TNM (regional lymph nodes – N)									
N_0	95,2	86,1 – 98,0	60,5	39,1 - 81,9	n/d	n/d	48,0	30,0; n/d	30,0 - 48,0
N_1	96,3	92,2 - 99,4	50,6	39,7 - 61,5	37	26,5 - 47,5	42,0	24,0; n/d	30,0 - 48,0
N_{2-3}	98,8	96,4 - 100,0	26,3	16,6 - 36	12,5	5,2 - 19,8	30,0	24,0; 42,0	24,0 - 30,0
p the level of differences according to χ2 based on the generalized log-rank test									*0,009*
Immediate results of combined treatment									
full regression	98,1	94,5 - 99,7	87,0	78,0 – 96,0	79,6	68,9 - 90,3	56,0	n/d	18,0 – 60,0
partial regression	97,7	93,2 - 98,9	25,0	16,7 - 33,3	5,76	1,3 - 10,2	30,0	24,0; 36,0	24,0 - 48,0
stabilization	82,6	67,1 - 98,1	4,4	-4,0 - 12,7	n/d	n/d	18,0	18,0; 30,0	18,0 - 48,0
p the level of differences according to χ2 based on the generalized log-rank test									*<0,001*
Reaction with $p16^{INK4}$ tumor suppressor (n=64)									
negative	33,3	-20,0 - 86,6	n/d	n/d	n/d	n/d	18,0	18,0; n/d	18,0 - 30,0
available	n/d	n/d	33,3	2,5 - 64,1	n/d	n/d	30,0	24,0; n/d	24,0 - 30,0
p the level of disagreement by the log-rank test									*0,134*

Note. n/d – not defined.

Table 5. Cox proportional hazards regression model of the influence of independent prognostic factors on the survival of patients with malignant neoplasms of the oral part of the pharynx.

Factors	Regression coefficient β	Standard error β	χ^2 Valda	p-value χ^2 Valda	RR	95 % CI
Direct results of treatment in the form of tumor growth progression (x_1)	0,932	0,145	41,16	*p<0,001*	3,72	2,78 – 5,0
Age (**x_2**)	0,018	0,009	3,86	*0,037*	1,17	1,07 - 1,46
N stage (**x_3**)	0,184	0,028	2,55	*0,049*	1,38	1,06 - 1,78

CI 36, 6 - 54.4) and 31.2% (95% CI 22.9 - 39.5), while in those of over 65 - the figures are lower and make up 31.8 respectively (95% CI 20.3 – 43.4) and 9.1% (95% CI - 0.6 - 8.8), although the latter indicator did not reach a statistically significant level (95% CI included zero in the range).

Differences in the survival rate in patients with different diagnoses by ICD and, accordingly, different localization of the pathological process *(p <0.001*) were revealed (Fig. 7).

The highest survival rates are observed in localization of the tumor on the palatine tonsil - median survival is 42.0 months (95% CI 36.0 - 48.0), lower - in localization on the vallecules pharynx and on the lingual surface of the epiglottis - 30.0 months (95% 24.0 - 36.0) and the lowest – in localization on the soft palate and on the lateral and posterior wall of the oral pharynx - 24.0 months (95% 24.0 - 30.0).

Analysis of the survival of the examined patients depending on the stage of the disease showed the worst results in patients with stage IV - so three-year survival rate in the examined patients of this group was 22.7% (95% CI 13.7 - 31.7), while in patients with stage II and III - 62.5 (95% CI 29.0 - 96.0) and 55.7% (95% CI 45.4 - 66) (p <0.001) respectively. (Fig. 8).

A similar trend in the decrease in survival rate with the deterioration of the stage of the pathological process is observed in the analysis of survival by TNM classification (Fig. 9, 10).

Analysis of patient survival rate depending on the immediate results of combined treatment showed that (Fig. 11), the probability of survival is higher (*p <0,001*) during three years in patients with complete regression of the tumor - 87.0% (95% CI 78.0 - 96.0) compared with patients with partial regression - 25.0% (95% CI 16.7 - 33.3) and stabilization of the process 4.4% (95% CI -4.0 - 12.7).

Regarding the choice of treatment strategy, the analysis of survival proved the adequacy of the applied approaches, as the best survival rates were observed in case of the best short-term results of the applied combined treatment. This was also confirmed by the analysis of factors influencing the survival rate of patients through the analysis of Cox's proportional risks. Based on the results of multiple analysis of Cox's proportional intensities, a significant (*p <0.001*) proportional model was constructed with independent prognostic factors for survival of patients with malignant oropharyngeal neoplasms - age, N stage of tumor process and short-term results of combined treatment in the form of progression of tumor growth (Table 5).

The probability of the endpoint (death of the patient) according to the regression model of proportional risks of Cox is modeled as follows:

$$H(t) = H_0(t) * \exp(b_1 \times x_1 + b_2 \times x_2 + b_3 \times x_3) \quad (1)$$

where - b_1 and b_2 - regression coefficients;

x_1 and x_2 are predictor variables presented in Table 5; $H_0(t)$ is the basic danger at time t, which represents the risk of death for a patient with a value of 0 of all predictor variables.

The regression coefficients (beta weights) are the weights for each variable in the equation. Therefore, the most important factor influencing the survival rate of the examined patients from the studied ones is the direct result of treatment, then in descending order of N stage and age of the patient.

A positive regression coefficient in predictor variable of relapse means an increase in risk and, consequently, a worsening of the prognosis in its presence. That is, the prognosis of survival deteriorates with age, N stage of the disease and the progression of tumor growth.

Based on equation 1, the risk ratio is calculated by the formula:

$$\ln(H(t) / H_0(t)) = b_1 \times x_1 + b_2 \times x_2 + b_3 \times x_3$$

Hazard ratio (or risk levels) is the degree of risk associated with each variable (factor) in fixing all other variables. HR greater than 1 indicates an increased risk for patients with this characteristic; less than 1 - a reduced risk.

Survival rate of the examined patients statistically significantly reduces in case of deterioration of direct results of treatment in the form of progression of tumor growth - the adjusted hazard ratio HR = 3,72 (95% of CI 02,78 - 5,0).

DISCUSSION

Treatment of patients with oropharyngeal cancer is still multidisciplinary with the use of surgery, chemotherapy and radiation. Surgery may be an option

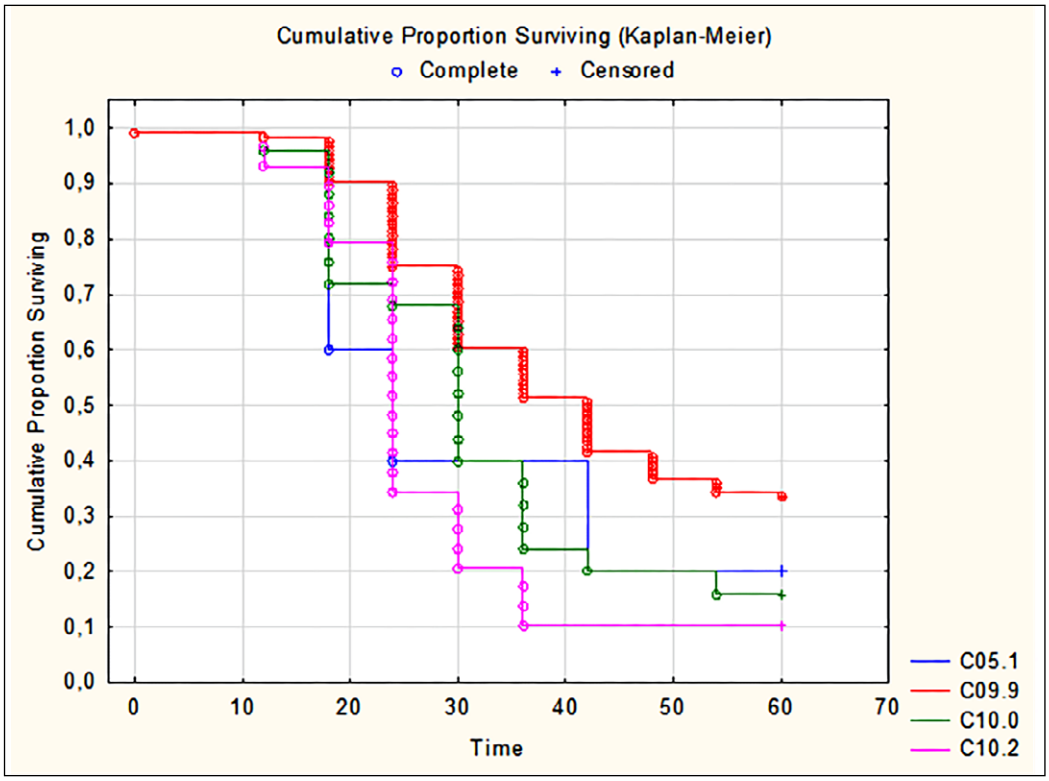

Fig. 7. Cumulative survival rate of the examined patients with oropharyngeal carcinoma depending on the diagnosis by ICD (survival period in months).

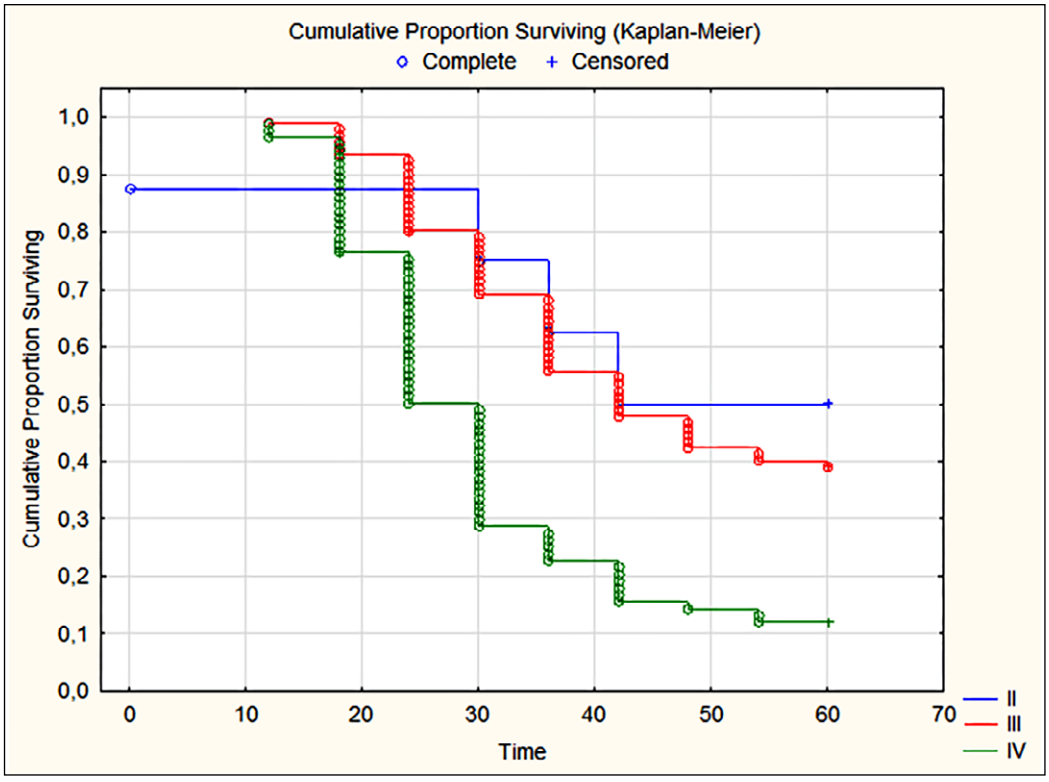

Fig. 8. Cumulative survival rate of the examined patients with oropharyngeal carcinoma depending on the disease stage (survival period in months).

for some early stages of oropharyngeal tumors. Patients with later stages of cancer or those who are inoperable usually receive radiation with or without chemotherapy.

Because toxicity is higher when chemotherapy is added, combination therapy in patients with multiple medical conditions increases the risk of treatment intolerance, which may lead to treatment interruption.

Treatment methods for cancer of head and neck tumors differ from localization in this part of the body. However, the effectiveness of primary surgical removal has been proven for tumors of the oral cavity. The protocols and tactics of laryngeal cancer treatment and their applica-

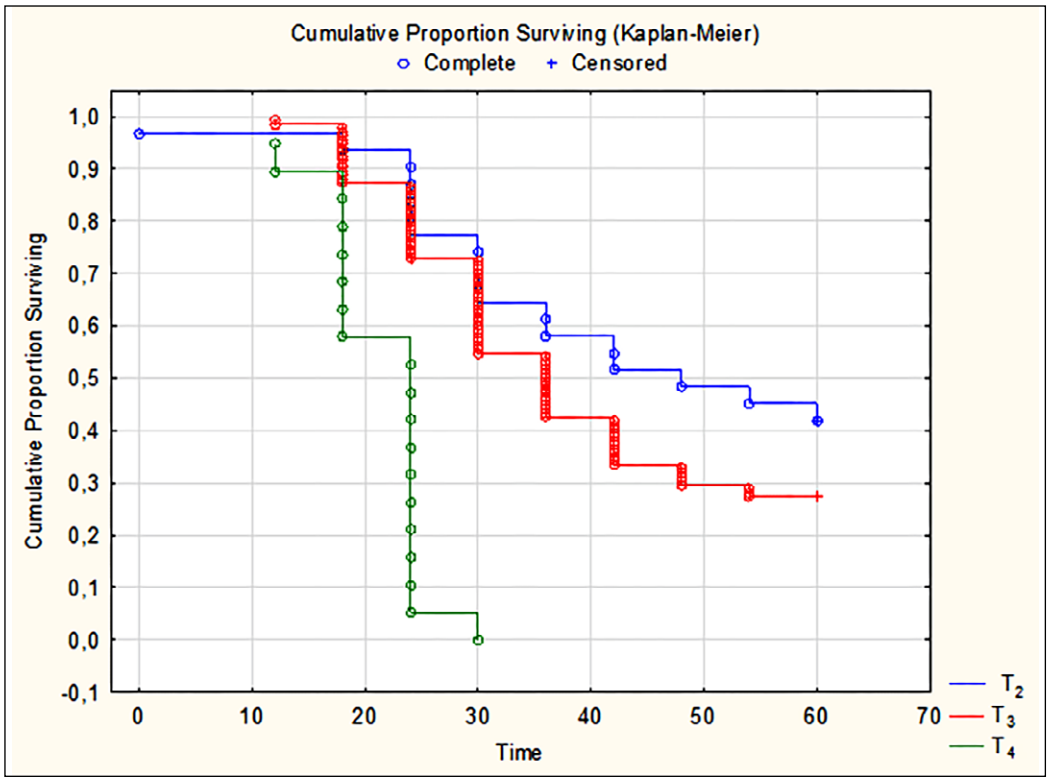

Fig. 9. Cumulative survival rate of patients examined with oropharyngeal carcinoma depending on stage of tumor process by TNM classification (tumor – T) (survival period in months).

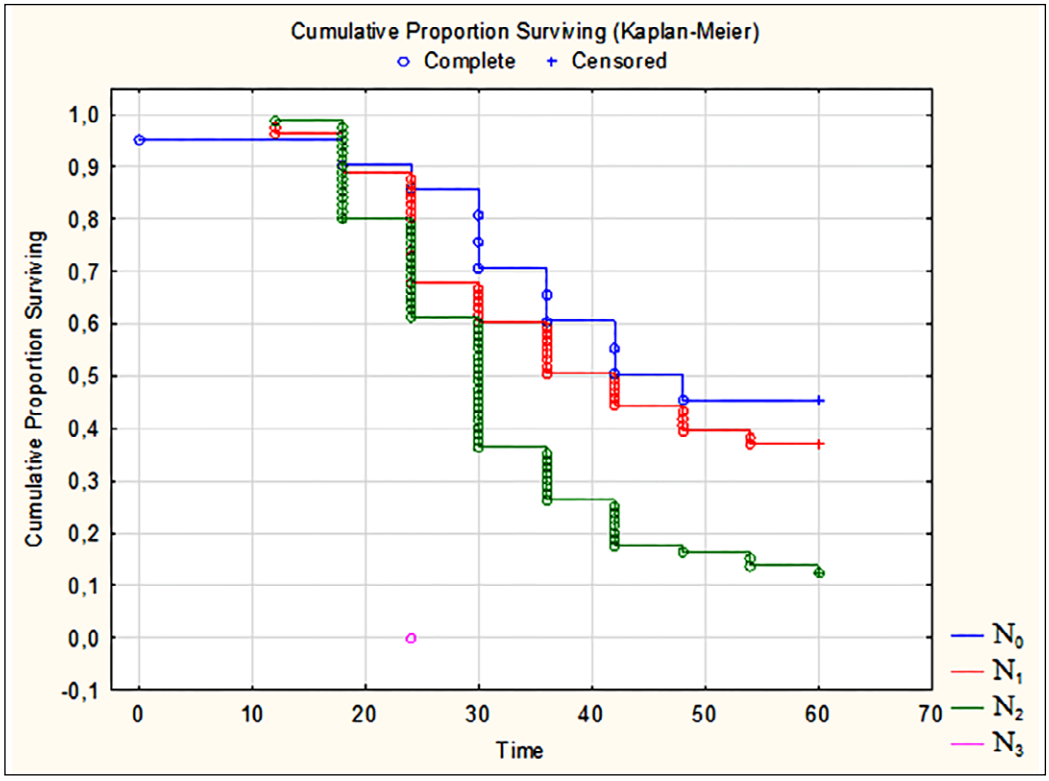

Fig. 10. Cumulative survival rate of the examined patients with oropharyngeal carcinoma depending on the stage of tumor process by TNM classification (regional lymph nodes – N)
(survival period in months).

tion in European countries provide for radiation therapy in the first stage. In the case of cancerous neoplasms of the oral part of the pharynx, meta-analyses demonstrate the usefulness of chemotherapy at the first stage.

In 2017, the staging of cancer of the oral part of the pharynx was changed depending on the association with the human papillomavirus (p16). Human papillomavirus (HPV) is detected in 20-60% of patients with oropharyngeal cancer.

The diagnosis of HPV is based on the study of its specific DNA or mRNA in a tumor cell using the polymerase chain reaction (PCR), enzyme analysis during immunohistochemical study of the p16 gene expression product - INK4A protein, or sequencing.

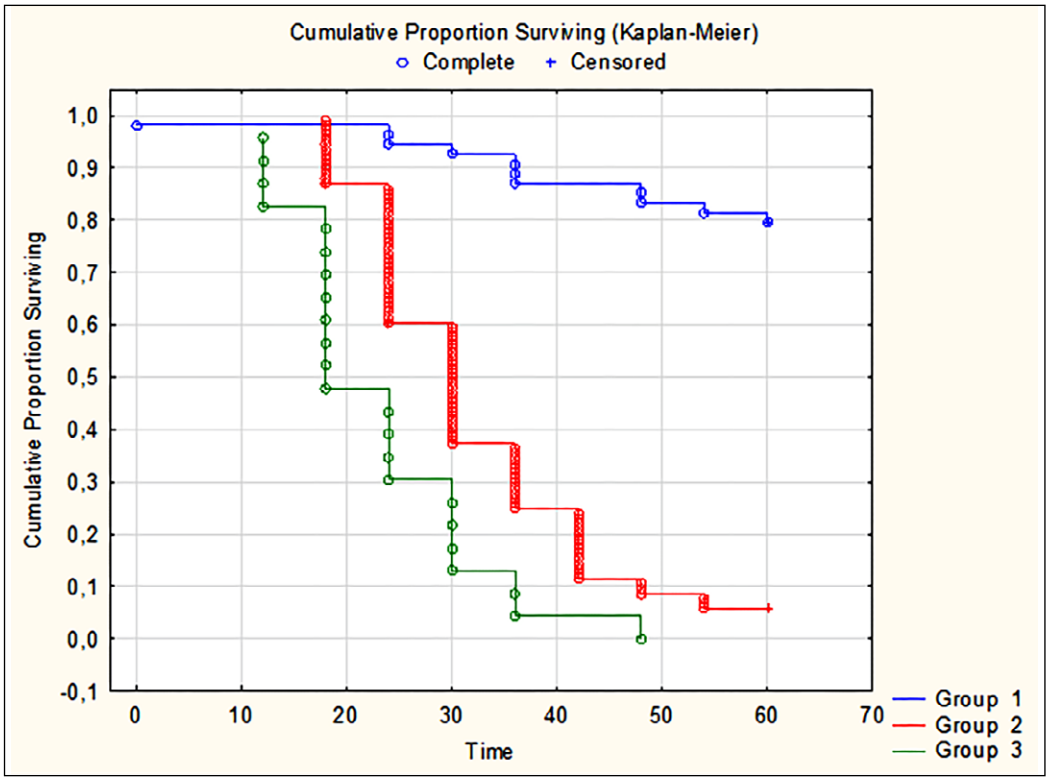

Fig. 11. Cumulative survival rate of patients with oropharyngeal carcinoma depending on short-term results of combination treatment (survival period in months)
Note. Group 1 – complete regression; Group 2 – partial regression; Group 3 – stabilization.

Overexpression of p16 protein INK4a serves as an excellent surrogate biomarker of HPV causation in oropharyngeal cancer because the early E7 protein of HPV leads to overexpression of p16 in HPV-related cancers.

In a multicenter cohort study of 7,895 patients with oropharyngeal cancer from Great Britain, Canada, Denmark, Sweden, France, Germany, the Netherlands, Switzerland, and Spain, the authors identified 4 groups of patients depending on immunohistochemical detection of p16 and HPV testing.

Thus, group 1 - patients with oropharyngeal cancer p16+/HPV– was the largest in subsites outside the tonsils and the base of the tongue (29.7% vs. 9.0%, p<0.0001). 5-year overall survival was 81·1% (95% CI 79·5–82·7).

The second group - patients with p16+/HPV+ had a 5-year survival = 40·4% (38·6–42·4).

The third group of patients with indicators - p16–/HPV–, total survival, respectively, 53·2% (46·6–60·8)

The fourth group of patients with p16–/HPV+ had a 5-year overall survival rate of 54·7% (49·2–60·9).

5-year disease-free survival for patients of the first p16+/HPV– group was 84.3% (95% CI 82.9–85.7), for the second p16+/HPV+= 60.8% (58.8–62, 9), for the third p16–/HPV–= 71·1% (64·7–8·2), for the fourth - p16–/HPV+ = respectively - 67·9% (62·5–73·7).

The study concluded that patients with discordant oropharyngeal cancer (p16–/HPV+ or p16+/HPV–) had a significantly worse prognosis than patients with p16+/HPV+ oropharyngeal cancer and a significantly better prognosis than patients with p16–/HPV– oropharyngeal cancer.

Along with routine p16 immunohistochemistry, HPV testing should be mandatory in clinical trials for all patients (or at least after a positive p16 test result). This is recommended if the HPV status may affect the treatment of patients [13].

These interesting data of the latest study, which indicate the presence of 4 groups of patients with squamous cell carcinoma of the oropharynx (SCCOPH) with different survival results depending on the detection of HPV by two different methods, can be used by clinicians in the future for more effective treatment.

Today, according to the protocols, the treatment of patients with oropharyngeal cancer (SCCOPH) is prescribed depending on the detection of the human papilloma virus.

For patients with cancerous neoplasms of the oral part of the pharynx, the meta-analyses discussed below demonstrate the usefulness of chemotherapy at the first stage.

Thus, in the MACH-NC 5872 meta-analysis, the treatment of head and neck cancer patients with the use of chemotherapy was considered. Individual data of 16,192 patients with an average follow-up period of 5.6 years were analyzed. The benefit of chemotherapy was similar for all head and neck tumor sites, with a hazard ratio for death or recurrence between 0.87 and 0.88 (p-value for interaction = 0.99). The best treatment effect was with combined chemoradiation therapy (simultaneous chemotherapy) for all tumor sites, but the test of interaction between time and treatment effect was significant only for tumors of the oropharynx

(p<0.0001) and larynx (p=0.05). The 5-year absolute effect rate associated with concomitant chemotherapy is 8.9%, 8.1%, 5.4%, and 4% for tumors of the oral cavity, oropharynx, larynx, and hypopharynx, respectively [14].

Other authors also conducted a meta-analysis of 87 trials of 16,485 treatment trials for head and neck cancer. Most patients received concomitant chemotherapy. The hazard ratio for death or recurrence was 0.88 (p<0.0001) with an absolute advantage for chemotherapy of 4.5% at 5 years and a significant interaction (p<0.0001) between time of chemotherapy (adjuvant, induction or concomitant) and treatment . Both direct (6 studies) and indirect comparison showed a more pronounced effectiveness of combined care with induction chemotherapy. For 50 related studies, the hazard ratio for death or recurrence was 0.81 (p<0.0001), and the absolute incidence was 6.5% at 5 years. There was a decrease in the effect of chemotherapy with age (p=0.003, test for trend). The authors conclude that when using concomitant chemotherapy was confirmed and was greater than from induction chemotherapy [15].

Somewhat better than our results of survival are reported by Ukrainian authors in patients with stage III-IV cancer of the oral cavity who received induction chemotherapy followed by radiation therapy. With the TPF scheme (docetaxel or paclitaxel + cisplatin + 5 fluorouracil), the 3- and 5-year survival rates were 51.4% and 42.6%, respectively.[16]

Three-year survival in patients with oral cavity and oropharyngeal cancer stage III-IV with the use of taxane-polyplatylene in the neoadjuvant regimen in another study was 40%, and with induction polychemotherapy with cisplatin - 5.3% [17] .

Our analysis of the treatment of 276 patients with cancer of the oral part of the pharynx with the use of neoadjuvant chemotherapy showed its good effectiveness despite the large number of patients with neglected stages (94%) and the presence of metastases in the lymph nodes of the neck (89.9%). Despite the fact that chemotherapy is ineffective for the treatment of metastases, we observed complete regression of regional metastases in 15% of cases.

The analysis of the survival rate of the examined patients depending on the stage of the disease showed the worst results in patients of stage IV - for example, the three-year survival rate of the examined patients of this group was 22.7% (95% CI 13.7 - 31.7), while in patients of II and III stages, respectively, 62.5 (95% CI 29.0 – 96.0) and 55.7% (95% CI 45.4 – 66) (p<0.001).

The highest survival rates are observed when the tumor is located on the palatine tonsil - median survival 42.0 months (95% CI 36.0 - 48.0), lower - when the tumor is located on the valeculus and on the lingual surface of the epiglottis - 30.0 months (95% 24 .0 - 36.0) and names when located on the soft palate and localization on the side and back wall of the oropharynx - 24.0 months (95% 24.0 - 30.0).

Diverse data on 3- and 5-year survival rates, risk ratio of death or recurrence, median survival value) in meta-analyses and articles by foreign and domestic authors indicate a considerable range of treatment schemes for oropharyngeal cancer and require further study.

Thus, the scientific goal of our work has been achieved, the dependence of the treatment results on the localization of the tumor in the oropharynx, association with the human papillomavirus, age, gender, and response of the tumor (full or partial) after primary chemotherapy has been proven. The results of the work are original for characterizing the treatment of oropharyngeal cancer patients in Ukraine.

The scientific goal was achieved, to the dependence of treatment results on the localization of relapse in the oropharynx, association with the human papillomavirus, age, gender and compliance shown (full or partial) after primary chemotherapy. The results of the work are original for the characteristics of the treatment of oropharyngeal cancer patients in Ukraine.

CONCLUSIONS

Studies of patients with malignant oropharyngeal neoplasms in which squamous cell carcinoma (90.6%) predominated, localized mainly in the palatine tonsil (73.2%), with the most frequent stages $T_3N_1M_0$ (30.1%) and $T_3N_1M_0$ %), with regional metastases to the lymph nodes of the neck (89.9%), showed that the effectiveness of treatment and rehabilitation of patients is quite high, as in most examined in the short term after combined treatment there was a complete or partial regression of the tumor (91.7%), no progression of the oncological process was detected.

In the presence of a reaction with the tumor suppressor $p16^{INK4}$, the chances of achieving complete regression of the tumor increase by 4.2 times compared to its absence (OR = 4.2; *p = 0.010*).

It was determined that with complete and partial tumor regression, a more positive reaction in patients associated with the human papilloma virus (P16 +) with the biomarker $p16^{INK4}$ (r_s = 0.33; *p = 0.007*), which can be used for screening diagnostic purposes as for tumor regression, but has a medium prognostic ability to predict complete regression.

The annual, three- and five-year survival rates of the examined patients with malignant oropharyngeal neoplasms after treatment were 97.3%, respectively

(95% CI 94.9 - 99.7); 40.8% (95% CI 33.7 - 47.9) and 27.0% (95% CI 20.6 - 33.4) with a median survival of 36 months with 95% CI (35.5 – 40.2).

Survival analysis proved the adequacy of the applied approaches to the management of patients, as the highest survival rates were observed at complete regression of the tumor - median survival of 56.0 months (95% CI 18.0 - 60.0) compared to patients with partial regression - 30.0 months (95% CI 24.0 - 48.0) and process stabilization - 18.0 months (95% CI 18.0 - 48.0) ($p<0.001$).

The effectiveness of the applied approaches is also indicated by the fact that in the direct results of combined treatment in the form of progression of tumor growth, survival rate decreases by 3.72 times (95% CI 02.78 - 5.0) and vice versa, if tumor regression is achieved - it significantly increases ($p<0,001$).

REFERENCES

1. Fedorenko ZP, Hulak LO, Mykhailovych YuI et al. Rak v Ukraini. 2019–2020. Zakhvoriuvanist, smertnist, pokaznyky diialnosti onkolohichnoi sluzhby [Cancer in Ukraine. 2019–2020. Morbidity, mortality, indicators of the oncology service]. Biuleten Natsionalnoho kantser-reiestru Ukrainy. Kyiv. 2020;22:132. (Ukrainian)
2. Amini A, Eguchi M, Jones BL et al. Comparing Outcomes of Concurrent Chemotherapy Regimens in Patients 65 Years or Older With Locally Advanced Oropharyngeal Carcinoma. Cancer. 2018;124(22):4322–4331. doi: 10.1002/cncr.31740. DOI
3. Hruzieva TS, Lekhan VM, Ohniev VA et al. Biostatystyka [Biostatistics]. Vinnytsia: Nova Knyha. 2020, p.384. (Ukrainian)
4. Siegel RL, Miller KD, Jemal A. Cancer statistics. CA Cancer J Clin. 2023 Jan;73(1):17-48. doi: 10.3322/caac.21763. DOI
5. Lang TA, Secic M. How to Report Statistics in Medicine: Annotated Guidelines for Authors, Editors, and Reviewers. 2nd ed. USA. Philadelphia: American College of Physicians. 2006, p.490.
6. Pencina MJ, D'Agostino RB. Overall C as a measure of discrimination in survival analysis: model specific population value and confidence interval estimation. Stat Med. 2004;15;23(13):2109-23. doi: 10.1002/sim.1802. DOI
7. Šimundić AM. Measures of Diagnostic Accuracy: Basic Definitions. EJIFCC. 2009;19(4):203-11.
8. Chaturvedi AK, Anderson WF, Lortet-Tieulent J et al. Worldwide trends in incidence rates for oral cavity and oropharyngeal cancers. J Clin Oncol. 2013;31(36):4550-4559. doi: 10.1200/JCO.2013.50.3870. DOI
9. Glantz SA. Primer of Biostatistics. Seventh Ed. New York McGraw-Hill. 2011, p.320.
10. Petrie A, Sabin C. Medical Statistics at a Glance, 4th Ed. Wiley-Blackwell. 2019, p.208.
11. Park SY, Park JE, Kim H et al. Review of Statistical Methods for Evaluating. The Performance of Survival or Other Time-to-Event Prediction Models (from Conventional to Deep Learning Approaches). Korean J Radiol. 2021;(10):1697-170. doi: 10.3348/kjr.2021.0223. DOI
12. Pencina MJ, D'Agostino RB. Overall C as a measure of discrimination in survival analysis: model specific population value and confidence interval estimation. Stat Med. 2004;23(13):2109-23. doi: 10.1002/sim.1802. DOI
13. Mehanna H, Taberna M, von Buchwald C at al. Prognostic implications of p16 and HPV discordance in oropharyngeal cancer (HNCIG-EPIC- OPC): a multicentre, multinational, individual patient data analysis. Lancet Oncol. 2023;24(3):239–51. doi: 10.1016/S1470-2045(23)00013-X. DOI
14. Blanchard P, Baujat B, Holostenco V. Meta-analysis of chemotherapy in head and neck cancer (MACH-NC): a comprehensive analysis by tumour site. Radiother. Oncol. 2011;100(1):33–40. doi: 10.1016/j.radonc.2011.05.036. DOI
15. Pignon JP, Maître A, Maillard E at al. Meta-analysis of chemotherapy in head and neck cancer (MACH-NC): an update on 93 randomised trials and 17,346 patients. 2009;92(1):4-14. doi: 10.1016/j.radonc.2009.04.014. DOI
16. Korobko VE, Protsyk VS. Vykorystannya induktsinoyi khimioterapiyi v kompleksnomu likuvanni khvorykh na rak rotovoyi porozhnyny z urakhuvannyam immunohistokhimichnych faktoriv [The use of induction chemotherapy in the complex treatment of patients with oral cavity cancer, taking into account immunohistochemical factors]. Klinichna onkolohiya. 2015;4(20):53-56. (Ukrainian)
17. Vorobyov OM, Shmykova OV, Vorobyov MO. Neoad"yuvantna polikhimioterapiya v kompleksnomu likuvanni khvorykh zloyakisnymy novoutvorennyamy porozhnyny rota, rotovoyi ta hortannoyi chastyny hlotky III,ta IV A ta IVB stadiyi [Neoadjuvant polychemotherapy in the complex treatment of patients with stage III, IV A and IV B malignant neoplasms of the oral cavity, oral and laryngeal part of the pharynx]. Klinichna onkolohiya. 2014;3(15):53-56. (Ukrainian)

The work was carried out within the framework of the work Institute of Otolaryngology named after Prof. O.S. Kolomiichenko of the National Academy of Sciences of Ukraine: «To determine the effectiveness of various options for the combined treatment of patients with cancer of the pharynx and larynx», state registration number 019U10493.

CONFLICT OF INTEREST

The Authors declare no conflict of interest

CORRESPONDING AUTHOR
Anatoliy A. Bakaiev
Dnipro State Medical University
12/83 Budivelnikiv St., 52005 Dnipro, Ukraine
e-mail: anatoliybakaev@gmail.com

ORCID AND CONTRIBUTIONSHIP
Ervin V. Lukach: 0000-0003-3262-4996 A D F
Viktor Ya. Dikhtiaruk: 0000-0001-9940-896X B D F
Oleksandr V. Kovtunenko: 0000-0002-0562-7684 A D F
Anatolii A. Bakaiev: 0000-0003-4192-7614 C D E F

A – Work concept and design, B – Data collection and analysis, C – Responsibility for statistical analysis, D – Writing the article, E – Critical review, F – Final approval of the article

RECEIVED: 17.03.2024
ACCEPTED: 19.07.2024

ORIGINAL ARTICLE

CONTENTS

Endoscopic light-guided choledochoduodenostomy in the treatment of the distal common bile duct obstruction

Valerii Vovk[1,2], Valerii Boyko[3], Vasyl Hroma[3], Igor Duda[1], Kyrylo Parkhomenko[4], Alla Vovk[2]

[1]TRNAVA UNIVERSITY IN TRNAVA, TRNAVA, SLOVAK REPUBLIC

[2]TRNAVA UNIVERSITY HOSPITAL, TRNAVA, SLOVAK REPUBLIC

[3]STATE ORGANIZATION «V.T. ZAYTSEV INSTITUTE OF GENERAL AND EMERGENCY SURGERY OF THE NATIONAL ACADEMY OF MEDICAL SCIENCES OF UKRAINE», KHARKIV, UKRAINE

[4]KHARKIV NATIONAL MEDICAL UNIVERSITY OF THE MINISTRY OF HEALTH OF UKRAINE, KHARKIV, UKRAINE

ABSTRACT

Aim: Experimental justification for creation of bile offtake into the duodenum with minimally invasive methods in cases of obstruction of the distal part of common bile duct and failure of transpapillary interventions and studying the first results of such intervention application.

Materials and Methods: The anatomical relationships between the duodenum and the common bile duct in its distal parts starting from its retroduodenal part to the sphincter of Oddi were studied. The possibility of transillumination of the walls of the common bile duct and the duodenum by a light source introduced into the lumen of the common bile duct is determined.

Results: The length of a conventional straight line between the lumens is from 7.1±0.2 mm at a distance of 50 mm from the sphincter of Oddi to 4.7±0.1 mm at a distance of 30 mm from the sphincter of Oddi. In the distance up to 40 mm from the sphincter of Oddi, the common bile duct and the duodenum are in close proximity to each other without free spaces, that predispose for the connection formation between the lumens of the duodenum and the common bile duct. The technology of endoscopic light-guided choledochoduodenostomy is substantiated, developed and implemented.

Conclusions: Created method of endoscopic light-guided choledochoduodenostomy allows to perform a conjunction between the lumens of the duodenum and the common bile duct. This intervention can be used when endoscopic transpapillary drainage of the common bile duct is impossible and has advantages over open draining bile duct operations in patients with tumor distal common bile duct obstruction.

KEY WORDS: cholangitis, biliary obstruction, minimally invasive interventions

Wiad Lek. 2024;77(8):1547-1553. doi: 10.36740/WLek202408103 DOI

INTRODUCTION

Obstruction of the distal common bile duct due to benign or malignant process in most cases requires primary drainage of the biliary tract [1,4]. Endoscopic retrograde cholangiopancreatography (ERCP) with stenting of the common bile duct (with or without papillosphincterotomy) is recognized as the "gold standard" of biliary tract drainage, and technical success is usually obtained in most cases [2,4]. However, according to the literature data, failed biliary cannulation or stenting of the choledochus are observed in up to 10% of cases when distal common bile duct is obstructed due to oncological processes and the rigidity of tumorous tissues in this area [3,6].

In cases of failed transpapillary cannulation and stenting, alternative access methods to biliary decompression are needed: percutaneous transpapillary external drainage, open or laparoscopic external and internal drainage, endoscopic ultrasound (EUS) internal biliary drainage (most often in the form of EUS-guided choledochoduodenostomy) [4,5]. It should be noted that percutaneous transhepatic biliary drainage is traditionally attempted as an alternative drainage method, but adverse event rates are reportedly relatively high. These negative aspects are directly related to the peculiarities of performing this intervention, as well as that is an external drainage method, which leads to indigestion because of bile absence in the duodenum and reduced quality of life. In general, laparoscopic external drainage interventions have similar disadvantages [7,8]. Open surgical interventions for biliary obstruction, compared with minimally invasive, are associated with much greater surgical trauma, which in turn leads to greater postoperative pain, longer postoperative period, increased postoperative complications, morbidity and mortality [9,10]. The hybrid approaches

such us EUS-guided choledochoduodenostomy or laparoscopic-cholangioscopic cooperative technique require careful patient selection, appropriate special equipment, experienced operator supported by a well-trained team in a multidisciplinary setting and has its own complications, for example, in the form of bleeding [4,11].

Thus, despite the fact that many scientific and practical efforts are devoted to the topic of bile ducts drainage in the case of distal lesions of common bile duct, this problem remains relevant due to its difficulty, that confirmed by numerous publications.

AIM

Experimental justification for creation of bile offtake into the duodenum with minimally invasive methods in cases of malignant obstruction of the distal part of common bile duct and failure of transpapillary interventions and studying the first results of such intervention application.

MATERIALS AND METHODS

During the primary drainage of the biliary system among patients with obstruction of the common bile duct of tumor etiology, in 19.7% cases transpapillary drainage was unsuccessful due to the technical impossibility of cannulating the bile ducts or the impossibility of papillosphincterotomy and stent placement due to the rigidity of the tissues near the large duodenal papilla. All these patients underwent percutaneous transhepatic and open draining surgical interventions for bile duct decompression. The fails in performing transpapillary biliary drainage in case of obstruction of the distal common bile duct dictated the need to develop other minimally invasive ways of diverting bile to the duodenum.

To solve the issue of alternative ("extrapapillary") bile drainage from the common bile duct to the duodenum, the anatomical relationships between the duodenum and the common bile duct in its distal parts were studied on the sectional material, starting from its retroduodenal part to the sphincter of Oddi. During the morphological study, the distance between the lumens of the choledochus and the duodenum was measured at different levels from 0 to 50 mm from the sphincter of Oddi.

The possibility of passing light through the walls of the common bile duct and duodenum by a light source introduced into the lumen of the common bile duct is also determined. A new method of bile drainage in the case of obstruction of the distal part of the choledochus has been developed. The first results of using this technique are compared with the results of treatment with transpapillary interventions and open interventions.

ETHICS

Ethical approval was obtained from the ethics committee of the State Organization «V.T. Zaytsev Institute of General and Emergency Surgery of the National Academy of Medical Sciences of Ukraine», Kharkiv, Ukraine, including the aim of the study and confirmation that all data collected, will be kept confidential and used for scientific research only. The Study complies with the Declaration of Helsinki.

STATISTICAL ANALYSIS

Data were presented using descriptive statistics in the form of frequencies and percentages. The average values were used with a standard deviation; for the comparison of non-parametric values an $\chi 2$ criterion was used; according to this criterion, p was determined ($p < 0,05$ was considered statistically significant).

RESULTS

Microscopic measurement of tissues cross-sections in the area of adjacency of the common bile duct to the duodenal wall revealed that the distance between the lumens of the common bile duct and the duodenum is unequal at different levels (Fig. 1).

According to the data obtained, the gap between the duodenal wall and the common bile duct has no free spaces starting from 50,1 ± 0,2 mm from the sphincter of Oddi. Therefore, the distance between the lumens of the duodenum and the common bile duct was measured during microscopic investigation at the distance of 50 mm, 40 mm, 30 mm, 20 mm and 10 mm from the sphincter of Oddi and directly in the area of the sphincter.

The results of measurements between the lumens of the common bile duct and duodenum are presented in Table 1.

Almost throughout the entire study area, the space between the lumens of the duodenum and the common bile duct consists of duodenal mucosa, its submucosal and muscle layers, adipose tissue and directly the wall of the common bile duct.

The length of the conditional straight line between the lumens is from 7.1 ± 0.2 mm at a distance of 50 mm from the sphincter of Oddi to 4.7 ± 0.1 mm at a distance of 30 mm from the sphincter of Oddi. Then, closer to the sphincter of Oddi, the length of the conditional straight line between

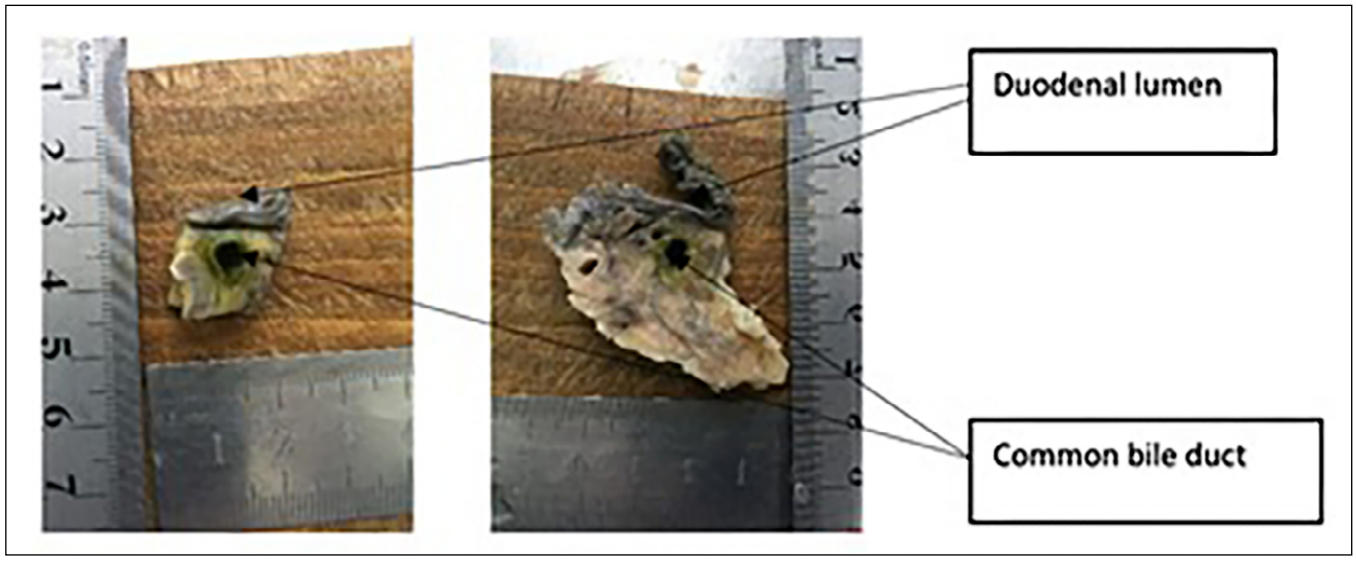

Fig. 1. Morphological sample of arrangement of the common bile duct and duodenum (cross section).

Table 1. Results of measurements between the lumens of the common bile duct and duodenum

Distance from Oddi's sphincter	The distance between the lumens of the common bile duct and the duodenum
50 mm	7,1±0,2 mm
40 mm	5,2±0,1 mm
30 mm	4,7±0,1 mm
20 mm	6,2±0,2 mm
10 mm	6,0±0,2 mm
0	3,5±0,1 mm

the duodenal lumen and lumen of the common bile duct increases to 6-6.5 mm at a distance of 10-20 mm from the sphincter of Oddi. The cause for increasing this distance is the artery, that occurs in about 85%, which follows the curvature of the common bile duct wall. (Fig. 2).

Further, even closer to the Oddi's sphincter, there is a significant shift of the common bile duct in the direction of the duodenal mucosa. The length of the straight line connecting the lumens of the duodenum and the common bile duct is reduced to 4-5 mm. Directly next to the sphincter of Oddi, the common bile duct is adjacent to the duodenal muscular layer, and the measured distance is 3.5 ± 0.1 mm.

Thus, in the area up to 40 mm from the sphincter of Oddi, the common bile duct and the duodenum are in close proximity to each other without voids, which is a prerequisite for the formation of a connection between the lumens of the duodenum and the common bile duct. A warning factor is the presence of an artery near the wall of the choledochus at a distance of 10-20 mm from the sphincter of Oddi.

Based on the above data, the possibility of establishing a connection between the lumens of the duodenum and the common bile duct due to the short distance between these formations is substantiated. It should be noted that to prevent bleeding, you need to avoid damage to the artery in this area.

Visibility from the duodenal lumen of the light source introduced into the common bile duct was checked on the cadaver material. Through the opening in the hepaticocholedochus, a light source was passed on a conductor to the retroduodenal part of the common bile duct, and the translucency of this light source through the open wall of the duodenum was observed (Fig. 3).

It was revealed that the light source inserted the common bile duct is visualized from the lumen of the duodenum with different intensities up to 50 mm from the sphincter of Oddi (Fig. 4).

To perform a connection between the lumens of the duodenum and the common bile duct, the technology of endoscopic light-guided choledoduodenostomy (ELCD) was created and implemented.

The insertion of a light source into the common bile duct to the site of its obstruction allows to identify the location of the obstruction, that visible from the adjacent part of the duodenum (i.e. to determine the point of the future junction). Also, it can be clarified the location of tissue dissection so that it does not fall into vessels and did not lead to bleeding. The light flux passes through optically inhomogeneous biological tissues, that allows to detect the presence of denser structures (bile stones, vessels).

PROCEDURE TECHNIQUE

A light source is inserted into the common bile duct through a dilated cystic duct laparoscopically to the point of its obstruction. Then endoscopically from the duodenum through its wall it is performed connection

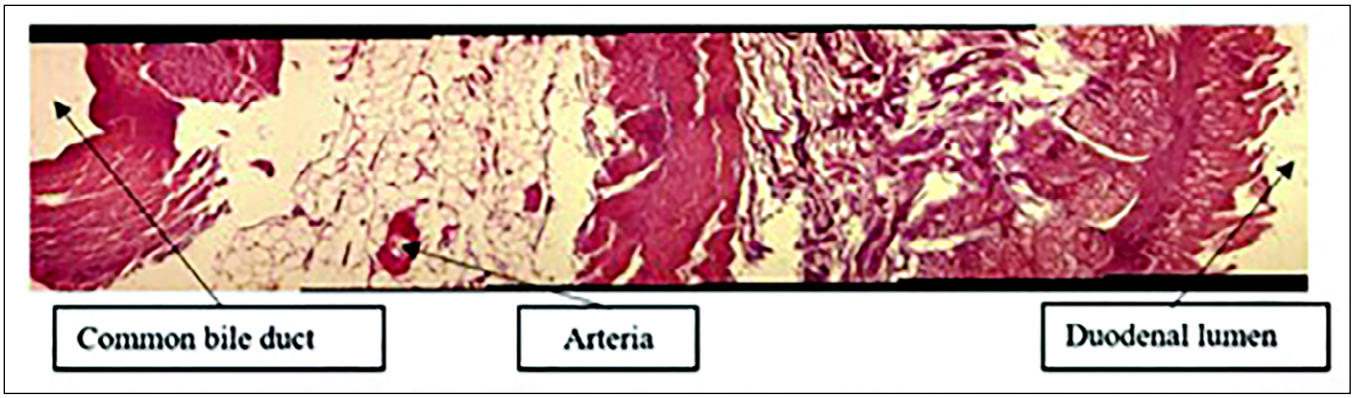

Fig. 2. Microscopy of the area between the lumens of the duodenum and the common bile duct (x60).

Table 2. Results of comparing after ELCD, ETD and BDA.

Parameter	ELCD (n=7)	ETD (n=10)	BDA (n=10)
Average indicator of PS *, points	3,6	2,2	7,5
Average duration of the postoperative period, days	6,7±0,5	5,3±0,3**	9,2±1,2
Complications,%	-	10%	20%
Beginning of enteral nutrition, days	1,5±0,3	0,9±0,1	2,8±0,5

* - PS (pain scale) 12 hours after surgery, points
** - the duration from the intervention to the patient's discharge or to the next stage of treatment.

Table 3. Dynamics of blood bilirubin decrease after ERLDC, EPDC and BDA, μmol/l

Type of intervention	Before intervention	After intervention		
		1st day	3d day	5th day
ELCD	170,2±13,4	113,8±12,5	67,1±6,7	20,6±4,9
ETD	181,5±9,8	105,7±10,3	59,3±7,5	17,5±3,4
BDA	203,6±15,8	130,7±11,5	79,5±9,1	35,9±5,2

between the lumens of the duodenum and the common bile duct with endoscopic knives or otherwise, focusing on light from the common bile duct (Fig. 5).

The criteria of the effectiveness of the intervention is the appearance of the contents of the common bile duct (bile, pus) in the duodenum lumen. Stenting of a new choledochoduodenal connection is not principally. The light source in the common bile duct to point of its obstruction can be delivered percutaneously transhepatic, percutaneously or laparoscopically through the gallbladder or cystic duct.

Thus, this procedure allows under visual (most informative) control to perform mini-invasive provision of bile outflow from the common bile duct to the duodenum in case of obstruction of choledoch's distal part and the impossibility of transpapillary interventions. The duration of the intervention was from 75 to 170 minutes.

According to this method it was performed 7 ELCD. The results after procedure in these patients were compared with the period after endoscopic transpapillary drainage (ETD) and open biliodigestive anastomoses (BDA). The results of the comparison are presented in Table 2.

The changes in bilirubin concentration in the blood after ELCD, ETD and BDA are presented in Table 3.

DISCUSSION

Obstruction of the distal part of the common bile duct in the vast majority of cases is managed by endoscopic transpapillary interventions. However, in some cases drainage of the biliary tree using transpapillary interventions is unsuccessful for various reasons. This especially applies to patients with tumor lesions of the distal part of the common bile duct and large duodenal papilla. Alternative methods to biliary decompression (percutaneous external drainage, open or laparoscopic external and internal drainage and endoscopic ultrasound internal biliary drainage) have their own disadvantages [7]. Therefore, still it has been created new methods for draining bile to the duodenum when

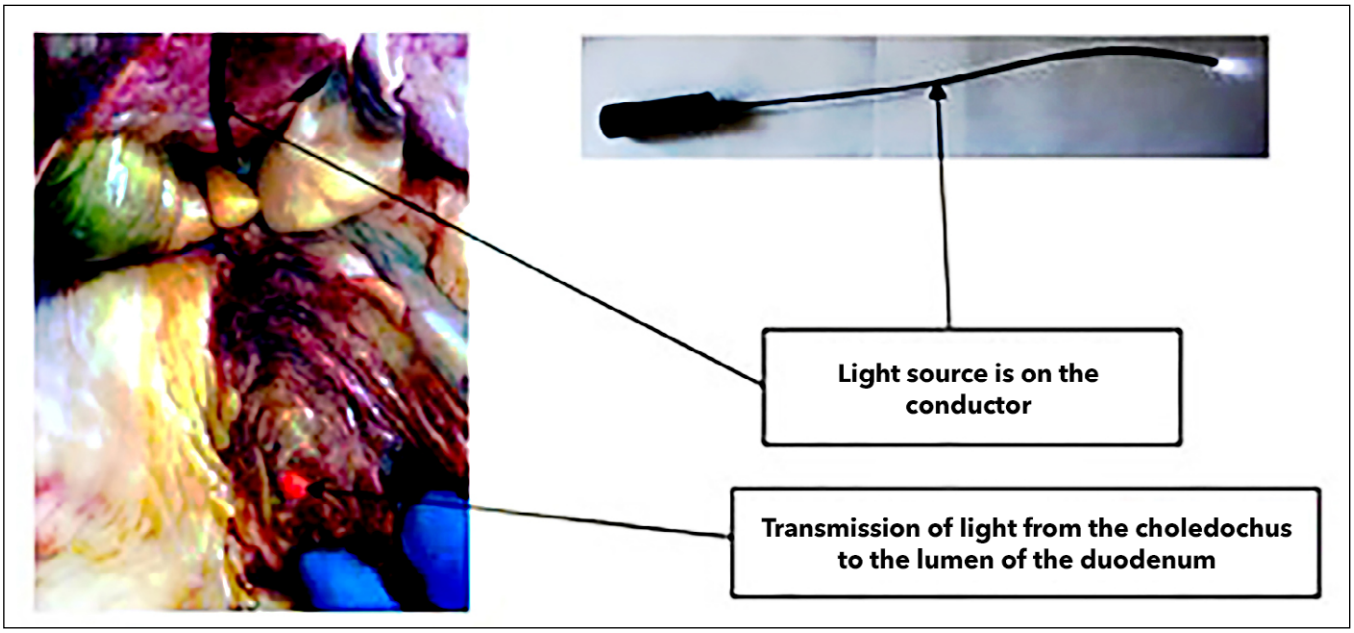

Fig. 3. A light source on a conductor introduced into the hepaticocholedochus (morphological material).

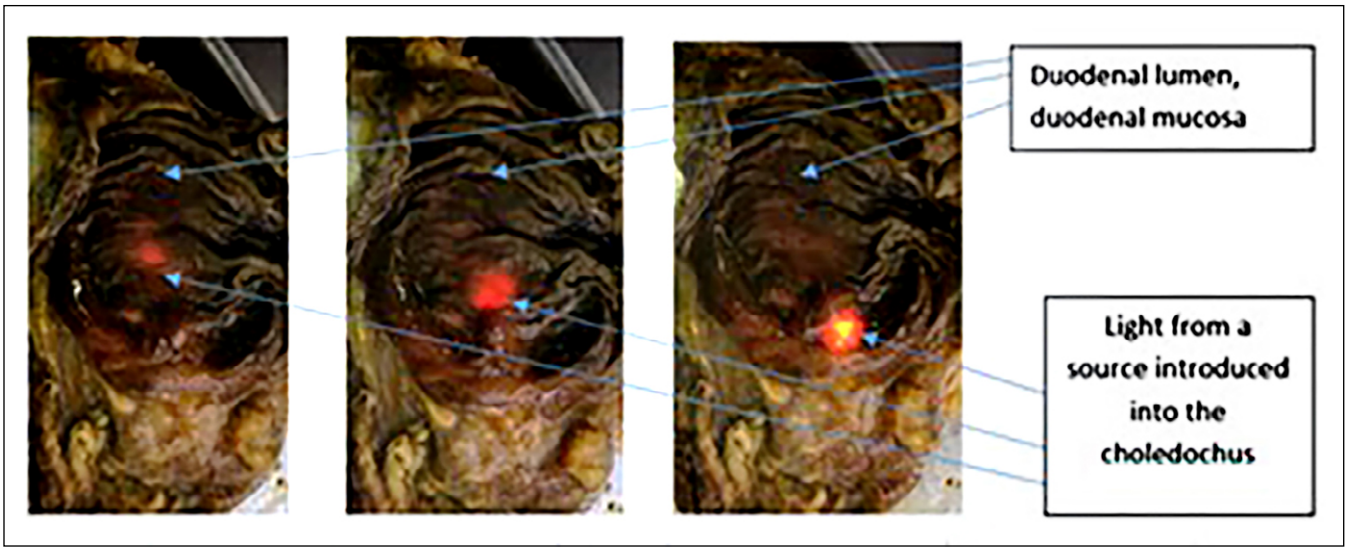

Fig. 4. Transillumination of light from the lumen of the common bile duct through the wall of the duodenum (morphological material).

transpapillary cannulation and stenting is failed. Based on the study of the anatomical relationship between duodenum and choledochus retroduodenal part, as well as on study of light transillumination through the walls of the common bile duct and duodenum, it was developed method of endoscopic light-guided choledoduodenostomy (ELCD). This technique was performed in 7 patients, and we have analyzed fist results.

According to the comparison data, the results of ELCD are not statistically different from endoscopic transpapillary drainage of the common bile duct in dynamics of bilirubin decrease, pain assessment, duration of postoperative period and beginning of enteral nutrition. At the same time, there is statistically significant differences ELCD with open biliodigestive anastomoses for all studied parameters: significantly lower pain rating scale ($p < 0.05$), shorter postoperative period ($p < 0.05$), less postoperative complications ($p < 0.05$), earlier possibility of the enteral nutrition ($p < 0.05$) and a more pronounced dynamic of bilirubin reducing in the blood ($p < 0.05$).

CONCLUSIONS

Thus, created method of endoscopic light-oriented choledochoduodenostomy allows to perform a conjunction between the lumens of the duodenum and the common bile duct. The results of this intervention are statistically better than the results of open biliodigestive anastomoses and comparable to endoscopic transpapillary drainage of the common bile duct. At present, this intervention can be used when endoscopic transpapillary

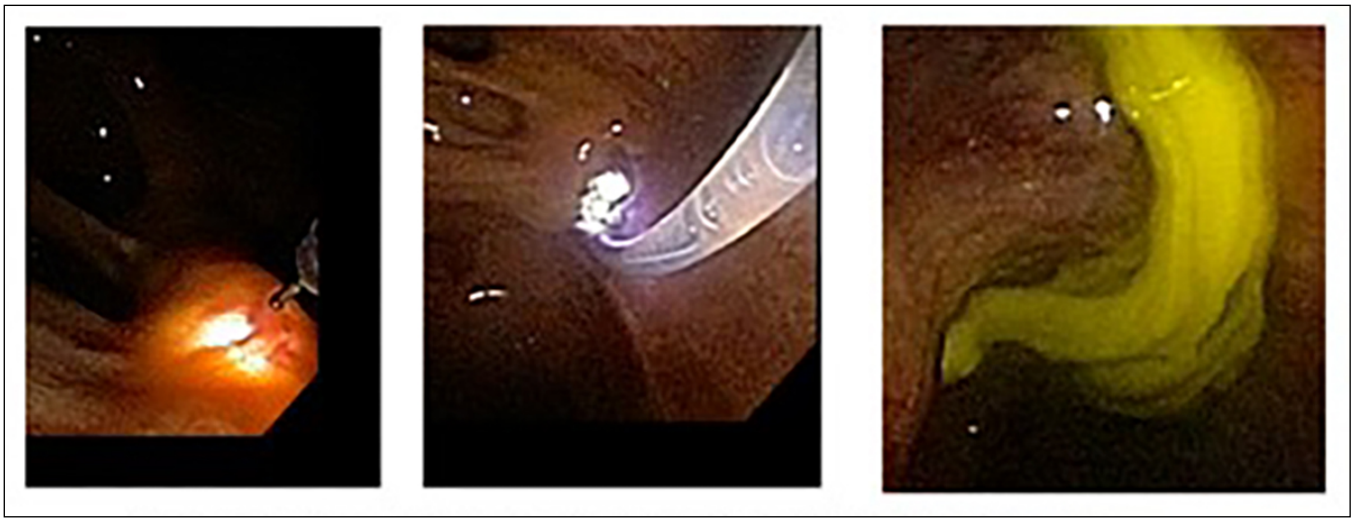

Fig. 5. Endoscopie light-guided choledochoduodenostomy.

drainage of the common bile duct is impossible and has advantages over open draining bile duct operations in patients with tumor distal common bile duct obstruction.

We would like to note that this article presents only the first results of implementing the Endoscopic light-guided choledochoduodenostomy. We publish them to inform the public about the technique itself and about the first good results of its application. In the future, we will continue research and collect material so that the results will be more relevant.

REFERENCES

1. Boyko VV, Maloshtan AV, Vovk VA et al. Fiziko-khimicheskiye svoystva zhelchi v period vozniknoveniya i proyavleniya kholangita. Ostryy kholangit: vozmozhnyye puskovyye mekhanizmy [Physical and chemical properties of bile during the onset and manifestation of cholangitis. Acute cholangitis: Possible triggering mechanisms]. Novosti Khirurgii. 2021;29(1):20-7. doi: 10.18484/2305-0047.2021.1.20. (Russian) DOI
2. Jinjiao Lu, Zhen F. ERCP endoscopic minimally invasive treatment of acute suppurative obstructive cholangitis: A study of 47 patients. Exp Ther Med. 2024;27(4):128. doi: 10.3892/etm.2024.12416. DOI
3. Bonnel D, André T, Mader B et al. Malignant biliary obstruction, general review and clinical practice. Bull Du Cancer. 2013;100(5):443–52. doi: 10.1684/bdc.2013.1736. DOI
4. Doyle JB, Sethi A. Endoscopic Ultrasound-Guided Biliary Drainage. J Clin Med. 2023;12(7):2736. doi: 10.3390/jcm12072736. DOI
5. Zhang GY, Li WT, Peng WJ et al. Clinical outcomes and prediction of survival following percutaneous biliary drainage for malignant obstructive jaundice. Oncol Lett. 2014;7(4):1185–90. doi: 10.3892/ol.2014.1860. DOI
6. Yamazaki H, Yamashita Y, Shimokawa T et al. Endoscopic ultrasound–guided hepaticogastrostomy versus choledochoduodenostomy for malignant biliary obstruction: A meta–analysis. DEN Open. 2024;4(1):e274. doi:10.1002/deo2.274. DOI
7. Lorenz JM. Management of malignant biliary obstruction. Semin Intervent Radiol. 2016;33(4):259. doi: 10.1055/s-0036-1592330. DOI
8. Mao XN, Lu ZM, Wen F et al. Bare-metal stents across the Vater's ampulla is a safe method for patients with lower bile duct obstruction. Medicine (Baltimore). 2017;96(45):e7475. doi: 10.1097/MD.0000000000007475. DOI
9. Tringali A, Costa D, Fugazza A, Colombo M et al. Endoscopic management of difficult common bile duct stones: Where are we now? A comprehensive review. World J Gastroenterol. 2021;27(44):7597–7611. doi: 10.3748/wjg.v27.i44.7597. DOI
10. Rimbas M, Anderloni A, Napoléon B et al. Common bile duct size in malignant distal obstruction and lumen-apposing metal stents: a multicenter prospective study. Endosc Int Open. 2021;9(11):E1801–10. doi: 10.1055/a-1526-1208. DOI
11. Chi Thanh Ho, Trung Hieu Le, Van Thanh Le et al. Laparoscopic-cholangioscopic cooperative modified tunnel technique for hepatolithiasis combined with dilated common bile duct: A case report and literature review. Int J Surg Case Rep. 2024;116:109369. doi: 10.1016/j.ijscr.2024.109369. DOI

CONFLICT OF INTEREST

The Authors declare no conflict of interest

CORRESPONDING AUTHOR
Valerii Vovk
Trnava University in Trnava
23 Hornopotochna st, 91843 Trnava, Slovak Republic
e-mail: valery_vals@ukr.net

ORCID AND CONTRIBUTIONSHIP
Valerii Vovk: 0000-0003-0888-1837 A B C D E F
Valerii Boyko: 0000-0002-3455-9705 A E F
Vasyl Hroma: 0000-0003-1886-3181 A E F
Igor Duda: 0009-0003-1550-6864 E F
Kyrylo Parkhomenko: 0000-0002-0004-2417 C E
Alla Vovk: 0009-0005-7497-0784 B C E

A – Work concept and design, B – Data collection and analysis, C – Responsibility for statistical analysis, D – Writing the article, E – Critical review, F – Final approval of the article

RECEIVED: 11.10.2023
ACCEPTED: 17.07.2024

ORIGINAL ARTICLE

CONTENTS

Changes in lipid profile parameters depending on the a1166c polymorphism of the angiotensin II type I receptor gene as a predictor of arterial hypertension

Volodymyr V. Shmanko[1], Svitlana R. Pidruchna[1], Roman V. Hnizdyukh[1], Alla E. Mudra[1], Uliana M. Zakharchuk[2], Iryna P. Kuzmak[1], Tetiana Y. Yaroshenko[1], Lylya M. Palytsya[1], Iryna A. Bandas[1], Volodymyr H. Dzhyvak[1], Iryna M. Nikitina[3], Iryna F. Zavarynska[4]

[1]I. YA. HORBACHEVSKY TERNOPIL NATIONAL MEDICAL UNIVERSITY, TERNOPIL, UKRAINE

[2]MSD BIOTECH, SWORDS, IRELAND

[3]SUMY STATE UNIVERSITY, SUMY, UKRAINE

[4]TERNOPIL VOLODYMYR HNATIUK NATIONAL PEDAGOGICAL UNIVERSITY, TERNOPIL, UKRAINE

ABSTRACT

Aim: To investigate lipid profile parameters depending the polymorphism of the A1166C I type gene receptor of the angiotensin II as a predictor of arterial hypertension.

Materials and Methods: The study involved 86 patients with arterial hypertension. The control group consisted of 30 practically healthy individuals. Indicators of lipid metabolism in the blood serum of patients were determined using "Lachema" kits on an analyzer. The the polymorphism of the A1166C I type gene receptor of the angiotensin II was studied by polymerase chain reaction with electrophoretic detection of the results.

Results: Higher levels of total cholesterol were found in patients with CC genotype compared to AA genotype carriers ((8.94±0.09) vs (5.18±0.02) mmol/L). The level of low-density lipoprotein in CC-genotype carriers was (7.43±0.03) versus (3.66±0.02) mmol/L in A-allele homozygotes. Triglycerides and very low density lipoproteins were also significantly higher in CC genotype carriers compared to patients with AA genotype. The level of high-density lipoprotein was lower in homozygotes with C-allele than in patients with the AA genotype, and was (0.59±0.12) versus (0.99±0.03) mmol/L.

Conclusions: The presence in the CC genotype the I type gene receptor of the angiotensin II type is a predictor of dyslipidemia. In patients with arterial hypertension, the presence in the C-allele of the I type gene of the angiotensin II type contributes to a significant increase in serum adipokines and a decrease in ghrelin levels.

KEY WORDS: arterial hypertension, polymorphism of the A1166C gene, lipidogram, predictor, lipid profile, ghrelin

Wiad Lek. 2024;77(8):1554-1561. doi: 10.36740/WLek202408104 DOI

INTRODUCTION

The clinical and pathogenetic heterogeneity of arterial hypertension (AH) and insufficient study of the mechanisms of blood pressure regulation and, as a result, the improvement of the schematics of complex therapy of AH, stipulates further study of the pathogenetic mechanisms of persistent high blood pressure. A unique feature of AH is the dominance of disorders of functional mechanisms of blood pressure regulation (nervous and humoral), which cover the main homeostatic systems of the body, the formation of vicious circles and the so-called cardiovascular continuum [1, 2].

Functionally, blood pressure regulatory systems are genetically determined. In view of this, the combination of genetic predisposition with living conditions and environmental factors allowed us to classify hypertension as a multifactorial pathology. The stratification of risk factors for hypertension has led to the most significant mutational changes in the genes responsible for the balance of the pressor (tissue and renal renin-aldosterone-angiotensin system (RAAS) vasoconstrictors-endothelin 1, 2, 3, vasopressin, aldosterone, leukotrienes C and D, prostaglandin-E2) and depressor (NO, Na-urethic peptides, kallikrein-kinin system, prostacyclin) long-acting circuits [3, 4].

The realization of pathophysiological effects of these «mediators» of hypertension is possible only in cases of expression of the corresponding receptors on target cells and organs. In addition, non-peptide components of the

Table 1. Characteristics of the examined patients (n=86)

Indicator	Meaning
Average age, years	61,35±13,3
Men, % (n)	45 (39)
Women, % (n)	55 (47)
Duration of the disease, years	12,6±1,8
BMI, kg/m^2	32,6±1,1
Obesity (BMI > 30 kg/m2), % (n)	34,9 (30)
Smoking	31,4 (27)
Alcohol abuse	12,8 (11)
Burdened heredity for early development of CVD (for men age < 55 years, for women < 65 years), % (n)	54,7 (47)
Grade 1 hypertension, % (n)	24,4 (21)
Grade 2 hypertension, % (n)	54,6 (47)
Grade 3 hypertension, % (n)	21 (18)

pressor and depressor circuits realize their physiological and pathophysiological effects only in the case of the activity of the corresponding enzymes. Mutational processes affecting the synthesis, production, and reception of these mediators of hypertension are an important component of this disease. The identification of specific polymorphisms associated with hypertension and their involvement in pathogenetic patterns of blood pressure dysregulation gave rise to the definition of these genes as candidate genes for hypertension. The most relevant polymorphisms in hypertension are the polymorphisms of the angiotensin-converting enzyme (ACE) gene, the angiotensin (AGT) gene polymorphism, the angiotensin II receptor (AGTR) gene polymorphism, and the NO-synthase gene polymorphism [5, 6, 7].

There are many gene-candidates, whose SNP-mutations are associated with a predisposition to cardiovascular disease, and one of the most common is undoubtedly arterial hypertension (AH). Despite some progress in the study of the pathogenesis and diagnosis of arterial hypertension, most patients fail to achieve adequate control of high blood pressure, which leads to an increased risk of developing complications of AH [8, 9].

The results of numerous studies confirm the relationship between arterial hypertension and genes of the renin-angiotensin-aldosterone system, namely the polymorphism of the A1166C I type gene receptor of the angiotensin II (AGTR1) in patients with hypertension and the evaluation of the relationship between polymorphism, high blood pressure and dyslipidemia [10, 11].

Given the material we have accumulated, we considered it appropriate to conduct additional research to help understand the interaction of genes with the environment to obtain a complete picture of the complex genetic architecture of AH.

AIM

The aim of the work is to investigate lipid profile parameters depending on the polymorphism of the A1166C I type gene receptor of the angiotensin II (AGTR1) as a predictor of arterial hypertension.

MATERIALS AND METHODS

86 patients (47 (55 %) women and 39 (45 %) men) with arterial hypertension, who were treated and examined in the therapeutic department of Koziv Central District Hospital were examined. Their age ranged from 45 to 76 years, with a mean age of (61.35 ± 13.30) years. The control group consisted of 30 people without signs of arterial hypertension. The criteria for inclusion in the study was the presence of arterial hypertension of 1-3 degrees. The diagnosis of hypertension was established in accordance with the orders of the Ministry of Health of Ukraine No. 54 and 436 and the Recommendations of the Ukrainian Association of Cardiologists on the prevention and treatment of hypertension on the basis of anamnestic data, complaints, physical and clinical examination data.

The study was conducted in accordance with the principles of bioethics, which are set out in the Declaration of Helsinki «Ethical Principles for Medical Research Involving Human Subjects», the Universal Declaration on Bioethics and Human Rights (UNESCO), and the Order of the Ministry of Health of Ukraine «On Approval of the Procedure for Conducting Clinical Trials of Medicines and Examination of Clinical Trial Materials and the Model Regulations on Ethics Commissions» No. 690 of 23.09.2009. Written informed consent for the study was obtained from all patients (Conclusion of the Biomedical Ethics Committee of the Ternopil National Medical University No. 69 dated 12.04.2022).

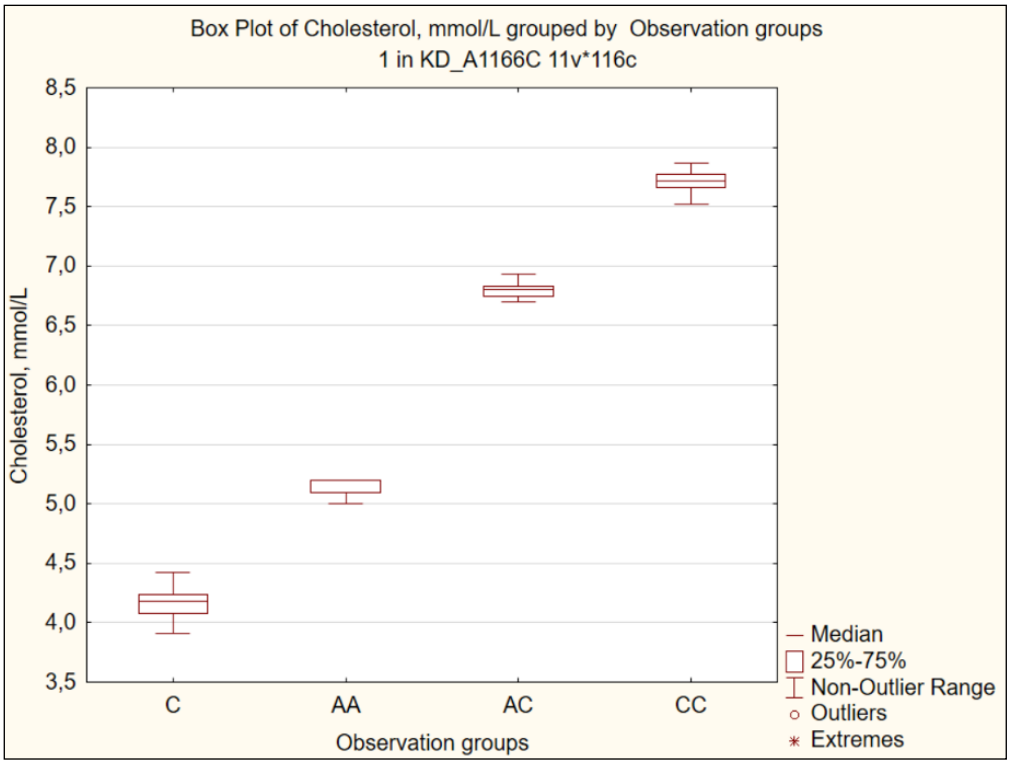

Fig. 1. Changes in general cholesterol level in patients with arterial hypertension depending on the polymorphism of the A1166C gene receptor of the of AA, AC and CC type carriers.

The study did not include patients with a history of myocardial infarction and stroke, secondary arterial hypertension, congenital or acquired heart disease, rhythm and conduction disorders, functional class III-IV heart failure by NYHA, chronic obstructive pulmonary disease, diabetes mellitus, chronic kidney disease, cancer, and mental illness. The clinical and anamnestic characteristics of the patients are shown in Table 1.

All patients underwent the following studies: measurement of body weight and height, office blood pressure, electrocardiography (ECG), lipid profile, and the polymorphism of the A1166C I type gene receptor of the angiotensin II was determined.

The lipid profile in the blood serum of the studied patients was measured in the laboratory of the Koziv Central District Hospital of the CEB. Concentrations of total cholesterol (TC), triglycerides (TG), low-density lipoprotein (LDL), very low-density lipoprotein (VLDL), and high-density lipoprotein (HDL) were determined using commercially available kits on a Biochem FC-200 analyzer (HTI, USA).

The allelic polymorphism of the A1166C I type gene receptor of the angiotensin II was studied by polymerase chain reaction with electrophoretic detection of the results using SNP-EXPRESS reagent kits (Litex Ltd.).

Statistical processing of the study materials was performed using biostatistical analysis methods implemented in the licensed software packages Microsoft Office 2010 Professional Plus (Microsoft Access 2010, Microsoft Excel 2010) - registration number 49521210; software product STATISTICA 6.1 (StatSoftInc., serial number AGAR909E415822FA).

The following basic statistical characteristics were calculated: number of observations (n), arithmetic mean (M), relative values (P), mean error of the mean (mM), mean error of the relative value (mr), standard deviation (SD), 95% confidence interval (95% CI); median (Me) with interquartile range (25% and 75% percentile) in case of asymmetric data distribution. These values are presented in the figures and text.

RESULTS

The state of lipid metabolism in patients with arterial hypertension depended on the A1166C polymorphism.

Analyzing the lipid status, we found the presence of pathological changes in lipid metabolism in all patients with AH, but in patients with the CC genotype compared with carriers of the AA genotype of the A1166C gene, lipid homeostasis disorders were more profound, as evidenced by a statistically significant increase in the levels of GCL, TG, VLDL, LDL. There was a tendency to a greater increase in all atherogenic blood fractions in the group of patients carrying the CC genotype compared with carriers of the AA genotype of the AGTR1 gene.

When analyzing the lipid profile of patients with arterial hypertension, higher cholesterol values were noted in all groups compared to controls.

All indicators were distributed according to a non-normal distribution law, so all their numerical values

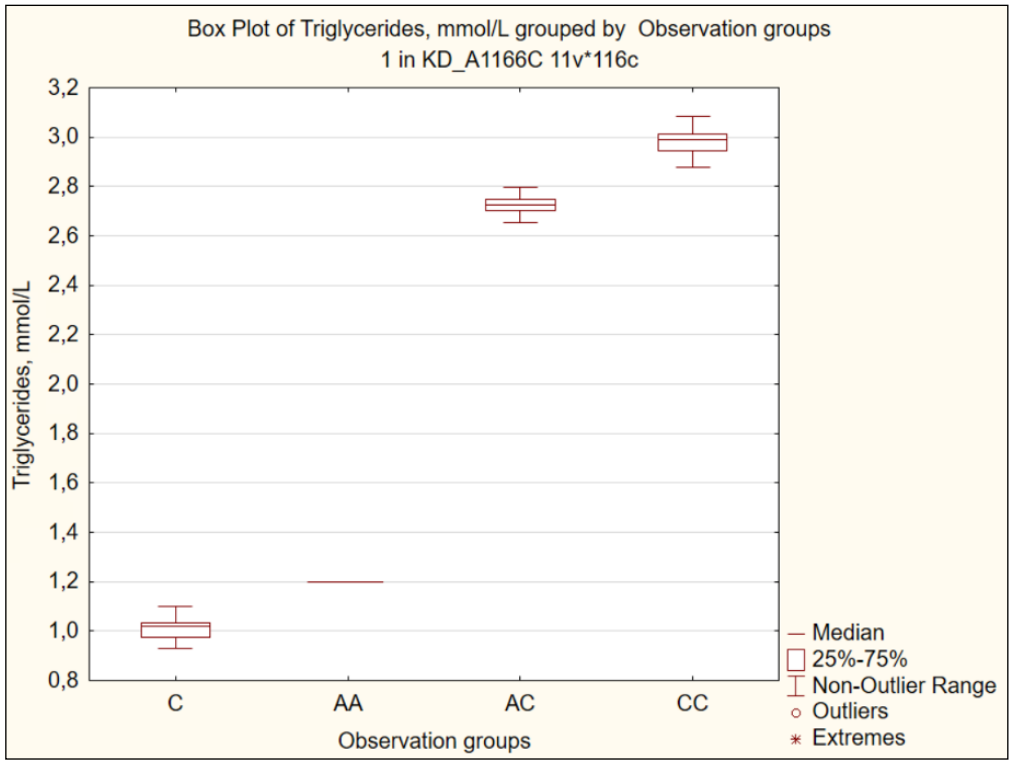

Fig. 2. Changes in triglycerol content in patients with hypertension depending on the polymorphism of the A1166C gene receptor of AA, AC and CC type carriers.

are presented in the form of medians and quartiles in the form of Me (IQR). Based on the results of the comparative analysis presented in Fig. 1, it can be concluded that a statistically significant difference for total cholesterol is observed when comparing the control group (C) (Me (IQR) 4.1 (4.1; 4.2)) and the groups of patients with arterial hypertension of AA carriers (Me (IQR) 5.1 (5.1; 5.2)), AC (Me (IQR) 6.8 (6.7; 6.8)) and CC genotype Me (IQR) 7.7 (7.7; 7.8)) of the A1166C gene, statistically significant differences were found with significance levels of $p<0.001$.

Our studies have shown that the level of general cholesterol in carriers of the homozygous AA genotype (n=18) is 1.23 times higher than in the control group (n=30). In patients with the AC genotype (n=38), the general cholesterol level was 1.68 times higher than in the control group. The most significant increase in the study index was recorded in patients with the CC genotype (n=30). In these patients, the level of general cholesterol was 2.14 times higher than in the control group.

Our next task was to analyze the value of triglycerols. TG had a similar trend to general cholesterol in the group of carriers of the CC genotype of the AGTR1 gene and was statistically significantly higher than in the group of carriers of the AA genotype.

According to the results of the comparative analysis shown in Fig. 2, it can be concluded that a statistically significant difference for triglycerols is observed when comparing the control group (C) (Me (IQR) 1.0 (0.9; 1.0)) and groups of patients with hypertension with AA (Me (IQR) 1.2 (0; 0)), AC (Me (IQR) 2.7 (2.7; 2.7)) and CC genotype Me (IQR) 3.0 (2.9; 3.0)) of the A1166C gene, statistically significant differences were found with significance levels of $p<0.001$.

According to the results of the comparative analysis shown in Fig. 3, it can be concluded that a statistically significant difference for LDL was observed when comparing the control group (C) (Me (IQR) 2.7 (2.6; 2.7)) and the groups of patients with hypertension of AA carriers (Me (IQR) 3.6 (0; 0)), AC (Me (IQR) 5.1 (5.1; 5.2)) and CC genotype Me (IQR) 5.4 (5.4; 5.5)) of the A1166C gene, statistically significant differences were found with significance levels of $p<0.001$.

The level of low-density lipoprotein (LDL) in patients with arterial hypertension with the CC genotype was 5.43 ± 0.03 mmol/L versus 3.66 ± 0.02 mmol/L in the group with AA genotype carriers.

We observed a similar trend in changes in VLDL content in patients with the CC genotype.

According to the results of the comparative analysis shown in Fig. 4, it can be concluded that a statistically significant difference for VLDL is observed when comparing the control group (C) (Me (IQR) 0.2 (0.2; 0.3)) and the groups of patients with hypertension of AA carriers (Me (IQR) 0.5 (0; 0)), AC (Me (IQR) 0.8 (0.8; 0.9)) and CC genotype Me (IQR) 1.7 (1.6; 1.8)) of the A1166C gene, statistically significant differences were found with significance levels of $p<0.001$.

Our studies have shown that the VLDL content in carriers of the homozygous AA genotype (n=18)

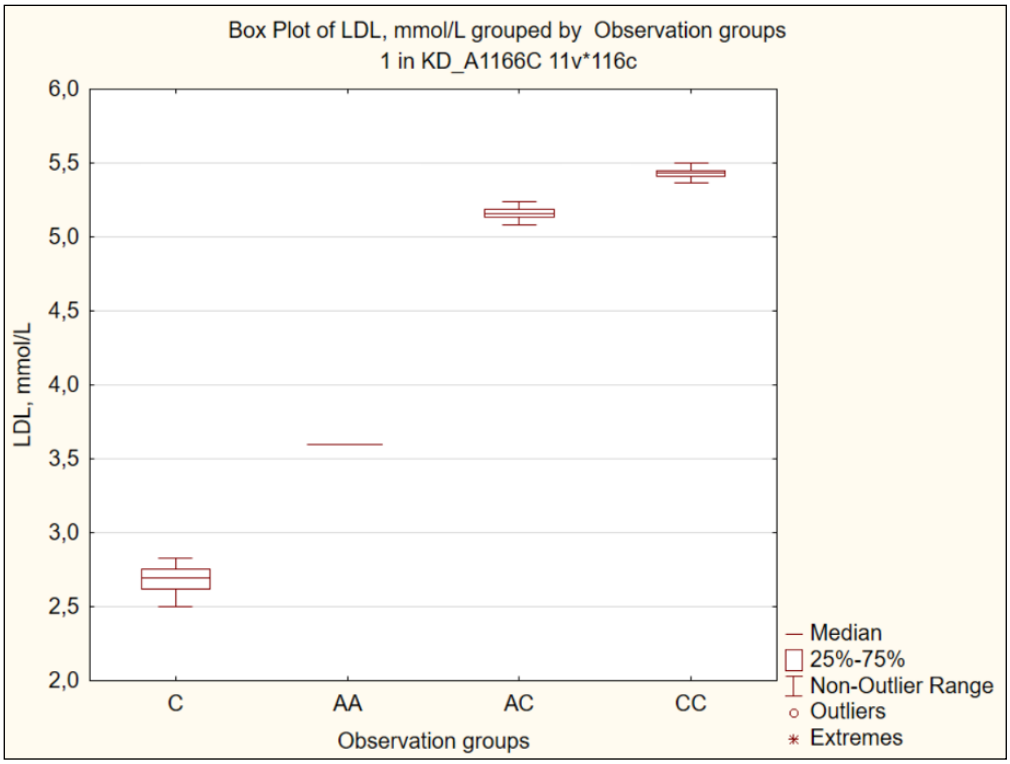

Fig. 3. Changes in low-density lipoprotein (LDL) content in patients with arterial hypertension depending on the polymorphism of the A1166C gene receptor of AA, AC and CC type carriers.

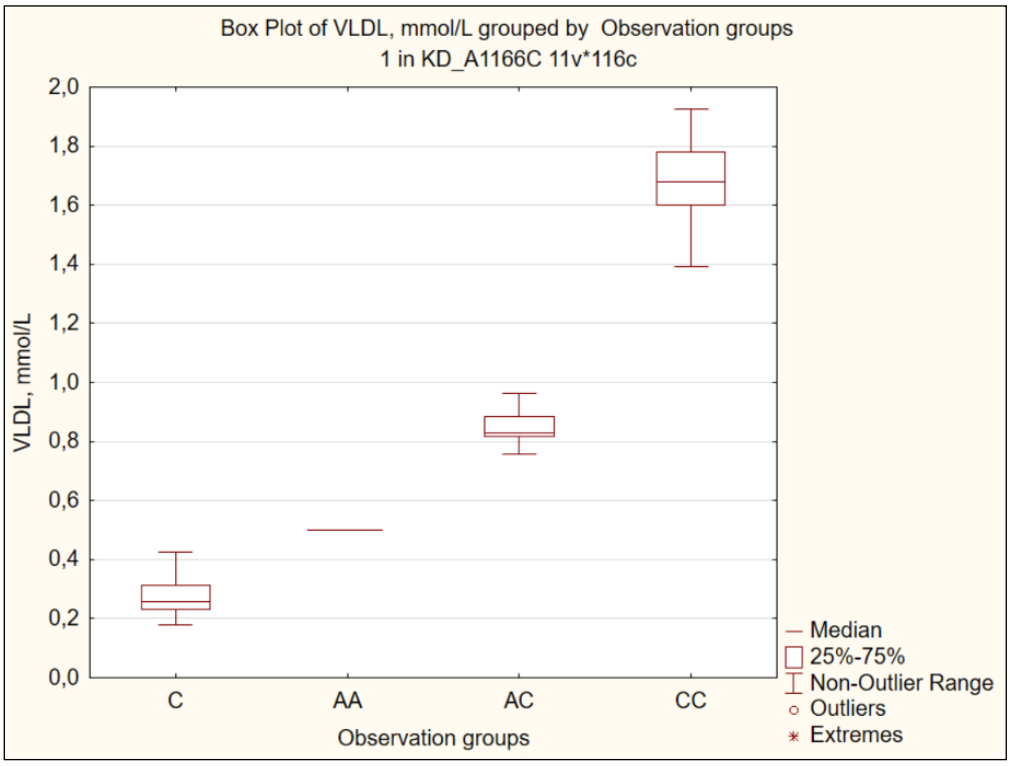

Fig. 4. Changes in the content of very low-density lipoprotein (VLDL) in patients with hypertension depending on the polymorphism of the A1166C gene receptor of AA, AC and CC type carriers.

differed from the patients of the control group and was 1.96 times higher. In patients with the AC genotype (n=38), the VLDL content was 3.14 times higher than in the control group (n=30). The most significant increase in the studied index was recorded in patients with the CC genotype (n=30). In these patients, VLDL content was 6.29 times higher than in the control group. A statistically significant increase in this indicator by 3.2 times in patients with CC genotype was observed relative to AA genotype carriers.

Regarding the level of HDL as an antiatherogenic factor, in the group of carriers of the CC genotype of the A1166C gene, this indicator was statistically significantly lower and amounted to 0.59 ± 0.12 mmol/l compared to the group with carriers of the AA genotype of 0.99 ± 0.03 mmol/l (Fig. 5). The decrease in HDL against the

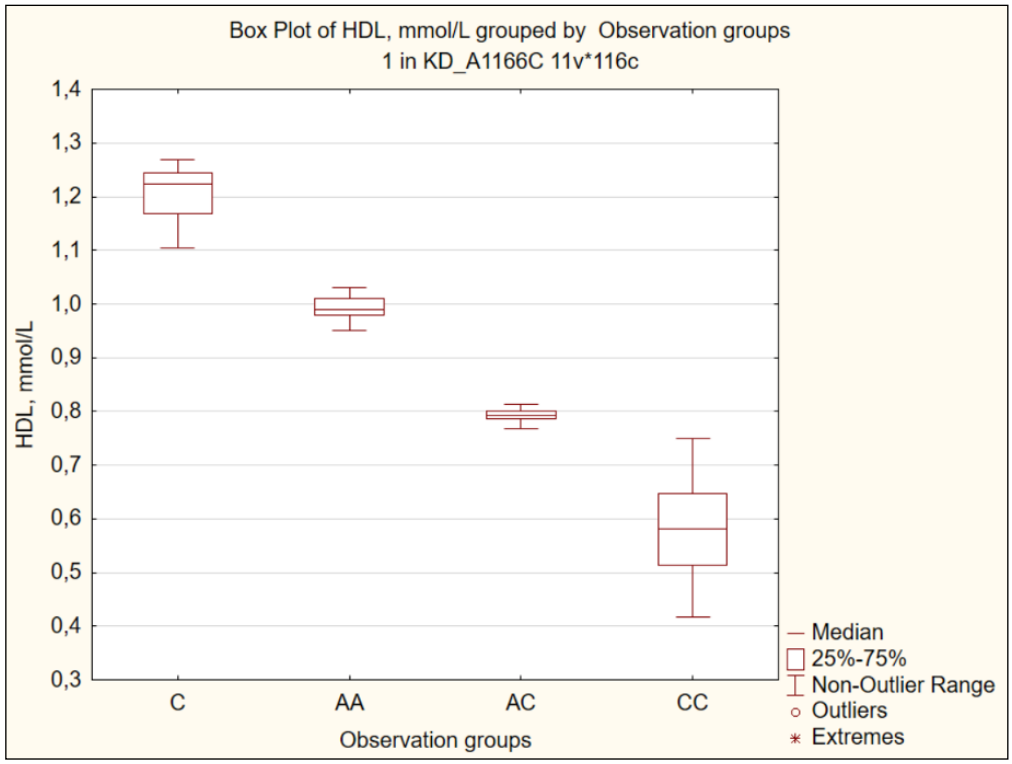

Fig. 5. Changes in the content of high-density lipoprotein (HDL) in patients with hypertension depending on the polymorphism of the A1166C gene receptor of AA, AC and CC type carriers.

background of increased LDL and VLDL in patients with arterial hypertension contributes to the formation of secondary IV type dyslipidemia according to the classification of D.S. Fredrickson [12].

According to the results of the comparative analysis presented in Fig. 5, it can be concluded that a statistically significant difference for HDL is observed when comparing the control group (C) (Me (IQR) 1.2 (1.1; 1.2)) and the groups of patients with hypertension with AA (Me (IQR) 0.9 (0.9; 1.0)), AC (Me (IQR) 0.7 (0.7; 0.8)) and CC genotype Me (IQR) 0.5 (0.5; 0.7)) of the A1166C gene, statistically significant differences were found with significance levels of $p<0.001$.

DISCUSSION

Many of the direct effects of angiotensin II (e.g., vasoconstriction) are realized through AGTR1. Stimulation of AGTR1 also activates membrane-binding H oxidase, which leads to the formation of reactive oxygen species. A number of authors describe that in almost all organ systems, activation of RAAS is associated with regeneration, remodeling, and tissue dysfunction, which are probably secondary to reactive oxygen species. All of this, when chronically activated, will contribute to inflammation, atherosclerosis, thrombosis and fibrogenesis in the vessels [13]. According to Lastra-Lastra G., the role of RAAS in the development of cardiovascular pathology is probably mediated by activation of I type receptor of angiotensin II and increased production of aldosterone, which is involved in the development of hypertension, endothelial dysfunction and fibrosis of cardiovascular tissue, remodeling, inflammation and oxidative stress [14, 15, 16].

Abdollahi M. (2007) described a new approach to the quantitative evaluation of transcriptional haplotypes of the AGTR1 gene [8]. According to his data, there were no significant differences in mRNA levels for rs5182: C > T alleles, but allele haplotypes and mRNA carrying A1166C showed a reduced widespreadness. The effect was much greater in CC homozygotes than in heterozygotes. It was also confirmed that the promoter region is located in a separate haplotype block from the 3'-region of AGTR1 containing rs5182: C > T and rs5186: A > C. The associations with metabolic syndrome symptoms were strongest for the 3'-block in general and for the C allele of rs5186: A > C allele, specifically [17]. All effects were expressed in homozygotes, possibly reproducing the mutual interaction through mRNA regulation feedback loops.

P. Palatini and colleagues (2009) studied the polymorphism of the A1166C gene AGTR1 for the frequency of arterial hypertension and metabolic syndrome in young patients with hypertension and found that this polymorphism is a predictor of hypertension and metabolic syndrome in the European population. Carriers of the C allele were more likely to develop resistant hypertension, and patients with the CC genotype had a 60 % increased risk compared with

patients with the AA genotype. At the beginning of the study, the authors noted higher fasting glucose levels, a significant increase in triglycerides, overweight, and other clinical signs of insulin resistance and hypertension in patients with the CC genotype. These results provide insight into the mechanisms that link obesity, arterial hypertension, and other features, and indicate that the polymorphism of the AGTR1 gene is involved in the pathogenesis of these clinical conditions. The authors propose to consider the polymorphism of the A1166C gene AGTR1 as a possible marker of the severity and development of arterial hypertension [18, 19]. Carriers of the C-allele also had an increased risk of MS, which is partly explained by a tendency to weight gain, but the occurrence of arterial hypertension was associated not only with the development of MS. The authors note that patients with the CC genotype at the beginning of the study had higher fasting glucose, significantly higher triglycerides, and were overweight. Their findings provide insight into the mechanisms linking obesity, hypertension, and MS, indicating that the polymorphism of the AGTR1 gene is involved in the pathogenesis of these conditions. It is likely that activation of RAAS in adipose tissue may be a link between obesity, AH and MS [20, 21]. The authors propose to consider the AGTR1 gene polymorphism (A1166C) as a possible marker of the severity and development of arterial hypertension. Our data match with those of these researchers. We have found a significant increase in all atherogenic lipid parameters (general cholesterol, trislycerides, LDL and VLDL) against the background of a decrease in HDL in patients with AH.

CONCLUSIONS

A statistically significant increase in all atherogenic lipid parameters of the lipidogram of patients with arterial hypertension and a worsening of dyslipidemia in carriers of the CC genotype compared with carriers of the AA genotype of the AGTR1 gene were found, which suggests that carriers of the CC genotype are predictors of dyslipidemia.

REFERENCES

1. Gintoni I, Adamopoulou M, Yapijakis C. The Angiotensin-converting Enzyme Insertion/Deletion Polymorphism as a Common Risk Factor for Major Pregnancy Complications. In Vivo. 2021;35(1):95-103. doi:10.21873/invivo.12236. DOI
2. Dziubanovskyi IY, Prodan AM, Pidruchna SR, Melnyk NA, Dzhyvak VG, Nikitina IM. Pathogenetic aspects of metabolic syndrome in experimental animals. Wiad Lek. 2022;75(2):514-519. doi: 10.36740/WLek202202134. DOI
3. Dungan JR, Conley YP, Langaee TY, et al. Altered beta-2 adrenergic receptor gene expression in human clinical hypertension. Biol Res Nurs. 2009;11(1):17-26. doi:10.1177/1099800409332538. DOI
4. Arendse LB, Danser AHJ, Poglitsch M, et al. Novel Therapeutic Approaches Targeting the Renin-Angiotensin System and Associated Peptides in Hypertension and Heart Failure. Pharmacol Rev. 2019;71(4):539-570. doi:10.1124/pr.118.017129. DOI
5. Chandra S, Narang R, Sreenivas V, Bhatia J, Saluja D, Srivastava K. Association of angiotensin II type 1 receptor (A1166C) gene polymorphism and its increased expression in essential hypertension: a case-control study. PLoS One. 2014;9(7):e101502. doi:10.1371/journal.pone.0101502. DOI
6. Castellano M, Glorioso N, Cusi D, et al. Genetic polymorphism of the renin-angiotensin-aldosterone system and arterial hypertension in the Italian population: the GENIPER Project. J Hypertens. 2003;21(10):1853-1860. doi:10.1097/00004872-200310000-00012. DOI
7. Shahid M, Rehman K, Akash MSH, et al. Genetic Polymorphism in Angiotensinogen and Its Association with Cardiometabolic Diseases. Metabolites. 2022;12(12):1291. doi:10.3390/metabo12121291. DOI
8. Abdollahi MR, Lewis RM, Gaunt TR, et al. Quantitated transcript haplotypes (QTH) of AGTR1, reduced abundance of mRNA haplotypes containing 1166C (rs5186:A>C), and relevance to metabolic syndrome traits. Hum Mutat. 2007;28(4):365-373. doi:10.1002/humu.20454. DOI
9. Aune D, Mahamat-Saleh Y, Kobeissi E, Feng T, Heath AK, Janszky I. Blood pressure, hypertension and the risk of atrial fibrillation: a systematic review and meta-analysis of cohort studies. Eur J Epidemiol. 2023;38(2):145-178. doi:10.1007/s10654-022-00914-0. DOI
10. Zeng Y, Jiang Y, Huang Z, Li K, Zhou Y. Association between AGTR1 (c.1166 A>C) Polymorphisms and Kidney Injury in Hypertension. Front Biosci (Landmark Ed). 2023;28(7):146. doi:10.31083/j.fbl2807146. DOI
11. Yaremchuk O, Posokhova K, Kuzmak I, Kulitska M, Klishch I, Korda M. Indexes of nitric oxide system in experimental antiphospholipid syndrome. Ukrainian Biochemical Journal. 2020;92(1):75-83. doi: 10.15407/ubj92.01.075. DOI
12. Sathiyakumar V, Pallazola VA, Park J, et al. Modern prevalence of the Fredrickson-Levy-Lees dyslipidemias: findings from the Very Large Database of Lipids and National Health and Nutrition Examination Survey. Arch Med Sci. 2019;16(6):1279-1287. doi:10.5114/aoms.2019.86964. DOI
13. Mehta PK, Griendling KK. Angiotensin II cell signaling: physiological and pathological effects in the cardiovascular system. Am J Physiol Cell Physiol. 2007;292(1):C82-C97. doi:10.1152/ajpcell.00287.2006. DOI
14. Lastra-Lastra G, Sowers JR, Restrepo-Erazo K, Manrique-Acevedo C, Lastra-González G. Role of aldosterone and angiotensin II in insulin resistance: an update. Clin Endocrinol (Oxf). 2009;71(1):1-6. doi:10.1111/j.1365-2265.2008.03498.x. DOI

15. Jiao K, Su P, Li Y. FGFR2 modulates the Akt/Nrf2/ARE signaling pathway to improve angiotensin II-induced hypertension-related endothelial dysfunction. Clin Exp Hypertens. 2023;45(1):2208777. doi:10.1080/10641963.2023.2208777. DOI
16. Underwood PC, Adler GK. The renin angiotensin aldosterone system and insulin resistance in humans. Curr Hypertens Rep. 2013;15(1):59-70. doi:10.1007/s11906-012-0323-2. DOI
17. Herrera CL, Castillo W, Estrada P, et al. Association of polymorphisms within the Renin-Angiotensin System with metabolic syndrome in a cohort of Chilean subjects. Arch Endocrinol Metab. 2016;60(3):190-198. doi:10.1590/2359-3997000000134. DOI
18. Palatini P, Ceolotto G, Dorigatti F, et al. Angiotensin II type 1 receptor gene polymorphism predicts development of hypertension and metabolic syndrome. Am J Hypertens. 2009;22(2):208-214. doi:10.1038/ajh.2008.319. DOI
19. Ceolotto G, Papparella I, Bortoluzzi A, et al. Interplay between miR-155, AT1R A1166C polymorphism, and AT1R expression in young untreated hypertensives. Am J Hypertens. 2011;24(2):241-246. doi:10.1038/ajh.2010.211. DOI
20. Kozak K, Pavlyshyn H, Kamyshnyi O, Shevchuk O, Korda M, Vari SG. The Relationship between COVID-19 Severity in Children and Immunoregulatory Gene Polymorphism. Viruses. 2023;15(10):2093. doi:10.3390/v15102093. DOI
21. Pidruchna SR, Benedyct VV, Piatnochka VI, Melnyk NA, Mykhailivna Zakharchuk U. Changes of pro- and antioxidant indicators in experimental animals under acute small bowel obstructions. J Med Life. 2021;14(1):32-36. doi:10.25122/jml-2020-0066. DOI

CONFLICT OF INTEREST

The Authors declare no conflict of interest

CORRESPONDING AUTHOR

Volodymyr H. Dzhyvak
I. Horbachevsky Ternopil National Medical University
1 Voli Square, 46001 Ternopil, Ukraine
e-mail: djyvak@tdmu.edu.ua

ORCID AND CONTRIBUTIONSHIP

Volodymyr V. Shmanko: 0000-0003-1128-200X A E F
Svitlana R. Pidruchna: 0000-0002-5607-5680 A B D F
Roman V. Hnizdyukh: 0000-0003-2833-0661 A B D
Alla E. Mudra: 0000-0003-3219-931X B E
Uliana M. Zakharchuk: 0000-0003-4346-0974 B C
Iryna P. Kuzmak: 0000-0002-5035-8815 C
Tetiana Y. Yaroshenko: 0000-0001-8434-3446 C
Lylya M. Palytsya: 0000-0003-0794-0911 E
Iryna A. Bandas: 0000-0002-3451-3192 B
Volodymyr H. Dzhyvak: 0000-0002-4885-7586 B D
Iryna M. Nikitina: 0000- 0001-6595-2502 F
Iryna F. Zavarynska: 0000-0002-1343-3505 C

A – Work concept and design, B – Data collection and analysis, C – Responsibility for statistical analysis, D – Writing the article, E – Critical review, F – Final approval of the article

RECEIVED: 11.03.2024
ACCEPTED: 18.07.2024

ORIGINAL ARTICLE

CONTENTS

Prognostic factors for low- and high grade squamous intraepithelial lesions in histological preparations following LLETZ procedure

Yonka Ivanova[1], Yavor Kornovski[1], Stoyan Kostov[1,2], Stanislav Slavchev[1], Dimitar Metodiev[3,4], Angel Yordanov[5]

[1]DEPARTMENT OF GYNECOLOGY, HOSPITAL "SAINT ANNA", MEDICAL UNIVERSITY "PROF. DR. PARASKEV STOYANOV", VARNA, BULGARIA
[2]RESEARCH INSTITUTE, MEDICAL UNIVERSITY PLEVEN, PLEVEN, BULGARIA
[3]CLINICAL PATHOLOGY LABORATORY, MHAT "NADEZDA" WOMEN'S HEALTH HOSPITAL, SOFIA, BULGARIA
[4]NEUROPATHOLOGICAL LABORATORY, UNIVERSITY HOSPITAL "SAINT IVAN RILSKI", SOFIA, BULGARIA
[5]DEPARTMENT OF GYNECOLOGIC ONCOLOGY, MEDICAL UNIVERSITY PLEVEN, PLEVEN, BULGARIA

ABSTRACT

Aim: To investigate the influence of the following prognostic factors: age, parity, hormonal status (premenopausal, postmenopausal), histological result from targeted biopsy (LSIL, HSIL), adequacy of colposcopic examination (satisfactory, unsatisfactory colposcopy), type of TZ (type 1, 2, 3), type of cervical lesions (type 1, 2, 3), the colposcopic impression (diagnosis) of the cervical lesion (LSIL, HSIL/Ca colli uteri in situ), lesion size (up to 1/3; up to 2/3; more than 2/3 of the cervical circumference) for the occurrence of LSIL and HSIL/Ca colli uteri in situ in the final histological result after LLETZ procedure.

Materials and Methods: This is a prospective study (01.01.2017 – 31.07. 2021) including 189 patients with cervical precancerous lesions received LLETZ treatment One gynaecologic oncologist performed video colposcopy, targeted biopsy, and LLETZ. One histopathologist diagnosed histological specimens from the biopsy and LLETZ procedure

Results: We found a statistically significant correlation between the histological result of the targeted biopsy factor and the colposcopic diagnosis factor concerning the final histological result of LLETZ. The cervical lesion size factor and cervical lesion type factor have prognostic significance for the histological outcome following LLETZ.

Conclusions: The histological result of targeted biopsy and colposcopic diagnosis are significant factors for the final histological result after LLETZ. Cervical lesion invasion into the endocervical canal is a prognostic factor for HSIL, and its invisible borders – for carcinoma (in situ or microinvasive/invasive). Lesion size up to 1/3 of the cervix is a prognostic factor for LSIL and large lesions (2/3 of the cervix) – for HSIL and cervical cancer (in situ, microinvasive/invasive).

KEY WORDS: prognostic factors, HSIL, LSIL, LLETZ

Wiad Lek. 2024;77(8):1562-1568. doi: 10.36740/WLek202408105 DOI

INTRODUCTION

Ablative and excisional treatment represent the two forms of outpatient surgical treatment of low- and high grade squamous intraepithelial lesion (LSIL, HSIL). LSIL covers the condition previously known as cervical intraepithelial neoplasia grades 1 (CIN 1) and HSIL covers the conditions known as cervical intraepithelial neoplasia grades 2 and 3 (CIN 2 and CIN 3)

While ablative methods destroy the affected cervical tissue, excisional methods remove the affected tissue and provide preparation for histological examination [1]. Ablative methods include cryotherapy, laser ablation, electrocoagulation and cold coagulation [2 – 12].

Excisional methods include scalpel conization, electroconization (loop electrosurgical conization), electrosurgical excision procedures - loop electrosurgical excision procedure or large loop excision of the transformation zone (LEEP or LLETZ), laser conization and electrosurgical needle conization. LEEP uses wire loop electrodes and electrosurgical cylindrical excision with long-armed loop electrodes to remove cells and tissue) and this is the most common technique for outpatient treatment of LSIL and HSIL [13 – 18].

The most common excisional methods are laser cone biopsy and LLETZ. Excisional techniques offer the following advantages: they provide histological material for pathological evaluation and determine the extent of the disease; in many cases, they are not only a diagnostic method but curative, and are performed with local analgesia. LLETZ has become the standard-of-care for cervical premalignant lesions in many clinics. Because it preserves the reproductive function of the cervix, it

Table 1. The characteristics of patients included in the study

Patients' characteristics	N	%
Total	189	100.0
Age groups		
20-29	35	18.5
30-39	85	45
40-49	60	31.7
50-59	8	4.2
60-69	1	0.5
Parity		
Nulliparous	45	23.8
Parous	144	76.2
Menstrual status		
Menstrual	177	93.7
Menopausal	12	6.3
Adequacy of colposcopy		
Satisfactory	69	36.5
Unsatisfactory Type of TZ	120	63.5
Type 1 Type 2 Type 3	7 37 145	3.7 19.6 76.7
Colposcopic diagnosis		
LSIL	47	24.9
HSIL	142	75.1
Cervical lesion size	41	7.9
Up to 1/3 To 2/3 Up to 2/3	147 38 4	77.8 20.1 2.1
Histological result of the biopsy		
LSIL	57	30.2
HSIL	117	61.9
Not performed	15	7.9

is suitable for patients who wish to retain fertility [19]. One drawback of LLETZ is the potential for thermal damage to the resection lines. This occurs due to the simultaneous use of coagulation and cutting modes during LLETZ.

In some cases, this can result in uncertainty for the histopathologist regarding the resection-line involvement in the dysplastic process. Both ablative and excisional methods are similarly effective – approximately 90% elimination of CIN lesions and reducing the risk of future invasive cervical cancer [1]. The choice of ablation versus excision is based on many factors, such as the severity of the disease, visibility of the squamocolumnar junction (SCJ), lesion size, and gland involvement. Excisional treatment is recommended when a glandular or invasive squamous lesion is suspected or when the patient does not meet the criteria for ablative therapy. Indications for excisional therapy are: suspected microinvasion, unsatisfactory colposcopy (the transformation zone is not fully visualized), lesion extending into the endocervical canal (including LSIL), endocervical curettage showing CIN or glandular atypia, lack of correlation between cytology, colposcopy, and biopsy, suspected adenocarcinoma in situ, recurrence after an ablative or previous excisional procedure.

A correlation is not always present between the histological findings from the targeted biopsy and that in the LLETZ preparation, nor between the colposcopic impression and the final histological result.

AIM

To investigate the influence of the following prognostic factors: age, parity, hormonal status (premenopausal, postmenopausal), histological result from targeted biopsy (LSIL, HSIL), adequacy of colposcopic examination (satisfactory, unsatisfactory colposcopy), type of TZ (type 1, 2, 3), type of cervical lesions (type 1, 2, 3), the colposcopic impression (diagnosis) of the cervical lesion (LSIL, HSIL/Ca colli uteri in situ), lesion size (up to 1/3; up to 2/3; more than 2/3 of the cervical circumference) for the occurrence of LSIL and HSIL/Ca colli uteri in situ in the final histological result after LLETZ procedure.

MATERIALS AND METHODS

STUDY POPULATION

This is a prospective study (01.01.2017 – 31.07. 2021) including 189 patients with cervical precancerous lesions received LLETZ treatment at Prof. Yavor Kornovski Medical Centre in an outpatient setting.

The indications for the LLETZ procedure are: histologically proven by targeted biopsy under video colposcopic control HSIL and LSIL, which colposcopically enters the cervical canal and its distal border is not visualized. The clinicopathological features of the patients are shown in Table 1.

The mean age of the patients is 37.06 ± 8.12 years ranging between 21 and 66.

METHODOLOGY

VIDEOCOLPOSCOPY

It was performed on all patients by one specialist with additional qualification in colposcopy. An Alyn Welch device was used until Feb. 10th, 2020, and then a Leisegang video colposcope with original software and monitor, model 2020. The examination was per-

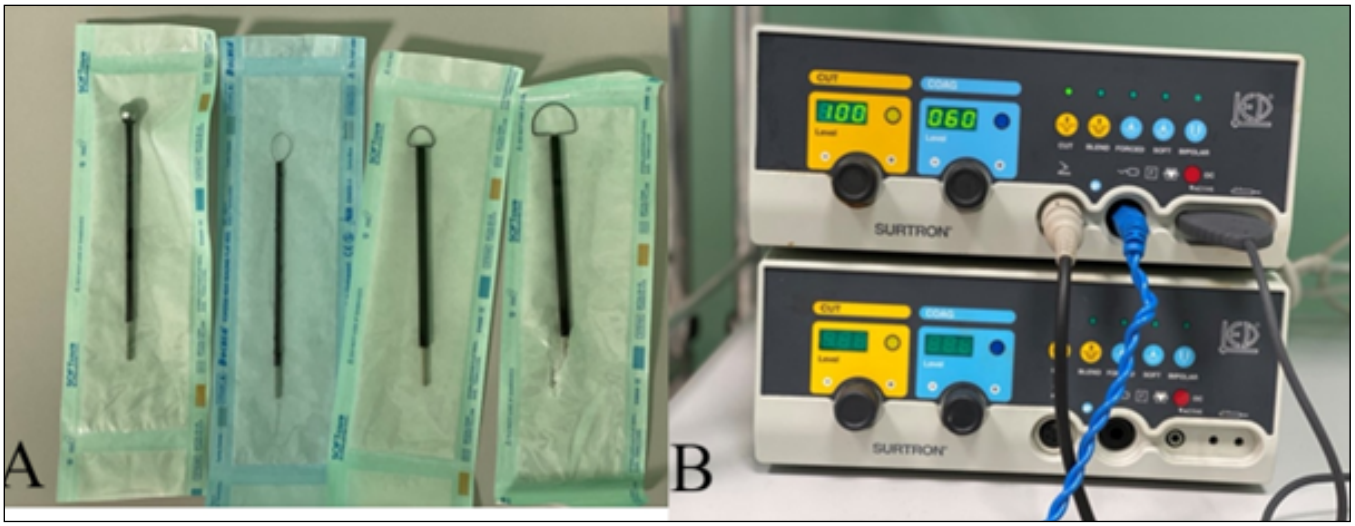

Fig. 1. A) Types of loop and ball electrodes for coagulation; B) Electrosurgical apparatus for cutting and coagulation.

formed after treatment of the cervix with 5% acetic acid solution, prepared every 2 days, and Lugol's solution, replaced every month. The colposcopic examination of each patient was saved, documented, and archived in the medical centre's patient database.

The colposcopic examination provides information on: adequacy (colposcopy is satisfactory and unsatisfactory); type of TZ; type of cervical lesion (its location relative to the exo- and endocervix); colposcopic diagnosis and cervical lesion size.

- Colposcopy is satisfactory if the junction between the squamous epithelium and the columnar epithelium (a line called the SCJ) is fully visible, and unsatisfactory if SCJ is partially visible or invisible;
- Type of TZ (the SCJ is on the ectocervix – type 1; the SCJ is in the cervical canal but visible – type 2; and the SCJ is in the cervical canal and invisible – type 3);
- Type of cervical lesion – located entirely on the ectocervix – type 1; the distal end of the lesion is on the endocervix but is visible – type 2; the distal end of the lesion is invisible – type 3;
- Colposcopic diagnosis (colposcopic impression) – LSIL/grade 1 colposcopic findings; HSIL/grade 2 colposcopic findings;
- Lesion size relative to its involvement of the cervical circumference – up to 1/3; up to 2/3; over 2/3.

HISTOLOGICAL EXAMINATION

Histological examination of previously taken biopsy

A biopsy is taken with biopsy forceps from the most affected area without anaesthesia under video colposcopic control. It is performed by the same gynaecologic oncologist who performed the colposcopies. Bleeding is controlled by gauze-based pressure, with a pack soaked in Monsel's solution, by surgical insertion and, as a last resort, by tamponade with a sterile roll gauze for several hours or one day. The histological preparation is placed in a 10% formalin solution.The histological result is reported as LSIL and HSIL.

Histological examination of the specimen after LLETZ procedure

Performed by the same highly qualified pathologist who examined the biopsy material.

LLETZ PROCEDURE

The procedure was performed by the same gynaecologic oncologist who performed the biopsy under local infiltration anaesthesia with lidocaine. SURTRON electrosurgical apparatus was used (cutting mode: cutting – 100W, and coagulation – 60W; coagulation mode – SOFT 100W 60W), and smoke evacuation apparatus (Fig.1).

STATISTICAL METHODS

Data were entered and processed with IBM SPSS Statistics 25.0. and MedCalc Version 19.6.3 statistical package. The level of significance for rejecting the null hypothesis was established as $p < 0.05$.

RESULTS

The histological results after the LLETZ procedure are: LSIL in 60 patients (31.75%); HSIL in 108 (57.14%); In situ cervical cancer in 14 (7.41%); microinvasive cervical cancer in 7(3.7%).

The correlation between patients' age and the histological outcome after LLETZ procedure is shown in Table 2.

The results presented in this table demonstrate no significant correlation between age and histological

Table 2. Analysis of the correlation between patient's age and the histological outcome after LLETZ (ANOVA, df = 2, F = 0.618, p = 0.540)

Histological result after LLETZ procedure	Age (years)		
	n	X^-	SD
LSIL	60	37.65	8.09
HSIL	108	36.25	8.07
In situ cervical cancer	14	37.21	6.34
Microinvasive cervical cancer*	7	44.29	9.98

* The category was not included in the analysis due to a lack of statistical representativeness.

Table 3. Analysis of the correlation between the histological results after LLETZ and the indicators parity, hormonal status, histological result from targeted biopsy, adequacy of the colposcopic examination and colposcopic diagnosis

Indicators	Frequency	Histological result after LLETZ procedure				P					
		1. LSIL	2. HSIL	3. In situ cervical cancer	4. Microinvasive cervical cancer	1-2	1-3	1-4	2-3	2-4	3-4
Parity											
Parous	n	49	76	13	6	0.155					
	%	81.7	70.4	92.9	85.7						
Non-parous	n	11	32	1	1						
	%	18.3	29.6	7.1	14.3						
Hormonal status											
Perimenopause	n	57	100	14	6	0.471					
	%	95.0	92.6	100.0	85.7						
Postmenopause	n	3	8	0	1						
	%	5.0	7.4	0.0	14.3						
Histological result from targeted biopsy											
LSIL	n	46	11	0	0	< 0.001	< 0.001	< 0.001	0.357	1.000	-
	%	82.1 a	11.1 b	0.0 c	0.0 c						
HSIL	n	10	88	13	6						
	%	17.9 a	88.9 b	100.0 c	100.0 c						
Adequacy of colposcopic examination											
Satisfactory	n	42	65	9	4	0.611					
	%	70.0	60.2	64.3	57.1						
Unsatisfactory	n	18	43	5	3						
	%	30.0	39.8	35.7	42.9						
Colposcopic diagnosis											
LSIL	n	43	4	0	0	< 0.001	< 0.001	< 0.001	1.000	1.000	-
	%	71.7 a	3.7 b	0.0 c	0.0 c						
HSIL	n	17	104	14	7						
	%	28.3 a	96.3 b	100.0 c	100.0 c						

The same letters in the horizontal lines indicate the absence of a significant difference, and the different ones – the presence of a significant difference ($p < 0.05$).

outcome after LLETZ. The group with microinvasive cervical cancer did not participate in the analysis due to the lack of statistical representativeness.

Table 3 examines the influence of the following factors: parity, hormonal status, histological biopsy result, adequacy of colposcopic examination, and colposcopic diagnosis (impression) on the final histological result after LLETZ procedure.

We found a statistically significant correlation between the factors targeted biopsy histological results and colposcopic diagnosis on the final histological result of LLETZ. We did not find a statistically significant correlation with the

Table 4. Analysis of the relationship between the histological result after LLETZ and the parameters of the ZT (zone of transformation) types, cervical lesion type and lesion size

Indicators	Frequency	Histological result after LLETZ procedure				P					
		1. LSIL	2. HSIL	3. In situ cervical cancer	4. Microinvasive cervical cancer	1 - 2	1 - 3	1 - 4	2 - 3	2 - 4	3 - 4
Zone of transformation (ZT)											
Type 1	n	42	65	9	4						
	%	70.0	60.2	64.3	57.1						
Type 2	n	4	20	2	1			0.486			
	%	6.7	18.5	14.3	14.3						
Type 3	n	14	23	3	2						
	%	23.3	21.3	21.4	28.6						
Type of cervical lesion											
Type 1	n	0	6	1	0	0.063	0.039	-	0.822	0.522	0.481
	%	0.0 a	5.6 ac	7.1 bc	0.0 ac						
Type 2	n	0	35	1	1	< 0.001	0.039	0.003	0.052	0.319	0.605
	%	0.0 a	32.4 b	7.1 b	14.3 b						
Type 3	n	60	67	12	6	< 0.001	0.003	0.003	0.082	0.209	1.000
	%	100.0 a	62.0 b	85.7 b	85.7 b						
Lesion size											
Up to 1/3	n	54	82	9	2	0.445	0.016	< 0.001	0.350	0.006	0.132
	%	90.0 a	75.9 ac	64.3 bcd	28.6 bd						
2/3	n	5	24	5	4	0.023	0.007	< 0.001	0.266	0.038	0.362
	%	8.3 a	22.2 b	35.7 bd	57.1 cd						
Over 2/3	n	1	2	0	1	0.926	0.626	0.067	0.604	0.049	0.157
	%	1.7 ac	1.9 a	0.0 ac	14.3 bc						

The same letters in the horizontal lines indicate the absence of a significant difference, and the different ones - the presence of a significant difference ($p < 0.05$).

histological outcome after LLETZ procedure for the other three indicators: parity, hormonal status and adequacy of colposcopic examination.

Table 4 shows the correlation between the histological outcome after LLETZ procedure and indicators such as transformation zone type, cervical lesion type and lesion size.

Data in Table 4 show that the cervical lesion size and cervical lesion type indicators have prognostic significance for the histological outcome after LLETZ.

DISCUSSION

Age is an essential factor contributing to the occurrence of high-grade precancerous changes in the cervix. The risk of their occurrence increases 4.5 and 11 times after the age of 30 and 50 years, respectively [20]. Chen et al. found increased risk in patients older than 45 years [21]. Conversely, some publications point out that age younger than 35 is associated with a higher risk for high-grade lesions [22].

Menopause as a factor influences the occurrence of colposcopic and cytological changes in the cervix. In menopause, as a result of estrogen deficiency, the SCJshifts into the cervical canal, making colposcopic examination often unsatisfactory [23]. In addition, chronic inflammation, reactive atypia, and atrophy occur, which may mask severe precancerous changes and even microinvasive carcinoma. In menopausal patients, cytology can also be misleading. Atrophic vaginal mucosa is dominated by basal and parabasal cells that have an altered nuclear-cytoplasmic index, leading to false-positive Pap test results. In these cases, it is appropriate to test for high-risk human papilloma virus(HPV) strains as well before deciding on excisional biopsy (LLETZ). Moore et al. found that 30% of their study patients over 50 years had unsatisfactory colposcopy, and 50% showed a discrepancy between cytology and colposcopic diagnosis. The authors recommended LLETZ without a correlation between cytology and colposcopy-guided biopsy [24].

Childbirth as a factor in the occurrence of cervical precancerous lesions is also of interest. The causes are found in changes in the SCJ after vaginal delivery. In nulliparous women and those who delivered by caesarean section, the cervix and cervical canal were not subjected to trauma, respectively, to a change in this junction. In a study of HIV-positive patients, it was suggested that nulliparous women had a higher risk of developing CIN [25].

We conventionally divide cervical lesions into 3 types: type 1 – located on the exocervix, fully visible; type 2 – intruding into the cervical canal (endocervix) but with visible borders; type 3 – entering into the cervical canal, with invisible borders. Table 3 shows that HSIL was found in type 2 cervical lesions in 35/37 cases (95%). Therefore, the involvement of the endocervix/endocervical glands is a prognostic marker for a high-grade lesion.

In cervical type 3 lesions, 18/21(86%) cases of carcinomas (in situ, microinvasive/invasive) were diagnosed. In these cases, the LLETZ procedure was performed mainly for diagnostic purposes – detecting invasion or microinvasion. This is often necessary because of atrophy in menopause or due to a process developing in the endocervical canal. Then, there is a discrepancy between the colposcopic findings and cytology, which is one of the indications for an excisional procedure.

Table 3 demonstrates that the size of the precancerous area has a prognostic significance for the histological outcome after LLETZ. Low-grade lesions are more common in small cervical lesions (up to 1/3 of cervical size), with 54/60 (90%) of LSILs being less than 1/3 of the cervical size. On the other hand, cervical lesions occupying 2/3 of the cervix were found to be HSIL, in situ cervical cancer, and microinasive/invasive cervical cancer in 33/38 (87%). The association between cervical lesion size (more than 2/3 of the cervical circumference) and HSIL histological score has been established by other researchers as well.

CONCLUSIONS

Histological results of targeted biopsy and colposcopic diagnosis are significant indicators for the final histological results after LLETZ. Cervical lesion invasion into the endocervical canal is a prognostic factor for HSIL and its invisible borders – for carcinoma (in situ or microinvasive/invasive). Lesion size up to 1/3 of the cervix is a prognostic factor for LSIL and large lesions (2/3 of the cervix) – for HSIL and cetrvical cancer (in situ, microinvasive/invasive).

REFERENCES

1. Martin-Hirsch PP, Paraskevaidis E, Bryant A, Dickinson HO. Surgery for cervical intraepithelial neoplasia. Cochrane Database Syst Rev. 2013;2013(12):CD001318. doi: 10.1002/14651858.CD001318.pub3. DOI
2. Basu P, Taghavi K, Hu SY et al. Management of cervical premalignant lesions. Curr Probl Cancer. 2018;42(2):129-136. doi: 10.1016/j.currproblcancer.2018.01.010. DOI
3. Nazari Z, Torabizadeh G, Khalilian A et al. Is cryotherapy effective in all women with low-grade cervical intraepithelial neoplasia? Eur Rev Med Pharmacol Sci. 2021;25(12):4211-4218. doi: 10.26355/eurrev_202106_26126. DOI
4. Wojciech R. The importance of cryosurgery in gynecological practice. Ginekol Pol. 2011;82(8):618-22.
5. Santesso N, Mustafa RA, Wiercioch W et al. Systematic reviews and meta-analyses of benefits and harms of cryotherapy, LEEP, and cold knife conization to treat cervical intraepithelial neoplasia. Int J Gynaecol Obstet. 2016;132(3):266-71.
6. Hurtado-Roca Y, Becerra-Chauca N, Malca M. Efficacy and safety of cryotherapy, cold cone or thermocoagulation compared to LEEP as a therapy for cervical intraepithelial neoplasia: Systematic review.Rev Saude Publica. 2020;54:27. doi: 10.11606/s1518-8787.2020054001750. DOI
7. Singh A, Arthur B, Agarwal V.J LEEP Verses Cryotherapy in CIN. Obstet Gynaecol India. 2011;61(4):431-5.
8. Navarro Santana B, Sanz Baro R, Orozco R, Plaza Arranz J. Cervical vaporization in LSIL and persistent HPV infection. Taiwan J Obstet Gynecol. 2018;57(4):475-478. doi: 10.1016/j.tjog.2018.06.010. DOI
9. Chen F, Gan Y, Wang HW. Investigation of the efficiency and stability of a novel visualized lattice CO2 laser-based gynecological therapeutic apparatus for the treatment of cervical diseases in rhesus monkeys. Lasers Med Sci. 2022;37(5):2413-2420. doi: 10.1007/s10103-021-03499-4. DOI
10. Shimada C, Todo Y, Yamazaki H et al. Cervical laser vaporization for women with cervical intraepithelial neoplasia-3. Jpn J Clin Oncol. 2019;49(5):447-451. doi: 10.1093/jjco/hyz001. DOI
11. Dolman L, Sauvaget C, Muwonge R et al. Meta-analysis of the efficacy of cold coagulation as a treatment method for cervical intraepithelial neoplasia: a systematic review. BJOG. 2014;121(8):929-42. doi: 10.1111/1471-0528.12655. DOI
12. Chanen W. Electrocoagulation diathermy. Baillieres Clin Obstet Gynaecol. 1995;9(1):157-72.
13. Wright TC, Massad S, Dunton CJ et al. 2006 consensus guidelines for the management of women with cervical intraepithelial neoplasia or adenocarsinoma in situ. American Journal of Obstetrics and Gynecology. 2007;197(4):340-345. doi: 10.1016/j.ajog.2007.07.050. DOI

14. Cooper DB, Carugno J, Dunton CJ et al. Cold Knife Conization of the Cervix. In: StatPearls. Treasure Island (FL): StatPearls Publishing; 2023.
15. Jiang Y, Chen C, Li L. Comparison of Cold-Knife Conization versus Loop Electrosurgical Excision for Cervical Adenocarcinoma In Situ (ACIS): A Systematic Review and Meta-Analysis. PLoS One. 2017;12(1):e0170587. doi: 10.1371/journal.pone.0170587. DOI
16. Jiang YM, Chen CX, Li L. Meta-analysis of cold-knife conization versus loop electrosurgical excision procedure for cervical intraepithelial neoplasia. Onco Targets Ther. 2016 29;9:3907-15. doi: 10.2147/OTT.S108832. DOI
17. El-Nashar SA, Shazly SA, Hopkins MR et al. Loop Electrosurgical Excision Procedure Instead of Cold-Knife Conization for Cervical Intraepithelial Neoplasia in Women With Unsatisfactory Colposcopic Examinations: A Systematic Review and Meta-Analysis. J Low Genit Tract Dis. 2017;21(2):129-136. doi: 10.1097/LGT.0000000000000287. DOI
18. Gao S, Huang L, Wang T et al. The Effect of Cervical Cold-Knife Conization (CKC) on HPV Infection in Patients with High-Grade Cervical Intraepithelial Neoplasia: A Retrospective Study. Int J Womens Health. 2023;15:1681-1691. doi: 10.2147/IJWH.S429749. DOI
19. Köse FM, Naki MM. Cervical premalignant lesions and their management. J Turk Ger Gynecol Assoc. 2014;15(2):109-21. doi: 10.5152/jtgga.2014.29795. DOI
20. Costa S, Nuzzo MD, Rubino A et al. Independent determinants of inaccuracy of colposcopically directed punch biopsy of the cervix. Gynecol Oncol. 2003;90:57–63. doi: 10.1016/s0090-8258(03)00202-6. DOI
21. Chen RJ, Chang DY, Yen ML et al. Independent clinical factors which correlate with failures in diagnosing early cervical cancer. Gynecol Oncol. 1995;58:356–361. doi: 10.1006/gyno.1995.1242. DOI
22. Kobelin MH, Kobelin CG, Burke L et al. Incidence and predictors of cervical dysplasia in patients with minimally abnormal Papanicolaou smears. Obstet Gynecol. 1998;92:356–359. doi: 10.1016/s0029-7844(98)00234-8. DOI
23. Wetrich DW. An analysis of the factors involved in the colposcopic evaluation of 2194 patients with abnormal Papanicolaou smears. Am J Obstet Gynecol. 1986;154:1339–1349. doi: 10.1016/0002-9378(86)90722-2. DOI
24. Moore KN, Bannon RJ, Lanneau GS et al. Cervical dysplasia among women over 35 years of age. Am J Obstet Gynecol. 2008;199:471.e1–471.e5. doi: 10.1016/j.ajog.2008.03.048. DOI
25. Lehtovirta P, Paavonen J, Heikinheimo O. Risk factors, diagnosis and prognosis of cervical intraepithelial neoplasia among HIV-infected women. Int J STD AIDS. 2008;19:37–41. doi: 10.1258/ijsa.2007.005672. DOI

CONFLICT OF INTEREST

The Authors declare no conflict of interest

CORRESPONDING AUTHOR

Angel Yordanov
Medical University Pleven
1 Saint Kliment Ohridski St., Pleven, Bulgaria
e-mail: angel.jordanov@gmail.com

ORCID AND CONTRIBUTIONSHIP

Yonka Ivanova: 0000-0001-5518-5186 B C
Yavor Kornovski: 0009-0001-0470-0819 A B D
Stoyan Kostov: 0000-0002-5279-3095 A E F
Stanislav Slavchev: 0000-0003-4830-6159 B F
Dimitar Metodiev: 0000-0001-8056-3580 B C
Angel Yordanov: 0000-0002-7719-382X D E F

A – Work concept and design, B – Data collection and analysis, C – Responsibility for statistical analysis, D – Writing the article, E – Critical review, F – Final approval of the article

RECEIVED: 10.03.2024
ACCEPTED: 17.07.2024

ORIGINAL ARTICLE

CONTENTS

Introduction of the modern 3d modeling method into the theory and practice of forensic medicine ballistics, caused by gunshot wounds inflicted by firearms with 9mm caliber ammunition

Yulia Zmievska, Ivan Savka
BUKOVINIAN STATE MEDICAL UNIVERSITY, CHERNIVTSI, UKRAINE

ABSTRACT

Aim: To explore the capabilities of the modern 3D modeling method for various elements of gunshot wounds caused by 9 mm caliber bullets, intending to integrate these findings into the theory and practice of forensic medicine.

Materials and Methods: The research began with a series of experimental shots, during which the morphological features were examined through their 3D spatial reconstruction. The entire series of experimental shots was conducted using an automatic pistol IZH 70-01 equipped with 9.0 mm caliber bullets. The ballistic clay Roma Plastilina No.1, manufactured in the USA, was utilized as a material for conducting standard ballistic tests according to the standards of the NIJ (National Institute of Justice) and HOSDB (Home Office Scientific Development Branch).

Results: The research was continued during the performance of forensic examinations involving actual cases of gunshot injuries. The dimensions of individual elements of the wound channel were measured in both experimental and expert cases using conventional measuring tools, as well as after their 3D modeling, utilizing graphic editors such as "Agisoft Photoscan" and "3ds max".

Conclusions: In the course of creating and studying experimental and expert 3D models, the dimensions of individual morphological elements of the wound channel were recorded with an accuracy that exceeded the results obtained through measurements using traditional measurement methods by ten times.

KEY WORDS: three-dimensional modeling, gunshot injuries, forensic-medical expertise

Wiad Lek. 2024;77(8):1569-1574. doi: 10.36740/WLek202408106 DOI

INTRODUCTION

More and more frequently, cases involving the use of firearms become the subjects of forensic investigations worldwide, occurring in civilian life as well as armed conflicts that constantly erupt in various parts of the globe. Additionally, firearms undergo constant modernization and improvement, often involving classified developments in the armaments sector of various countries. This, in turn, necessitates the development of new methods for diagnosing gunshot injuries caused by various types of firearms.

On the one hand, in the theory of forensic medicine, standardized approaches to examining such injuries have already been developed. Therefore, as of today, the results of forensic examination must provide answers to a series of fundamental questions: whether the injury is gunshot-related, the type of firearm used, and the distance from which it was fired, the locations of the entrance and exit gunshot wounds, the direction of the wound channel, the relative positions of the shooter and the victim, and so on. In a whole range of cases, the knowledge accumulated in forensic medicine over the entire period of studying gunshot injuries is sufficient to prepare positive responses to these questions for investigative and judicial authorities.

However, on the other hand, the performance of such forensic examinations encounters objective difficulties due to the use of new, unfamiliar types of firearms. In this context, traditional methodologies may not always ensure a comprehensive and objective determination of the individual identifying morphological features of the fired projectile.

Therefore, the logical and sequential solution for forensic medicine scientists was the pursuit of modern, high-precision research methods that would effectively address these new challenges.

One of the most promising directions in this field is considered to be the implementation of 3D modeling of bodily injuries caused by blunt, sharp, and firearms factors. Photogrammetry of such injuries has yielded significantly more precise and well-founded results [1].

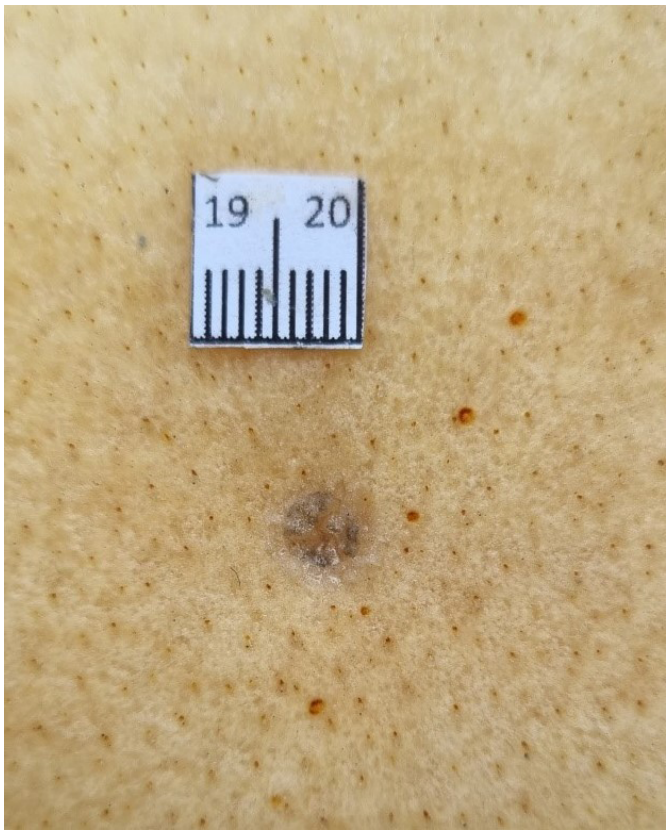

Fig. 1. Gunshot injury of the skin, caliber 9,0 mm.

Other researchers have assessed the effectiveness of studying gunshot injuries using traditional methods such as radiological and ultrasonic techniques. They unequivocally favored more advanced computer tomography, which enables the reproduction of the wound channel in its 3D spatial dimension [2].

Researchers have also demonstrated the high effectiveness of studying gunshot injuries to the skin, internal organs, and bones through their 3D modeling in living individuals and corpses during post-mortem examinations [3].

Some researchers point to the efficiency of the 3D modeling method in the identification of bullets by examining their traces at the micro level [4].

Additionally, the application of this method in computer modeling of damage to protective helmets and their comparison with gunshot injuries in the head region is noteworthy for reproducing the real circumstances of acquiring combat gunshot trauma [5].

AIM

Taking this into account, the primary aim of the research was to explore the capabilities of the modern 3D modeling method for various elements of gunshot injuries, illustrated through experimental and expert cases caused by 9mm caliber ammunition.

Fig. 2. Gunshot injury of the subcutaneous tissue, caliber 9,0 mm.

MATERIALS AND METHODS

These researches were carried out in agreement with the basic bioethical principles of the Council of Europe Convention on Human Rights and Biomedicine (dated 04.04.1997), the Helsinki Declaration of the World Medical Association on the Ethical Principles of Scientific Medical Research with Human Participation (1964-2013), the Order of the Ministry of Health of Ukraine №6 "Instruction on forensic-medical examination" (dated January 17, 1995), the Order of the Ministry of Health of Ukraine №690 (dated September 23, 2009), and taking into account the methodological recommendations of the Ministry of Health of Ukraine "Procedure of exemption of biological objects from dead persons whose bodies are subject to forensic medical examination and pathological examination for scientific purposes" (2018). The Committee on Biomedical Ethics of the Bukovinian State Medical University did not reveal any violations of moral and legal norms during these scientific researches (Protocol No1 dated 21.09.2023).

The series of experiments were conducted at the Chernivtsi Scientific Research Expert-Criminalistic Center, equipped with the projectile flight speed recorder VBX-2020. An example of a firearm used in the experiments was the IZH 70-01 automatic pistol loaded with 9.0 mm caliber ammunition. Targets were covered with pigskin, including the subcutaneous adipose layer, and were placed at a distance of 1.5 meters from the muzzle of the firearm. As a target, ballistic clay Roma Plastilina No.1, produced in the USA for conducting stand ballistic tests according to the standards of the National Institute

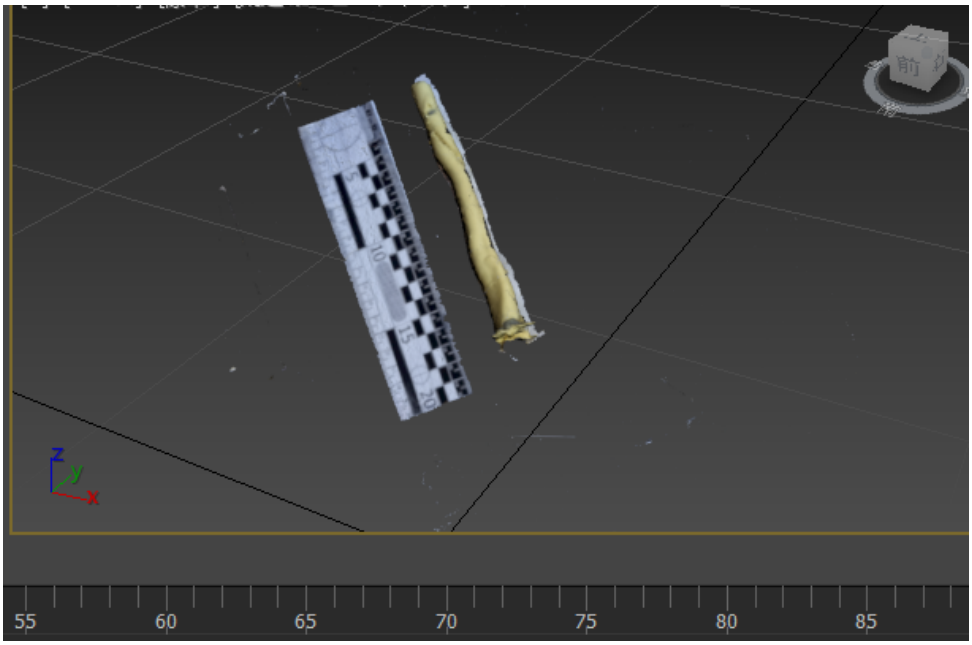

Fig. 3. 3D model of the gunshot wound canal caused by bullet, caliber 9,0 mm.

of Justice (NIJ) and Home Office Scientific Development Branch (HOSDB), was used. This ballistic clay, due to its physical and technical characteristics, accurately reproduces the soft tissues of the human body (skin, subcutaneous adipose tissue, muscles, parenchymal organs), especially when heated to a temperature of 35-38 °C.

After the shots were fired, digital photographs of the injuries on the skin, subcutaneous adipose tissue, and the plastiline block at the entry and exit points of the bullet were taken. Subsequently, all elements of the gunshot injuries were measured using traditional methods for investigating linear dimensions of objects – rulers and calipers. Circular photogrammetry of the entrance wound and subcutaneous adipose tissue was then carried out at different angles: 30°, 45°, 60°, and 90°. For this purpose, the skin fragment with the injury was placed on a turntable with a white background and additional lighting provided by spherical LED lamps (Fig. 1 and Fig. 2).

The next step involved uploading all the JPEG format photos into the computer program "Agisoft Photoscan". In this program, 3D models were constructed, and then textures were created, resulting in a textured 3D model of the entrance wound in the skin and subcutaneous adipose tissue. These textured models were exported in "OBJ" format to the "3ds max" program, where scaling and measurements of the wound dimensions were performed.

In the process of progressively investigating the wound channel, the next step was to create its volumetric cast in a ballistic clay block. For this purpose, we utilized alginate material Tropicalgin (by "Zhermack", Italy), prepared according to the manufacturer's recommended instructions. This material is characterized by high precision in capturing object impressions and allows for the reproduction of the finest details of the wound channel. After pouring, solidifying, and cleaning the material from clay, a clear sample of the wound channel was obtained. It represented an accurate replica made from the alginate material, which underwent photography, photogrammetry, and the creation of a 3D model using the same methodologies as with the skin and subcutaneous adipose tissue (Fig. 3).

The obtained digital data were initially recorded in electronic spreadsheets to standardize their input, grouping, storage, and computation. Calculations and statistical analysis were performed using the Statistica 13.5.0.17 software by TIBCO Software Inc. (ZZS9990000099100363DEMO-L).

The assessment of the distribution type of the data was conducted by determining the measure of central tendency between the mean, mode, and median, as well as skewness (symmetry) and kurtosis (excess). In the computation of statistical values, the following were calculated: the sample mean (M), standard deviation (SD), standard error of the mean (m), as well as the minimum (min) and maximum (max) values of the variables.

For assessing the strength of relationships, Pearson's correlation analysis was employed. In this context, the evaluation of the strength of correlational ties utilized a six-level gradation: up to 0.16 – unsatisfactory, 0.17-0.33 – satisfactory, 0.34-0.50 – below average, 0.51-0.67 – average, 0.68-0.84 – above average, and greater than 0.85 – high. Results were considered statistically significant at $p<0.05$.

Table 1. Parameters and morphological signs of experimental gunshot injuries caused by the automatic pistol IZH 70-01, caliber 9,0 mm (N=15)

Parameter	Average value and mean arithmetic error (M±m)	Minimum value (min)	Maximum value (max)	Standard deviation (S.D.)
1.Physical parameters of the bullet				
Initial velocity, m/sec	310±0,9411	304	315	3,6450
Kinetic energy of the bullet, (Joule)	302,732±6,4905	284,641	390,287	25,1378
Specific energy of the bullet, (Joule/mm^2)	4,461±0,0277	4,284	4,599	0,1072
2.Morphological signs of the gunshot entry wound				
Diameter of the entry wound, cm	0,887±0,0091	0,8	0,9	0,0352
Dimensions of the defect tissue, cm	0,367±0,0187	0,3	0,5	0,0724
Dimensions of the abrasion ring, cm	0,320±0,0175	0,2	0,4	0,0676
Dimensions of the deposition ring, cm	0,380±0,0175	0,3	0,5	0,0676
3. Morphological signs of the gunshot wound canal				
Diameter of the wound canal in the initial part, cm	0,7±0,0507	0,5	0,9	0,1964
Diameter of the wound canal in the initial part (3D modelling), cm	0,9158±0,0090	0,841	0,949	0,0349
Diameter of the wound canal in the middle part, cm	1,63±0,0621	1,2	2,1	0,2404
Diameter of the wound canal in the middle part (3D modelling), cm	1,655±0,0643	1,215	2,142	0,2490
Diameter of the wound canal in the exit part, cm	2,19±0,0636	1,8	2,6	0,2463
Diameter of the wound canal in the exit part (3D modelling), cm	2,227±0,0627	1,836	2,638	0,2430

ETHICAL APPROVAL

The research protocol and informed consent form were approved by the Commission on Biomedical ethics in biomedical scientific research of the Bukovinian State Medical University (Protocol No.1 dated 21.09.2023).

RESULTS

The results of all 15 shots, after statistical processing, were grouped into three data blocks. The first data block provided characteristics of the bullet's physical parameters after the shot and included initial velocity, kinetic energy, and specific energy of the bullet. The second data block pertained to the morphological features of the entrance gunshot wound and was represented by measurements of the entrance wound diameter, measured with traditional measuring tools and established during 3D modeling, as well as the dimensions of tissue defects and deposition rings. The third data block illustrated the morphological features of the wound channel, measured at various intervals using traditional methods and during its 3D modeling. All three data blocks were grouped into a table and subjected to a comparative analysis (Table 1).

The digital data in this table indicate a slight discrepancy between the values of the average initial bullet velocity and its specific energy in shots fired from the IZH 70-01 automatic pistol, as well as their minimum and maximum values. At the same time, a somewhat larger range of values was observed in the minimum, average, and maximum values of its kinetic energy.

As for the morphological features of the wound, 3D technologies have enabled the recording of significantly more precise average dimensions, as well as minimum and maximum values of the entrance wound diameter, tissue defect, and the dimensions of the ring of deposition and abrasion than previously achieved using calipers and rulers.

This also applies to the morphological features of the wound channel. The diameters of its middle portion, at the exit, and especially in the initial part were determined with greater precision through 3D modeling and the use of computer technologies in determining the linear dimensions of the investigated objects.

All described injuries had a perforating nature with a wound channel length of 16.0 cm (across the entire length of the ballistic gel block), and the skin wounds were round in shape with finely serrated edges.

Table 2. Morphological signs of the gunshot injury (forensic medicine case, determined caliber – 9,0 mm)

Part of the wound canal	Dimensions measured by traditional means, centimeters	Dimensions fixed by 3D modelling, centimeters	Additional characteristics
Entry wound	0,87x0,6	0,884x0,603	Presence of the defect tissue, abrasion ring up to 0,5 mm, margins are fine notched
Buttonhole fracture of the right temporal bone (external plate)	0,91x0,6	0,914x0,613	Round form with fine notched edges
Buttonhole fracture of the right temporal bone (internal plate)	1,2x1,0	1,245x1,124	Crater-like form
Injury of the right temporal lobe of brain	1,3x1,1	1,343x1,150	Entry
Injury of the left temporal lobe of brain	1,5x0,9	1,512x0,934	Exit
Buttonhole fracture of the left temporal bone	1,6x0,9	1,628x0,941	Margins are uneven with small fissured cracks
Exit wound	1,9x0,5	1,932x0,542	Fissured form, margins without abrasions, turned outwards

DISCUSSION

The subsequent scientific discussion revolved around establishing and analyzing correlational relationships between shooting parameters and identified morphological features of individual elements of gunshot injuries. Correlational analysis revealed direct average-strength correlations between the diameter of the wound channel at its entrance, determined by 3D modeling methods, and the initial velocity of the bullet and its specific energy (r=+0.55), with p=0.04.

Strong (high) direct correlations were identified between the diameters of the wound channel in its middle part and the initial velocity of the bullet and its specific energy, measured both by traditional methods (r=+0.90 and r=+0.85) and 3D modeling techniques (r=+0.89 and r=+0.85) respectively (p=0.02).

Even stronger direct correlation links were found between the diameters of the wound channel at its exit and the initial velocity of the bullet and its specific energy, measured by both traditional methods (r=+0.94 and r=+0.89) and 3D modeling techniques (r=+0.94 and r=+0.90) respectively (p=0.01).

Average direct correlations were observed between the initial velocity of the bullet and tissue defect (r=+0.54), as well as between the initial velocity of the bullet and the dimensions of the ring of deposition (r=+0.55), at p=0.04.

The described direct correlation relationships discussed may indicate an objective dependence and an increase in the dimensions of the diameters of the initial section of the wound channel during 3D modeling, especially the dimensions of the wound channel in its middle part and at the exit, as the initial velocity and specific energy of the bullet increase. The indicators of the initial velocity also directly influence the enlargement of tissue defects and the ring of deposition around the entrance wound in cases involving the use of a 9.0 mm caliber automatic short-barreled weapon.

Other researchers have also utilized 3D modeling of firearm injuries caused by short-barreled automatic weapons with a 9.0 mm caliber (Luger pistol). They observed similar morphological changes that assisted them in conducting differential diagnoses from firearms of larger calibers [6]. Objective morphological differences identified through 3D modeling of gunshot wounds caused by 9.0 mm firearms, compared to other calibers, have been described by other authors as well [7].

The described methodologies were applied by us during a forensic examination in the case of a fatal injury to the victim from automatic firearms. The body of an unidentified person was brought to the morgue with a through gunshot wound to the head. During the examination, a gunshot wound was found in the right temporal region, a perforated fracture of the right temporal bone, damage to the brain, and a perforated fracture of the left temporal bone.

All elements of the gunshot wound channel were measured using standard metric methods, followed by circular photogrammetry, and their 3D model was created (Table 2). This provided a factual basis for determining the caliber of the unknown firearm – 9.0 mm, along with a series of three-dimensional illustrations that assisted in the successful investigation of this crime later on.

CONCLUSIONS

The implementation of 3D modeling techniques allows for a 10-fold increase in accuracy in capturing the morphological features of the main elements of gunshot wounds. It enables the creation of 3D models of both individual components of gunshot injuries and the entire wound channel, opening up new possibilities for visualization, long-term storage, and expert analysis.

Example of 3D modeling of gunshot wounds caused by automatic firearms with a caliber of 9.0 mm demonstrates new directions in the theory and practice of forensic medicine regarding the possibilities of conducting differential diagnostics between gunshot projectiles of different calibers in the future.

REFERENCES

1. Villa C. Forensic 3D documentation of skin injuries. International Journal of Legal Medicine. 2017;131(3):751-59. doi: 10.1007/s00414-016-1499-9. DOI
2. Stevenson T, Carr DJ, Harrison K et al. Ballistic research techniques: visualizing gunshot wounding patterns. International Journal of Legal Medicine. 2020;134(3):1103-14. doi: 10.1007/s00414-020-02265-5. DOI
3. Villa C, Olsen KB, Hansen SH. Virtual animation of victim-specific 3D models obtained from CT scans for forensic reconstructions: Living and dead subjects. Forensic Sci Int. 2017;278:e27-e33. doi: 10.1016/j.forsciint.2017.06.033. DOI
4. Banno A, Masuda T, Ikeuchi K. Three dimensional visualization and comparison of impressions on fired bullets. Forensic Sci Int. 2004;140(2-3):233-40. doi: 10.1016/j.forsciint.2003.11.025. DOI
5. Mahoney P, Carr D, Harrison K et al. Forensic reconstruction of two military combat related shooting incidents using an anatomically correct synthetic skull with a surrogate skin/soft tissue layer. International Journal of Legal Medicine. 2019;133(1):151-62. doi: 10.1007/s00414-018-1802-z. DOI
6. Costa ST, Freire AR, Matoso RI et al. Computational Approach to Identify Different Injuries by Firearms. J Forensic Sci. 2017;62(2):361-368. doi: 10.1111/1556-4029.13387. DOI
7. Matoso RI, Freire AR, Santos LS et al. Comparison of gunshot entrance morphologies caused by .40-caliber Smith & Wesson, .380-caliber, and 9-mm Luger bullets: a finite element analysis study. PLoS One. 2014;9(10):e111192. doi: 10.1371/journal.pone.0111192. DOI

Authors would like to thank all participants of this study.

CONFLICT OF INTEREST

The Authors declare no conflict of interest

CORRESPONDING AUTHOR

Ivan Savka
Bukovinian State Medical University
2 Teatralna sq., 58002 Chernivtsi, Ukraine
e-mail: savka.ivan@bsmu.edu.ua

ORCID AND CONTRIBUTIONSHIP

Yulia Zmievska: 0009-0008-5771-0114 B C D
Ivan Savka: 0000-0002-2969-1306 A E F

A – Work concept and design, B – Data collection and analysis, C – Responsibility for statistical analysis, D – Writing the article, E – Critical review, F – Final approval of the article

RECEIVED: 21.11.2023
ACCEPTED: 17.07.2024

ORIGINAL ARTICLE

CONTENTS

Diet control and BMI impact on Metformin response in type 2 Diabetes mellitus patients

Alaa Abd AL-Hussain Naem[1], Fadhaa Abdulameer Ghafil[1], Mona N. Al-Terehi[2], Sahar Majeed[1], Defaf Al-Mudafer[3], Najah Rayish Hadi[1]

[1]DEPARTMENT OF PHARMACOLOGY AND THERAPEUTIC, FACULTY OF MEDICINE, UNIVERSITY OF KUFA, KUFA, IRAQ
[2]DEPARTMENT OF MOLECULAR BIOLOGY, FACULTY OF SCIENCE, UNIVERSITY OF BABYLON, BABYLON, IRAQ
[3]DEPARTMENT OF MICROBIOLOGY, FACULTY OF MEDICINE, UNIVERSITY OF KUFA, KUFA, IRAQ

ABSTRACT

Aim: To assess the impact of BMI and diet control on variation in response to metformin monotherapy in Iraqi people with type 2 DM.

Materials and Methods: a cross-sectional study included 150 patients who met specific criteria, such as being between 30 and 70 years old, diagnosed with type 2 diabetes, and on a daily dose of 1000 mg metformin as a monotherapy for at least three months. Data collected included body mass index (BMI) and glycemic control parameters such as: glycated hemoglobin (HbA1c) levels, fasting blood glucose levels, fasting serum insulin levels, HOMA-IR, and insulin sensitivity. The patients according to their metformin response classified into two groups based on HbA1c as following: poor (HbA1c≥6.5% and good (HbA1c≤6.5%) responder's patients.

Results: The statistical analysis suggests that there is no meaningful distinction in glycemic control parameters when comparing good and poor responders within specific BMI subgroups and among individuals practicing diet control. However, in a broader context, it is evident that glycemic control parameters tend to be lower in patients with lower BMI and those who are following a controlled diet.

Conclusions: The correlation between diet control and BMI with glycemic control in diabetic patients, underscoring the significance of lifestyle adjustments in the management of diabetes.

KEY WORDS: BMI, metformin response, type 2 diabetes mellitus, diet control

Wiad Lek. 2024;77(8):1575-1581. doi: 10.36740/WLek202408107 DOI

INTRODUCTION

Type 2 Diabetes Mellitus (T2DM), a prevalent metabolic disorder, results from the interplay of two main factors: impaired insulin secretion by pancreatic β-cells and the reduced responsiveness of insulin-sensitive tissues to insulin [1]. Insulin synthesis, release, and recognition are tightly regulated molecular processes that are essential for maintaining glucose balance. Any disruptions in these mechanisms can lead to metabolic disturbances, potentially contributing to the development of certain medical conditions [2]. Metformin is extensively employed as the initial medication for managing type 2 diabetes (T2D). Acting primarily on the liver, metformin effectively reduces hepatic glucose production [3]. Metformin helps maintain glucose balance by inhibiting gluconeogenesis, encouraging glycolysis, and suppressing glycogenolysis, which is closely linked to increased hepatic glucose production (HGP). Furthermore, metformin improves insulin sensitivity and lowers abnormal lipid levels in individuals with type 2 diabetes (T2D) [4-5]. Diet control is a cornerstone of managing T2DM. Patients are often advised to adopt a diet that helps regulate blood sugar levels. Maintaining a balanced intake of carbohydrates, proteins, and healthy fats, along with portion control and carbohydrate counting, can lead to better blood sugar control. This, in turn, can reduce the need for medications or insulin therapy [6]. The recommended nutritional therapy for diabetic patients includes a balanced nutritional calculation from carbohydrates, fruits, vegetables, whole grains, nuts, and low-fat milk [7]. Measuring diet control in diabetic patients is crucial for managing their condition and preventing complications. Several ways are used to assess and monitor diet control in diabetic individuals such as blood glucose monitoring and HbA1c test [8]. BMI is a measure of body weight relative to height and is commonly used to assess whether an individual is underweight, normal weight, overweight, or obese. Excess

body weight, especially obesity, is a major risk factor for the development of T2DM. High BMI is associated with insulin resistance, where the body's cells do not respond effectively to insulin, leading to elevated blood sugar levels. Weight loss and maintaining a healthy BMI can improve insulin sensitivity and help manage T2DM [9]. Both diet control and achieving a healthy BMI can improve insulin sensitivity in patients with T2DM. When the body's cells become more responsive to insulin, it becomes easier to regulate blood sugar levels. Weight loss, in particular, has been shown to have a positive impact on insulin sensitivity [10]. In clinical settings, it is frequently observed that patients diagnosed with type 2 diabetes (T2DM) and given the same antidiabetic treatments often exhibit significant variability in their capacity to manage blood sugar levels, their HbA1c levels, the efficacy of the prescribed medications, their ability to tolerate these drugs, and the occurrence of adverse side effects [11].

AIM

To assess the impact of BMI and diet control on variation in response to metformin monotherapy in Iraqi people with type 2 DM.

MATERIALS AND METHODS

STUDY DESIGN

A cross-sectional study was conducted between April 2022 and June 2023, involving a sample of 150 individuals diagnosed with type 2 diabetes mellitus based on the 2012 American Diabetes Association criteria. These criteria define type 2 diabetes using parameters such as HbA1c levels ≥6.5%, fasting plasma glucose (FPG) levels ≥126 mg/dl, 2-hour plasma glucose levels ≥200 mg/dl during an oral glucose tolerance test (OGTT), or random plasma glucose levels ≥200 mg/dl. The study participants were recruited randomly from the diabetes center at Al-Sadar Teaching Hospital in Najaf, Iraq, and the study received ethical clearance from the Medical Ethics Committee of the Faculty of Medicine at Kufa University.

STUDY POPULATION

The study population comprised 150 individuals with type 2 diabetes, encompassing both males and females, who had been undergoing a monotherapy regimen of metformin tablets (1000 mg once daily) for a minimum of three months [12]. These participants fell within the age range of 30 to 70 years. Exclusion criteria for the study encompassed patients with significant organ dysfunction, including heart, liver, and renal failure, individuals above 70 years of age, those with a BMI exceeding 30 kg/m2, pregnant women, patients with chronic gastrointestinal disorders or malabsorption syndrome, and individuals concurrently using other oral hypoglycemic agents (OHAs) or insulin. The participants in the study were divided into two groups based on their adherence to diet control criteria recommended by the American Diabetic Association in 2018. These criteria include: low carbohydrate/high protein intake. Patients choose complex carbohydrates like whole grains and distributed carbohydrate intake evenly throughout the day to prevent spikes in blood sugar levels, avoided refined carbohydrates, sugary food, and beverages. Patients taken lean protein which include: fish, legumes, and low-fat dairy. Patients incorporated high-fiber foods like vegetables, fruits, whole, beans, and nuts into their diet. As well as increased intake of healthy fats like those found in nuts, seeds, and olive oil and limited saturated and trans fats found in fried foods, fatty cuts of meat, and processed snacks. According to the glycemic control the patients were classified into two groups based on HbA1c into well (HbA1c levels≤6.5%) ≤ and poor responders (HbA1c levels ≥6.5%).

DATA COLLECTION

The data collection process involved the investigator administering a standardized questionnaire to gather demographic and clinical information from patients. This information encompassed their names, ages, body weight, and height, duration of illness, medical history, family medical history, dietary habits, sleep patterns, and occupations. To calculate the Body Mass Index (BMI), measurements for weight and height were taken. Height measurements were acquired with subjects standing upright, barefoot, with arms at their sides, and feet close together. Weight measurements were recorded with patients standing on a scale, wearing lightweight clothing, and without shoes or socks. BMI was calculated using the formula BMI = weight (in kilograms) / height (in meters squared), and it was used to categorize patients as either normal (BMI < 25 kg/m^2), overweight (BMI between 25 and 29.9 kg/m^2), or obese (BMI ≥ 30 kg/m^2) [12]. The glycemic control parameters measured include:

- **FBG (fasting blood glucose):** measured by "RanDox kit-UK", which is rely on the "PAP enzymatic" measurement of glucose.
- **HbA1c:** the percentage assessed by using immune assay method by Stanbio/USA kit.
- **Serum insulin:** assayed according to the procedure recommended by (BTLAB®) company.

- **Homeostasis-Model Assessment for Insulin Resistance (HOMA-IR):** The approach presented by used the "Homeostasis-Model Assessment for Insulin Resistance (HOMA-IR)" index to measure insulin resistance [13].

The of HOMA-IR was calculated in the following manner: "HOMA-IR = Fasting-insulin (μU/L) * Fasting-glucose (mmol/L)/22.5."

- **Insulin sensitivity:** the quantitative insulin sensitivity check index (QUICKI) is derived using the inverse of the sum of the logarithms of the fasting insulin and fasting glucose [13]:
- 1 / (log(fasting insulin μU/mL) + log(fasting glucose mg/dL)

BLOOD SAMPLE COLLECTION

Morning blood samples were collected from each patient after an overnight fast of 8-12 hours. While patients were seated, about 5mL of venous blood was drawn using disposable syringes. This blood collection involved distributing 3mL of blood into tubes containing EDTA and cautiously transferring the remaining 2mL into serum tubes equipped with separating gel. The blood is stored in EDTA tubes for assessing HbA1c via Immunoassay technique. Blood within the serum tubes was allowed to coagulate at room temperature for around 10-15 minutes, followed by centrifugation at approximately 3000 × g for approximately 3 minutes. The resulting serum was then stored at a temperature of -80°C until analysis. Serum insulin levels were measured using the BT LAB® ELISA kit, following the manufacturer's recommended procedure. Fasting blood glucose was measured utilizing the RanDox® kit, which relies on the PAP enzymatic method for determining glucose levels. All data was managed by using SPSS version 22, ANOVA test and t-test used for multiple comparisons, and chi-square test for utilization of non-numerical variables. Values of ≤ 0.05 will be considered to be statistically significant.

Table 1. Mean differences of variables in study subjects

Variables	Patients
FBG	219.46±8.80
HbA1c	8.77±0.203
Insulin	8.67±1.103
HOMA-IR	84.76±12.002
Insulin sensitivity	1.14±1.03
age	53.97±1.86
BMI	28.34±1.58

RESULTS

150 T2DM patients as shown in Table 1 with an average age of 53.97±1.86 years and a mean BMI of 28.34±1.58 kg/m2 were included in the study. Socio-demographic data as in table 2 like BMI, age, duration of disease, and diet control shows there is a difference between the two groups but statistically is non-significant (p-value ≥ 0.05).

The patients were classified into two subgroups according to their glycemic control; poorly controlled diabetics (HbA1c ≥ 6.5%) who were 73.82% compared to good glycemic control (HbA1c ≤ 6.5%) who were 26.17% as expressed in Fig. 1.

The difference in glycemic parameters between the good and poor responders is represented in table 3. As shown by the mean difference in glycemic parameters between good and poor responders to metformin there was a highly significant difference between the two groups about the FBS, HbA1c, and HOMA-IR (p-value 0.000), (p-value 0.000), and (p-value: 0.019) respectively.

Table 2. Socio-demographic distribution of study groups

Variables	<6.5	>6.5	X^2	P value
		Diet		
No	20	57	0.00331407	0.9541
Yes	19	52		
Age	52.00±1.648	53.90±1.82	1.131	0.260
BMI	27.93±0.58	28.01±0.63	0.076	0.940
Duration	6.13±0.94	7.94±0.55	1.681	0.095
BMI category				
Normal	8	33	1.61206	0.4466
Overweight	21	48		
Obese	11	28		
Gender				
Male	10	44	2.99042	0.08376
Female	30	65		

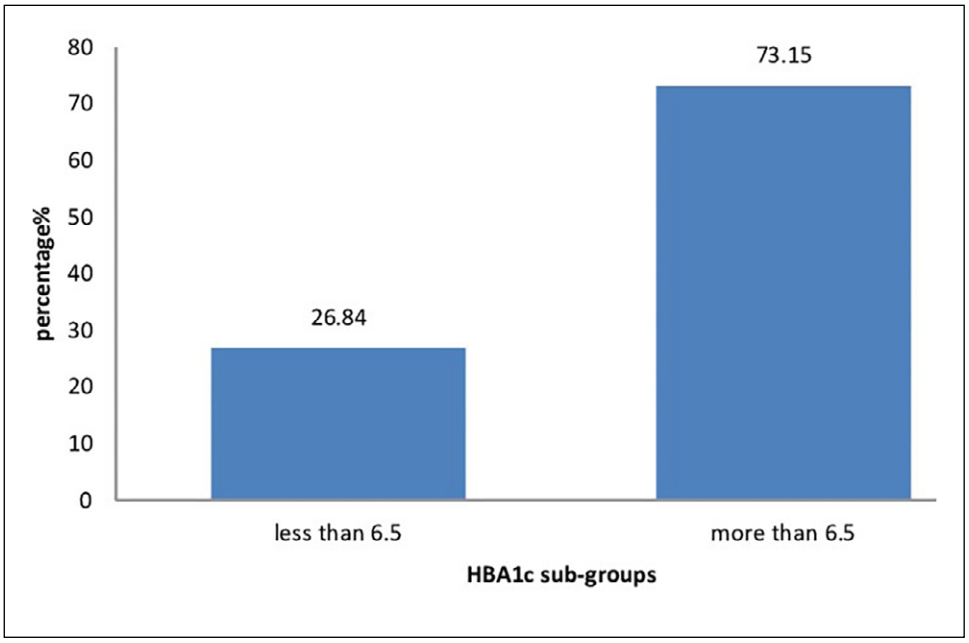

Fig. 1. The percentage of HBA1c sub-groups.

Table 3. Glycemic variables in study groups. All data is expressed as mean ± SD

Variables	<6.5	>6.5	P value
FBC	138.7±9.755	248.62±8.843	0.000
HbA1c	6.036±0.070	9.77±0.203	0.000
Insulin	7.148±1.701	9.57±1.26	0.355
HOMA- IR	45.59±11.55	105.05±14.39	0.019
Insulin sensitivity	1.18±0.08	1.03±0.047	0.587

Serum insulin was higher in poor responders than in good responders but this difference was statistically non-significant.

The association of BMI and glycemic control parameters is shown in table (4). Based on the data presented in table 4, the statistical analysis indicates that there is no significant difference in glycemic factors such as Fasting Blood Sugar (FBS), HbA1c, serum insulin, insulin sensitivity, and HOMA-IR when comparing patients who responded well to those who responded poorly. It's worth noting that in both groups, patients with a body mass index (BMI) greater than 30 kg/m^2, indicating overweight, exhibited higher levels of all these glycemic control parameters. Insulin sensitivity was higher in normal-weight patients (BMI<25 kg/m^2) in both groups.

The association between diet control and glycemic parameters illustrated in table 5, the result shows there is a difference in glycemic parameters (FBS, HbA1c, serum insulin, insulin sensitivity, and HOMA-IR) between good and poor responder patients as well as there is difference within the group itself but statistically non-significant. All glycemic parameters show a higher mean in patients without diet control than those with a restricted diet. The HbA1c shows a significant difference between patients with diet control and non-good responders' patients.

In this study, the correlation between the studied glycemic control parameters in two groups is clarified in table 6:

1- FBG in good responder has a positive correlation (R = 0.393) with HbA1c, which is statistically highly significant (P = 0.000). Also in poor responders, the FBG has a positive correlation (R = 0.327) with HbA1c which is statistically significant (P = 0.018). This suggests that as FBG levels increase, HbA1c levels also tend to increase.

2- In good responders, BMI has a positive correlation with FBG (R = 0.240) and HbA1c (R = 0.258) but is statistically non-significant (P = 0.292), (P = 0.113) respectively. In poor responders, BMI has a negative correlation with FBG (R =-0.041) statistically non-significant (P =0.671), while a positive correlation with HbA1c (R = 0. 0.795) statistically non-significant (P =0.782).

3- HOMA-IR has a positive non-significant correlation with FBG (R = 0. 0.159), (P =0.095).

4- Insulin sensitivity has an inverse correlation non-significant with FBG (R = -0.008), (P =0.938).

5- Age has a non-significant inverse correlation with FBG (R = -0.050), (p= 0. 0.602).

6- Serum insulin has an inverse correlation non-significant with FBG (R = -0.016), (P =0.867).

DISCUSSION

Prior research has established that being overweight or obese significantly increases the risk of inadequate blood glucose control in people with diabetes. Nevertheless, the precise impact of obesity on both metabolic

Table 4. Means differences of study variables according to BMI categories

Variables	<6.5				>6.5			
	<25	25-29.9	>30	p	<25	25-29.9	>30	P value
FBG	132.25±11.21	133.14±17.71	133.40±6.69	0.500	256.81±14.12	241.43±14.37	259.20±16.72	0.749
HbA1C	5.78±0.17	6.13±0.09	6.17±0.12	0.177	41.27±27.27	9.63±0.316	49.58±19.58	0.369
IN	6.67±1.85	7.17±2.90	7.47±2.45	0.988	6.06±1.05	10.20±2.47	6.97±2.16	0.257
IR	40.75±12.22	40.89±20.65	41.54±13.97	0.972	74.30±11.78	108.79±27.63	133.59±26.21	0.298
IS	1.23±0.09	0.95±0.13	1.20±0.122	0.358	1.11±0.07	1.10±0.07	1.05±0.09	0.339

IN:: serum insulin, IR: insulin resistant, IS: insulin sensitivity

Table 5. Differences in study variables according to diet control. All data is expressed as mean ± SD

Variables	<6.5			>6.5		P value
	no	Yes	P	No	Yes	
FBG	151.95±12.086	125.45±15.03	0.178	253.46±12.29	251.23±12.374	0.560
HbA1C	6.19±0.07	5.88±0.112	0.024	10.03±0.26	9.84±0.30	0.178
IN	5.04±0.70	4.56±3.22	0.171	10.95±1.379	10.18±2.25	0.634
IR	35.73±5.96	35.05±22.40	0.400	111.64±15.429	110.08±25.770	0.747
IS	1.04±0.090	1.11±0.138	0.665	1.12±0.06217	1.13±0.072	0.894

Table 6. The correlation coefficients among study variables in study groups

Variables		FBG	HBA1C	BMI
FBG	R		0.372	0.240
	P		0.018	0.292
HBA1C	R	0.393		0.258
	P	0.000		0.113
IN	R	-0.016-		0.121
	P	0.867		0.463
HOMA-IR	R	0.159		0.086
	P	0.098		0.601
INS	R	-0.008-		0.131
	P	0.938		0.425
Age	R	-0.050-		-0.064-
	P	0.602		0.700
Bmi	R	-0.041-	0.795	
	P	0.671	0.782	

regulation and the emergence of microvascular and macrovascular complications remains incompletely comprehended [14]. In our research, as illustrated in Tables (4), we found that individuals with a BMI of 30 kg/m^2 or higher had higher levels of glycemic parameters. This finding aligns with a separate study that also observed significant differences in HbA1c levels between individuals who were obese and those who were either pre-obese or had a normal weight [15]. In 2004, Koro et al. documented that various diabetic characteristic, such as their BMI, affected glycemic control parameters. Specifically, they found that higher HbA1c levels were related to obesity [16]. A Turkey-wide survey has unveiled a significant incidence of obesity, including severe obesity, in individuals diagnosed with type 2 diabetes. This research indicates that obesity worsens the management of blood sugar levels and increases the likelihood of cardiovascular diseases in this patient group [17]. Our study demonstrated that patients with diet control had a lower glycemic parameter as compared to those who did not. These findings consistent with multiple systematic reviews and meta-analyses have consistently found that diets emphasizing a lower glycemic index are associated with decreased fasting blood glucose levels and reduced glycation markers such as HbA1c. Additionally, these reviews have offered compelling evidence supporting the notion that the consumption of foods with a lower glycemic index substantially enhances insulin sensitivity [18].

CONCLUSIONS

The impact of BMI and diet control on metformin response in diabetic patients is a complex and multifaceted issue, while it is well-established that metformin is an effective medication for managing blood glucose levels in type 2 diabetes, the relationship between BMI, diet, and metformin response is influenced by various factors. Research suggests that individuals with higher BMIs may initially require higher doses of metformin to achieve adequate glycemic control. However, weight loss through diet control and lifestyle modifications can improve the efficacy of metformin and reduce the insulin resistance commonly associated with obesity. Additionally, dietary changes can contribute to better overall diabetes management by promoting healthier

eating habits and weight reduction. However, a personalized and comprehensive approach to diabetes care, including regular medical supervision and ongoing lifestyle modifications, remains the cornerstone of successful diabetes management.

LIMITATION OF STUDY

To draw more robust conclusions about the impact of BMI and diet control on diabetic patients using metformin, you may consider conducting a longitudinal cohort study or a randomized controlled trial (RCT) with appropriate controls and follow-up periods. These study designs can help establish causation, control for confounding variables, and provide insights into the temporal relationships between variables. It's important to note that the impact of diet control and BMI on T2DM can vary from person to person, and individualized care is essential. A healthcare provider or registered dietitian can work with patients to develop a personalized diabetes management plan that takes into account their unique needs, preferences, and medical history. Additionally, regular monitoring and follow-up are crucial to assess progress and make any necessary adjustments to the treatment plan.

REFERENCES

1. Roden M, Shulman GI. The integrative biology of type 2 diabetes. Nature. 2019;576(7785):51-60. doi: 10.1038/s41586-019-1797-8. DOI
2. Galicia-Garcia U, Benito-Vicente A, Jebari S et al. Pathophysiology of type 2 diabetes mellitus. Int J Mol Sci. 2020;21(17):6275. doi: 10.3390/ijms21176275. DOI
3. Foretz M, Guigas B, Bertrand L et al. Metformin: from mechanisms of action to therapies. Cell metabolism. 2014;20(6):953-66. doi: 10.1016/j.cmet.2014.09.018. DOI
4. Zheng J, Woo S-L, Hu X et al. Metformin and metabolic diseases: a focus on hepatic aspects. Frontiers of medicine. 2015;9:173-86. doi: 10.1007/s11684-015-0384-0. DOI
5. LaMoia TE, Shulman GI. Cellular and molecular mechanisms of metformin action. Endocrine reviews. 2021;42(1):77-96. doi: 10.1210/endrev/bnaa023. DOI
6. Major CA, Henry MJ, de Veciana M, Morgan MA. The effects of carbohydrate restriction in patients with diet-controlled gestational diabetes. Obstetrics & Gynecology. 1998;91(4):600-604. doi: 10.1016/s0029-7844(98)00003-9. DOI
7. Shalahuddin I, Maulana I, Pebrianti S, Eriyani T. Blood Sugar Levels Regulation in Diabetes Mellitus Type 2 Patients Through Diet Management. Jurnal Aisyah: Jurnal Ilmu Kesehatan. 2022;7(2):413-422. doi: 10.30604/jika. v7i2.911. DOI
8. Kalyani RR, Corriere M, Ferrucci L. Age-related and disease-related muscle loss: the effect of diabetes, obesity, and other diseases. The lancet Diabetes & endocrinology. 2014;2(10):819-829. doi: 10.1016/S2213-8587(14)70034-8. DOI
9. Narayan KV, Boyle JP, Thompson TJ et al. Effect of BMI on lifetime risk for diabetes in the US. Diabetes care. 2007;30(6):1562-1566. doi: 10.2337/dc06-2544. DOI
10. Verma S, Hussain ME. Obesity and diabetes: an update Diabetes & Metabolic Syndrome: Clinical Research & Reviews. 2017;11(1):73-79. doi: 10.1016/j.dsx.2016.06.017. DOI
11. Potenza MA, Nacci C, De Salvia MA et al. Targeting endothelial metaflammation to counteract diabesity cardiovascular risk: Current and perspective therapeutic options. Pharmacol Res. 2017;120:226-241. doi: 10.1016/j.phrs.2017.04.009. DOI
12. Hakooz N, Jarrar YB, Zihlif M et al. Effects of the genetic variants of organic cation transporters 1 and 3 on the pharmacokinetics of metformin in Jordanians. Drug Metabolism and Personalized Therapy. 2017;32(3):157-62. doi: 10.1515/dmpt-2017-0019. DOI
13. Katz A, Nambi SS, Mather K et al. Quantitative insulin sensitivity check index: a simple, accurate method for assessing insulin sensitivity in humans. The Journal of Clinical Endocrinology & Metabolism. 2000;85(7):2402-2410. doi: 10.1210/jcem.85.7.6661. DOI
14. Khoury M, Manlhiot C, McCrindle BW. Role of the waist/height ratio in the cardiometabolic risk assessment of children classified by body mass index. Journal of the American College of Cardiology. 2013;62(8):742-751. doi: 10.1016/j.jacc.2013.01.026. DOI
15. Chen S, Zhou J, Xi M et al. Pharmacogenetic variation and metformin response. Current Drug Metabolism. 2013;14(10):1070-82. doi: 10.2174/13892002146661312111539 33. DOI
16. Koro CE, Bowlin SJ, Bourgeois N, Fedder DO. Glycemic control from 1988 to 2000 among US adults diagnosed with type 2 diabetes: a preliminary report. Diabetes care. 2004;27(1):20-17. doi: 10.2337/diacare.27.1.17. DOI
17. Sonmez A, Yumuk V, Haymana C et al. Impact of obesity on the metabolic control of type 2 diabetes: results of the Turkish nationwide survey of glycemic and other metabolic parameters of patients with diabetes mellitus (TEMD obesity study). Obesity facts. 2019;12(2):167-78. doi: 10.1159/000496624. DOI
18. Livesey G, Taylor R, Hulshof T, Howlett J. Glycemic response and health-a systematic review and meta-analysis: relations between dietary glycemic properties and health outcomes. The American journal of clinical nutrition. 2008;87(1):258S-68S. doi: 10.1093/ajcn/87.1.258S. DOI

CONFLICT OF INTEREST
The Authors declare no conflict of interest

CORRESPONDING AUTHOR
Najah Rayish Hadi
University of Kufa
299G+HPX Kufa, Najaf Governorate, Iraq
e-mail: sgahmed1331962@outlook.com

ORCID AND CONTRIBUTIONSHIP
Alaa Abd AL-Hussain Naem: 0009-0005-6658-1121 B C
Fadhaa Abdulameer Ghafil: 0000-0002-1998-9459 B C D
Mona N. Al-Terehi: 0000-0002-9244-6709 C D E
Sahar Majeed: 0000-0002-7296-499 D E
Defaf Al-Mudafer: 0009-0008-8200-0800 E F
Najah Rayish Hadi: 0000-0002-8415-5311 A F

A – Work concept and design, B – Data collection and analysis, C – Responsibility for statistical analysis, D – Writing the article, E – Critical review, F – Final approval of the article

RECEIVED: 16.09.2023
ACCEPTED: 17.07.2024

ORIGINAL ARTICLE

CONTENTS

The association of inflammatory changes of the uterus and chorioamniotic membranes with different types of labor activity anomalies

Kateryna L. Shatylovych, Leonid B. Markin
DANYLO HALYTSKY LVIV NATIONAL MEDICAL UNIVERSITY, LVIV, UKRAINE

ABSTRACT

Aim: To clarify the association between different types of uterine contractility dysfunction and the inflammation of the uterus and chorioamniotic membranes.
Materials and Methods: The association between the inflammation of the uterine layers, chorioamniotic membranes, umbilical cord, and different types of labor activity abnormalities was examined in 382 patients with singleton pregnancies at 28-42 weeks' gestation who underwent Caesarean section (CS) for abnormal uterine contractions and other complications. Statistical analyses included the Mann-Whitney U, Chi-squared test, and logistic regression.
Results: In the control group, slight infiltration with polymorphonuclear leukocytes (PMNs) and macrophages of the myometrium and decidua of the lower uterine segment at term pregnancy was found in 59.7% and 73.6% of cases. The main clinical risk factors for placental and decidual membrane inflammation in patients with excessive uterine activity (EUA) were prematurity, multiparity, group B streptococcus (GBS) colonization, and duration of ruptured fetal membranes before the CS. Moderate or marked myometrial inflammation of both uterine segments in the EUA group was diagnosed only in patients with cervical dilation of >6 cm and duration of labor of >8h. In women with hypotonic uterine activity (HUA), decidual and myometrial inflammation was significantly associated with nulliparity and intrapartum factors, such as protracted active first stage of labor, advanced cervical dilation, and number of vaginal examinations. In all cases, inflammation of the myometrium was accompanied by deciduitis.
Conclusions: Mild inflammation of the decidual membrane and myometrium of the lower segment at term pregnancy is a common physiological phenomenon contributing to labor initiation. Uterine hyperfunction comes as the response of the unaffected myometrium to the release of high concentrations of pro-inflammatory cytokines produced by the inflamed decidual and chorioamniotic membranes into the bloodstream. Marked myometrial inflammation that occurs in prolonged labor is an additional factor aggravating the hypotonic uterine activity.

KEY WORDS: hypotonic uterine activity, excessive uterine activity, uterus, inflammation, chorioamniotic membranes

Wiad Lek. 2024;77(8):1582-1592. doi: 10.36740/WLek202408108 DOI

INTRODUCTION

Abnormal labor patterns are relatively prevalent obstetric complications that justify medical intervention during labor. Approximately 20% of labors are thought to be affected by these conditions [1-4]. Hypotonic uterine activity (HUA) is one of the most common reasons for labor arrest in primiparous women that increases the risk of operative vaginal delivery, CS, and postpartum hemorrhage [3-7]. Excessive uterine activity (EUA) or uterine tachysystole produce a significant negative impact on the mothers (uterine and birth canal trauma, amniotic fluid embolism, postpartum hemorrhage) and neonates (hypoxia, intracranial hemorrhage, trauma) due to excessive myometrial stimulation [2, 7-11].

Over the last decade, it has been established that intraamniotic inflammatory response represented by chorioamnionitis (CAM) and funisitis is characterized by an increased amniotic fluid white blood cell count [12-15] and increased concentrations of inflammatory mediators which play a crucial role in human parturition [16-20]. In more recent publications, Gonzales J.M. et al. (2011), Hamilton S. et al. (2012), Hamilton S. et al. (2013), Keelan J. et al. (2018), Shynlova O. et al. (2020) [21-25] have demonstrated intense inflammatory myometrial infiltration of monocytes, neutrophils and macrophages before labor and have shown that inflammatory cytokines, bacterial lipopolysaccharide and monocytes themselves can increase myometrial cell contractions and cause a hypertonic uterine dysfunction. On the contrary, other authors [26–33] have reported that intrauterine inflammation and/or hyperthermia associated with CAM reduces uterine contractility.

Despite a better understanding of the etiology and management of labor abnormalities [1–3, 7-10, 34], our knowledge about the effect of intrauterine inflammation on the course of labor is limited. Whether preexistent

inflammation produces abnormal labor or labor aberrations contribute to the development of inflammatory complications intrapartum is an issue that appears never to have been raised. There is no unequivocal data on whether inflammatory lesions of the myometrium are associated with different types of uterine activity pathology. Since there is currently no published data on the availability of a correlation between different types of dysfunctional labor and the inflammatory changes of the uterus and chorioamniotic membranes, the measurement of such potential complications is important for the development of possible preventive measures.

AIM

The aim of our study was to examine the association between different types of uterine contractility dysfunction and the inflammation of the uterus and chorioamniotic membranes.

MATERIALS AND METHODS

The study comprised 382 women with singleton pregnancy at 28-42 weeks' gestation who underwent CS due to abnormal uterine contractions and other complications.

Maternal information included maternal age, parity, gestational age (based on the last menstrual period and/or ultrasound examination findings), GBS colonization, clinical CAM status, duration of labor (defined as the presence of true labor pain and partograph data until the CS), duration of ruptured fetal membranes period prior to operation, level of cervical dilation at the surgery, number of vaginal examinations, oxytocin usage, antibiotic, antipyretic and tocolytic treatment.

The first observation group enrolled 168 women with HUA who were operated on due to the absence of labor progress. The second observation group consisted of 70 women with EUA who were made to deliver abdominally because of intrapartum cardiotocography (CTG) abnormalities, placental abruption, and combined indications. The control group included 144 women (65 women in the first stage of labor with regular uterine contractions and 79 women without labor) who underwent CS due to different indications.

Oxytocin was used for augmentation of labor in all patients in HUA group when the action line on partograph (four hours to the right of the alert line) was crossed [35–38] and for induction of labor in GBS-infected women with premature rupture of membranes in EUA and control group patients [39–40]. Prophylactic antibiotics were always administered after cord clamping and biopsy removal. Intrapartum antibiotics were administered to patients with GBS colonization, in the setting of prolonged membrane rupture (>18 hours) in women with an unknown GBS status as well as to patients with symptoms of clinical CAM [39–40]. Women with hyperthermia received antipyretic therapy [29–30, 32]. In cases of acute fetal distress combined with tachysystole, acute tocolysis with selective beta$_2$ (ß$_2$)-adrenergic agonists was used [10].

CARDIOTOCOGRAPHY

The CTGs on admission and during labor were carefully analyzed to define fetal heart rate and uterine activity abnormalities. The following criteria of fetal distress were applied: diminished short-term heart rate variability (variability < 5 beats per minute (bpm) persisting for >20 minutes); sustained tachycardia (basal heart rate > 160 bpm for > 20 minutes); sustained bradycardia (basal heart rate < 100 bpm >20 minutes); repetitive late or variable decelerations; sinusoidal pattern (visually apparent, smooth, sine wave-like, undulating pattern in fetal heart rate baseline with a cycle frequency of 3-5 per minute persisting for >20 minutes) [41].

External monitoring of uterine contractions using a tocodynamometer evaluates increased myometrial tension measured through the abdominal wall. 5 contractions with an intensity of >200 Montevideo units (MU) were considered to be adequate uterine activity (peak intensity of each contraction calculated in millimeters of mercury (mm Hg) minus basal uterine tone, summed over a 10-min period) but <300 MU with basal tone < 25 mmHg and > 50 mmHg contraction peak/active pressure in a 10-minute period for 2 hours [41]. Excessive uterine activity (EUA) was defined as increased intensity of contractions (MU >300), uterine tachysystole (the CTG showed more than 5 contractions in a 10-minute period, averaged over a 30-minute window), uterine hypertonus (a single contraction lasting for more than 2 min or contractions of normal duration occurring with a relaxation time of less than 60 seconds or resting pressure >25 mmHg) [2, 41]. Hypotonic uterine activity (HUA) was diagnosed when more than one of the following criteria was met: decreased intensity of contractions (MU <200), the frequency of contractions is <2 within 10 minutes, the peak/active pressure during contraction is < 25 mmHg at the cervical dilation of 4 to 8 cm and <40 mmHg at the cervical dilation of >9 cm, the duration of contraction is <20 to 30 seconds at the cervical dilation of >4 cm [41]. A protracted active first stage (once 4-cm cervical dilation is achieved) was defined as no cervical dilation after 6 hours of inadequate contractions, with ruptured membranes, despite oxytocin administration [1, 38].

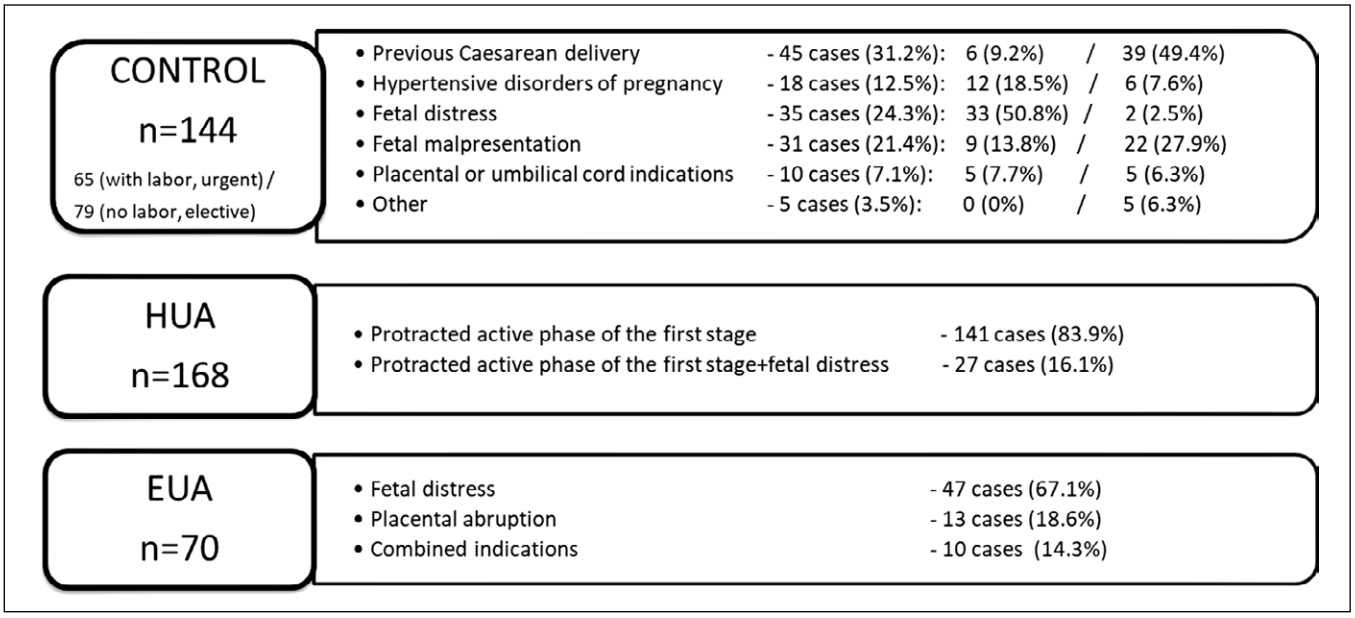

Fig. 1. Indications for Caesarean section.

HISTOLOGICAL EXAMINATION

Full-thickness biopsy specimens of endometrium (decidua) and myometrium from the upper margin of the lower uterine segment incision and upper uterine segment obtained through the dissection of a strip of myometrium from the inner surface of the posterior uterine wall during the CS were received immediately after delivery of the child and taken for histopathologic assessment. In 5 women in the HUA group, myometrial biopsies were taken from the anterior wall of the lower segment and upper uterine body, immediately following the hysterectomy.

The following sites of the placentas were sampled: chorion-amnion, the chorionic plate, and the umbilical cord. Three to nine sections of the placenta were examined, and at least one full-thickness section was taken from the center of the placenta; others were taken randomly from the placental disc [42].

Each of the samples was placed in 10% neutral buffered formalin for fixation and embedded in paraffin. Sections of tissue blocks were stained with hematoxylin and eosin. Samples were fixed for 24 hours at 4°C.

The presence of inflammatory reaction in the myometrium and endometrium (decidual tissue) was analyzed and correlated with the clinical parameters of the case. Evaluation of specimens was modified from the scale described by Keski-Nisula L.T. et al., 2003 [43]. Normal samples were graded 0, and those that contained clearly identifiable polymorphonuclear leukocytes (PMNs) and monocytes/macrophages were graded as positive for acute inflammation using a scale of 1 to 4: 1, or mild: 1 focus of at least 5 PMNs and 3 macrophages; 2, or moderate: >1 focus of grade 1 inflammation or at least 1 focus of 5-20 PMNs and 3-10 macrophages; 3, or marked: multiple and/or confluent foci of grade 2; 4, or very marked: diffuse and dense acute inflammation.

Inflammatory lesions of the placenta and umbilical cord were diagnosed according to established criteria [44-46]. Placental inflammation was defined as the infiltration of neutrophils into the chorion and amnion. Histologic chorioamnionitis (hCAM) was defined as the presence of acute inflammatory changes on examination of a membrane roll and chorionic plate of the placenta: stage 1 (hCAM1) – acute subchorionitis or chorionitis; stage 2 (hCAM2) – acute chorioamnionitis: PMNs extend into fibrous chorion and/or amnion; stage 3 (hCAM3) – necrotizing chorioamnionitis: karyorrhexis of PMNs, amniocyte necrosis, and/or amnion basement membrane hypereosinophilia. Funisitis was diagnosed in the presence of neutrophil infiltration into the umbilical vessel walls or Wharton's jelly, according to criteria of Amsterdam Placenta Workshoup Group [47]: stage 1 – chorionic vasculitis or umbilical phlebitis; stage 2 – involvement of the umbilical vein and one or more umbilical arteries; stage 3 – necrotizing funisitis.

The present study was approved by the institutional review board (Bioethics Commission) of Danylo Halytsky Lviv National Medical University (No. 156). All procedures in this study were performed in accordance with the ethical standards of the institutional and national research committee.

STATISTICAL ANALYSIS

Mann-Whitney U test and one-way analysis of variance were used to compare the continuous

Table 1. Clinical characteristics of the patients in the HUA, EUA, and control groups

Variable	Groups of patients			p-value
	HUA n=168	EUA n=70	Control n=144	
Maternal age, years (mean±SD)	27.6±5.7	32.1±4.8	30.3±4.2	NS
Gestational age at delivery, weeks (mean±SD)	40.2±1.4	33.3±4.6	38.4±4.1	<0.01[a]
Multiparous, n (%)	65 (38.7)	53 (75.7)	82 (56.9)	<0.05[b]
Primiparous, n (%)	103 (61.3)	17 (24.3)	62 (43.1)	<0.05[b]
Birth weight at delivery, g (mean±SD)	3680±458	1920±814	3440±465	<0.01[a]
GBS-colonization, n (%)	16 (9.5)	10 (14.3)	9 (6.3)	NS
Clinical CAM:	14 (8.3)	13 (18.6)		<0.05[b]
antenatally, n (%)	2 (1.2)	9 (12.9)	0	<0.01[b]
intrapartum, n (%)	12 (7.1)	4 (5.7)		<0.05[b]

Values are given as mean±standard deviation (SD) unless specified otherwise
[a] – p-value: one-way analysis of variance
[b] – p-value: chi-squared test
NS – p-value: not significant (p>0.05).

Table 2. Obstetric characteristics of the patients in the HUA, EUA, and control groups

Variable	Groups of patients			p-value
	HUA n=168	EUA n=70	Control n=65	
Mean interval from onset of labor to the surgery, h (mean±SD)	18.4±6.9	5.6±4.2	8.8±3.3	<0.05[a]
Premature rupture of fetal membranes, n (%)	81 (48.2)	57 (81.4)	14 (21.5)	< 0.05[b]
Duration of ruptured fetal membranes before the surgery, h (mean±SD)	16.2±8.0	51.7±41.7	6.2±1.4	<0.01[a]
Mean cervical dilation at the surgery, cm (mean±SD)	8.1±1.7	4.4±1.8	5.6±2.5	<0.05[a]
Number of vaginal examinations with membrane rupture before the surgery >4, n (%)	81 (48.2)	0	4 (6.2)	<0.01[b]
Uterine activity in the 0.5 h prior to delivery, MU (mean±SD)	94±37	422±66	168±53	<0.05[a]
Use of oxytocin, n (%)	168 (100)	6 (8.6)	3 (4.6)	<0.01[b]
Intrapartum antibiotics, n (%)	53 (31.6)	43 (61.4)	3 (4.6)	<0.01[b]
Use of antipyretics, n (%)	10 (5.9)	9 (12.9)	0	<0.05[b]
Acute tocolysis, n (%)	0	22 (31.4)	0	NS

Results are expressed as mean ±standard deviation (SD) unless specified otherwise
MU - Montevideo units
[a] - p-value: one-way analysis of variance
[b] - p-value: chi-squared test
NS – p-value: not significant (p>0.05).

variables. Chi-squared test was used to compare the categorical variables. Comparative analysis of the development of HUA, EUA, and availability of inflammation in the tissue samples, as well as identification of univariate associations between the labor abnormalities and preoperative clinical factors were carried out through logistic regression analysis performance. For each variable, one category as the control was chosen, and odds ratios (ORs) or adjusted odds ratios (aORs) and 95% confidence intervals (CI) for the other categories were calculated. Probability values p<0.05 were considered to be statistically significant. Statistica 10 software (StatSoft, USA) was used for the statistical analyses.

RESULTS

Figure 1 shows the main indications for cesarean section of the study participants.

Table 1 and Table 2 show the clinical and obstetric characteristics of the study patients in observed groups.

The mean maternal age was not different among the groups (p>0.05), although the HUA group tended to have more patients aged 18–25 years. The mean gestational age at delivery in patients in the HUA and control groups differed significantly from patients in the EUA group (40.2, 38.4 and 33.3 weeks, respectively (p<0.01). The rate of primiparous in the HUA group (61.3%) was far above that of the EUA (24.3%) and control groups (43.1%) (p<0.05).

Table 3. The grade of inflammatory infiltration of decidua and myometrium in the HUA, EUA, and control groups patients

Grade	Groups of patients			p-value[a]
	HUA, n=168	EUA, n=70	Control, n=144	
Decidual samples, n (%)				
0	0	0	14 (9.7)	NS
1	49 (29.2)	17 (24.3)	106 (73.6)	< 0.01
2	54 (32.1)	23 (32.9)	16 (11.1)	< 0.05
3	55 (32.7)	18 (25.7)	8 (5.6)	< 0.05
4	10 (6.0)	7 (10)	0	< 0.05
Grade ≥2	119 (70.8)	48 (68.6)	24 (16.7)	< 0.01
Myometrial samples (lower segment), n (%)				
0	0	0	48 (33.4)	NS
1	58 (34.5)	38 (54.3)	86 (59.7)	NS
2	82 (48.8)	14 (20)	10 (6.9)	< 0.01
3	23 (13.7)	3 (4.3)	0	< 0.01
4	5 (3)	0	0	NS
Grade ≥2	110 (65.5)	17 (24.3)	10 (6.9)	< 0.01
Myometrial samples (upper segment), n (%)				
0	13 (7.7)	18 (25.7)	122 (84.7)	< 0.01
1	55 (32.7)	25 (35.7)	15 (10.4)	< 0.05
2	74 (44.1)	12 (17.1)	7 (4.9)	< 0.01
3	11 (6.5)	0	0	NS
4	5 (3)	0	0	NS
Grade ≥2	90 (53.6)	12 (17.1)	7 (4.9)	< 0.01

[a] - p-value: chi-squared test

NS – p-value: not significant (p >0.05).

Due to the prevalence of preterm labor, the mean weight of newborns was much higher in the HUA and control groups than in the EUA group patients (3,680 g and 3,440 g vs 1,920 g, p<0.01).

Clinically evident CAM was diagnosed more frequently in the EUA group patients compared to those in the HUA group (18.6% vs 8.3%, p <0.05). However, in the HUA group, 12 out of 14 women developed clinical CAM intrapartum due to prolonged labor. The EUA group was dominated by the patients with clinical CAM (9/13), which developed antenatally against the background of a prolonged period (> 72 h) from rupture of the fetal membranes prior to delivery.

In the process of comparing the course of labor (Table 2), the following statistically significant differences among the study patients were found between the groups. Women in the EUA group had a higher incidence of premature rupture of membranes than women in the HUA and control groups (81.4% (EUA group) vs 48.2% (HUA group), and 21.5% (control group), p<0.05); a shorter mean interval from onset of labor to the CS (5.6±4.2 h vs 18.4±6.9 h, and 8.8±3.3 h, p< 0.05); a longer period of rupture of fetal membranes (51.7±41.7 h vs 16.2±8.0 h, and 6.2±1.4 h, p<0.01); a lower level of cervical dilation (4.4±1.8 cm vs 8.1±1.7 cm, and 5.6±2.5 cm, p<0.05) and stronger uterine activity (422±66 MU vs 94±37 MU, and 168±53 MU, p<0.05). More than 4 vaginal examinations after membrane rupture during the management of labor were performed in 81 (48.2%) women in the HUA group and in 4 (6.2%) women in the control group (p<0.01).

Intrapartum antibiotics in the HUA, EUA, and control groups were administered to 99 parturients (in all GBS-colonized women after rupture of membranes or beginning of labor (n=16; n=8; n=3); in patients with an unknown GBS status and the duration of ruptured fetal membranes >18h (n=25; n=26; n=0); in patients with symptoms of clinical CAM in labor (n=12; n=4; n=0). In all cases with CAM and fever (n=10 in the HUA group and n=9 in the EUA group) antipyretics were prescribed. 22 patients in the EUA group underwent acute tocolysis before surgery due to fetal distress.

The data of histological analysis of the uterine walls layers and fetal and placental membranes in studied groups are presented in Table 3 and Table 4.

Absence of decidual inflammation (0 grade) was found only in 14 patients in the control group (9.7%)

Table 4. The stage of hCAM and funisitis in the HUA, EUA, and control group patients

Stage	Groups of patients			p-value[a]
	HUA, n=168	EUA, n=70	Control, n=144	
hCAM stage, n (%)				
Not present	93 (55.4)	9 (12.9)	121 (84)	< 0.01
1	37 (22)	7 (10)	17 (11.8)	< 0.05
2	9 (5.4)	20 (28.6)	3 (2.1)	< 0.05
3	11 (6.5)	19 (27.1)	3 (2.1)	< 0.05
hCAM	57 (33.9)	46 (65.7)	23 (16)	< 0.05
Stage ≥2	20 (11.9)	39 (55.7)	6 (4.2)	< 0.01
Funisitis stage, n (%)				
Not present	140 (83.3)	46 (65.7)	139 (96.5)	< 0.05
1	16 (9.5)	6 (8.6)	3 (2.1)	NS
2	9 (5.4)	11 (15.7)	1 (0.7)	< 0.05
3	3 (1.8)	7 (10)	1 (0.7)	< 0.05
Funisitis	28 (16.7)	24 (34.3)	5 (3.5)	< 0.05
Stage ≥2	12 (7.2)	18 (25.7)	2 (1.4)	< 0.05

[a] - p-value: chi-squared test
NS – p-value: not significant.

who were delivered by elective CS at less than 36 weeks' gestation. Decidual PMN and macrophage infiltration of mild grade was detected in the HUA, EUA, and control groups in 29.2%, 24.3%, 73.6% cases, respectively (p<0.05). Moderate to marked decidual inflammation was diagnosed more frequently in the samples from the HUA and EUA groups than from the control group parturients (70.8% and 68.6% vs 16.7%, p<0.05).

In contrast to the decidual tissue, the 1st grade of inflammatory changes in the myometrium of the lower uterine segment was diagnosed more frequently, although no significant difference was noted between the observation groups (Table 3). Moderate to marked myometrial inflammation of both uterine segments was identified in 53.6%, 17.1%, and in 4.9% patients of the HUA, EUA, and control group, respectively (p<0.05). In all cases, inflammation of the myometrium was accompanied by inflammatory changes in the decidual tissue. Very marked myometrial inflammation of both uterine segments was detected in the tissue samples of 5 women in the HUA group who underwent hysterectomy due to hypotonic bleeding during the CS.

In contrast to clinical CAM, acute hCAM was diagnosed significantly more frequently and was observed in 33.9% of patients in the HUA group, in 65.7% of patients in the EUA group and in 16% of patients in the control group. It was noted that the incidence of histologically confirmed acute CAM of stage 2+ was only 11.9% among the HUA group cases but as high as 55.7% among the EUA group cases, p<0.01. The combination of hCAM and funisitis of stage 2+ was reported in the HUA, EUA, and control groups in 12 (7.2%), 18 (25.7%), and 2 (1.4%) cases, respectively (p< 0.05). There were no cases of isolated funisitis in all observation groups.

The presence of an inflammatory reaction in the myometrium, endometrium (decidual tissue), placental, and fetal membranes was analyzed and correlated with clinical parameters of the cases in the HUA and EUA groups (Table 5).

Analysis of data (Table 5) showed rather contradictory results in the observation groups, due to the pathophysiologic opposite of the main clinical complication by which the patients were selected into groups - excessive or hypotonic uterine activity in labor.

Multiple logistic regression analysis indicated that the frequency of deciduitis was associated with the gestational age (>37 weeks in the HUA group, but <37 weeks in the EUA group), parity (nulliparity in the HUA group, but multiparity in the EUA group), GBS colonization (in the EUA group), duration of active first stage before operation (>12 h in the HUA group and >8 h in the EUA group), duration of ruptured fetal membranes before the surgery (>24 h in both groups), cervical dilation (>6 cm in both groups), and a high number of vaginal examinations in labor (in the HUA group).

The odds of myometritis in both observation groups increased with the duration of labor, advanced cervical dilation, quantity of vaginal examinations, and nulliparity (in the HUA group).

hCAM and funisitis were significantly associated in both groups with GBS colonization, parity (nulliparity in the HUA group, multiparity in the EUA group), gestational age (>37 weeks in the HUA group, but <37 weeks in the EUA group), and prolonged (>24 h) duration of ruptured fetal membranes.

Table 5. Unadjusted odds ratios and 95% confidence intervals for grade 2+ deciduitis and myometritis, stage 2+ inflammation of the placental and fetal membranes associated with various clinical preoperative factors among parturients with HUA and EUA

Factors	Decuduitis		Myometritis (lower segment)		Myometritis (both segments)		hCAM		Funisitis	
	HUA	EUA	HUA	EUA	HUA	EUA	HUA	EUA	HUA	EUA
	Odds ratio (95% CI) p-value		Odds ratio (95% CI) p-value		Odds ratio (95% CI) p-value		Odds ratio (95% CI) p-value		Odds ratio (95% CI) p-value	
Gestational age (weeks) <37	0.4 (0.1-1.3) p < 0.05	6.9 (2.2-21.9) p < 0.001	0.9 (0.04-0.7) p < 0.05	0.8 (0.5-9.3) p < 0.05	0.7 (0.03-11.8) NS	0.3 (0.02-7.1) p < 0.05	0.1 (0.02-10.6) NS	1.7 (0.3-10.6) p < 0.01	0.1 (0.05-13.7) NS	1.9 (0.3-22.8) p < 0.001
37-41	2.1 (0.9-5.2) p < 0.001	0.9 (0.3-2.5) p < 0.05	0.8 (0.6-4.6) p < 0.05	0.3 (0.08-4.9) p < 0.05	0.6 (0.1-6.1) p < 0.01	0.8 (0.7-7.7) p < 0.05	0.9 (0.2-21.2) p < 0.05	0.5 (0.2-14.5) p < 0.05	0.2 (0.04-33.4) p < 0.05	0.5 (0.04-22.1) NS
>41	1.6 (0.2-3.4) p < 0.01	-	0.6 (0.1-2.2) p < 0.05	-	0.7 (0.1-3.3) p < 0.05	-	1.2 (0.6-9.2) p < 0.05	-	0.7 (0.2-9.7) p < 0.01	-
Nulliparous	1.8 (0.5-6.2) p < 0.05	0.7 (0.3-2.8) p < 0.05	1.6 (0.5-4.8) p < 0.05	0.1 (0.2-1.6) p < 0.05	1.4 (0.2-14.2) p < 0.05	0.2 (0.07-2.1) p < 0.05	1.1 (0.3-7.3) p < 0.05	0.3 (0.05-1.7) p < 0.05	0.7 (0.2-9.2) p < 0.05	2.9 (0.2-55.8) p < 0.05
Multyparous	0.6 (0.3-1.9) p < 0.05	1.4 (0.9-16.7) p < 0.05	0.3 (1.5-7.5) p < 0.05	0.9 (0.1-8.5) p < 0.05	0.1 (0.2-7.2) p < 0.05	0.1 (0.05-1.4) p < 0.05	0.7 (0.1-4.0) p < 0.05	4.4 (3.1-14.8) p < 0.05	0.1 (0.01-6.9) p < 0.05	4.8 (0.9-24.0) p < 0.01
GBS colonization	0.7 (0.1-1.2) p < 0.05	3.5 (0.6-26.6) p < 0.001	0.7 (0.08-8.1) p < 0.05	0.1 (0.05-18.0) NS	0.6 (0.05-16.9) NS	0.8 (0.04-14.9) NS	1.3 (0.2-4.8) p < 0.01	2.7 (0.5-14.9) p < 0.05	1.2 (0.01-9.7) p < 0.05	3.5 (0.5-23.3) p < 0.01
Duration of ruptured fetal membranes before the CS >24 h	1.9 (1.0-4.4) p < 0.001	2.6 (1.0-4.4) p < 0.001	0.7 (0.2-1.3) p < 0.05	0.3 (0.08-2.7) p < 0.05	0.9 (0.2-5.5) p < 0.01	0.5 (0.05-10.4) p < 0.01	0.6 (0.2-7.9) p < 0.05	1.3 (0.2-7.8) p < 0.001	1.1 (0.02-21.2) p < 0.05	1.2 (0.8-54.5) p < 0.01
Duration of active first stage before the CS 8-12h	0.7 (0.1-3.2) p < 0.01	1.6 (0.4-12.9) p < 0.05	0.8 (0.2-2.7) p < 0.05	1.9 (1.1-18.4) p < 0.05	0.8 (0.2-3.8) p < 0.01	1.5 (0.8-21.1) p < 0.05	0.6 (0.3-9.6) p < 0.01	0.7 (0.2-5.5) p < 0.01	0.5 (0.04-31.8) NS	0.6 (0.2-28.4) NS
>12h*	2.7 (0.9-8.3) p < 0.001	-	3.5 (1.2-10.4) p < 0.001	-	4.8 (1.5-15.7) p < 0.001	-	1.2 (0.4-3.8) p < 0.01	-	0.8 (0.02-50.6) NS	-
Advanced cervical dilation at CS (>6 cm)	3.8 (1.7-8.6) p < 0.001	1.8 (0.3-10.5) p < 0.01	1.3 (0.4-3.8) p < 0.001	4.3 (1.8-9.9) p < 0.001	1.7 (0.8-6.3) p < 0.01	3.9 (1.5-10.6) p < 0.01	1.6 (0.1-5.1) p < 0.05	0.7 (0.09-34.9) NS	0.3 (0.05-13.7) NS	0.4 (0.06-22.1) NS
Number of vaginal examinations >4	7.8 (2.8-21.9) p < 0.001	-	5.4 (7.1-23.8) p < 0.001	-	1.7 (0.3-10.2) p < 0.001	-	1.1 (0.1-9.8) p < 0.01	-	0.2 (0.04-31.4) p < 0.05	-

CI - confidence interval
NS – p-value: not significant
*Oxytocin usage.

After adjustment was made for clinically relevant variables, multiple logistic regression analysis indicated that a significant relationship remained between HUA and decidual and myometrial inflammation, between EUA and deciduitis, hCAM, and funisitis (Table 6).

DISCUSSION

The correlation between two different types of labor anomalies and availability of inflammation in the uterus, placental, and fetal membrane samples was examined. The results obtained in the control group confirmed the results of the previous researchers, according to whom macrophages and neutrophils infiltrate the uterine lower segment myometrium and decidua parietalis before and at the beginning of the physiological term labor [18, 21, 22, 25, 43]. Activated macrophages and neutrophils themselves are a powerful source of pro-inflammatory cytokines, prostaglandins, proteases, and reactive oxygen species [16-18, 23-24], which are capable of initiating and amplifying inflammatory responses of the decidua, adjacent myometrium, cervix, placental and fetal membranes, and finally triggering labor. Inflammatory mediators have many diverse functions in different parts of the uterus. Within the lower segment, they take part in connective tissue remodeling

Table 6. Unadjusted odds ratios, adjusted odds ratios and 95% confidence intervals for grade 2+ deciduitis and myometritis, stage 2+ inflammation of the placental and fetal membranes in the presence of HUA and EUA

Grade/Stage 2+	HUA			EUA		
	OR (95% CI)	aOR (95% CI) *	p-value	OR (95% CI)	aOR (95% CI) *	p-value
Deciduitis	3.1 (1.0-11.1)	1.4 (0.6-3.6)	p < 0.01	5.9 (3.1-11.3)	2.6 (1.4-4.8)	p < 0.01
Myometritis (lower segment)	5.4 (2.4-8.0)	2.1 (1.2-6.2)	p < 0.01	4.3 (1.8-9.9)	0.5 (0.4-1.3)	p < 0.01
Myometritis (both segments)	9.5 (8.6-21.3)	3.9 (1.3-14.7)	p < 0.01	4.1 (1.5-10.8)	0.7 (0.3-2.4)	p < 0.05
hCAM	1.8 (0.9-28.4)	0.8 (0.3-4.9)	p < 0.05	11.0 (2.9-32.8)	4.5 (3.4-12.1)	p < 0.01
Funisitis	1.5 (1.2-24.8)	0.3 (0.6-2.7)	p < 0.05	4.7 (1.9-12.6)	2.9 (1.3-10.6)	p < 0.01

OR - odds ratio
aOR - adjusted odds ratio
CI - confidence interval
*Adjusted for gestational age, parity, GBS colonization, duration of ruptured fetal membranes, duration of active first stage, cervical dilation, number of vaginal examinations before operation.

and thereby facilitate cervical dilation and passage of the fetus. In the upper segment, leukocyte products, including eicosanoids, interleukins, and tumor necrosis factor α may stimulate uterine contractions directly or indirectly by facilitating the production of prostaglandins [18, 22]. Thus, mild inflammatory changes in the decidual membrane and slight leukocyte infiltration of the lower segment of the uterus constitute a necessary prerequisite for the physiological onset of labor.

A significant difference in parity, gestational age, and birth weight at delivery among the HUA and EUA observation groups was found. Multiparity, early gestational age, and low birth weight of newborns were strongly associated with EUA. In contrast to the EUA group, primiparous patients at term pregnancies dominated in the HUA group.

When comparing the histological findings, the localisation of inflammatory changes between the groups also differed: myometritis prevailed in the HUA group, while hCAM and funisitis were predominant in the EUA group. Both groups had a high incidence rate of decidual inflammation. It should be noted that severe deciduitis was also diagnosed in the control group (16.7%), but only in those patients who underwent surgery after several hours of regular labor against the background of premature rupture of the amniotic membranes.

The main clinical risk factors for placental and decidual membrane inflammation in the EUA group were prematurity, multiparity, GBS colonization, and duration of ruptured fetal membranes before the CS (Table 5), which is indicative of the occurrence of inflammatory changes antenatally. Despite high incidence of deciduitis (68.6%) and hCAM (55.7%) in this group, moderate to marked myometrial inflammation of both uterine segments was diagnosed in only 17.1% of patients, mostly in women with cervical dilation of >6 cm and duration of labor of >8h. In all cases, myometrial changes occurred along with severe deciduitis.

We attribute such a low incidence of myometrial lesions in the EUA group to the rapid progression of labor (mean time from the beginning of contractions to the CS was 5.6±4.2 h), and insufficient time for significant leukocyte penetration into the deeper myometrial layers of the lower and upper uterine segments. High magnitude of aORs for deciduitis, hCAM and funisitis (2.6, 4.5, 2.9, respectively, p<0.01 (Table 6) in patients in the EUA group indicate involvement of not only the decidual but also the chorioamniotic membranes in the synthesis of proinflammatory cytokines. If physiological levels of inflammatory agents contribute to normal uterine contraction, it is reasonable to assume that their significantly elevated rates will cause stronger contractions and lead to hypertensive uterine dysfunction. In our opinion, the key factor in this process is that the myometrium remains intact by inflammation.

The inflammatory nature of tachysystole was also confirmed by some of our clinical and therapeutic observations. We noted the ineffectiveness of acute tocolysis in 13 of 22 patients (59.1%) who received tocolytic drugs alone, and a decrease of the uterine activity in the remaining 9 of 22 women (40.9%) who were prescribed tocolytics in combination with antipyretics against the background of clinical CAM symptoms (hyperthermia). Thus, uterine hyperfunction, which is insensitive to tocolytic agents, comes as a response of the unaffected myometrium to the release of huge concentrations of pro-inflammatory cytokines into the bloodstream. In such situations, the use of anti-inflammatory drugs rather than tocolytic agents may be more effective in the treatment of uterine tachysystole.

It is well-known that hCAM and funisitis demonstrate an inflammatory response of the placenta, fetal mem-

branes, and amniotic fluid to microbial invasion of the amniotic cavity [12-14, 19], and deciduitis indicates an ascending pathway of infection [15, 22-23]. However, in the HUA group our data showed the association of decreased uterine contractility with grade 2+ deciduitis (aOR: 1.4, 95% CI: 0.6-3.6), but no association with stage 2+ hCAM (aOR: 0.8, 95% CI: 0.3-4.9) and stage 2+ funisitis (aOR: 0.3, 95% CI: 0.6-2.7) (Table 6). The limitation of our study was the inability to obtain histological specimens before or at least at the beginning of labor in the observation groups. Therefore, we are unable to deny or state with certainty that inflammation of parietal decidua was present or absent before the labor. Such clinical risk factors for the development of severe deciduitis as protracted active first stage, advanced cervical dilation, and a large number of vaginal examinations (Table 5) revealed during statistical analysis in the HUA group indicate the progression of inflammatory pathology of the decidual membrane intrapartum. The latter suggests that progressive severe deciduitis may be an additional risk factor for the development of hypotonic uterine activity.

In contrast to the EUA group, moderate to severe myometritis was a common finding in patients of the HUA group (53.6% of cases). In multiple stepwise logistic regression analysis, myometrial inflammation was largely associated with nulliparity, protracted active first stage with oxytocin augmentation, advanced cervical dilation, and the number of vaginal examinations (Table 5). The results of our study partially coincide with the earlier works by L.T. Keski-Nisula and coauthors (2003) [43], and J.M. Gonzalez and coauthors (2011) [21] who noted inflammatory cell infiltration of the myometrium with an increase in the duration of labor and cervical dilation.

Severe myometrial inflammation in all cases was detected in conjunction with severe deciduitis (84/84), much less frequently with severe hCAM (15/84) and funisitis (7/84). Long-term weak contractions, only temporarily enhanced by oxytocin, allow decidual inflammation to spread deeper into the myometrium of both the lower and upper segments of the uterus. According to our histological data, it can be concluded that development of myometritis in patients with HUA is the result of ascending deciduitis that gradually progresses to grade 2+ during prolonged labor. Slow penetration of leukocytes into the myometrium leads to remodeling of the extracellular matrix, dysregulation of oxytocin receptor synthesis, and a decrease in the uterine response to both intrinsic and extrinsic oxytocin [26, 33, 37]. The consequence of long-lasting labor augmentation with oxytocin is insensitivity to this agent, complete uterine inertia, and postpartum hemorrhage [26, 27]. The latter occurred in 5 parturients with total leukocyte infiltration of the myometrium who underwent hysterectomy due to atonic uterine bleeding. In such situations, the possibility of prescribing other groups of uterotonics should be considered when choosing drugs for the prevention or treatment of postpartum bleeding.

CONCLUSIONS

Mild inflammation of the decidual membrane and the myometrium of the lower uterine segment at term pregnancy is a physiological phenomenon that contributes to the initiation of labor. Inflammation of the chorioamniotic and decidual membranes against the background of intact myometrium plays a fundamental role in the occurrence of hypertensive uterine dysfunction, particularly in preterm birth. Inflammatory changes in the myometrium of the lower and especially upper uterine segment arising during prolonged term labor are an additional factor contributing to the onset or aggravation of the hypotonic uterine activity. Strategies aimed at preventing the influx of inflammatory cells into the uterine cavity can be crucial for the prevention of preterm labor, as well as for the coordination of uterine activity at term labor.

REFERENCES

1. Gill P, Henning JM, Carlson K et al. Abnormal Labor. Treasure Island (FL): StatPearls Publishing. 2023.
2. Hobson SR, Abdelmalek MZ, Farine D. Update on uterine tachysystole. J Perinat Med. 2018;0(0):1-9. doi:10.1515/jpm-2018-0175. DOI
3. LeFevre NM, Krumm E, Cobb WJ. Labor dystocia in nulliparous women. Am Fam Physician. 2021;103(2):90-96.
4. Blankenship SA, Raghuraman N, Delhi A et al. Association of abnormal first stage of labor duration and maternal and neonatal morbidity. Am J Obstet Gynecol. 2020;223(3):445.e1-445.e15. doi:10.1016/j.ajog.2020.06.053. DOI
5. Ragusa A, Gizzo S, Noventa M et al. Prevention of primary caesarean delivery: comprehensive management of dystocia in nulliparous patients at term. Arch Gynecol Obstet. 2016;294(4):753–761. doi:10.1007/s00404-016-4046-5. DOI
6. Ende HB, Lozada MJ, Chestnut DH et al. Risk factors for atonic postpartum hemorrhage: a systematic review and meta-analysis. Obstet Gynecol. 2021;137(2):305-323. doi:10.1097/AOG.0000000000004228. DOI
7. Heuser CC, Knight S, Esplin MS et al. Tachysystole in term labor: incidence, risk factors, outcomes, and effect on fetal heart tracings. Am J Obstet Gynecol. 2013;209(1):32.e1–6. doi:10.1016/j.ajog.2013.04.004. DOI

8. Smith S, Zacharias J, Lucas V et al. Clinical associations with uterine tachysystole". J Matern Fetal Neonatal Med. 2014;27:709-13. doi:10.3109/14767058.2013.836484. DOI
9. Sims ME. Legal briefs: tachysystole, uterine rupture, and a bad outcome. Neoreviews. 2019;20(2):e110-e112. doi:10.1542/neo.20-2-e110. DOI
10. Leathersich SJ, Vogel JP, Tran TS et al. Acute tocolysis for uterine tachysystole or suspected fetal distress. Cochrane Database Syst Rev. 2018;7(7):CD009770. doi: 10.1002/14651858.CD009770.pub2. DOI
11. Reynolds AJ, Geary MP, Hayes BC. Intrapartum uterine activity and neonatal outcomes: a systematic review. BMC Pregnancy Childbirth. 2020;20(1):532. doi:10.1186/s12884-020-03219-w. DOI
12. Kim CJ, Romero R, Chaemsaithong P et al. Acute chorioamnionitis and funisitis: definition, pathologic features, and clinical significance. Am J Obstet Gynecol. 2015;213:S29–52. doi:10.1016/j.ajog.2015.08.040. DOI
13. Tita ATN, Andrews WW. Diagnosis and management of clinical chorioamnionitis. Clinics in Perinatology. 2010;37(2):339–354. doi:10.1016/j.clp.2010.02.003. DOI
14. Romero R, Chaemsaithong P, Korzeniewski SJ et al. Clinical chorioamnionitis at term III: how well do clinical criteria perform in the identification of proven intra-amniotic infection? J Perinat Med. 2015. doi:10.1515/jpm-2015-0044. DOI
15. Markin LB, Tatarchuk TF, Shatylovych KL. Pathogenetic therapeutic and preventive measures in women of risk group of isthmicocervical incompetence. Reprod Endocrin. 2017;4(36):44-47. doi:10.18370/2309-4117.2017.36.44-47. DOI
16. Slutsky R, Romero R, Xu Y et al. Exhausted and senescent T cells at the maternal-fetal interface in preterm and term labor. J Immunol Res. 2019;23:1–16. doi:10.1155/2019/3128010. DOI
17. Than NG, Hahn S, Rossi SW et al. Editorial: fetal-maternal immune interactions in pregnancy. Front Immunol. 2019;10:2729. doi:10.3389/fimmu.2019.02729. DOI
18. Gomez-Lopez N, StLouis D, Lehr MA et al. Immune cells in term and preterm labor. Cell Molecul Immunol. 2014;11(6):571-581. doi:10.1038/cmi.2014.46. DOI
19. Romero R, Chaemsaithong P, Korzeniewski SJ et al. Clinical chorioamnionitis at term II: the intra-amniotic inflammatory response. J Perinat Med. 2015;44(1):5-22. doi:10.1515/jpm-2015-0045. DOI
20. Sklyarova VO, Filipyuk AL, Shatylovych KL et al. Platelet-rich plasma in the management of chronic endometritis treatment in women with reproductive health disorders. Eur J Med Health Sci. 2020;2(6):1-3. doi:10.24018/ejmed.2020.2.6.560. DOI
21. Gonzalez JM, Franzke C-W, Yang F et al. Complement activation triggers metalloproteinases release inducing cervical remodeling and preterm birth in mice. Amer J Pathol. 2011;179(2):838–849. doi:10.1016/j.ajpath.2011.04.024. DOI
22. Hamilton S, Oomomian Y, Stephen G et al. Macrophages infiltrate the human and rat decidua during term and preterm labor: evidence that decidual inflammation precedes labor. Biol Reprod. 2012;86(2):39. doi:10.1095/biolreprod.111.095505. DOI
23. Hamilton SA, Tower CL, Jones RL. Identification of chemokines associated with the recruitment of decidual leukocytes in human labour: potential novel targets for preterm labour. PLoS ONE. 2013;8(2):e56946. doi:10.1371/journal.pone.0056946. DOI
24. Keelan JA. Intrauterine inflammatory activation, functional progesterone withdrawal, and the timing of term and preterm birth. J Reprod Immunol. 2018;125:89-99. doi:10.1016/j.jri.2017.12.004. DOI
25. Shynlova O, Nadeem L, Zhang J et al. Myometrial activation: Novel concepts underlying labor. Placenta. 2020;92:28-36. doi:10.1016/j.placenta.2020.02.005. DOI
26. Zackler A, Flood P, Dajao R et al. Suspected chorioamnionitis and myometrial contractility: mechanisms for increased risk of cesarean delivery and postpartum hemorrhage. Reprod Sci. 2019;26(2):178-183. doi:10.1177/1933719118778819. DOI
27. Wetta LA, Szychowski JM, Seals S et al. Risk factors for uterine atony/postpartum hemorrhage requiring treatment after vaginal delivery. Am J Obstet Gynecol. 2013;209(1):51.e1-e6. doi:10.1016/j.ajog.2013.03.011. DOI
28. Wiley RL, Racusin D, Chen HY et al. Chorioamnionitis and adverse outcomes in low-risk pregnancies: a population based study. Am J Obstet Gynecol. 2020;222:S244-S245. doi:10.1080/14767058.2021.1887126. DOI
29. Conde-Agudelo A, Romero R, Jung EJ et al. Management of clinical chorioamnionitis: an evidence-based approach. Am J Obstet Gynecol. 2020;223(6):848-869. doi:10.1016/j.ajog.2020.09.044. DOI
30. Wisner K. Intrapartum management of chorioamnionitis. MCN Am J Matern Child Nurs. 2018;43(1):52. doi:10.1097/NMC.0000000000000396. DOI
31. Burgess APH, Katz JE, Moretti M et al. Risk factors for intrapartum fever in term gestations and associated maternal and neonatal sequelae. Gynecol Obstet Invest. 2017;82(5):508-16. doi:10.1159/000453611. DOI
32. Wang C, Sirluck Schroeder I, Sosa Cazales A et al. Management of fever in labor after institution of a standardized order set at a maternity quaternary care center. Am J Obstet Gynecol. 2019;221(6):687. doi:10.1016/j.ajog.2019.10.041. DOI
33. Dior UP, Kogan L, Eventov-Friedman S et al. Very high intrapartum fever in term pregnancies and adverse obstetric and neonatal outcomes. Neonatology. 2016;109(1):62-8. doi:10.1159/000440938. DOI
34. Kissler K, Hurt KJ. The pathophysiology of labor dystocia: theme with variations. Reprod Sci. 2023;30(3):729-742. doi:10.1007/s43032-022-01018-6. DOI

35. Friedman EA, Cohen WR. The active phase of labor. Am J Obstet Gynecol. 2023;228(5S):S1037-S1049. doi:10.1016/j.ajog.2021.12.269. DOI
36. WHO recommendations for augmentation of labor. Executive summary. Geneva: World Health Organization. 2014. https://www.ncbi.nlm.nih.gov/books/NBK258881/. [Accessed 14 April 2023]
37. Brüggemann C, Carlhäll S, Grundström H et al. Labor dystocia and oxytocin augmentation before or after six centimeters cervical dilatation, in nulliparous women with spontaneous labor, in relation to mode of birth. BMC Pregnancy Childbirth. 2022;22(1):408. doi:10.1186/s12884-022-04710-2. DOI
38. Dike NO, Ibine R. Hypotonic Labor. StatPearls [Internet]. Treasure Island (FL): StatPearls Publishing. 2023.
39. Prevention of Group B Streptococcal Early-Onset Disease in Newborns: ACOG Committee Opinion, Number 797. Obstet Gynecol. 2020;135(2):e51-e72. doi: 10.1097/AOG.0000000000003668. DOI
40. Committee Opinion No. 797: Prevention of Group B Streptococcal Early-Onset Disease in Newborns: Correction. Obstet Gynecol. 2020;135(4):978-979. doi: 10.1097/AOG.0000000000003824. DOI
41. Ayres-de-Campos D, Arulkumaran S. FIGO intrapartum fetal monitoring expert consensus panel. FIGO consensus guidelines on intrapartum fetal monitoring: Introduction. Int J Gynaecol Obstet. 2015;131(1):3-4. doi:10.1016/j.ijgo.2015.06.017. DOI
42. Altemani A, Gonzatti A, Metze K. How many paraffin blocks are necessary to detect villitis? Placenta. 2003;24(1):116-117. doi:10.1053/plac.2002.0875. DOI
43. Keski-Nisula LT, Aalto M-L, Kirkinen PP. Myometrial inflammation in human delivery and its association with labor and infection. Am J Clin Pathol. 2003;120:217-224. doi:10.1309/KC6KDTX98LFYB3J7. DOI
44. Nath CA, Ananth CV, Smulian JC et al. Histologic evidence of inflammation and risk of placental abruption. Am J Obstet Gynecol. 2007;197:319e1–319e6. doi:10.1016/j.ajog.2007.06.012. DOI
45. Keski-Nisula L, Aalto ML, Katila ML et al. Intrauterine inflammation at term: a histopathologic study. Hum Pathol. 2000;31:841–846. doi:10.1053/hupa.2000.8449. DOI
46. Redline RW. Placental pathology: a systematic approach with clinical correlations. Placenta. 2008;29:S86–91. doi:10.1016/j.placenta.2007.09.003. DOI
47. Khong TY, Mooney EE, Ariel I. Sampling and definitions of placental lesions Amsterdam placental workshop group consensus statement. Arch Pathol Lab Med. 2016;140:698–713. doi:10.5858/ arpa.2015-0225-CC. DOI

CONFLICT OF INTEREST

The Authors declare no conflict of interest

CORRESPONDING AUTHOR

Kateryna L. Shatylovych
Danylo Halytsky Lviv National Medical University
64 Pekarska st., 79010 Lviv, Ukraine
e-mail: shatik2@ukr.net

ORCID AND CONTRIBUTIONSHIP

Kateryna L. Shatylovych: 0000-0002-8465-0355 A B C D
Leonid B. Markin: 0000-0003-0237-7808 E F

A – Work concept and design, B – Data collection and analysis, C – Responsibility for statistical analysis, D – Writing the article, E – Critical review, F – Final approval of the article

RECEIVED: 13.10.2023
ACCEPTED: 17.07.2024

ORIGINAL ARTICLE

CONTENTS

The influence of the psychosocial stress on oral health status in the conditions of being in Ukraine during the prolonged state of martial law

Yulia G. Kolenko, Iryna A. Volovyk, Iryna E. Voronina, Olena V. Dementieva, Evelina A. Chumak
BOGOMOLETS NATIONAL MEDICAL UNIVERSITY, KYIV, UKRAINE

ABSTRACT

Aim: To study the presence of clinical and biochemical correlations between psycho-emotional stress, level of cortisol and periodontal oral health status of the patients in Ukraine during prolonged martial law.

Materials and Methods: The comprehensive clinical and laboratory study covered 49 persons, including 20 patients with Gingivitis (40.8%) and 29 with Periodontitis (59.2%). Biochemical blood test was performed to determine the level of "stress hormone" – cortisol. Patients filled out the questionnaire by the method of V. Zung (low mood-subdepression scale) to determine psycho-emotional state in the conditions of prolonged martial law in Ukraine.

Results: The research results showed that in the conditions of martial law in Ukraine, "stabilization" and "improvement" of the process of patients with Gingivitis was established in 50%, with Periodontitis - only in 41.4% of patients. In 54% of patients, a significant deterioration of clinical indices was established, compared to the indicators before the war. In patients with Periodontitis, PBI index was 1.33 (0.62-1.43) score, which was not statistically significantly different from the initial level ($p>0.05$). Biochemical blood tests revealed an increased level of the hormone cortisol in 18% of patients. According to the method by V. Zung scale of mental states, the majority of patients (87%) showed low mood and emotional instability within the medium level (range 2 and 3). Correlation was identified, according to the Spearman coefficient ($R=0.39$, $p<0.05$), between scale assessments by V.Zung and the blood level of cortisol.

Conclusions: Psycho-emotional stress is one of the leading pathogenetic factors in the deterioration of oral health status and the development of periodontal diseases, especially in people in Ukraine during prolonged martial law. Indicators of method by V. Zung scale of mental states and the level of cortisol are optimal markers of the need to correct the psycho-emotional state. For patients with increased levels of stress and fear, it is necessary to create special treatment-prevention schemes, taking into account greater attention to motivation to maintain the health of the oral cavity, as well as more frequent hygiene procedures.

KEY WORDS: oral health status, periodontium, stress, cortisol, martial law in Ukraine

Wiad Lek. 2024;77(8):1593-1602. doi: 10.36740/WLek202408109 DOI

INTRODUCTION

Currently, more attention should be paid to the study of indicators of the emotional state and content of feelings of people living in the conditions of prolonged martial law in Ukraine [1]. For more than a year now (February 2022 – February 2023) they experience stressful situations, causing various physical, emotional or mental reactions.

The studies performed show that negative emotional events in the life of a human cause strong negative influence on his or her body, leading to the occurrence or aggravation of specific diseases. There is a connection between negative emotional events in a person's life and changes in the immune system, which leads to the occurrence of a disease. It was established that psycho-emotional stress modulates the immune system through the nervous and endocrine systems. This causes and aggravates many chronic diseases: cardiovascular, endocrine, gastroenterological, pulmonary and rheumatological, as well as conditions of infectious, allergic, autoimmune or neoplastic etiology. Various clinical observations and epidemiological studies point to a correlation between the state of suspense and uncertainty in which the patient is in a stressful situation, and the development and progression of periodontal tissue diseases [2].

Literature has it that stress plays a significant role in the etiology, progression and the outcome of treatment of periodontal diseases, in particular, generalized periodontitis. Distress, anxiety, depression, loneliness, adverse life circumstances cause a deterioration in the general state of human health, facilitating bacterial invasion due to poor oral cavity hygiene and leading to the destruction of periodontal tissues. Prolonged depressive and anxiety states can have the most adverse effect on the degree, severity and course of periodontal

diseases [3]. There is also a connection between the severity of periodontal tissue diseases and the mechanism of behavioral stress, due to the indirect effect of stress on the health of the periodontium through lifestyle changes, such as smoking, alcohol consumption, unhealthy diet and careless oral cavity hygiene [4].

Stress factors cause induced modulation of the immune system, which leads to an increase in the level of adrenocorticoid hormones in the blood, stimulation of chemotaxis and phagocytosis of polymorphonuclear leukocytes, a decrease in the proliferation of lymphocytes, changes in the level of cytokines, changes in blood circulation and regeneration, modification of saliva (saliva pH and IgA secretion) [5].

The key steroid hormones, which are synthesized by the adrenal cortex and whose level increases in stressful situations, include cortisol. Cortisol hormone is one of the main human hormones that influences the vital activity of the body, proper functioning of organs and systems, our mood, the level of aggression, loyalty [6]. Cortisol helps the body timely recover in order to adequately resist negative influences, such as physical injuries, strong fear, tension, pain, fatigue, lack of sleep, constant emotional overload and stress. Cortisol is called the "stress hormone"; when its balance is disturbed, a person may experience quite strong physical and emotional sensations that deteriorate the quality of life [7].

AIM

The aim is to study the presence of clinical and biochemical correlations between psycho-emotional stress and periodontal condition of the patients staying in Ukraine during prolonged martial law.

MATERIALS AND METHODS

In January-February, 2021, 61 young persons in the age of 18-35 years applied to the Dental Medical Center of NMU named after O.O. Bogomolets for examination and treatment. The study covered 49 persons, including 22 men (44.9%) and 27 women (55.1%). Examined patients were divided into two clinical groups, dependent on the diagnosis: group I consisted of 20 (40.8%) patients with Gingivitis: dental biofilm-induced; group II included 29 (59.2%) patients with stage I Periodontitis. Before the beginning of examination and treatment, voluntary informed consent was obtained from all the patients in accordance with the protocol. Those patients underwent a comprehensive clinical, radiological and laboratory examination; a treatment and prevention scheme was developed for them in accordance with the protocols (depending on the established diagnosis), recommendations were issued, and they were entered into the dispensary register.

Oral health status examination of the patients included diagnostics of the key indicators of the oral cavity state and periodontal screening with determination of clinical indices. The intensity of dental caries was assessed using the CFE index. The hygienic condition of the oral cavity was assessed using the oral cavity hygiene index OHI-S (Green-Vermillion index) and approximal plaque index – API (Lange). Periodontal examination included determination of the PMA index (C. Parma), periodontal screening and registration (PSR), probing pocket depth (PPD), loss of the clinical attachment level (CAL), presence of recession, nature of exudate. Probing was performed with a periodontal probe at six points around each tooth. Gum bleeding was determined by the papillary bleeding index (PBI, H.R. Muhlemann). The results of all examinations and measurements were entered in the periodontal card of the patient.

The condition of the teeth, bone tissue of the alveolar process, and jaws was assessed using orthopantomography and the data of targeted contact intraoral radiographs.

The diagnosis of periodontal diseases was established according to the new classification of periodontal and peri-implant diseases and conditions of the World Working Group, sponsored by the American Academy of Periodontology (AAP) and the European Federation of Periodontology (EFP) in 2017.

To assess the physiological level of stress resistance, a laboratory biochemical blood test was performed to determine the "stress hormone", cortisol – a marker of the endocrine system for the protection of the psycho-emotional sphere from negative influences.

In 2022-2023, patients underwent control examinations in the near and distant observation periods. It should be noted that in 2023, before the start of the comprehensive follow-up clinical and laboratory examination, all patients filled out a questionnaire to determine their psycho-emotional state in the conditions of prolonged martial law in Ukraine. This questionnaire was specially developed for the differentiated diagnostics of depressive and similar conditions by the method of V. Zung (Low mood-subdepression Scale (LMSS)) [8].

The statistical analysis of the obtained data was carried out on a PC using Microsoft Excel 2021, StatSoft Statistica 12 software. For the samples, the conformity of the empirical distributions to the normal law (Gaussian distribution) was assessed according to the Kolmogorov-Smirnov and Shapiro-Wilk criteria, being the basis for selection of

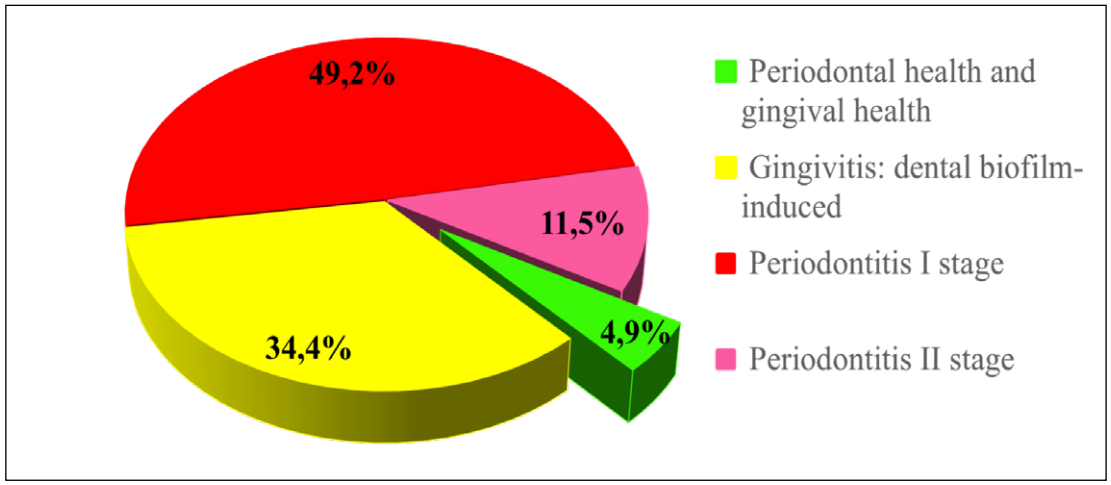

Fig. 1. Prevalence of periodontal diseases in young people in Ukraine.

Table 1. State of Periodontal oral health status in patients with Gingivitis and Periodontitis

Index	Group I, M±m, Me (Q_I-Q_{III})		Group II, M±m, Me (Q_I-Q_{III})	
	2021, initial state	2022, control, before the war	2021, initial state	2022, control, before the war
OHI-S, score	1.98±0.1	0.73±0.1; *p<0.05*	2.67±0.07	1.25±0.07; p<0.05
API, %	96.6 (90.0-100)	54.8 (46.5-56.5); p<0.05	100 (96.8-100)	56.3 (53.1-63.3); p<0.05
PMA, %	27.4 (20.4-38.2)	10.4 (9.5-11.9); p<0.05	41.4 (30.0-48.9)	13.5 (12.2-14.4); p<0.05
PBI, score	1.02 (0.81-1.22)	0.31 (0.26-0.35); p<0.05	1.47 (1.29-1.60)	0.43 (0.33-0.47); p<0.05
PPD, mm	1.81 (1.63-2.0)	1.03 (1.00-1.07); p<0.05	3.05 (2.64-3.17)	2.00 (1.75-2.13); p<0.05
PSR, code	1.50 (1.08-1.83)	0.67 (0.67-0.83); p<0.05	2.17 (1.83-2.33)	1.17 (0.83-1.33); p<0.05

Notes: p – indicator of probability of differences, compared to the initial data.

the statistical criteria: Student's t-test, analysis of variance (ANOVA), analysis of variance according to Friedman's test, Mann-Whitney U-test, Wilcoxon's test, Spearman's correlation coefficient. In the work, the studied values are presented in the form of the mean value of the variant M, the standard error of the mean value m, the median value of the median Me and the interquartile range QI-QIII.

RESULTS

DEMOGRAPHIC AND CLINICAL DATA

In January-February, 2021, 61 young persons in the age of 18-35 years applied to the Dental Medical Center of NMU named after O.O. Bogomolets for examination and treatment: 24 (39.3%) – men, and 37 (60.7%) – women. The prevalence of periodontal diseases among young patients was as follows: 3 persons (4.9%) – Periodontal and Gingival health; 21 persons (34.4%) – Gingivitis: dental biofilm-induced; 30 persons (49.2%) – Periodontitis stage I; 7 persons (11.5%) – Periodontitis stage II (Fig. 1).

Out of 61 persons, the research covered 49 persons: 22 male (44.9%) and 27 female (55.1%). Patients were divided into two clinical groups, dependent on the diagnosis: group I consisted of 20 (40.8%) patients with Gingivitis: dental biofilm-induced; group II included 29 (59.2%) patients with stage I Periodontitis.

Following a biochemical blood test among 49 patients at the beginning of clinical examination for the level of cortisol hormone in 2021, indicators within the physiological norm were detected in 48 patients (97.9%). Only in 1 patient (2.1%), an insignificant increase in its level was detected. By its clinical diagnosis patient belonged to group II with Periodontitis stage I.

PERIODONTAL ORAL HEALTH STATUS

Periodontal oral health status in 49 patients in the respective clinical groups with dental biofilm-induced Gingivitis (group I) and stage I Periodontitis (group II) in January-February 2021 (initial state) and January-February 2022, that is, after 1 year of observation but before the introduction of martial law in Ukraine, is described in Table 1.

During the control examination of patients with Gingivitis in group I in 2022, OHI-S index on average equaled 0.73±0.1 points, which corresponded to satisfactory hygiene (p<0.05). API index on average equaled

Table 2. Clinical efficiency of treatment of patients with Gingivitis and Periodontitis after a remote observation period (2 years in total and 1 year of war)

	Treatment results						Total	
	Stabilization		Unchanged		Progression			
	abs.	%	abs.	%	abs.	%	abs.	%
Clinical group I	10	50	3	15	7	35	20	100
Clinical group II	12	41.4	5	17.2	12	41.4	29	100
Total	22	44.9	8	16.3	19	38.8	49	100

Table 3. State of Periodontal oral health status in patients with Gingivitis and Periodontitis after a remote observation period (2 years in total and 1 year of war)

Index	Group I, M±m, Me (Q_I-Q_{III})			Group II, M±m, Me (Q_I-Q_{III})		
	2021, initial state	2022, control, before the war	2023, control, after 1 year of war	2021, initial state	2022, control, before the war	2023, control, after 1 year of war
OHI-S, score	1.98±0.1	0.73±0.1; p<0.05	1.25±0.15; p<0.05	2.67±0.07	1.25±0.07; p<0.05	2.10±0.13; p<0.05
API, %	96.6 (90.0-100)	54.8 (46.5-56.5); p<0.05	93.4 (85.7-100); p>*0.05*	100 (96.8-100)	56.3 (53.1-63.3); p<0.05	100 (96.7-100); p>*0.05*
PMA, %	27.4 (20.4-38.2)	10.4 (9.5-11.9); p<0.05	17.7 (14.0-31.3); p<0.05	41.4 (30.0-48.9)	13.5 (12.2-14.4); p<0.05	31.1 (19.5-37.5); p>*0.05*
PBI, score	1.02 (0.81-1.22)	0.31 (0.26-0.35); p<0.05	0.59 (0.39-1.07); p<0.05	1.47 (1.29-1.60)	0.43 (0.33-0.47); p<0.05	1.33 (0.62-1.43); p>*0.05*
PPD, mm	1.81 (1.63-2.0)	1.03 (1.00-1.07); p<0.05	1.37 (1.13-1.95); p<0.05	3.05 (2.64-3.17)	2.00 (1.75-2.13); p<0.05	2.82 (2.07-3.05); p>*0.05*
PSR, code	1.50 (1.08-1.83)	0.67 (0.67-0.83); p<0.05	0.83 (0.67-1.50); p<0.05	2.17 (1.83-2.33)	1.17 (0.83-1.33); p<0.05	1.83 (1.33-1.83); p<0.05

Notes: p – indicator of probability of differences, compared to the initial data.

54.8 (46.5-56.5)%, which corresponded to satisfactory interdental hygiene (p<0.05). PMA index on average equaled 10.4 (9.5-11.9)%, which corresponded to the light degree of inflammation (p<0.05). PBI index on average equaled 0.31 (0.26-0.35) points (p<0.05). Periodontal indicator of probing pocket depth (PPD) on average equaled 1.03 (1.00-1.07) mm (p<0.05). PSR code on average equaled 0.67 (0.67-0.83) (p<0.05).

In group II patients with stage I Periodontitis, OHI-S index on average equaled 1.25±0.07 points, which corresponded to satisfactory hygiene (p<0.05). API index on average equaled 56.3 (53.1-63.3)%, which corresponded to satisfactory interdental hygiene (p<0.05). PMA index on average equaled 13.5 (12.2-14.4)%, which corresponded to the light degree of inflammation (p<0.05). PBI index on average equaled 0.43 (0.33-0.47) points (p<0.05). PPD index on average equaled 2.00 (1.75-2.13) mm (p<0.05). PSR code on average equaled 1.17 (0.83-1.33) (p<0.05).

In February-March, 2023, that is, after 2 years of observation and 1 year of life of Ukrainians in the in the conditioned of prolonged martial law in Ukraine, control examination and analysis of data of the patients in the study groups were performed. Their data have shown that in group I with Gingivitis, "stabilization" of the process was observed in 50% of patients; the process in periodontal tissues remained "unchanged" in 15%; 35% of patients met the criteria of "progression". In group II with stage I Periodontitis, "stabilization" of the process was observed in 41.4% of patients; the process in periodontal tissues remained "unchanged" in 17.2%; 41.4% of patients met "progression" criteria (Table 2).

Therefore, the results of clinical and laboratory examination have shown that out of 49 patients with periodontal diseases, positive results and stabilization of the pathological processes were achieved only by 22 patients, that is, in 44.9% of cases. This is a very low treatment efficiency indicator, which may be attributed to the extremely difficult psycho-emotional, physical and financial standing of the Ukrainian population during the war in Ukraine.

Periodontal oral health status in patients of two clinical groups with Gingivitis and Periodontitis, stage I, in 2023, that is, after 1 years of martial law in Ukraine, is described in Table 3.

The dynamic of most patients in both clinical groups with Gingivitis and Periodontitis stage I after 2 years of observation and one year of war in Ukraine has

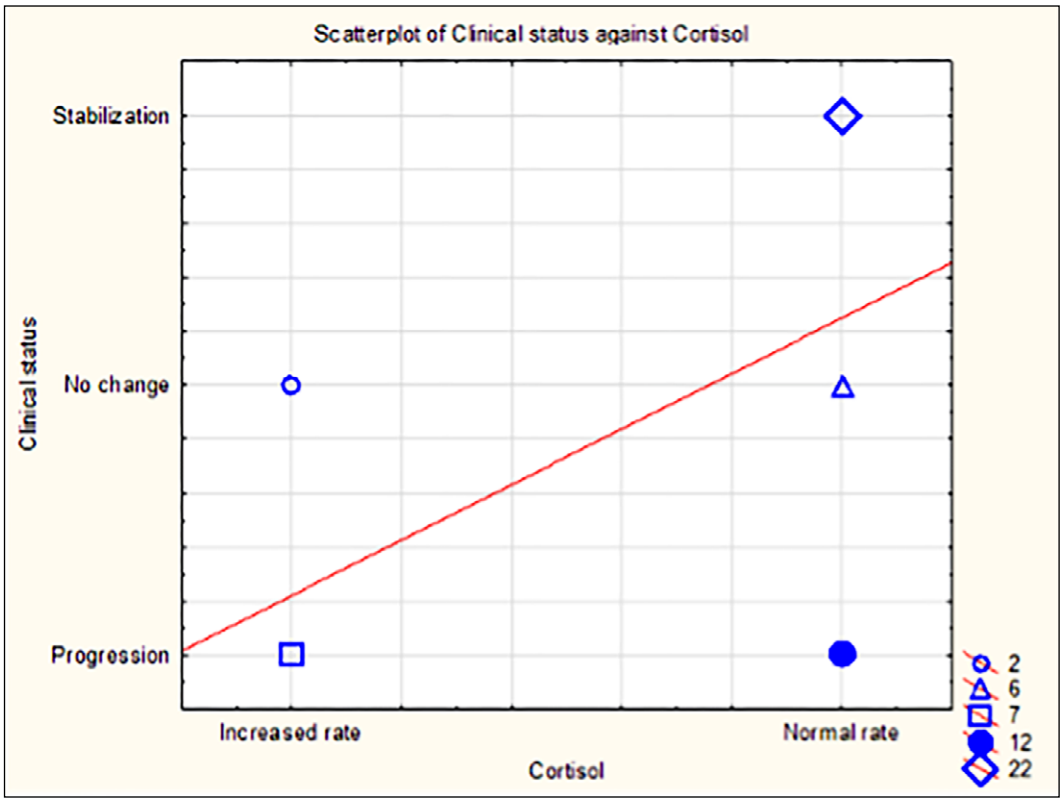

Fig. 2. Scatterplot of indicator of Clinical status against level of Cortisol.

shown a significant deterioration of the indices of hygiene, PMA inflammation, PBI bleeding, periodontal indicators of PPD and PSR, as compared to the data of follow-up control after 1 year of observation, before the introduction of martial law, in almost 55% of patients, compared to the initial examination data. Only 45% of patients demonstrated positive dynamics after a long observation period.

In group I of patients with Gingivitis OHI-S index in 2023 (that is after 1 year of war) on average equaled 1.25±0.15 points, which corresponded to satisfactory hygiene, while remaining 35.9% lower, compared to the initial level ($p<0.05$). API index deteriorated substantially, on average equaling 93.4 (85.7-100)%, which corresponded to unsatisfactory interdental hygiene, and did not statistically differ from the initial level ($p>0.05$). PMA index also declined, on average equaling 17.7 (14.0-31.3)%, which corresponded to the light degree of inflammation, while remaining 35.4% lower, compared to the initial level ($p<0.05$). PBI index on average equaled 0.59 (0.39-1.07) points, remaining 42.1% lower, compared to the initial level ($p<0.05$). Periodontal indicator PPD on average equaled 1.37 (1.13-1.95) mm, while remaining 24.3% lower, compared to the initial level ($p<0.05$). PSR code on average equaled 0.83 (0.67-1.50), remaining 44.6% lower, compared to the initial level ($p<0.05$).

Among patients with Periodontitis stage I in group II, OHI-S index after 1 year of war deteriorated substantially and on average equaled 2.10±0.13 points, which corresponded to unsatisfactory hygiene, while remaining 21.3% lower, compared to the initial level ($p<0.05$). API index also sharply declined, on average equaling 100 (96.7-100)%, which corresponded to unsatisfactory interdental hygiene, and did not substantially differ from the initial level ($p>0.05$). PMA index sharply declined, too, on average equaling 31.1 (19.5-37.5)%, which corresponded to average inflammation, and did not statistically differ from the initial level ($p>0.05$) either. PBI index on average equaled 1.33 (0.62-1.43) points, and also did not statistically differ from the initial level ($p>0.05$). Periodontal PPD indicator on average equaled 2.82 (2.07-3.05) mm, and did not statistically differ from the initial level ($p>0.05$). PSR code on average equaled 1.83 (1.33-1.83), while remaining 15,7% lower, compared to the initial level ($p<0.05$).

Evaluation of the biochemical marker of stress of the cortisol hormone was carried out before the clinical and laboratory examination of patients of both groups in 2023, that is, 2 years after the first visit. The biochemical blood test showed a slight increase in the level of cortisol in 9 out of 49 patients, making 18.4%. Noteworthy, exactly these 9 patients during the control examination in 2023 were diagnosed with the clinical state of "unchanged" or "progression" of the pathological process in the periodontal tissues: 2 patients of clinical group I with Gingivitis had «progression»; 2 patients of clinical group II with Periodontitis stage I had an «unchanged»

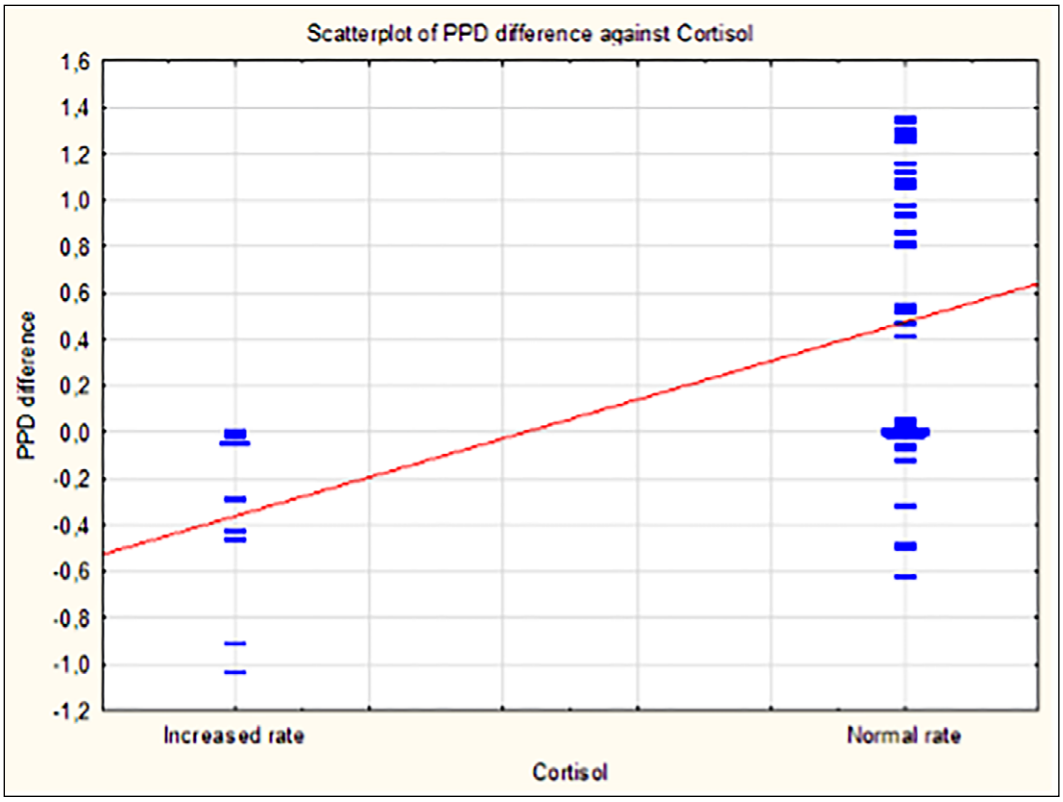

Fig. 3. Scatterplot of PPD difference against level of Cortisol.

condition, and 5 patients of clinical group II with Periodontitis stage I had «progression».

Statistical analysis revealed a weak correlation, according to the Spearman correlation coefficient (R=0.36, p<0.05), between the periodontal oral health status in patients with Gingivitis and Periodontitis in 2023 and the elevated level of cortisol in their blood (Fig. 2). It also established a weak correlation, according to the Spearman correlation coefficient (R=0.45, p<0.05), between the indicator of changes in the periodontal PPD index in the dynamics of treatment and the elevated level of blood cortisol (Fig. 3).

PSYCHOLOGICAL ASSESSMENT

Extreme living conditions, martial law and combat factors in Ukraine, in which the Ukrainian population appeared at the beginning of 2022, exert rather strong influence on the psycho-emotional sphere and the quality of life of a human. The intensity of perception of combat stress depends on the interaction of two main factors: the power and length of influence of combat factors on the mind, and the specific individual response to the effect of these factors.

At the beginning of 2023, before the follow-up clinical and laboratory examination, all patients were interviewed (V.Zung) to identify their psycho-emotional state in the conditions of prolonged martial law in Ukraine.

By the Zung (low mood-subdepression scale), the average value of the index of depression equals 61.2±0.91 points. In most patients – 32 out of 49 patients, making 65.3% – a substantial deterioration of the spirit and emotional instability (range 3) were detected. Only in 4 patients, making 8.2%, no deterioration of the spirit (range 1) was observed. In 11 patients, making 22.4%, a slight but clear deterioration of the spirit was observed (range 2). Unfortunately, 3 patients, making 6.1%, demonstrated deep depression and suspense (range 4).

Distribution of 49 patients in both clinical groups with Gingivitis and Periodontitis by the range of scale assessments according to the V.Zung method dependent on periodontal oral health clinical status in 2023 – «stabilization», «unchanged» and «progression» – is shown on Fig. 4. The condition of «stabilization» was observed in 22 patients, in that, 4 patients – range 1 according to the V.Zung method, 6 patients – range 2, 12 – range 3, 0 patients – range 4. The «unchanged» condition was observed in 8 patients, in that, 0 patients – range 1, 2 patients – range 2, 5 patients – range 3, 1 patient – range 4. The condition of «progression» was observed in 19 patients, in that, 0 patients – range 1, 3 patients – range 2, 14 patients – range 3, 2 patients – range 4 (Fig. 4).

Distribution of patients in both clinical groups by the range of scale assessments according to the V.Zung method.

Statistical analysis revealed a weak correlation, according to the Spearman correlation coefficient (R=0.40, p<0.05), between the periodontal oral health status in

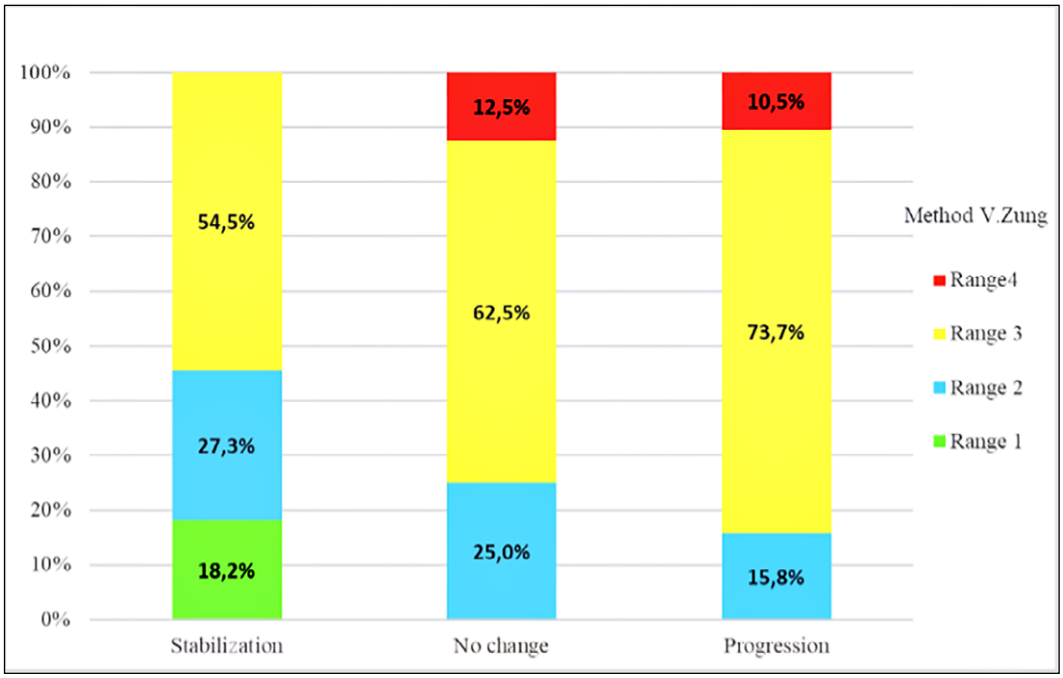

Fig. 4. Distribution of patients in both clinical groups by the range of scale assessments according to the V. Zung method.

patients with Gingivitis and Periodontitis in 2023 and the scale assessments of adverse mental conditions according to V.Zung (Fig. 5).

Correlation of weak strength was identified, according to the Spearman correlation coefficient (R=0.39, p<0.05), between scale assessments of adverse mental conditions according to V.Zung and the blood level of cortisol (Fig. 6).

Weak correlation was identified, according to the Spearman correlation coefficient (R=0.36, p<0.05), between scale assessments of adverse mental conditions according to V.Zung and the change of the periodontal index PPD in the dynamics of treatment (Fig. 7).

DISCUSSION

The possible correlation between psychological stress and generalized periodontitis was covered in a number of clinical studies. It was suggested that stress might play an important role in the development and severity of periodontal diseases [9]. It was established that individuals who experienced stress were more prone to the development and progression of periodontal diseases than subjects without stress [10, 11]. Our study identified correlations between scale assessments of adverse mental conditions according to V.Zung and periodontal oral health status in both observation groups, using the Spearman correlation coefficient (R=0.36, p<0.05).

Over the past decade, it has become more obvious that stress can negatively affect the health of the oral cavity, which can lead to increased plaque and gum inflammation [12].

Ravishankar et al. (2014) discovered that psychological stress can disrupt the lifestyle and hygienic condition of the oral cavity. Poor hygiene of the oral cavity due to stress can contribute to the accumulation of dental plaque and, over time, occurrence of gingivitis and periodontitis [13]. We observed a similar situation in our study: the indices of OHI-S and ARI significantly worsened in both groups after the beginning of the war.

Experimental studies *in vitro* have shown that the elevated level of cortisol in the blood plasma can provoke an inappropriate response of T-helpers to a microbial stressor and contribute to the destruction of the periodontium [14]. Psycho-emotional stress, which was determined by the increase in the level of cortisol in the oral fluid, is believed to be a risk factor in the pathogenesis of periodontal diseases (generalized periodontitis) [15].

Our study has established correlations according to the Spearman correlation coefficient (R=0.36, p<0.05) between the clinical periodontal oral health status in patients with Gingivitis and Periodontitis and their elevated blood level of cortisol. Correlations were also established according to Spearman's correlation coefficient (R=0.39, p<0.05) between V. Zung's scale assessments of adverse mental conditions and the blood level of cortisol. Glucocorticosteroids, in particular, cortisol, suppress immunity, including secretory IgA, IgG and functions of neutrophilic granulocytes. All these factors may be important in the protection of the periodontium from infection of the periodontium by pathogenic microorganisms. Secretory IgA antibodies can protect the periodontium by reducing the initial colonization of periodontium pathogens. IgG antibodies can provide protection through opsonization of periodontium pathogenic microorganisms for

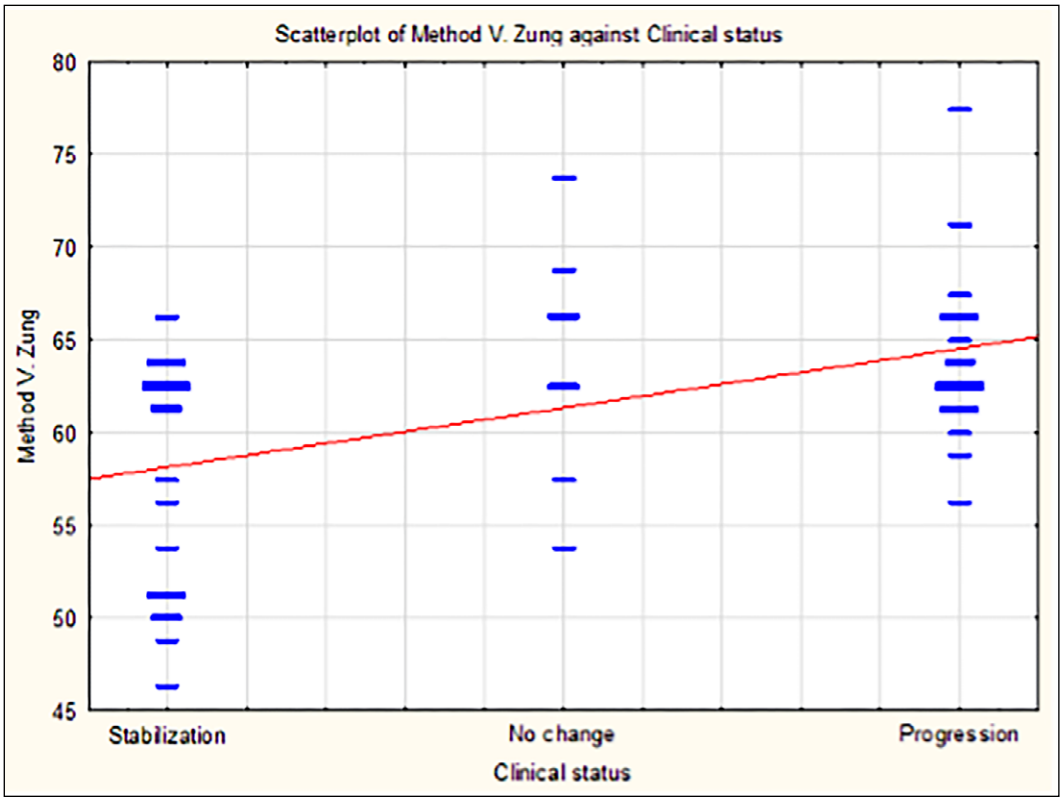

Fig. 5. Scatterplot of rate of Method V. Zung against of indicator of Clinical status.

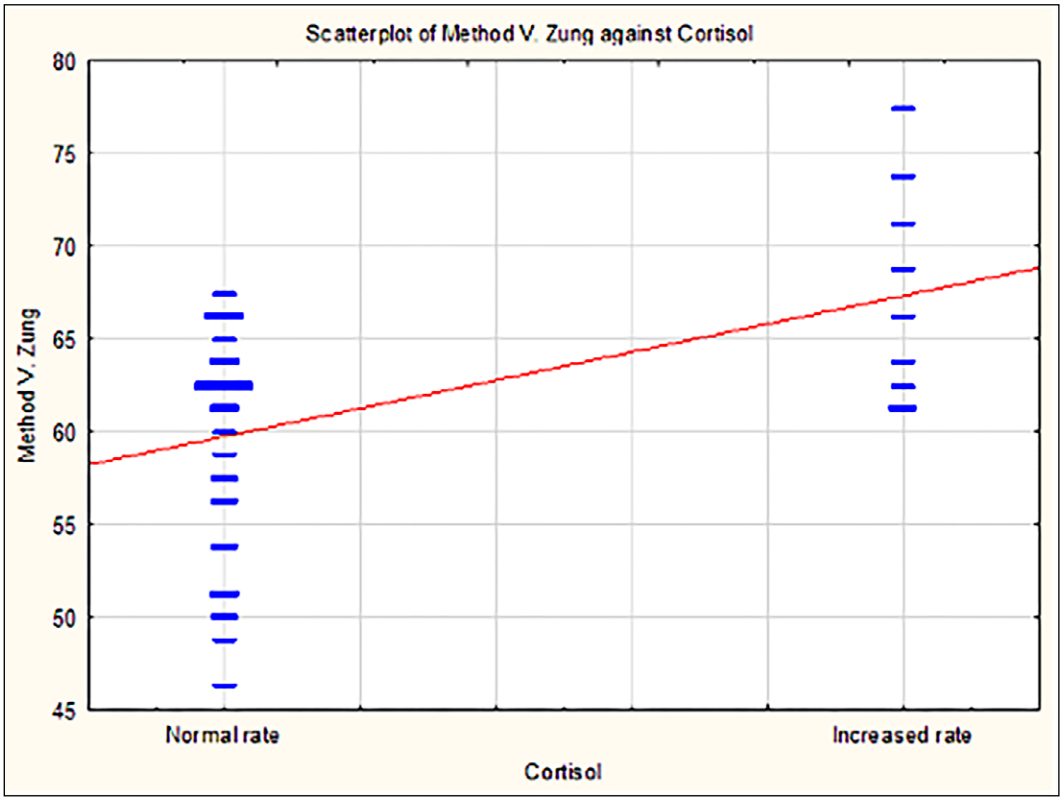

Fig. 6. Scatterplot of rate of Method V.Zung against level of Cortisol.

phagocytosis and their destruction by neutrophils. This leads to an increased susceptibility to infection of periodontal tissues, which, in turn, leads to the development of destruction of the periodontium and generalized periodontitis.

CONCLUSIONS

The our research results have shown that psycho-emotional stress is a factor that contributes to the pathogenesis of periodontal diseases and an increase in the level of cortisol in blood serum.

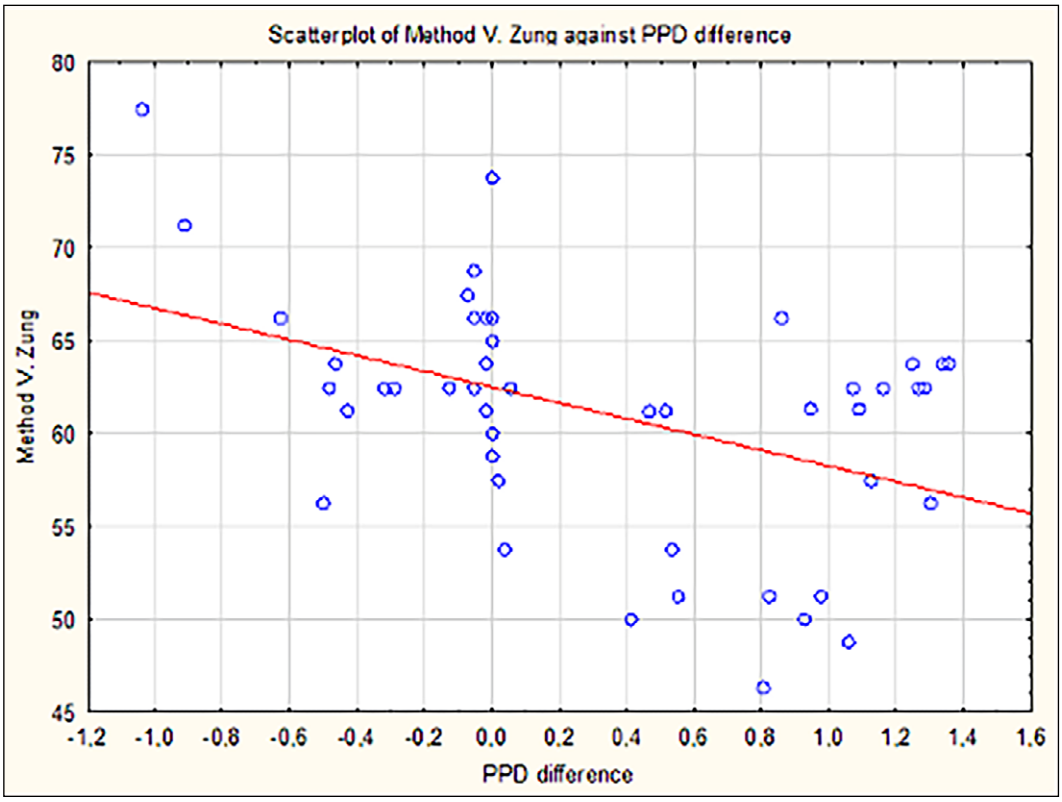

Fig. 7. Scatterplot of rate of Method V.Zung against PPD difference.

Stress also negatively influences the health of the periodontium through behavioral and lifestyle changes, increasing careless attitude to the oral cavity hygiene. It also influences the health of the periodontium through a direct biological effect, mediated by a change in the state of saliva, changes in the blood circulation of the gums and an effect on the body's immune response.

The obtained by us results give reason to consider it necessary to receive a consultation and, if required, treatment from a related specialist: an endocrinologist for the purpose of correcting the imbalance of the hormonal state and a psychologist (neuropathologist) for the purpose of normalizing and improving the psycho-emotional state of patients with increased indicators of stress and fear.

Considering the results of the research, it is important that dentists take into account stress factors as risks of periodontal diseases, their severity and reduction of the efficiency of treatment. Patients with chronic stress should be regularly reminded to maintain the health of periodontal tissues through constant motivation and an increase in the number of oral cavity hygiene procedures.

REFERENCES

1. Kanyura OA, Bidenko NV, Kolenko YuG. Dosvid nadannya stomatologichnoyi dopomogi v umovah vijskovogo stanu [Experience of providing dental care in the conditions of the military state]. Suchasna stomatologiya. 2022;3-4:38-44. doi: 10.33295/1992-576X-2022-3-38. (Ukrainian) DOI
2. Penmetsa GS, Seethalakshmi P. Effect of stress, depression, and anxiety over periodontal health indicators among health professional students. J Indian Assoc Public Health Dent. 2019;17:36-40. doi: 10.4103/jiaphd.jiaphd_53_18. DOI
3. Trombelli L, Scapoli C, Tatakis DN, Grassi L. Modulation of clinical expression of plaque-induced gingivitis: Effects of personality traits, social support and stress. J Clin Periodontol 2005;32:1143-50. doi: 10.1111/j.1600-051X.2005.00835.x. DOI
4. Kolenko YuG, Volovik IA, Myalkivskij KO. Vpliv zahvoryuvan tkanin parodonta na yakist zhittya paciyentiv [The influence of periodont tissue diseases on the quality of life of patients.] Suchasna stomatologiya. 2021;2:36-42. doi: 10.33295/1992-576X-2021-2-36. (Ukrainian) DOI
5. Goyal S, Gupta G, Thomas B et al. Stress and periodontal disease: The link and logic! Ind. Psychiatry J. 2013;22:4-11. doi: 10.4103/0972-6748.123585. DOI
6. Obulareddy VT, Chava VK, Nagarakanti S. Association of Stress, Salivary Cortisol, and Chronic Periodontitis: A Clinico-biochemical Study. Contemp. Clin. Dent. 2018;9(2):S299-S304. doi: 10.4103/ccd.ccd_289_18. DOI
7. Bawankar PV, Kolte AP, Kolte RA. Evaluation of stress, serum and salivary cortisol, and interleukin-1β levels in smokers and non-smokers with chronic periodontitis. J. Periodontol. 2018;89:1061-1068. doi: 10.1002/JPER.18-0028. DOI

8. Agayev NA, Kokun OM, Pishko IO. Zbirnik metodik dlya diagnostiki negativnih psihichnih staniv vijskovosluzhbovciv: Metodichnij posibnik. K.: NDC GP ZSU. 2016, p.234. (Ukrainian)
9. Corridore D, Saccucci M, Zumbo G et al. Impact of Stress on Periodontal Health: Literature Revision. Healthcare. 2023;11:1516. doi: 10.3390/healthcare11101516. DOI
10. D'Ambrosio F, Caggiano M, Schiavo L et al. Chronic Stress and Depression in Periodontitis and Peri-Implantitis: A Narrative Review on Neurobiological, Neurobehavioral and Immune-Microbiome Interplays and Clinical Management Implications. Dent. J. 2022;10:49. doi: 10.3390/dj10030049. DOI
11. Maruyama T, Ekuni D, Higuchi M et al. Relationship between Psychological Stress Determined by Voice Analysis and Periodontal Status: A Cohort Study. Int. J. Environ. Res. Public Health. 2022;19:9489. doi: 10.3390/ijerph19159489. DOI
12. Varshini VV, Rajasekar A. Effect of Stress on Periodontal Health: A Clinical Study. J. Res. Med. Dent. Sci. 2020;8:259-263.
13. Ravishankar TL, Ain TS, Gowhar O. Effect of academic stress on plaque and gingival health among dental students of Moradabad, India. J. Int. Acad. Periodontol. 2014;16(4):115-120.
14. Rahate PS, Kolte RA, Kolte AP et al. Evaluation of stress, serum, and salivary ghrelin and cortisol levels in smokers and non- smokers with Stage III periodontitis: A cross-sectional study. J. Periodontol. 2022;93:1131-1140. doi: 10.1002/JPER.21-0373. DOI
15. Ramesh A, Malaiappan S, Prabhakar J. Relationship between clinical depression and the types of periodontitis–A cross-sectional study. Drug Invent. Today. 2018;10(5):659-663.

The topic of the research is "A multidisciplinary approach to the prevention and treatment of hard tooth tissues and periodontal diseases in persons of working age" (State registration number No. 0119U104010).

CONFLICT OF INTEREST
The Authors declare no conflict of interest

CORRESPONDING AUTHOR
Yulia G. Kolenko
Bogomolets National Medical University
1 Zoologichna st., 03057 Kyiv, Ukraine
e-mail: kolenko.julia@gmail.com

ORCID AND CONTRIBUTIONSHIP
Yulia G. Kolenko: 0000-0003-1659-3333 A B C D E F
Iryna A. Volovyk: 0000-0003-2063-0758 A D E
Iryna E. Voronina: 0000-0002-4917-8518 A B C
Olena V. Dementieva: 0000-0002-7049-518X C E
Evelina A. Chumak: 0000-0003-2967-5346 A D F

A – Work concept and design, B – Data collection and analysis, C – Responsibility for statistical analysis, D – Writing the article, E – Critical review, F – Final approval of the article

RECEIVED: 17.03.2024
ACCEPTED: 23.07.2024

ORIGINAL ARTICLE

CONTENTS

Impact of cranioskeletal trauma on the development of endogenous intoxication syndrome in rats of different ages

Nataliya V. Izhytska[1,2], Yurii I. Sushko[1], Arsen A. Hudyma[3], Tetiana I. Pisklivets[3], Zoryana V. Smahlii[3], Narhiz Dzhavadova[3]

[1]DANYLO HALYTSKY LVIV NATIONAL MEDICAL UNIVERSITY, LVIV, UKRAINE

[2]UNIVERSITY OF ZIELONA GÓRA, ZIELONA GÓRA, POLAND

[3]I. YA. GORBACHEVSKY TERNOPIL NATIONAL MEDICAL UNIVERSITY, MINISTRY OF HEALTH OF UKRAINE, TERNOPIL, UKRAINE

ABSTRACT

Aim: The aim of the study was to determine the impact of cranioskeletal trauma (CST) on the development of endogenous intoxication syndrome in rats of different ages.

Materials and Methods: The experiments involved 147 white male Wistar rats of different age groups. The first experimental group included sexual immature rats aged 100-120 days. The second group includes sexually mature rats aged 6-8 months. The third group included old rats aged 19-23 months. In all experimental groups, CST was modelled under thiopentalonatrium anaesthesia. The control rats were only injected with thiopentalonatrium anaesthesia. The animals were withdrawn from the experiments under anaesthesia after 1, 3, 7, 14, 21 and 28 days by total bleeding from the heart. In blood serum, the content of fractions of molecules of middle mass was determined at a wavelength of 254 and 280 nm (MMM_{254}, MMM_{280}).

Results: As a result application of CST in rats of different age groups, an increase in the serum content of MMM_{254} and MMM_{280} was observed with a maximum after 14 days and a subsequent decrease by 28 days. At all times of the experiment, the indicators were statistically significantly higher compared to the control groups. The degree of growth of the MMM_{254} fraction after 1, 7 and 14 days was statistically significantly higher in sexual immature rats, and after 21 and 28 days – in old rats. In old rats after 21 and 28 days of the post-traumatic period, the content and degree of growth of the MMM_{280} fraction in the blood serum were also significantly higher.

Conclusions: Modelling of CST in rats of different age groups is accompanied by the development of endogenous intoxication syndrome, which is manifested by the accumulation of MMM_{254} and MMM_{280} fractions in the blood serum with a maximum after 14 days of the experiment. The content of the serum fraction of MMM_{254} in sexual immature rats in the dynamics of experimental CST exceeds other age groups after 1, 7 and 14 days, in old rats the content of the studied MMM fractions is significantly higher after 21-28 days.

KEY WORDS: traumatic brain injury, skeletal injury, endogenous intoxication of the kidney, age, molecular of middle mass

Wiad Lek. 2024;77(8):1603-1610. doi: 10.36740/WLek202408110 DOI

INTRODUCTION

Traumatic brain injury (TBI) in the structure of polytrauma trauma is a serious problem for health care [1]. Despite the creation of specialized department of trauma and intensive care units, which has led to a reduction in mortality in polytrauma from exsanguination, acute respiratory distress syndrome and multiple organ dysfunction syndrome, TBI-related mortality remains the most common cause of death in trauma [2, 3]. It has been proven that the severity of TBI is the dominant factor in the mortality of victims with polytrauma [4].

Combined trauma contributes to the worsening of secondary brain damage. It is based on coagulopathy, hypotension, fever and hypoxia, which initiate a sequence of ischemic and damaging biochemical processes [5].

Age has been shown to be an independent predictor of TBI mortality. In older people, the frequency and severity of brain injury is associated with deterioration in motor and physiological functions, a higher risk of low-energy falls, and the appearance of intracranial hematomas with slow exacerbation [6], while younger patients usually suffer injuries related to sports, work, and road accidents and are more prone to polytrauma [7]. The age characteristics of patients, mechanisms of injury, and kinetics of brain damage emphasise the difficulties of approaches to TBI [8], which requires further in-depth study of the pathogenesis of combined cranioskeletal trauma (CST) in the age-related aspect.

As a result of physical trauma, there are disorders of the protective layers of the skin, fascia, capsules and underlying tissues. These injuries lead to the gener-

ation and release of damage-associated molecular fragments, including membrane debris, mitochondrial components, histones, DNA and RNA fragments, and damaged proteins [9]. Together with the products of normal and impaired metabolism, trauma results in the formation of a toxic excess of biologically active substances of molecular of middle mass (MMM) of 300-5000 daltons. As shown in the study [10], an increase in the concentration of MMM is one of the markers of the transition of the inflammatory toxic stage of endogenous intoxication syndrome in TBI to the stage of systemic endogenous intoxication. However, in the age aspect, the dynamics of the content of MMM in the blood under conditions of CST has not been studied.

AIM

To determine the effect of CST on the development of endogenous intoxication syndrome in rats of different ages

MATERIALS AND METHODS

The experiments were performed out on 147 white male Wistar rats of different age groups, which were selected randomly and kept on a standard vivarium diet. The first experimental group included sexually immature rats aged 100-120 days and weighing 90-110 g. The second group included sexually mature rats aged 6-8 months and weighing 180-200 g. The third group included old rats aged 19-23 months and weighing 300-320 g.

In all experimental groups (49 rats each), according to the method described in the study [10], CST was modelled under thiopentalonatrium anaesthesia (40 $mg \cdot kg^{-1}$). To modelling skeletal trauma - a closed fracture of the femur, sexual immature rats were firstly subjected to a dosed mechanical impact with a steel object with a wedge-shaped nozzle on the projection of the middle third of the left femur with an energy of 0.320 J, sexually mature rats - with an energy of 0.637 J, and old rats - with an energy of 0.796 J. Next, a dosed blow to the skull was applied with a blunt object to sexual immature rats at a point 3 mm anterior to the interaural line with an energy of 0.226 J, to sexual mature rats at a point 5 cm anterior to the interaural line with an energy of 0.375 J, and to old rats at a point 6 mm anterior to the interaural line with an energy of 0.549 J. Impact energy caused moderate TBI in animals of different age groups. No animals with penetrating skull damage or open femur fracture were used in the experiments. In the control groups (7 rats each), animals were only put under thiopentalonatrium anaesthesia.

The rats were withdrawn from the experiments under anaesthesia after 1, 3, 7, 14, 21 and 28 days by total bleeding from the heart. In blood serum, the content of individual fractions of MMM was studied at 254 nm (MMM_{254}, peptide fraction) and 280 nm (MMM_{280}, chromatophore fraction) using an Ulab 108 UV spectrophotometer (China) [11].

The experiments were performed in accordance with the 'General Ethical Principles for Experiments on Animals' adopted by the First National Congress on Bioethics (Kyiv, 2001) and agreed with the provisions of the 'European Convention for the Protection of Vertebrate Animals Used for Experimental and Other Scientific Purposes' (Strasbourg, 1986), as well as the conclusion of the Bioethics Commission of the I. Ya. Horbachevsky Ternopil National Medical University, Ministry of Health of Ukraine No. 72 of 06.01.2023.

The obtained digital material was processed in the STATISTICA software package (StatSoft Inc., USA). The median (Me), lower and upper quartiles (LQ, UQ) were determined. For an independent comparison of the degree of deviation of indicators in animals of different age groups, the average ratio of individual values of the studied indicators to the average value of the control group was calculated [12]. The significance of differences was assessed by the nonparametric Mann-Whitney test.

RESULTS

As can be seen from Table 1, in the control groups of rats, the highest content of the fraction of MMM_{254} in the blood serum was observed in the group of sexually mature and old rats, which was 27.2 and 11.0 % higher, respectively, than in the group of sexually immature rats ($p_{1-2}<0.05$, $p_{1-3}<0.05$). In 1 day after the application of CST in the groups of experimental rats, the content of the MMM_{254} fraction in the blood serum increased significantly compared to the result of the control group - in sexually immature rats by 6.06 times ($p<0.05$), in mature rats – by 5.05 times ($p<0.05$), in old rats – by 4.71 times ($p<0.05$). The value of the studied index became statistically significantly higher in experimental groups 1 and 2 compared to experimental group 3 (by 15.9 and 22.8 %, respectively, p1-3<0.05, p2-3<0.05). Subsequently, after 3 days in the experimental groups of rats of different ages, the index significantly decreased compared to the result of day 1: in experimental group 1 – by 2.34 times ($p<0.05$), in experimental group 2 – by 2.25 times ($p<0.05$), in experimental group 3 - by 1.69 times ($p<0.05$), but in all experimental groups it remained statistically significantly higher than in the control (2.59, 2.24 and 2.79 times, respectively, $p<0.05$).

Under these conditions, the index in the group of old rats was significantly higher than in the group of sexually immature rats (by 19.6 %, $p_{1-3}<0.05$).

Further, up to 14 days, compared with the result of 3 days, the index in all experimental groups increased and reached the level of 1 day of the posttraumatic period ($p>0.05$), significantly exceeded the result of the control group ($p<0.05$) and significantly prevailed in the groups of sexually immature and mature rats compared with old rats ($p_{1-3}<0.05$, $p_{2-3}<0.05$). By day 28, the index in all experimental groups decreased. Compared with the result of the 14th day, the index in experimental group 1 decreased by 2.54 times ($p<0.05$), in experimental group 2 – by 3.27 times ($p<0.05$), in experimental group 3 – by 1.90 times ($p<0.05$), but in all experimental groups the index continued to remain significantly higher than in the control (respectively by 2.31, 1.46 and 2.62 times, $p<0.05$). At this time of the post-traumatic period in the group of old rats, the index was statistically significantly higher than in the groups of sexually immature and mature rats (by 24.1 and 57.1 %, respectively, $p_{1-3}<0.05$, $p_{2-3}<0.05$), and in the group of sexually immature rats it was significantly higher than in the group of sexually mature rats (by 26.6 %, $p_{1-2}<0.05$).

The analysis of the dynamics of the average ratio of individual values of MMM_{254} in the blood serum to the average value of the control group under the influence of cranioskeletal trauma in rats of different ages showed (Table 2) that 1 day after the application of CST, the index was significantly higher in experimental group 1 compared to experimental groups 2 and 3 (by 20.0 and 28.7 %, respectively, $p_{1-2}<0.05$, $p_{1-3}<0.05$). After 3 days, the index in all experimental groups decreased and was significantly higher in experimental group 3 compared to experimental group 2 (by 24.6 %, $p_{2-3}<0.05$). Up to 14 days, the index increased and at this time in experimental group 1 statistically significantly exceeded the result of experimental groups 2 and 3 (respectively by 25.4 and 19.9 % ($p_{1-2}<0.05$, $p_{1-3}<0.05$). Subsequently, the index decreased and after 28 days was significantly higher in experimental group 3 compared to experimental groups 1 and 2 (by 13.4 and 79.4 %, respectively, $p_{1-3}<0.05$, $p_{2-3}<0.05$). In experimental group 1, the index exceeded the result of experimental group 2 (by 58.2 %, $p_{1-2}<0.05$).

In turn, under the influence of CST, the content of the fraction of MMM_{280} in the blood serum (Table 3) in immature rats compared to the control also increased after 1 day of the experiment (by 44.2 %, $p<0.05$) and remained at the same level after 3 days ($p>0.05$). Subsequently, the index gradually increased up to day 14 of the experiment and at this time was 3.34 times higher than the control level ($p<0.05$) and was significantly higher than the result of the previous observation periods (2.32, 1.91 and 1.77 times, respectively, $p<0.05$). After 21 days, the index decreased, but the differences with respect to the result of the 14th day of the experiment were not statistically significant ($p>0.05$). Subsequently, after 28 days of the experiment, the index continued to decrease and was statistically significantly lower compared to the results of 14 and 21 days of the experiment ($p>0.05$), but remained significantly higher compared to the results of 1, 3 and 7 days of the experiment ($p<0.05$).

In sexually mature rats, the content of the MMM_{280} fraction in the blood serum under the influence of CST also increased compared to the control after 1 day of the experiment (by 77.7 %, $p<0.05$). Subsequently, the index continued to increase and reached the first "plateau" in 3-7 days. During these periods, the index was statistically significantly higher than the result of the 1st day of the experiment (by 13.5 and 16.1 %, respectively, $p<0.05$). After 14 and 21 days, the index continued to increase, reached the second "plateau" and exceeded the result of day 7 by 66.8 and 65.5 %, respectively ($p<0.05$). By day 28, the index decreased and was statistically significantly lower compared to the results of days 14 and 21 of the experiment ($p<0.05$), but significantly exceeded the results of days 1, 3 and 7 of the experiment ($p<0.05$).

In old rats, the content of the MMM_{280} fraction in the blood serum after modeling of CST increased by 65.0 % ($p<0.05$) compared to the control after 1 day of the experiment. Subsequently, the index after 3 and 7 days of the experiment continued to increase, reached the first "plateau" and was statistically significantly higher compared to the result of 1 day, respectively, by 45.6 and 45.9 % ($p<0.05$). Subsequently, the index gradually increased until day 21 of the experiment and was 55.7% higher compared to the result of day 7 of the experiment ($p<0.05$) and 17.4% higher compared to the result of day 14 ($p<0.05$). After 28 days, the index decreased and reached the level of day 14 ($p>0.05$). During this period of the experiment, the index was significantly lower compared to the result of 21 days ($p<0.05$), and statistically significantly higher than the result of 1, 3 and 7 days ($p<0.05$).

Comparison of the experimental groups showed that after 1, 3 and 14 days of the experiment, the differences in the content of the fraction of MMM_{280} in the blood serum were not statistically significant ($p_{1-2}>0.05$, $p_{1-3}>0.05$, $p_{2-3}>0.05$). At the same time, after 3, 7, 21 and 28 days of the experiment, the index was the highest in experimental group 3 and exceeded experimental group 1 by 35.7, 26.0, 24.0 and 33.9 %, respectively ($p_{1-3}<0.05$). After 3 and 28 days of the experiment, the

Table 1. The content of MMM_{254} in blood serum under the influence of cranioskeletal trauma in rats of different ages, Me (LQ;UQ) – median (lower and upper quartiles)

Animal Group	Control	Period after injury					
		1 day	3 day	7 day	14 day	21 day	28 day
Group 1 Sexually immature	0.136 (0.129; 0.138)	0.824* (0.788; 0.894) *	0.352*1 (0.320; 0.384) *1	0.559*1,3 (0.505; 0.580) *1,3	0.812*3,7 (0.771; 0.818) *3,7	0.353 (0.336; 0.386) *1,7,14	0.319 (0.287; 0.326) *1,7,14,21
Group 2 Sexually mature	0.173 (0.157; 0.196)	0.873 (0.822; 0.931) *	0.388 (0.365; 0.421) *1	0.556 (0.510; 0.590) *1,3	0.824 (0.805; 0.828) *3,7	0.377 (0.361; 0.401) *1,7,14	0.252 (0.239; 0.274) *1,3,7,14,21
Group 3 Old	0.151 (0.147; 0.166)	0.711 (0.672; 0.766) *	0.421 (0.390; 0.440) *1	0.542 (0.503; 0.602) *1,3	0.752 (0.748; 0.761) *3,7	0.452 (0.447; 0.471) *1,7,14	0.396 (0.391; 0.409) *1,7,14
p_{1-2}	<0.05	>0.05	>0.05	>0.05	>0.05	>0.05	<0.05
p_{1-3}	<0.05	<0.05	<0.05	>0.05	<0.05	<0.05	<0.05
p_{2-3}	<0.05	<0.05	>0.05	>0.05	<0.05	<0.05	<0.05

Notes. Here and in table 3:

1. * – differences in relation to the control group are statistically significant ($p<0.05$);
2. 1,3,7,14,21 – differences in the results of days 1, 3, 7, 14 and 21 of the experiment are statistically significant ($p<0,05$);
2. p_{1-2} – significance of differences between study groups 1 and 2;
3. p_{1-3} – significance of differences between study groups 1 and 3;
4. p_{2-3} – significance of differences between study groups 2 and 3.

Table 2. Dynamics of the average ratio of individual values of kidney MMM_{280} to the average value of the control group under the influence of cranioskeletal trauma in rats of different ages, Me (LQ;UQ) – median (lower and upper quartiles)

Animal Group	Control					
	1 day	3 day	7 day	14 day	21 day	28 day
Group 1 Sexually immature	6.06 (5.79; 6.57)	2.59 (2.35; 2.82)	4.11 (3.71; 4.26)	5.97 (5.67; 6.01)	2.60 (2.47; 2.84)	2.31 (2.11; 2.39)
Group 2 Sexually mature	5.05 (4,75; 5.38)	2.24 (2.11; 2.43)	3.21 (2.95; 3.41)	4.76 (4.65; 4.78)	2.18 (2.09; 2.32)	1.46 (1.38; 1.58)
Group 3 Old	4.71 (4.45; 5.07)	2.79 (2.58; 2.92)	3.59 (3.33; 3.99)	4.98 (4.95; 5.04)	2.99 (2.96; 3.12)	2.62 (2.59; 2.71)
p_{1-2}	<0.05	>0.05	<0.05	<0.05	<0.05	<0.05
p_{1-3}	<0.05	>0.05	>0.05	<0.05	<0.05	<0.05
p_{2-3}	>0.05	<0.05	>0.05	>0.05	<0.05	<0.05

Notes. Here and in table 4:

1. p_{1-2} – significance of differences between study groups 1 and 2;
2. p_{1-3} – significance of differences between study groups 1 and 3;
3. p_{2-3} – significance of differences between study groups 2 and 3.

index in experimental group 1 was also statistically significantly lower compared to experimental group 2 (by 9.4 and 9.2 %, respectively, $p_{1-2}<0.05$).

The dynamics of the average ratio of the individual values of the content of the fraction of MMM_{280} in the blood serum to the average value of the control group (Table 4) showed that the degree of growth of the studied indicator in all experimental groups after 1, 3 and 14 days of the experiment was almost the same ($p_{1-2}>0.05$, $p_{1-3}>0.05$, $p_{2-3}>0.05$). After 7, 21, and 28 days of experimentation, the degree of growth in experimental group 3 was statistically significantly higher

Table 3. The content of MMM_{254} in blood serum under the influence of cranioskeletal trauma in rats of different ages, Me (LQ;UQ) - median (lower and upper quartiles)

Animal Group	Control	Period after injury					
		1 day	3 day	7 day	14 day	21 day	28 day
Group 1 Sexually immature	0.226 (0.214; 0.245)	0.326 (0.319; 0.398) *	0.395 (0.374; 0.416) *	0.426 (0.410; 0.452) *1	0.755 (0.695; 0.795) *1,3,7	0.674 (0.600; 0.714) *1,3,7	0.502 (0.471; 0.527) *1,3,7,14,21
Group 2 Sexually mature	0.216 (0.206; 0.234)	0.384 (0.331; 0.399) *	0.436 (0.429; 0.460) *1	0.446 (0.433; 0.515) *1	0.744 (0.719; 0.756) *1,3,7	0.738 (0.705; 0.767) *1,3,7	0.553 (0.532; 0.591) *1,3,7,14,21
Group 3 Old	0.223 (0.212; 0.234)	0.368 (0.355; 0.399) *	0.536 (0.517; 0.564) *1	0.537 (0.515; 0.556) *1	0.712 (0.686; 0.750) *1,3,7	0.836 (0.793; 0.909) *1,3,7,14	0.672 (0.645; 0.692) *1,3,7,21
p_{1-2}	>0.05	>0.05	<0.05	>0.05	>0.05	>0.05	<0.05
p_{1-3}	>0.05	>0.05	<0.05	<0.05	>0.05	<0.05	<0.05
p_{2-3}	>0.05	>0.05	<0.05	>0.05	>0.05	<0.05	<0.05

Table 4. Dynamics of the average ratio of individual values of kidney MMM_{280} to the average value of the control group under the influence of cranioskeletal trauma in rats of different ages, Me (LQ;UQ) - median (lower and upper quartiles)

Animal Group	Control					
	1 day	3 day	7 day	14 day	21 day	28 day
Group 1 Sexually immature	1.44 (1.41; 1.76)	1.94 (1.89; 2.02)	1.88 (1.81; 2.00)	3.34 (3.07; 3.52)	2.98 (2.65; 3.16)	2.22 (2.08; 2.33)
Group 2 Sexually mature	1.78 (1.53; 1.84)	2.18 (2.13; 2.27)	2.06 (2.00; 2.38)	3.44 (3.33; 3.50)	3.42 (3.26; 3.55)	2.56 (2.46; 2.73)
Group 3 Old	1.65 (1.59; 1.79)	2.25 (2.12; 2.31)	2.41 (2.31; 2.49)	3.19 (3.08; 3.36)	3.75 (3.55; 4.08)	3.01 (2.89; 3.10)
p_{1-2}	>0.05	>0.05	>0.05	>0.05	<0.05	<0.05
p_{1-3}	>0.05	>0.05	<0.05	>0.05	<0.05	<0.05
p_{2-3}	>0.05	>0.05	>0.05	>0.05	<0.05	<0.05

compared to experimental group 1 (by 28.2, 25.8, and 35.6 %, respectively, $p_{1-3}<0.05$). Also, in study group 2, the index after 21 days was 14.8 % higher than in study group 1 ($p_{1-2}<0.05$), after 28 days – by 15.3 % ($p_{1-2}<0.05$).

DISCUSSION

The intensification of endogenous intoxication processes is one of the key syndromes of traumatic injury. According to the results of studies [13], one of the manifestations of endotoxemia in experimental moderate and severe TBI is the accumulation of MMM fractions in the blood serum. The dynamics of their content had a three-phase character: primary accumulation (3 hours after trauma), followed by a "plateau" period when the level of MMM did not change significantly (24-48 hours after trauma) and, finally, an avalanche-like accumulation of MMM starting from the 3rd day after trauma (72 hours – 5 days). The authors believe that the first stage is due to the entry of endotoxins into the bloodstream from damaged brain tissue (primary – "cerebral" posttraumatic endotoxemia). The reason for further stabilization of the level of endotoxemia could be the destruction of endotoxins and their excretion by the kidneys (the "plateau" period). At the third stage, a pronounced increase in all MMM fractions was noted, which is associated not only with the progression of nervous tissue damage but also with systemic damage to internal organs and tissues of the body due to the final formation of endogenous intoxication syndrome and multiple organ failure. According to data [14], increased endotoxicity is also characteristic of experimen-

tal skeletal trauma (fracture of both femurs). However, in the dynamics, the content of MMM fractions in the blood serum changed in a wave-like manner with a significant increase after 3 days of the experiment and a subsequent decrease by 7 days.

Work [15] showed that modeling of combined moderate TBI and skeletal trauma (femur fracture) in the acute period and the period of early manifestations of traumatic illness (1-7 days) causes a gradual increase in the content of MMM in the blood serum, indicating the leading role of TBI in the formation of endogenous intoxication syndrome in the conditions of CST.

Some studies have shown that after modeling of CST, the phenomena of endogenous intoxication do not subside even during the late manifestations of traumatic illness (14-35 days) [16]. The authors have shown that the content of serum fractions of MMM in the conditions of CST (moderate TBI and closed fracture of both femurs), the content of MMM fractions in the blood serum after 14 days of posttraumatic period significantly exceeds the control level, but by 21 days it increased even more, followed by a decrease by 35 days, which reached the control level. The authors conclude that in the period of late manifestations of traumatic disease in the body of experimental animals there are prerequisites for increasing the level of endotoxemia, which is primarily due to membrane-destructive and dysmetabolic processes.

Our studies have shown that in the acute period of traumatic illness (1 day) after modeling of CST, the content of the studied fractions of MMM increases in the blood serum compared to the control. At this stage, the serum is dominated by the content of the MMM_{254} fraction, which is considered a general integral indicator of the content of substances of low and medium molecular weight (from 500 to 5000 Da), which, in addition to peptides, include about 200 compounds of normal and abnormal metabolism [13]. Their appearance on the background of CST in the acute period of traumatic illness (1 day) is obviously due to the entry of endotoxins into the bloodstream from the damaged brain tissue, soft tissue, and femur of the injured limb. After 3 days, the index decreases, which indicates that the process of accumulation of endotoxins in the blood was balanced with the processes of their destruction and excretion from the body. However, later, after 7-14 days, the content of the MMM_{254} fraction in the blood serum increases again. During this period, the maximum increase in the concentration of the MMM_{280} fraction in the blood serum is also noted. Given that the MMM_{280} fraction characterizes an increase in the content of aromatic amino acids that are not normally formed, their accumulation, according to [13], may indicate systemic damage to internal organs. Subsequently, the content of the studied fractions of MMM gradually decreases and by day 28 does not reach the control level.

Analyzing the dynamics of the studied fractions of MMM in rats of different ages under the influence of CST, we first found that the degree of increase in the content of MMM_{254} fraction in the blood serum after 1 day significantly prevails in sexually immature rats compared to sexually mature and old rats. Consequently, the degree of destructive processes in the affected tissues of sexually immature rats is higher, which is obviously associated with more pronounced manifestations of hypermetabolism syndrome in this age group, which is characteristic of the acute period of traumatic illness [13]. Subsequently, after 3 days, the endotoxemia associated with the MMM_{254} fraction subsides, but its content does not reach the level of the control group. During this period, their lowest serum levels were observed in sexually mature rats, and the highest in old rats, which is obviously due to the different capacity of detoxification systems, which is lower in old rats. After 7 and 14 days, the rate increased again. The degree of increase is again significantly greater in sexually immature rats, with the lowest rate in sexually mature rats. It can be assumed that the repeated increase in the serum content of the MMM_{254} fraction in sexually immature rats is mainly due to secondary brain damage, which occurs in a delayed manner at a young age, due to the peculiarities of the structure of the skull (greater bone plasticity, wider subarachnoid space) and brain (greater tissue hydrophilicity) [17]. In other study groups, the increase in serum MMM_{254} fraction was due to venous damage to internal organs and the development of functional insufficiency of detoxification systems.

Subsequently, during the late manifestations of traumatic disease – after 21 and 28 days - the content of the fraction of MMM_{254} in the blood serum decreases, but does not reach the level of the control group and continues to remain significantly higher. At these times, the content of the fraction of MMM_{254} in the blood serum is statistically significantly higher in old rats and the lowest in mature rats. Thus, in old rats, the recovery of the affected structures is slower, and the recovery of detoxification systems is prolonged.

At the same time, the dynamics of the accumulation of the aromatic fraction of MMM_{280} in the blood serum indicates that the level of dysmetabolic disorders in internal organs due to CST in all age groups gradually increases from day 1 of the experiment. After 3 days, the index dominates in old rats, then in sexual mature and immature rats. In sexual immature rats, the maximum increase in the value of the studied index falls on day 14, in sexual mature rats – on days 14-21, in old rats – on day 21. By day 28, the index decreases in rats of all age

groups, but does not reach the control level. After 21 and 28 days, the index became significantly higher in old rats compared to immature rats. Thus, the intensity of dysmetabolic disorders that occurred at the systemic level is significantly higher in old rats, mainly during the period of late manifestations of traumatic disease.

Thus, local destructive processes of the brain, soft tissues, and bones as a source of endotoxins dominate in immature rats during the acute period (after 1 day) and the period of early manifestations of traumatic injury (after 7 and 14 days), and in old rats during the period of late manifestations of traumatic injury (21-28 days). At the same time, the maximum development of dysmetabolic disorders of internal organs as a source of endotoxins under conditions of CST occurs mainly in old rats and occurs during the period of late manifestations of traumatic disease. The revealed peculiarities of endotoxin accumulation in the dynamics of CST in rats of different ages indicate the high informativeness of the study of MMM fractions for understanding the mechanisms of development of endogenous intoxication syndrome in the age aspect and allow a pathogenetic approach to the choice of correction agents.

CONCLUSIONS

1. The modeling of CST in rats of different age groups is accompanied by the development of endogenous intoxication syndrome, the manifestation of which is the accumulation of MMM_{254} and MMM_{280} fractions in the blood serum, the content of which gradually increases by day 14 of the posttraumatic period, followed by a decrease by day 28 and at all times statistically significantly exceeds the control level.
2. The content of the serum fraction of MMM_{254} in immature rats in the dynamics of experimental CST statistically significantly exceeds other age groups in the acute period (after 1 day) and the period of early manifestations of traumatic illness (after 7 and 14 days). In the period of late manifestations of traumatic illness (21-28 days), the content of serum fractions of MMM_{254} and MMM_{280} significantly exceeds other age groups in old rats.

REFERENCES

1. Dewan MC, Rattani A, Gupta S et al. Estimating the global incidence of traumatic brain injury. J Neurosurg. 2018;130(4):1080-1097. doi:10.3171/2017.10.JNS17352. DOI
2. van Wessem KJP, Leenen LPH. Reduction in Mortality Rates of Postinjury Multiple Organ Dysfunction Syndrome: A Shifting Paradigm? A Prospective Population-Based Cohort Study. Shock. 2018;49(1):33-38. doi:10.1097/SHK.0000000000000938. DOI
3. Hietbrink F, Houwert RM, van Wessem KJP et al. The evolution of trauma care in the Netherlands over 20 years. Eur J Trauma Emerg Surg. 2020;46(2):329-335. doi:10.1007/s00068-019-01273-4. DOI
4. Niemeyer M, Jochems D, Houwert RM et al. Mortality in polytrauma patients with moderate to severe TBI on par with isolated TBI patients: TBI as last frontier in polytrauma patients. Injury. 2022;53(4):1443-1448. doi:10.1016/j.injury.2022.01.009. DOI
5. Robinson CP. Moderate and Severe Traumatic Brain Injury. Continuum (Minneap Minn). 2021;27(5):1278-1300. doi:10.1212/CON.0000000000001036. DOI
6. Karibe H, Hayashi T, Narisawa A et al. Clinical Characteristics and Outcome in Elderly Patients with Traumatic Brain Injury: For Establishment of Management Strategy. Neurol Med Chir (Tokyo). 2017;57(8):418-425. doi:10.2176/nmc.st.2017-0058. DOI
7. Peeters W, van den Brande R, Polinder S et al. Epidemiology of traumatic brain injury in Europe. Acta Neurochir (Wien). 2015;157(10):1683-1696. doi:10.1007/s00701-015-2512-7. DOI
8. Liew TYS, Ng JX, Jayne CHZ et al. Changing Demographic Profiles of Patients With Traumatic Brain Injury: An Aging Concern. Front Surg. 2019;6:37. doi:10.3389/fsurg.2019.00037. DOI
9. Huber-Lang M, Lambris JD, Ward PA. Innate immune responses to trauma. Nat Immunol. 2018;19(4):327-341. doi:10.1038/s41590-018-0064-8 DOI
10. Hozhenko AI, Sushko YuI, Hudyma AA et al. Osoblyvosti enzymnoi lanky antyoksydantnoho zakhystu nyrok shchuriv riznoho viku za umov eksperymentalnoi kranioskeletnoi travmy [The influence of unbalanced fat nutrition on the state of enzyme systems of the kidneys]. Actual problems of transport medicine. 2023;1-2(71-72):279–290. doi: 10.5281/zenodo.7617488. (Ukrainian) DOI
11. Syniachenko OV, Yermolaieva MV, Aliieva TIu et al. Riven molekul serednoi masy v synovialnii ridyni khvorykh na revmatoidnyi artryt [Level of middle mass molecules in synovial fluid of patients with rheumatoid arthritis]. Trauma. 2020; 21(60):21-26. doi: 10.22141/1608-1706.6.21.2020.223884. (Ukrainian) DOI
12. Sikirynska DO, Hudyma AA, Hospodarskyi Ila et al. Vplyv kranioskeletnoi travmy, uskladnenoi krovovtratoiu, na aktyvnist protsesiv tsytolizu ta endohennoi intoksykatsii v rannii period u shchuriv z riznoiu rezystentnistiu do hipoksii [Peculiarities of the enzyme link of antioxidant protection in the early period of cranioskeletal injury complicated by blood loss in rats with different hypoxia resistance]. Hospital Surgery. Journal named after L. Ya. Kovalchuk. 2021;2(94):33–40. doi:10.11603/mcch.2410-681X.2021.i2.12238. (Ukrainian) DOI

13. Ziablitsev SV, Yelskyi VM. Stadiinist rozvytku syndromu endohennoi intoksykatsii pry eksperymentalnii cherepno-mozkovii travmi [Stage of endogenous intoxication syndrome in experimental brain injury]. Trauma. 2019; 20(4):80-87. doi: 10.22141/1608-1706.4.20.2019.178750. (Ukrainian) DOI
14. Pysklyvets TI, Shulhai AH. Dynamika pokaznykiv tsytolizu ta endohennoi intoksykatsii za umov skeletnoi travmy, uskladnenoi hostroiu krovovtratoiu riznoho stupenia, ta yikh korektsiia [Indicators dynamics of cytolysis and endogenous intoxication under conditions of skeletal trauma complicated by acute blood loss of various degrees and their correction]. Hospital Surgery. Journal named after L. Ya. Kovalchuk. 2023; (3):51-63. doi: 10.11603/2414-4533.2023.3.14151. (Ukrainian) DOI
15. Sikirynska DO, Hudyma AA, Hospodarskyi Ila, Pokhodun KA. Vplyv kranioskeletnoi travmy, uskladnenoi krovovtratoiu, na aktyvnist protsesiv tsytolizu ta endohennoi intoksykatsii v rannii period u shchuriv z riznoiu rezystentnistiu do hipoksii [Effect of cranioskeletal trauma complicated with blood loss on the activity of cytolysis and endogenous intoxication in the early period in rats with different hypoxia resistance]. Medical and Clinical Chemistry. 2021;23(2):55-62. doi: 10.11603/mcch.2410-681X.2021.i2.12238. (Ukrainian) DOI
16. Prokhorenko OO, Tsymbaliuk Hlu. Dynamika pokaznykiv endohennoi intoksykatsii v period piznikh proiaviv kranioskeletnoi travmy za umov suputnoho khronichnoho hepatytu ta efektyvnist korektsii armadinom [Dynamics of endogenous intoxication parameters in period of late manifestations of cranioskeletal trauma in case of concomitant chronic hepatitis and effectiveness of correction with armadine]. Achievements of Clinical and Experimental Medicine. 2022;(2):115-123. doi: 10.11603/1811-2471.2022.v.i2.13141. (Ukrainian) DOI
17. Kurikeru M, Muravskyi A, Huk A. Patohenetychni mekhanizmy cherepno-mozkovoi travmy serednoho stupenia vazhkosti u patsiientiv riznoho viku [Pathogenetic mechanisms of mild traumatic brain injury in patients of different ages]. Experimental and Clinical Medicine. 2021;90(1):45-54. doi: 10.35339/ekm.2021.90.1.kmh. (Ukrainian) DOI

The article was made within the framework of a complex research topic of the Educational and Scientific Institute of Modelling and Analysis of Pathological Processes of the I. Horbachevsky Ternopil National Medical University of the Ministry of Health of Ukraine «Study of pathogenetic patterns of development of post-traumatic and inflammatory degenerative injuries of organs and systems and their correction» (State Registration No. 0122U000030).

CONFLICT OF INTEREST

The Authors declare no conflict of interest

CORRESPONDING AUTHOR

Arsen A. Hudyma
I. Ya. Gorbachevsky Ternopil National Medical University
Maidan Voli 1, 46001 Ternopil, Ukraine
e-mail: nataizhytska@gmail.com

ORCID AND CONTRIBUTIONSHIP

Nataliya V. Izhytska: 0000-0001-9406-5435 A E F
Yurii I. Sushko: 0000-0002-7601-7904 A B C D E
Arsen A. Hudyma: 0000-0002-1282-2728 A B E F
Tetiana I. Pysklivets: 0009-0005-2537-0897 B C
Zoryana V. Smahlii: 0000-0002-1370-9188 A D
Narhiz A. Dzhavadova: 0000-0002-4758-1039 C D

A – Work concept and design, B – Data collection and analysis, C – Responsibility for statistical analysis, D – Writing the article, E – Critical review, F – Final approval of the article

RECEIVED: 10.03.2024
ACCEPTED: 21.07.2024

REVIEW ARTICLE

CONTENTS

Phenylketonuria – newborn screening as a health protection in society

Katarzyna Piotrowicz[1], Hubert Piotrowicz[1], Jacek Kurzeja[2,3], Emilia Żurowska[3,4]
[1]STUDENT OF THE FACULTY OF MEDICINE, POZNAN UNIVERSITY OF MEDICAL SCIENCES, POZNAN, POLAND
[2]STUDENT SCIENTIFIC SOCIETY, POZNAN UNIVERSITY OF MEDICAL SCIENCES, POZNAN, POLAND
[3]GRADUATE OF THE FACULTY OF MEDICINE, POZNAN UNIVERSITY OF MEDICAL SCIENCES, POZNAN, POLAND
[4]FRANCISZEK RASZEJA MEMORIAL MUNICIPAL HOSPITAL IN POZNAN, POZNAN, POLAND

ABSTRACT

Aim: Phenylketonuria is the most prevalent inherited metabolic disorder. Early detection and prompt treatment can prevent serious neurological consequences. This has become possible thanks to the implementation of newborn screening programmes. The objective of this review is to provide readers with a comprehensive understanding of the phenylketonuria and the role that neonatal screening plays in the protection of public health.

Materials and Methods: A review of the literature was conducted using the PubMed database, with the search period encompassing the most recently published scientific sources. Analysis of the literature. This article presents phenylketonuria as an example of an inherited metabolic disorder, outlines the treatment options, and discusses the potential implications of hyperphenylalaninemia. Furthermore, it also delineates the various aspects of health that are influenced by newborn screening.

Conclusions: Phenylketonuria represents a significant health problem in the population. The development of screening tests has transformed healthcare, including improvements in quality of life, prognosis, and reductions in the number of comorbidities in patients. It is essential to disseminate knowledge among the society about the importance of newborn screening tests in order to enhance awareness and prevent refusal to participate.

KEY WORDS: phenylketonuria, inherited metabolic disorders, newborn screening, health protection

Wiad Lek. 2024;77(8):1611-1616. doi: 10.36740/WLek202408111 DOI

INTRODUCTION

Phenylketonuria (PKU) is an autosomal recessive error of amino acid metabolism, that affects about 1 in 10000 newborns in Europe [1]. The majority of cases are caused by a mutation in the phenylalanine hydroxylase (PAH) gene, which results in the absence or reduced activity of PAH, the liver's enzyme that catalyses the conversion of phenylalanine to tyrosine. Abnormalities in the enzyme's cofactor, tetrahydrobiopterin (BH4), are responsible for a small number of cases [2]. Table 1 illustrates the fundamental metabolic phenotypes in relation to blood phenylalanine (Phe) concentrations. The most common and severe phenotype is classical PKU [3]. High levels of Phe cross the blood-brain barrier and accumulate in the brain. In addition, lower levels of tyrosine lead to a reduced synthesis of neurotransmitters such as dopamine and noradrenaline [4]. The clinical manifestations include severe mental retardation, epilepsy, neurocognitive deficits and behavioural issues. Patients also experience a musty smell, hypopigmentation of the skin, hair, irises, and eczema [5]. It is crucial to highlight that these symptoms can be prevented through the immediate initiation of treatment [6]. This is made possible by the early diagnosis provided by newborn screening programmes.

AIM

The aim of the review is to increase awareness among the population about phenylketonuria and the importance of newborn screening. It emphasizes how their development has significantly enhanced the quality of life and prognosis of patients. The purpose is to demonstrate that participation in neonatal screening is a crucial aspect of health protection.

MATERIALS AND METHODS

A review of the literature was conducted using the PubMed database. In order to identify the most recent scientific sources, the results were limited to a period between 2015 and 2024. The search terms were formu-

Table 1. Metabolic phenotypes and corresponding pre-treatment blood Phe concentrations [3].

Metabolic phenotypes	Pre-treatment blood Phe concentrations
Classical PKU (cPKU)	> 1,200 µmol/L
Mild PKU (mPKU)	600–1,200 µmol/L
Mild hyperphenylalaninemia (MHP)	120–600 µmol/L

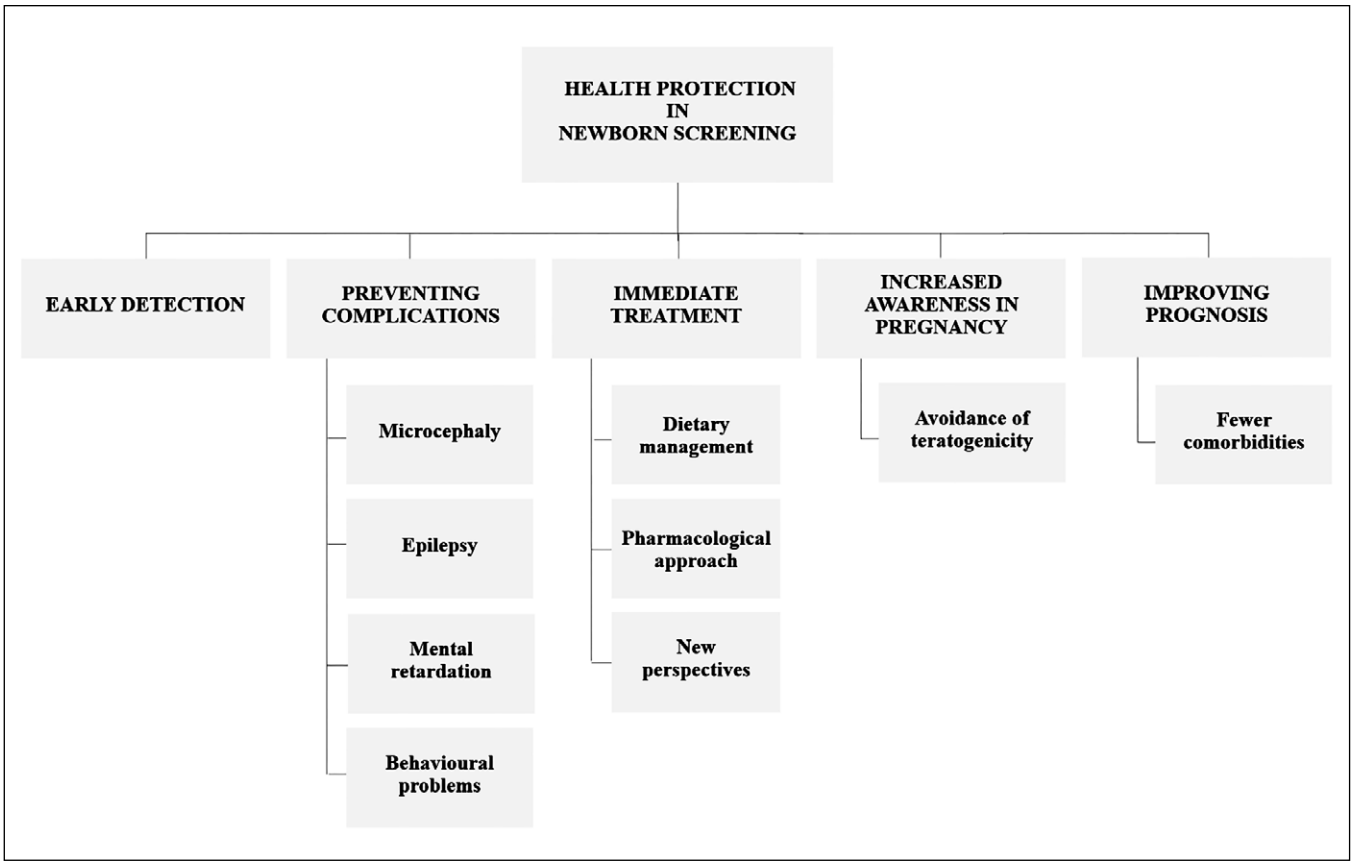

Fig. 1. Phenylketonuria: Key areas of health protection affected by neonatal screening.

lated as follows: "phenylketonuria", "phenylketonuria epidemiology", "phenylketonuria treatment", "newborn screening", "inherited metabolic disorders". All articles retrieved were subjected to analysis.

REVIEW AND DISCUSSION

INHERITED METABOLIC DISORDERS: A MARGINAL OR SIGNIFICANT HEALTH PROBLEM?

Phenylketonuria is one of the most prominent examples of inherited metabolic disorders (IMDs), which comprises over 750 diseases. The majority of these conditions are associated with an abnormality in an enzyme, cofactor or transporter, resulting in impaired functioning of the metabolic pathway [7, 8]. There is a common conception that they are very rare; however, their cumulative incidence is significant [1]. Their number is estimated to be 50.9 per 100,000 live births. Early detection and treatment of metabolic diseases can result in a favourable prognosis. In contrast, undetected and untreated cases have adverse consequences. IMDs are an important cause of mortality in children under the age of five. Approximately 23,500 children die each year from metabolic disease, which represents 0.4% of all child deaths worldwide [9].

MILESTONES IN THE HISTORY OF PHENYLKETONURIA AND NEWBORN SCREENING

The most pivotal event that started the history of metabolic diseases was the discovery of phenylketonuria in 1934 [10]. Dr Fölling examined two siblings who exhibited an intellectual disability and a musty odour. He identified phenylpyruvic acid in their urine. Two decades later, the description of a Phe-reduced dietary regimen marked the beginning of a new era in treatment [11]. Following the creation of a method for the diagnosis

of PKU, newborn screening was first implemented in the United States in 1963 [12]. Subsequently, screening tests were developed for other congenital disorders [13]. Another significant step was the introduction of tandem mass spectrometry (MS/MS) in the 1990s. This analytical technique allows the simultaneous measurement of multiple metabolites in one blood sample. This method has led to the expansion of newborn screening programmes worldwide. Today, approximately 25 million newborns are screened each year using MS/MS [14].

ABOUT NEWBORN SCREENING

The objective of Newborn Bloodspot Screening (NBS) is to identify presymptomatic, treatable congenital conditions at an early stage, allowing for prompt intervention [15]. This is important in preventing potentially severe complications and reducing mortality in infants and children [16]. NBS has evolved from the study of a limited number of disorders to complex programmes that cover over 50 diseases in some countries. In addition to inborn errors of metabolism, these include lysosomal storage disorders, immunodeficiencies, haemoglobin disorders, endocrine disorders, cystic fibrosis, and spinal muscular atrophy [17]. The screening process involves the testing of dried blood spots within the first few days of life [18]. The main motivation for parents to take part in the NBS is the prevention of health problems in their children. One of the primary reasons for declining newborn screening is the concern about potential pain from the heel prick [15]. Failure to inform parents of the purpose of NBS may cause them to opt out without fully understanding the potential risks and benefits [19].

HEALTH PROTECTION – IMPORTANCE OF THE NEWBORN SCREENING

In phenylketonuria, newborn screening plays a crucial role in the context of health protection. Figure 1 illustrates the manner in which NBS impacts health outcomes.

RAPID INTERVENTION FOR BRAIN PROTECTION

Early detection and immediate treatment can prevent the development of serious abnormalities associated with phenylketonuria [6]. Management should be initiated ideally before the age of 10 days [20]. Failure to diagnose and treat PKU can lead to acquired microcephaly, epilepsy and severe cognitive impairment as a result of synaptogenesis defects [4]. Neurological damage becomes irreversible within the first few months or years of life, depending on plasma Phe concentration [6].

THE ESSENCE OF PHENYLALANINE MONITORING IN SUBSEQUENT YEARS

Elevated levels of Phe during late childhood can cause changes in nervous system function, resulting in attention deficit hyperactivity disorder (ADHD), reduced intelligence quotient (IQ), and delayed speech. Adolescents and adults may experience impacts on executive function and mood. Nevertheless, cognitive and behavioural problems can be effectively reversed by maintaining optimal phenylalanine levels [4]. Adherence to treatment may improve intelligence quotient and neuropsychological results [21]. Inadequate management of phenylketonuria may lead to psychological comorbidities, such as phobias and depression [22].

TREATMENT DURATION

The duration of treatment should be determined using objective measurements of blood phenylalanine concentrations. For individuals with Phe blood levels between 360 µmol/L and 600 µmol/L, it is recommended up to the age of 12 years. Lifelong treatment is advised for those with concentrations exceeding 600 µmol/L [23].

DIETARY MANAGEMENT - FUNDAMENTAL OF TREATMENT

The primary treatment for phenylketonuria involves dietary management, specifically limiting natural protein intake and consuming low-protein foods [23]. It is recommended to avoid high-protein products, such as meat, eggs, dairy, cereals, and nuts. The consumption of phenylalanine should be adjusted based on individual tolerance, as determined by test results [24]. Regular monitoring of phenylalanine levels is an essential part of the management of phenylketonuria [25]. Supplementation with medical substitutes, such as Phe-free amino acids (AA) or low-Phe glycomacropeptide (GMP), is used to prevent protein and micronutrient deficiency [26]. The dietary treatment method that shows promise involves supplementing with large neutral amino acids (LNAAs). LNAAs can reduce phenylalanine levels in the brain by competing with phenylalanine for the transporter across the blood-brain barrier [27]. Treatment with these compounds could be an alternative to a demanding low-protein diet in the future [28].

PHARMACOLOGICAL APPROACH AND NEW PERSPECTIVES

Some patients report benefit from pharmacological treatments, such as sapropterin or pegvaliase. Oral

sapropterin is a synthetic form of BH4 that can activate residual PAH and reduce phenylalanine levels when used in conjunction with a controlled diet. However, its effectiveness is limited, with only 20-56% of patients responding to treatment with this medication [29]. Following a lifelong phenylalanine-restricted diet is demanding and burdensome [30]. It is estimated that only 32% of patients follow a Phe-restricted diet with protein replacement as prescribed, the rest are partially compliant or not at all [31]. Furthermore, dining out can pose several difficulties, with the primary obstacle being the restricted availability of low-protein options [32]. A drug that has the potential to improve the long-term outcome and quality of life for patients is pegvaliase. It is an injectable enzyme substitution treatment that degrades phenylalanine. Pegvaliase reduces Phe levels more effectively than standard therapy and allows for greater intact protein intake [29]. However, this treatment requires daily injections and carries the risk of immune-mediated hypersensitivity reactions. Genetic therapies are a promising area of research for directly restoring PAH activity in the liver [33, 34]. Clinical trials are currently underway [33].

INCREASED AWARENESS IN PREGNANCY

It is important for women with phenylketonuria to maintain metabolic control during pregnancy. If phenylalanine levels are high, it can result in maternal phenylketonuria (MPKU) syndrome in the fetus, which is one of the most severe teratogenic pregnancy syndromes [4, 35]. Untreated pregnant women with classical PKU have a 75-90% chance of their offspring developing intellectual disability and microcephaly [4, 36]. Additionally, there is an increased risk of retarded intrauterine growth, congenital heart disease and dysmorphic facial features [35, 37]. Spontaneous miscarriage and early neonatal mortality may also occur [35]. However, controlling the mother's blood phenylalanine levels during pregnancy can prevent MPKU syndrome [36]. It is crucial to monitor phenylalanine levels in the first trimester [37]. The most significant factors for pregnant women to achieve and maintain good metabolic control are the support of loved ones and personalized care from specialist metabolic centres [38].

PROGNOSIS IMPROVEMENT AND ONGOING CHALLENGES

The prognosis for individuals with phenylketonuria has improved significantly thanks to newborn screening and a low-phenylalanine diet [39]. Those who received treatment at a young age are now in their fifth and sixth decades of life and are expected to have a lifespan similar to that of the general population [39, 40]. However, individuals with this condition remain at a heightened risk of developing various health issues, including obesity, hypertension, and osteoporosis [41]. A common comorbidity, particularly in women, is obesity [42]. This condition leads to changes in body composition, including a significant increase in fat content and a decrease in muscle mass, protein, and mineral ingredients [43]. As a result, there may be an increased risk of developing metabolic disorders, such as insulin resistance and dyslipidaemia, which can elevate the likelihood of cardiovascular events [40]. Additionally, individuals with phenylketonuria may have a higher risk of osteoporosis due to low bone mineral density (BMD) [22, 41]. Patients who are diagnosed with PKU at an early age and promptly initiated on appropriate treatment are less prone to developing comorbidities [41].

CONCLUSIONS

The review emphasizes the significance of inherited metabolic disorders, using phenylketonuria as an example, as an important public health concern. Neonatal screening is a crucial aspect of healthcare, with a positive impact on the quality of life and prognosis of patients. Therefore, it is valuable to increase awareness about neonatal screening among parents, so that they can make an informed decision regarding participation. A failure to engage may result in the disease going undetected, which could lead to irreversible neurological complications.

REFERENCES

1. Guerra IMS, Ferreira HB, Neves B, et al. Lipids and phenylketonuria: Current evidences pointed the need for lipidomics studies. Arch Biochem Biophys. 2020;688:108431. doi: 10.1016/j.abb.2020.108431 DOI
2. Elhawary NA, AlJahdali IA, Abumansour IS, et al. Genetic etiology and clinical challenges of phenylketonuria. Hum Genomics. 2022;16(1):22. doi: 10.1186/s40246-022-00398-9. DOI
3. Hillert A, Anikster Y, Belanger-Quintana A, et al. The Genetic Landscape and Epidemiology of Phenylketonuria. Am J Hum Genet. 2020;107(2):234-250. doi: 10.1016/j.ajhg.2020.06.006. DOI
4. Rovelli V, Longo N. Phenylketonuria and the brain. Mol Genet Metab. 2023;139(1):107583. doi: 10.1016/j.ymgme.2023.107583 DOI

5. van Spronsen FJ, Blau N, Harding C, et al. Phenylketonuria. Nat Rev Dis Primers. 2021;7(1):36. doi: 10.1038/s41572-021-00267-0 DOI
6. Wiedemann A, Oussalah A, Jeannesson É, et al. Phenylketonuria, from diet to gene therapy. Med Sci (Paris). 2020;36(8-9):725-734. doi: 10.1051/medsci/2020127 DOI
7. Balakrishnan U. Inborn Errors of Metabolism-Approach to Diagnosis and Management in Neonates. Indian J Pediatr. 2021;88(7):679-689. doi: 10.1007/s12098-021-03759-9 DOI
8. Saudubray JM, Garcia-Cazorla À. Inborn Errors of Metabolism Overview: Pathophysiology, Manifestations, Evaluation, and Management. Pediatr Clin North Am. 2018;65(2):179-208. doi: 10.1016/j.pcl.2017.11.002 DOI
9. Waters D, Adeloye D, Woolham D, et al. Global birth prevalence and mortality from inborn errors of metabolism: a systematic analysis of the evidence. J Glob Health. 2018;8(2):021102. doi: 10.7189/jogh.08.021102 DOI
10. Villoria JG, Pajares S, López RM, et al. Neonatal Screening for Inherited Metabolic Diseases in 2016. Semin Pediatr Neurol. 2016;23(4):257-272. doi: 10.1016/j.spen.2016.11.001 DOI
11. Chen A, Pan Y, Chen J. Clinical, genetic, and experimental research of hyperphenylalaninemia. Front Genet. 2023;13:1051153. doi: 10.3389/fgene.2022.1051153 DOI
12. Spiekerkoetter U, Bick D, Scott R, et al. Genomic newborn screening: Are we entering a new era of screening? J Inherit Metab Dis. 2023;46(5):778-795. doi: 10.1002/jimd.12650 DOI
13. El-Hattab AW, Almannai M, Sutton VR. Newborn Screening: History, Current Status, and Future Directions. Pediatr Clin North Am. 2018;65(2):389-405. doi: 10.1016/j.pcl.2017.11.013 DOI
14. Millington DS. How mass spectrometry revolutionized newborn screening. J Mass Spectrom Adv Clin Lab. 2024;32:1-10. doi: 10.1016/j.jmsacl.2024.01.006 DOI
15. van der Pal SM, Wins S, Klapwijk JE, et al. Parents' views on accepting, declining, and expanding newborn bloodspot screening. PLoS One. 2022;17(8):e0272585. doi: 10.1371/journal.pone.0272585 DOI
16. IJzebrink A, van Dijk T, Franková V, et al. Informing Parents about Newborn Screening: A European Comparison Study. Int J Neonatal Screen. 2021;7(1):13. doi: 10.3390/ijns7010013 DOI
17. Conway M, Vuong TT, Hart K, et al. Pain points in parents' interactions with newborn screening systems: a qualitative study. BMC Pediatr. 2022;22(1):167. doi: 10.1186/s12887-022-03160-1 DOI
18. Pappas KB. Newborn Screening. Pediatr Clin North Am. 2023;70(5):1013-1027. doi: 10.1016/j.pcl.2023.06.003 DOI
19. Fabie NAV, Pappas KB, Feldman GL. The Current State of Newborn Screening in the United States. Pediatr Clin North Am. 2019;66(2):369-386. doi: 10.1016/j.pcl.2018.12.007 DOI
20. van Wegberg AMJ, MacDonald A, Ahring K, et al. The complete European guidelines on phenylketonuria: diagnosis and treatment. Orphanet J Rare Dis. 2017;12(1):162. doi: 10.1186/s13023-017-0685-2 DOI
21. Jameson E, Remmington T. Dietary interventions for phenylketonuria. Cochrane Database Syst Rev. 2020;7(7):CD001304. doi: 10.1002/14651858.CD001304.pub3 DOI
22. Kenneson A, Singh RH. Natural history of children and adults with phenylketonuria in the NBS-PKU Connect registry. Mol Genet Metab. 2021;134(3):243-249. doi: 10.1016/j.ymgme.2021.10.001 DOI
23. van Spronsen FJ, van Wegberg AM, Ahring K, et al. Key European guidelines for the diagnosis and management of patients with phenylketonuria. Lancet Diabetes Endocrinol. 2017;5(9):743-756. doi: 10.1016/S2213-8587(16)30320-5 DOI
24. MacDonald A, van Wegberg AMJ, Ahring K, et al. PKU dietary handbook to accompany PKU guidelines. Orphanet J Rare Dis. 2020;15(1):171. doi: 10.1186/s13023-020-01391-y DOI
25. Zuñiga Vinueza AM. Recent Advances in Phenylketonuria: A Review. Cureus. 2023;15(6):e40459. doi: 10.7759/cureus.40459 DOI
26. Manta-Vogli PD, Dotsikas Y, Loukas YL, et al. The phenylketonuria patient: A recent dietetic therapeutic approach. Nutr Neurosci. 2020;23(8):628-639. doi: 10.1080/1028415X.2018.1538196 DOI
27. Appaiah P, Vasu P. Improvement, cloning, and expression of an in silico designed protein enriched with large neutral amino acids in Pichia pastoris for possible application in phenylketonuria. J Food Biochem. 2020;44(3):e13151. doi: 10.1111/jfbc.13151 DOI
28. van Vliet D, van der Goot E, van Ginkel WG, et al. The increasing importance of LNAA supplementation in phenylketonuria at higher plasma phenylalanine concentrations. Mol Genet Metab. 2022;135(1):27-34. doi: 10.1016/j.ymgme.2021.11.003 DOI
29. Burton BK, Clague GE, Harding CO, et al. Long-term comparative effectiveness of pegvaliase versus medical nutrition therapy with and without sapropterin in adults with phenylketonuria. Mol Genet Metab. 2024;141(1):108114. doi: 10.1016/j.ymgme.2023.108114 DOI
30. McWhorter N, Ndugga-Kabuye MK, Puurunen M, et al. Complications of the Low Phenylalanine Diet for Patients with Phenylketonuria and the Benefits of Increased Natural Protein. Nutrients. 2022;14(23):4960. doi: 10.3390/nu14234960 DOI
31. Ilgaz F, Ford S, O'Driscoll MF, et al. Adult PKU Clinics in the UK-Users' Experiences and Perspectives. Nutrients. 2023;15(20):4352. doi: 10.3390/nu15204352 DOI
32. Poole G, Pinto A, Evans S, et al. Hungry for Change: The Experiences of People with PKU, and Their Caregivers, When Eating Out. Nutrients. 2022;14(3):626. doi: 10.3390/nu14030626 DOI

33. Martinez M, Harding CO, Schwank G, et al. State-of-the-art 2023 on gene therapy for phenylketonuria. J Inherit Metab Dis. 2024;47(1):80-92. doi: 10.1002/jimd.12651 DOI
34. Maestro S, Weber ND, Zabaleta N, et al. Novel vectors and approaches for gene therapy in liver diseases. JHEP Rep. 2021;3(4):100300. doi: 10.1016/j.jhepr.2021.100300 DOI
35. Alghamdi MA, O'Donnell-Luria A, Almontashiri NA, et al. Classical phenylketonuria presenting as maternal PKU syndrome in the offspring of an intellectually normal woman. JIMD Rep. 2023;64(5):312-316. doi: 10.1002/jmd2.12384 DOI
36. Waisbren SE, Rohr F, Anastasoaie V, et al. Maternal Phenylketonuria: Long-term Outcomes in Offspring and Post-pregnancy Maternal Characteristics. JIMD Rep. 2015;21:23-33. doi: 10.1007/8904_2014_365 DOI
37. Yıldız Y, Sivri HS. Maternal phenylketonuria in Turkey: outcomes of 71 pregnancies and issues in management. Eur J Pediatr. 2019;178(7):1005-1011. doi: 10.1007/s00431-019-03387-8 DOI
38. Rohde C, Thiele AG, Baerwald C, et al. Preventing maternal phenylketonuria (PKU) syndrome: important factors to achieve good metabolic control throughout pregnancy. Orphanet J Rare Dis. 2021;16(1):477. doi: 10.1186/s13023-021-02108-5 DOI
39. Vardy ERLC, MacDonald A, Ford S, et al. Phenylketonuria, co-morbidity, and ageing: A review. J Inherit Metab Dis. 2020;43(2):167-178. doi: 10.1002/jimd.12186 DOI
40. Luengo-Pérez LM, Fernández-Bueso M, Ambrojo A, et al. Body Composition Evaluation and Clinical Markers of Cardiometabolic Risk in Patients with Phenylketonuria. Nutrients. 2023;15(24):5133. doi: 10.3390/nu15245133 DOI
41. Charrière S, Maillot F, Bouée S, et al. Health status and comorbidities of adult patients with phenylketonuria (PKU) in France with a focus on early-diagnosed patients - A nationwide study of health insurance claims data. Mol Genet Metab. 2023;139(3):107625. doi: 10.1016/j.ymgme.2023.107625 DOI
42. Tankeu AT, Pavlidou DC, Superti-Furga A, et al. Overweight and obesity in adult patients with phenylketonuria: a systematic review. Orphanet J Rare Dis. 2023;18(1):37. doi: 10.1186/s13023-023-02636-2. DOI
43. Barta AG, Becsei D, Kiss E, et al. The Impact of Phenylketonuria on Body Composition in Adults. Ann Nutr Metab. 2022;78(2):98-105. doi: 10.1159/000520047. DOI

CONFLICT OF INTEREST

The Authors declare no conflict of interest

CORRESPONDING AUTHOR

Katarzyna Piotrowicz
Student of the Faculty of Medicine,
Poznan University of Medical Sciences,
Poznań, Poland
e-mail: katarzyna.piotrowicz@op.pl

ORCID AND CONTRIBUTIONSHIP

Katarzyna Piotrowicz: 0009-0009-3888-3885 A B D E F
Hubert Piotrowicz: 0009-0008-2453-3561 A B D E F
Jacek Kurzeja: 0009-0004-4075-7208 B D E
Emilia Żurowska: 0009-0006-5952-1064 B D

A – Work concept and design, B – Data collection and analysis, C – Responsibility for statistical analysis, D – Writing the article, E – Critical review, F – Final approval of the article

RECEIVED: 15.05.2024
ACCEPTED: 11.07.2024

REVIEW ARTICLE

CONTENTS

Novel non-pharmacological strategies for managing dentophobia in adult patients – literature review

Artur Los, Jakub Fiegler-Rudol, Monika Tysiąc-Miśta, Marta Tanasiewicz
DEPARTMENT OF CONSERVATIVE DENTISTRY AND ENDODONTICS, MEDICAL UNIVERSITY OF SILESIA, KATOWICE, POLAND

ABSTRACT

Dentophobia concerns a substantial portion of the adult population, often leading to avoidance of dental care and subsequent deterioration in oral health. This comprehensive review explores the multifaceted nature of odontophobia and examines various non-pharmacological strategies aimed at its management in adult patients. Factors contributing to dentophobia, including past traumatic experiences, feelings of vulnerability, and mistrust in dental professionals, are discussed, highlighting the complex interplay of psychological, physiological, and environmental influences. Novel approaches such as Virtual Reality Exposure Therapy offer promising avenues for systematically desensitising patients to their fears and enhancing treatment acceptance. Aromatherapy utilising essential oils like chamomile, orange, and lavender, as well as dog-assisted therapy, have shown potential in creating calming environments and reducing patient anxiety during dental procedures. Muscle relaxation therapy, biofeedback techniques, and process simulations provide additional tools for addressing the physiological and cognitive aspects of odontophobia. Cognitive-behavioural therapy interventions, including brief sessions focused on cognitive restructuring and exposure therapy, demonstrate efficacy in reducing fear of dentists and improving treatment outcomes. By incorporating these diverse non-pharmacological strategies into dental practice, clinicians can enhance patient experiences, increase treatment acceptance and adherence, and ultimately improve oral health outcomes. While these interventions show promising results, further research is needed to refine their implementation, optimize their effectiveness, and ensure accessibility to patients with dentophobia. By addressing the multifaceted nature of dental anxiety and adopting a patient-centred approach, clinicians can provide holistic care, fostering better oral health and overall well-being in their patients.

KEY WORDS: stress, dentistry, dentophobia

Wiad Lek. 2024;77(8):1617-1622. doi: 10.36740/WLek202408112 DOI

INTRODUCTION

Dentophobia is a significant issue affecting a large population of adults. This severe anxiety can lead to avoidance of dental care, resulting in potentially more complex and urgent dental conditions in the future such as periodontitis, which leads to tooth loss and general deterioration of oral health. Without proper management, odontophobia can prevent patients from seeking necessary dental treatments, which is detrimental not only to oral health but also general well-being [1].

The management of fear of dentists is crucial for the comfort and mental health of patients and the effectiveness of dental treatment. Adequate management strategies can significantly enhance patients' cooperation, reduce the stress associated with dental visits, and improve overall treatment outcomes [2, 3].

Dental anxiety can stem from various sources, both personal experiences and external influences. A traumatic dental encounter in the past can leave a lasting imprint, causing individuals to dread future visits. Feelings of vulnerability and loss of control while confined to the dental chair can also contribute to this anxiety. Furthermore, a sense of shame or embarrassment about one's teeth or oral health can exacerbate the discomfort associated with dental visits. In some cases, a lack of trust or confidence in the dentist's competence or bedside manner can fuel apprehension [4]. Dentophobia is among the most prevalent phobias globally, despite increased awareness and efforts to enhance the dentist - patient relationship [5].

AIM

The aim of this review is to provide information about less common non-pharmacological strategies for managing odontophobia in adult patients, discuss their effectiveness and encourage implementation of these methods into clinical practice to improve patient experiences and treatment outcomes. The review also highlights the need for further research to validate and optimize these strategies for use in routine clinical dental settings.

MATERIALS AND METHODS

The preparation of this review article involved a structured search of the PubMed and Scopus databases to identify relevant studies on non-pharmacological interventions for managing odontophobia in adult patients. Keywords used in the search included "odontophobia," "dental anxiety,""Virtual Reality Exposure Therapy,""aromatherapy,""muscle relaxation therapy,""biofeedback," "process simulations," and "Cognitive Behavioral Therapy." The search was restricted to peer-reviewed articles published in English. Studies were selected based on their relevance to adult patients, the robustness of their methodology, and the use of non-pharmacological interventions. Data were extracted regarding intervention type, study design, sample size, duration, outcome measures, and main findings.

REVIEW AND DISCUSSION

VIRTUAL REALITY EXPOSURE THERAPY (VRET)

VRET is a novel cognitive-behavioural approach that uses computer-generated virtual environments to treat specific anxieties through systematic and gradual desensitization until fear extinction occurs. It is considered an in vitro form of exposure therapy, where the patient can confront their fears in a controlled setting, reducing anticipatory anxiety and increasing treatment acceptance and completion rates [6, 7]. VRET is equally or slightly more effective than real-life exposure therapy for anxiety treatment. Studies like those by Guijar et al. (2018) have demonstrated that VRET can significantly reduce dentophobia and behavioural avoidance, with patients in the VRET group more likely to schedule follow-up appointments and no longer meet the criteria for dental anxiety after treatment [6,8].

Yamashita et al. evaluated the effect of Virtual Reality (VR) in alleviating anxiety during impacted mandibular third molar extractions under local anaesthesia. They found that anxiety decreased among patients who used VR, while it increased in those who did not apply it. Objective measures like heart rate variability and subjective questionnaires confirmed these findings. Notably, 92% of participants reported decreased anxiety, 100% wanted to use VR in future surgical treatments, and 96% desired it for future dental treatments [9, 10].

AROMATHERAPY

Chamomile oil is known for its aromatherapeutic properties, which can help patients maintain a calm mental state. A randomised controlled trial assessed the effect of chamomile oil on dentophobia in patients undergoing extractions. The oil was administered through inhalation using a diffuser. The results concluded that chamomile oil significantly decreased odontophobia levels, showcasing its effectiveness in creating a calming environment for patients [11]. Orange oil possesses sedative and anxiolytic properties, which are attributed to its ability to permeate through mucosal membranes and stimulate the central nervous system after crossing the blood-brain barrier. A study investigating the effect of ambient orange fragrance on patient anxiety during the surgical removal of impacted third molars found that the intervention group exhibited significantly lower mean blood pressure, pulse rate, and respiratory rate during the surgical procedure. This indicates that orange fragrance effectively reduces anxiety during dental procedures [12].

Lavender oil is one of the most preferred essential oils for aromatherapy due to its sedative properties. Linalool, a key component in lavender oil, acts on gamma-aminobutyric acid (GABA-A) receptors, causing an inhibitory effect on the limbic system and autonomic transmission. This results in a decrease in blood pressure and anxiety levels. Studies have shown that lavender oil inhalation can produce effects like lorazepam, making it a safer and more accessible option for reducing dental anxiety. Lavender oil has also been shown to have antidepressant, sedative, calmative, antibacterial, and antifungal properties, further supporting its use as an anxiolytic agent [13].

DOG-ASSISTED THERAPY CONCEPT AND POTENTIAL BENEFITS

Dog-assisted therapy involves the use of trained therapy dogs to provide comfort, reduce stress, and improve overall emotional well-being in therapeutic settings. This form of therapy leverages the innate bond between humans and animals, particularly dogs, to promote psychological and physiological healing. The presence of a therapy dog can help reduce blood pressure, heart rate, and anxiety while increasing feelings of comfort and safety. It is particularly beneficial in medical environments, where patients may feel anxious or uneasy about the procedures they are undergoing [14].

A pilot study conducted by Cruz-Fierro et al. evaluated the effectiveness of dog-assisted therapy in managing dentophobia. The findings from this study indicated that the presence of a therapy dog during dental sessions significantly improved the patients' emotional state. The study observed a notable decrease in blood pressure and neurohormone levels among patients interacting with the therapy dog, suggesting a physiological response to the calming presence of the dog.

Patients reported a reduction in discomfort and an overall improved experience during their dental visits [15]. This improvement in patient experience is crucial as it can lead to better compliance with dental treatments and less avoidance of future dental care. The therapy provided by the dog's presence helped significantly reducing the anxiety levels of the patients, making them more relaxed during the dental procedures.

The pilot study on dog-assisted therapy for dental anxiety demonstrated promising results, indicating that this therapy could be a valuable addition to traditional methods for managing dental anxiety. However, the study also noted the need for further research to fully establish the effectiveness and implement this therapy widely in dental practices [16].

MUSCLE RELAXATION THERAPY

Muscle relaxation therapy (MRT) is based on the principle that anxiety and stress lead to increased muscle tension. By consciously relaxing the muscles, the body's physiological response to stress and anxiety can be reduced. MRT help suppress the response of the sympathetic nervous system, which is activated during stressful situations like dental procedures. By inducing a relaxed state, muscle relaxation therapy lowers heart rate, respiratory rate, and blood pressure, which are elevated during anxiety. This therapy helps regulate both the peripheral and central nervous systems, reducing the overall stress response and promoting a calmer state. MRT has been shown to decrease levels of cortisol in the body. The most common form of muscle relaxation therapy used for dental anxiety is progressive muscle relaxation therapy (PMRT) [17, 18].

In PMRT, patients are guided to systematically tense and then relax different muscle groups throughout the body, helping them differentiate between tension and relaxation states. A study by Park et al. investigated the effectiveness of PMRT in alleviating dental anxiety. The study found that PMRT over four sessions effectively alleviated anxiety for at least three months following the intervention [17]. The intervention significantly reduced depressive symptoms, blood pressure, pulse rate, and salivary cortisol levels in participants. The study concluded that PMRT might be beneficial in reducing dentophobia. By lowering physiological parameters like heart rate, respiratory rate, and blood pressure, and regulating the nervous system, PMRT helps reduce stress, anxiety, and depression, thereby alleviating dental anxiety. Overall, the evidence presented in the study suggests that PMRT is an effective non-pharmacological intervention for managing odontophobia. It can help patients achieve a relaxed state, improve their ability to cope with the stress of dental procedures, and potentially enhance their overall experience and compliance with dental treatment [17, 19].

BIOFEEDBACK: CONCEPT AND POTENTIAL BENEFITS

Biofeedback is a technique that involves measuring and providing real-time feedback on an individual's physiological processes, such as heart rate, breathing rate, muscle tension, and skin temperature. The primary goal of biofeedback is to help individuals gain awareness and control over these physiological functions, which are often dysregulated during states of anxiety or stress. By providing visual or auditory feedback on physiological parameters like heart rate or breathing rate, patients become more aware of their body's stress response during dental procedures. With the help of biofeedback, patients can learn techniques to consciously regulate their physiological processes, such as slowing down their breathing or relaxing their muscles, which can counteract the anxiety response [20, 21].

Biofeedback empowers patients by giving them a sense of control over their body's reactions, which can be particularly helpful in situations where they feel a lack of control, such as during dental procedures. By promoting relaxation and self-regulation, biofeedback can effectively reduce anxiety, stress, and negative emotions associated with dental visits. A pilot study conducted by Morarend et al. investigated the use of a novel biofeedback device to reduce preoperative general anxiety levels in a dental setting. The results demonstrated the effectiveness of the biofeedback device in reducing dental anxiety and negative feelings associated with dental injections [22].

The biofeedback device allowed both the patient and the dentist to monitor the patient's physiological information, such as respiratory rate, which is often dysregulated during anxiety attacks. By providing real-time feedback, the device assisted patients in practising control and self-regulating their monitored physiological processes, thereby helping them down-regulate the sympathetic nervous system response associated with anxiety. Biofeedback offers a non-invasive and empowering approach to managing odontophobia by increasing awareness, promoting self-regulation, and reducing the physiological manifestations of anxiety [23].

CONCEPT OF PROCESS SIMULATIONS AND THEIR MECHANISMS

Process simulations (PSs) involve mentally simulating or imagining the process of undergoing a particular task

or procedure. In the context of dentophobia, PSs allow patients to mentally rehearse and familiarize themselves with the steps involved in a dental procedure before experiencing it.

By mentally simulating the process, patients can prepare themselves cognitively for what to expect during the actual procedure. This familiarity can help reduce anticipatory anxiety and fear of the unknown. PSs give patients a sense of control over the situation, as they can mentally rehearse and plan their responses and coping strategies. This perceived control can help mitigate feelings of helplessness and anxiety. Repeated mental simulations can lead to a gradual desensitization to the anxiety-provoking stimuli associated with the dental procedure, reducing the overall fear response. PSs can help patients identify and challenge irrational thoughts or beliefs related to dental procedures, allowing for cognitive restructuring and a more realistic perspective [24].

A study by Armitage and Reidy investigated the effectiveness of PSs in reducing anxiety before and after consultations. The key findings were that process simulations significantly reduced state anxiety (situational anxiety) before and after consultations. The results were consistent with previous research, demonstrating that PSs are clinically and statistically effective in reducing state anxiety [25]. The anxiety-reducing effects of process simulations had a prolonged effect, lasting even after the consultation. The study suggests that PSs can be effective in reducing anxiety in field settings, where there is an imminent threat of physical discomfort, such as dental procedures. Further research is needed to refine the technique of PSs and identify other active components that contribute to its effectiveness as an intervention for reducing anxiety [26].

COGNITIVE-BEHAVIORAL THERAPY

Cognitive-behavioral therapy (CBT) is a psychotherapeutic approach that focuses on modifying dysfunctional thoughts, beliefs, and behaviours that contribute to anxiety and other psychological distress. In the context of dentophobia, CBT aims to address the irrational thoughts, beliefs, and maladaptive behaviours that exacerbate fear and avoidance of dental procedures [1, 27].

The key principles of CBT for odontophobia include Identifying and challenging irrational or distorted thoughts and beliefs related to dental procedures, such as catastrophizing or overestimating the likelihood of negative outcomes. Gradually exposing the patient to anxiety-provoking dental stimuli in a controlled and safe environment, leading to desensitization and reduced fear response [27].

Teaching patients relaxation strategies, such as deep breathing exercises or progressive muscle relaxation, to manage physiological symptoms of anxiety during dental procedures. Developing coping strategies and problem-solving skills to better manage anxiety-provoking situations and increase a sense of control. Providing information about the nature of anxiety, its symptoms, and the rationale behind CBT techniques to promote understanding and engagement in the treatment process. The study highlights the potential effectiveness of brief CBT interventions, involving one to three sessions, in reducing dental anxiety.

Spindler et al.: investigated the effect of a brief dental fear intervention based on cognitive-behavioral principles specifically designed for dental practice. The findings showed that the immediate treatment group experienced a significant reduction in dental anxiety compared to the waiting list condition. After both groups completed the intervention, the reduction in anxiety were comparable and maintained at the two-year follow-up [28]. Previous studies suggest that brief interventions involving one to three sessions might effectively reduce odontophobia, even in the long term. Brief CBT interventions might be equal or superior to other forms of intervention, and their benefits persist over time. Brief cognitive-behavioural interventions performed by practising dentists might be sufficient for a significant proportion of patients with dental anxiety. However, it also acknowledges that the number of sessions in each study varies, and further research is needed to optimize the implementation of these interventions in dental settings [29, 30].

CONCLUSIONS

Dentophobia among adults can lead to avoidance of dental care, increased risk of periodontal diseases, tooth loss and general deterioration of oral health. Effective management of dental anxiety is crucial for patient comfort and treatment effectiveness. Various factors contribute to odontophobia, including past traumatic experiences and feelings of vulnerability. Non-pharmacological strategies such as VRET, aromatherapy, dog-assisted therapy, MRT, biofeedback, PSs, and CBT have shown promise in managing dental anxiety. VRET has been effective in reducing dental anxiety, while aromatherapy with oils like chamomile, orange, and lavender has demonstrated calming effects. Dog-assisted therapy has been shown to improve patient experience and reduce anxiety during dental visits. MRT, particularly PMRT, has been effective in suppressing the sympathetic nervous system response and reducing stress. Biofeedback helps patients gain awareness and control

over physiological functions, while PSs allow patients to mentally prepare for dental procedures. CBT, especially in brief interventions, addresses dysfunctional thoughts and behaviours contributing to anxiety. Overall, integrating these non-pharmacological strategies into dental practice can improve patient experiences and treatment outcomes, though further research is needed for optimization and widespread implementation.

REFERENCES

1. Hoffmann B, Erwood K, Ncomanzi S, Fischer V, O'Brien D, Lee A. Management strategies for adult patients with dental anxiety in the dental clinic: a systematic review. Aust Dent J. 2022 Mar;67 Suppl 1(Suppl 1):S3-S13. doi: 10.1111/adj.12926. Epub 2022 Jul 12. DOI
2. Armfield J, Heaton L. Management of fear and anxiety in the dental clinic: a review. Aust Dent J. 2013;58:390-407. doi: 10.1111/adj.12118 DOI
3. Sindhu R, Rajaram S, Bharathwaj VV, Mohan R, Manipal S, Prabu D. Is Individual deprivation measures associated with dental anxiety and socioeconomic status of patients visiting dentists. Indian J Dent Res. 2020;31:515-519.
4. Armfield JM. Towards a better understanding of dental anxiety and fear: Cognitions vs. experiences. Eur J Oral Sci. 2010;118:259-264. doi: 10.1111/j.1600-0722.2010.00740.x DOI
5. Sindhu R, Rajaram S, Bharathwaj VV, Mohan R, Manipal S, Prabu D. Is Individual deprivation measures associated with dental anxiety and socioeconomic status of patients visiting dentists. Indian J Dent Res. 2020;31:515-519. doi: 10.4103/ijdr.IJDR_802_18. DOI
6. Gujjar K, Sharma R, Jongh A. Virtual reality exposure therapy for treatment of dental phobia. Dent Update 2017;44:423-435. 10.12968/denu.2017.44.5.423.x
7. Gujjar K, Van Wijk A, Sharma R, De Jongh A. Virtual reality exposure therapy for the treatment of dental phobia: a controlled feasibility study. Behav Cogn Psychother 2018;46:367-373. doi: 10.1017/S1352465817000534 DOI
8. Boeldt D, McMahon E, McFaul M, Greenleaf W. Using Virtual Reality Exposure Therapy to Enhance Treatment of Anxiety Disorders: Identifying Areas of Clinical Adoption and Potential Obstacles. Front Psychiatry. 2019 Oct 25;10:773. doi: 10.3389/fpsyt.2019.00773. DOI
9. Yamashita Y, Shimohira D, Aijima R, Mori K, Danjo A. Clinical effect of virtual reality to relieve anxiety during impacted mandibular third molar extraction under local anaesthesia. J Oral Maxillofac Surg. 2020;78:545.e541–545.e546. 10.1016/j.joms.2019.11.016
10. Kothgassner OD, Goreis A, Kafka JX, Van Eickels RL, Plener PL, Felnhofer A. Virtual reality exposure therapy for posttraumatic stress disorder (PTSD): a meta-analysis. Eur J Psychotraumatol. 2019 Aug 19;10(1):1654782. doi: 10.1080/20008198.2019.1654782. DOI
11. Baskran R, Lakshmanan R. Assessment of effect of chamomile oil on dental anxiety for patients undergoing extraction – a randomized controlled trial. Drug Invent Today 2019;11:1875-1879.
12. Hasheminia D, Kalantar Motamedi M, Karimi Ahmadabadi F, Hashemzehi H, Haghighat A. Can ambient orange fragrance reduce patient anxiety during surgical removal of impacted mandibular third molars? J Oral Maxillofac Surg. 2014;72:1671-1676. doi: 10.1016/j.joms.2014.03.031 DOI
13. Karan N. Influence of lavender oil inhalation on vital signs and anxiety: a randomized clinical trial. Physiol Behav. 2019;211:112676. 10.1016/j.physbeh.2019.112676
14. Bert F, Gualano MR, Camussi E, Pieve G, Voglino G, Siliquini R. Animal assisted intervention: A systematic review of benefits and risks. Eur J Integr Med. 2016 Oct;8(5):695-706. doi: 10.1016/j.eujim.2016.05.005 DOI
15. Cruz–fierro N, Vanegas–Farfano M, González–Ramírez MT. Dog–assisted therapy and dental anxiety: a pilot study. Animals 2019;9. doi: 10.3390/ani9080512 DOI
16. Cherniack EP, Cherniack AR. The benefit of pets and animal-assisted therapy to the health of older individuals. Curr Gerontol Geriatr Res. 2014;2014:623203. doi: 10.1155/2014/623203. DOI
17. Park E, Yim H, Lee K. Progressive muscle relaxation therapy to relieve dental anxiety: a randomized controlled trial. Eur J Oral Sci. 2019;127:45-51. doi: 10.1111/eos.12585 DOI
18. Mejía-Rubalcava C, Alanís-Tavira J, Mendieta-Zerón H, Sánchez-Pérez L. Changes induced by music therapy to physiologic parameters in patients with dental anxiety. Complement Ther Clin Pract. 2015 Nov;21(4):282-6. doi: 10.1016/j.ctcp.2015.10.005. DOI
19. Mills MP. Periodontal implications: anxiety. Ann Periodontol. 1996 Nov;1(1):358-89. doi: 10.1902/annals.1996.1.1.358. DOI
20. Frank DL, Khorshid L, Kiffer JF, Moravec CS, McKee MG. Biofeedback in medicine: who, when, why and how? Ment Health Fam Med. 2010 Jun;7(2):85-91.
21. Schwartz MS, Andrasik F. Biofeedback: a practitioner's guide. New York: Guilford Press, 2003.
22. Morarend Q, Spector M, Dawson D, Clark S, Holmes D. The use of a respiratory rate biofeedback device to reduce dental anxiety: an exploratory investigation. Appl Psychophysiol Biofeed 2011;36:63-70. doi: 10.1007/s10484-011-9148-z DOI
23. Dou L, Vanschaayk MM, Zhang Y, Fu X, Ji P, Yang D. The prevalence of dental anxiety and its association with pain and other variables among adult patients with irreversible pulpitis. BMC Oral Health. 2018 Jun 7;18(1):101. doi: 10.1186/s12903-018-0563-x. DOI
24. Armitage CJ, Reidy JG. Evidence that process simulations reduce anxiety in patients receiving dental treatment: randomized exploratory trial. Anxiety Stress Coping. 2012 Mar;25(2):155-65. doi: 10.1080/10615806.2011.604727. DOI

25. Higgins D, Hayes M, Taylor J, Wallace J. A scoping review of simulation-based dental education. MedEdPublish (2016). 2020 Feb 27;9:36. doi: 10.15694/mep.2020.000036.1. DOI
26. Armitage C, Reidy J. Evidence that process simulations reduce anxiety in patients receiving dental treatment: randomized exploratory trial. Anxiety Stress Coping. 2012;25:155-165. 10.1080/10615806.2011.604727
27. Matsuoka H, Chiba I, Sakano Y, Toyofuku A, Abiko Y. Cognitive behavioral therapy for psychosomatic problems in dental settings. Biopsychosoc Med. 2017 Jun 13;11:18. doi: 10.1186/s13030-017-0102-z. DOI
28. Spindler H, Staugaard S, Nicolaisen C, Poulsen R. A randomized controlled trial of the effect of a brief cognitive–behavioral intervention on dental fear. J Publ Health. Dent 2015;75:64–73. 10.1111/jphd.12074
29. Blackwell SE, Heidenreich T. Cognitive behavior therapy at the crossroads. Int J Cogn Ther. 2021;8:1-22.
30. Curtiss JE, Levine DS, Ander I, Baker AW. Cognitive-behavioral treatments for anxiety and stress-related disorders'. Focus (Am Psychiatr Publ). 2021 Jun;19(2):184-189. doi:10.1176/appi.focus.20200045. DOI

CONFLICT OF INTEREST

The Authors declare no conflict of interest

CORRESPONDING AUTHOR

Jakub Fiegler-Rudol
Department of Conservative Dentistry and Endodontics
Medical University of Silesia, Poland
e-mail: jakub.fiegler@gmail.com

ORCID AND CONTRIBUTIONSHIP

Artur Los: 0009-0004-1743-7716 A B D
Jakub Fiegler-Rudol: 0009-0009-3173-9389 A D
Monika Tysiąc-Miśta: 0000-0001-5750-6174 E F
Marta Tanasiewicz: 0000-0002-8700-7381 E F

A – Work concept and design, B – Data collection and analysis, C – Responsibility for statistical analysis, D – Writing the article, E – Critical review, F – Final approval of the article

RECEIVED: 07.05.2024
ACCEPTED: 20.07.2024

CASE STUDY

CONTENTS

Orbital floor reconstruction based on 3d printed model – case report

Piotr Pławecki[1], Magdalena Jędrusik-Pawłowska[1], Agnieszka Rolek[2], Agata Cieślik-Bielecka[1]
[1]DEPARTMENT OF CRANIO-MAXILLO-FACIAL SURGERY, PROVINCIAL SPECIALIST HOSPITAL NO. 5 IN SOSNOWIEC, SOSNOWIEC, POLAND
[2]PRIVATE DENTAL PRACTICE - AGNIESZKA ROLEK, WROCLAW, POLAND

ABSTRACT
Orbital fractures, constituting 10-25% of facial traumas, result from diverse mechanisms such as traffic accidents and assaults. These fractures present with characteristic symptoms like edema, diplopia, and infraorbital paraesthesia. Timely diagnosis and surgical intervention are paramount to mitigate long-term complications. Recent advancements in materials science and surgical methodologies have ushered in innovative approaches including 3D printing and computer-aided design implants. This article details a case study of successful reconstructive orbital surgery in a patient following a traumatic incident where a car accident caused extensive facial fractures. Leveraging 3D printing technology, a precisely tailored titanium mesh aided in the meticulous restoration of the orbital floor. During surgery, entrapped soft tissues were released, and the zygomatic-maxillary complex was carefully repositioned. Postoperative evaluation revealed promising outcomes, affirming the efficacy of contemporary surgical strategies. This case highlights the evolving role of 3D printing in enhancing the accuracy, cost-effectiveness, and accessibility of orbital reconstruction procedures, demonstrating its potential for broader clinical applications.

KEY WORDS: trauma, 3d print, orbital floor reconstrution

Wiad Lek. 2024;77(8):1623-1626. doi: 10.36740/WLek202408113 DOI

INTRODUCTION
Orbital fractures occur through various mechanisms and account for 10-25% of facial fractures [1]. They most commonly result from traffic accidents and assaults [2]. The fracture patterns are stereotypical with predictable short, medium, and long-term symptoms such as edema, infraorbital paraesthesia, blurred vision, subconjunctival hemorrhage, diplopia, orbital dystopia, and enophthalmos [3, 4]. All of these can be minimized by rapid diagnosis and anatomical repair. An early aggressive surgical approach within 14 days is recommended and is more effective than secondary reconstructive procedures [5]. The development of materials science and surgical techniques has led to innovations such as prefabricated titanium mesh, computer-aided design implants, 3D printing, and surgical navigation [6, 7]. The origins of reconstructive orbital surgery date back to the late 19th century when reconstructions were performed using steel wires and antral bone grafts [8]. Since the 1950s, alloplastic materials and bone substitutes have been used [9]. Despite the advances in reconstructive techniques, the goal of treatment has remained the same: to restore the bony walls of the orbit, as well as function and aesthetics. Currently used materials include autogenous materials that are biocompatible, reliable, and cheap but offer limited shaping ability and are associated with donor site morbidity [4]. Allogenic materials are osteoconductive but carry the risk of severe disease transmission [10]. Alloplastic materials allow for the most precise implant design but always carry the risk associated with a permanent foreign body [11]. The disadvantage of resorbable alloplastic materials is that once resorption occurs, the orbital tissues, deprived of support, may tend to collapse [12].

AIM
This article details a case study of successful reconstructive orbital surgery in a patient following a traumatic incident where a car accident caused extensive facial fractures.

CASE REPORT
On April 4, 2023, shortly after midnight, a patient was hit by a car while crossing the street. Initially transported to the Emergency Department of the Hospital in Dąbrowa Górnicza with head injuries, a CT scan revealed a right subdural and epidural hematoma

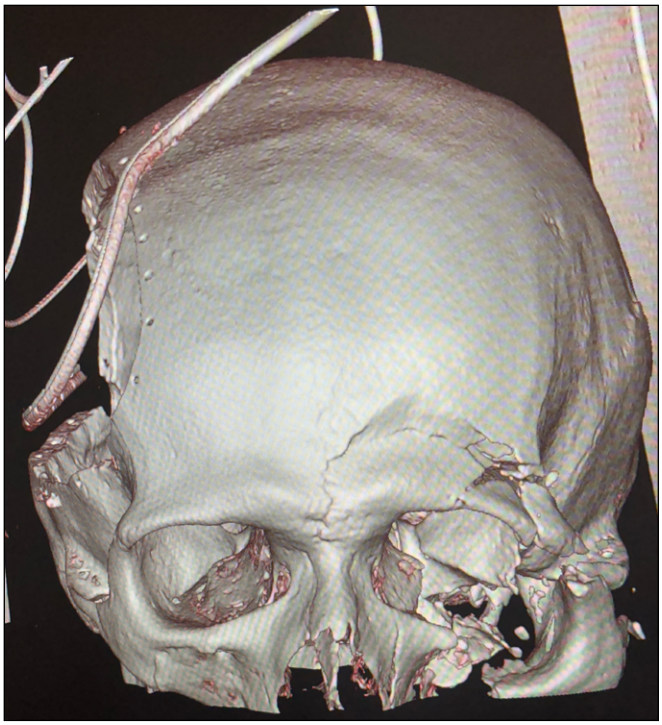

Fig. 1. CT scan before reconstruction.

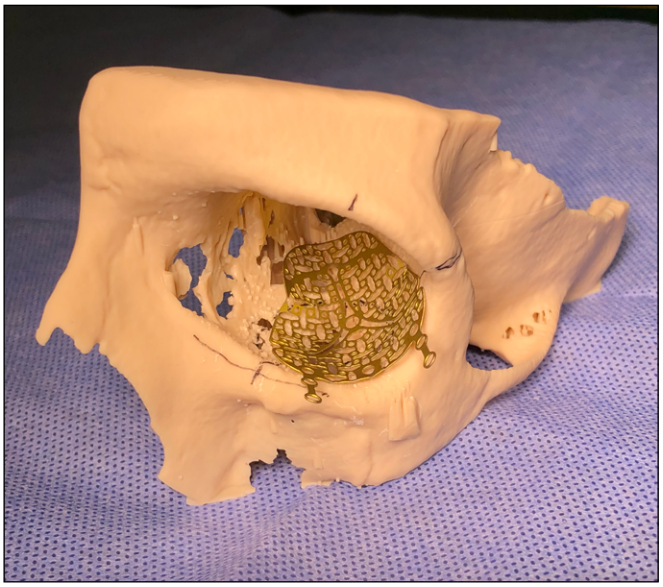

Fig. 2. 3d printed mirror image of the left orbit with shaped titanium mesh.

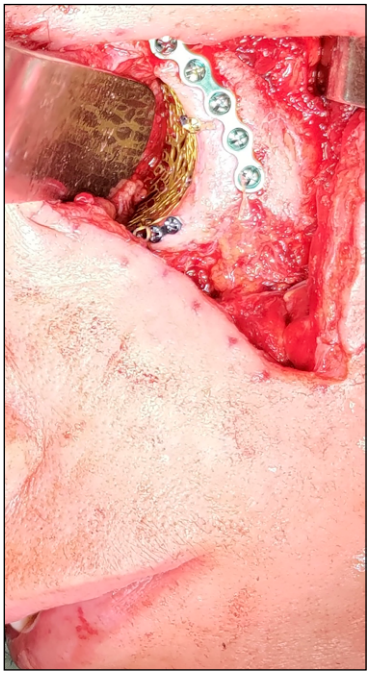

Fig. 3. Reconstructed orbital contour, intraoperative view.

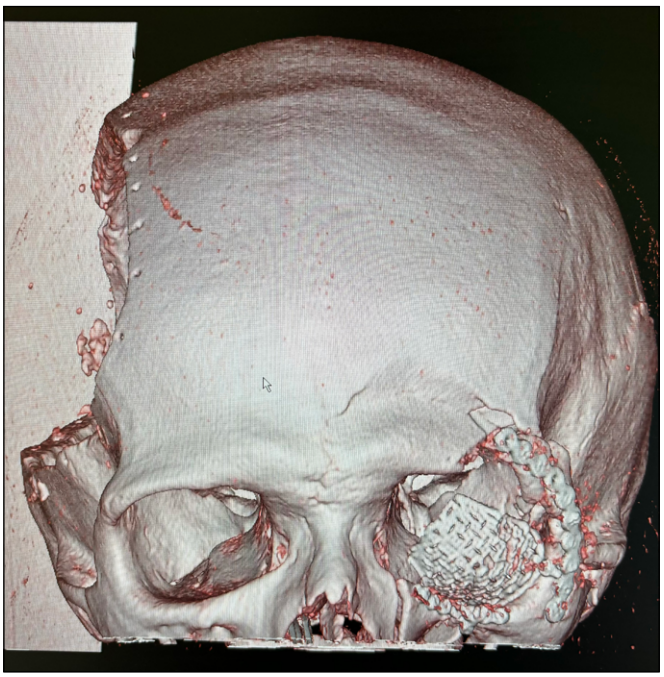

Fig. 4. CT scan after the reconstruction.

along with multiple facial fractures (Fig. 1). After initial wound management, the patient was transferred to Provincial Specialist Hospital No. 5 in Sosnowiec where a frontal-temporal-parietal craniotomy was performed 3 hours after the accident. Mechanically ventilated and pharmacologically sedated, the patient was admitted to the Department of Anesthesiology and Intensive Care, where on the 12th day, empirical antibiotic therapy with ceftriaxone 3x2 g was initiated. Additionally, edema treatment with mannitol 5x100 mg and hemostatic therapy using tranexamic acid 3x1 g were started. Based on follow-up brain CT scans and neurosurgical recommendations, anti-edema treatment was gradually reduced. 10 days after the injury, the patient, in stable general condition, sedated, mechanically ventilated, and with efficient circulatory and respiratory systems, was transported to the Maxillofacial Surgery operating room for the repositioning and osteosynthesis of the

right zygomatic-maxillary-orbital fracture. A mirror image of the left orbit, printed based on the CT scan, was prepared for the surgery. The model was used as a template to shape the titanium reconstruction mesh to restore the destroyed floor of the left orbit (Fig. 2). From an expanded approach in the traumatic wound, access to the orbital floor was gained. After releasing the entrapped soft tissues protruding into the maxillary sinus, the orbital floor was reconstructed using a titanium mesh shaped on the model. Subsequently, the zygomatic-maxillary complex was repositioned, the bony contour of the orbit was restored, and the fragments were fixed with two titanium plates (Fig. 3). The patient was transferred back to the Department of Anesthesiology and Intensive Care, where edema treatment with dexamethasone 3x4 mg was administered and a follow-up examination confirmed the reconstruction of the original shape of the orbit (Fig. 4). In the 12th day, antithrombotic treatment with dalteparin 5000 units were initiated. On the 13th day, due to the appearance of fever and increased inflammatory parameters, targeted antibiotic therapy with meropenem 3x1g and vancomycin 4x500 mg was started. The patient was extubated and weaned off the ventilator on the 16th day with inflammatory parameters decreasing. On the 21 day after the injury, she was transferred to the Department of Neurosurgery. The patient was in simple logical contact, with no signs of enophthalmos or impaired eye movement.

DISCUSSION

The advancement of medicine undoubtedly aims to optimize procedures to achieve the best postoperative results and patient satisfaction. One of the factors influencing positive outcomes in orbital reconstruction procedures, based on 3D printing and subsequent shaping of a titanium mesh on a model printed as the mirrored reflection of the healthy orbit, is undoubtedly the precision and individualization of this approach. Research by Hahn et al. has demonstrated the effectiveness of using "mirroring" in reconstructing orbital wall fractures, as there is no significant difference in the size of patients' orbits. Hahn et al. proved that using "mirroring" in the reconstruction of orbital wall fractures is a precise technique because there is no significant difference in the size of patients' orbits [14]. Reconstructive technologies are constantly evolving, as restoring function and appearance remains a paramount goal in trauma surgery. The most technologically advanced method of orbital reconstruction is patient-specific implants (PSI), designed individually for each patient in a computer program and then custom-made. A meta-analysis conducted by Sanjeev et al. showed that despite the tendency to favor PSI, no statistically significant differences were found compared to conventional methods in terms of postoperative outcomes [15]. Scientific literature focused on reconstructions of the maxillofacial area also agrees that the duration of surgical procedures is a significant factor affecting postoperative recovery time, and the restoration of function depends on the duration of the surgery. The study by Kallaverja et al. conducted research demonstrating greater accuracy and significantly shorter procedure times in orbital floor reconstruction using a preformed titanium mesh based on a stereolithographic model produced with 3D printers compared to intraoperatively shaped titanium mesh [13].

CONCLUSIONS

Although the patient's neurological deficits do not allow for a full assessment of the restoration of all functions, the examination and analysis of CT documentation indicate that the goals of the reconstructive surgery were achieved. 3D print is becoming an increasingly cost effective and accessible method that allows for more precise and predictable orbital reconstruction procedures.

REFERENCES

1. Brucoli M, Arcuri F, Cavenaghi R, Benech A. Analysis of complications after surgical repair of orbital fractures. J Craniofac Surg. 2011 Jul;22(4):1387-90. doi: 10.1097/SCS.0b013e31821cc317 DOI
2. Boffano P, Kommers SC, Karagozoglu KH, Forouzanfar T. Aetiology of maxillofacial fractures: a review of published studies during the last 30 years. Br J Oral Maxillofac Surg. 2014 Dec;52(10):901-6. doi: 10.1016/j.bjoms.2014.08.007 DOI
3. Bonavolonta P, Ortiz-Perez S, Caron CJJM, Koudstaal M, Holmes S. Orbital Injury – Anatomical Based Reconstruction. In: Quaranta Leoni F, Verity DH, Paridaens D (eds). Oculoplastic, Lacrimal and Orbital Surgery. Springer, 2024, pp.431-445.
4. Sivam A, Enninghorst N. The Dilemma of Reconstructive Material Choice for Orbital Floor Fracture: A Narrative Review. Medicines (Basel). 2022 Jan 13;9(1):6. doi: 10.3390/medicines9010006 DOI
5. Burnstine MA. Clinical recommendations for repair of orbital facial fractures. Curr Opin Ophthalmol. 2003 Oct;14(5):236-40. doi: 10.1097/00055735-200310000-00002 DOI
6. Bite U, Jackson IT, Forbes GS, Gehring DG. Orbital volume measurements in enophthalmos using three-dimensional CT imaging. Plast Reconstr Surg. 1985 Apr;75(4):502-8. doi: 10.1097/00006534-198504000-00009 DOI

7. Tuncer S, Yavuzer R, Kandal S, Demir YH, Ozmen S, Latifoglu O, Atabay K. Reconstruction of traumatic orbital floor fractures with resorbable mesh plate. J Craniofac Surg. 2007 May;18(3):598-605. doi: 10.1097/01.scs.0000246735.92095.ef DOI
8. Patel BC, Hoffmann J. Management of complex orbital fractures. Facial Plast Surg. 1998;14:83-104. doi: 10.1055/s-0028-1085305 DOI
9. Patterson RW Jr, McCoy WJ 3rd, Benedict WH. The use of processed bovine in orbital floor fractures. Arch Ophthalmol. 1967 Sep;78(3):360-4. doi: 10.1001/archopht.1967.00980030362019 DOI
10. Chowdhury K, Krause GE. Selection of materials for orbital floor reconstruction. Arch Otolaryngol Head Neck Surg. 1998 Dec;124(12):1398-401. doi: 10.1001/archotol.124.12.1398 DOI
11. Ellis E 3rd, Tan Y. Assessment of internal orbital reconstructions for pure blowout fractures: cranial bone grafts versus titanium mesh. J Oral Maxillofac Surg. 2003 Apr;61(4):442-53. doi: 10.1053/joms.2003.50085 DOI
12 Baumann A, Burggasser G, Gauss N, Ewers R. Orbital floor reconstruction with an alloplastic resorbable polydioxanone sheet. Int J Oral Maxillofac Surg. 2002 Aug;31(4):367-73. doi: 10.1054/ijom.2001.0219 DOI
13. Hahn HM, Jung YK, Lee IJ, et al. Revisiting bilateral bony orbital volumes comparison using 3D reconstruction in Korean adults: a reference study for orbital wall reconstruction, 3D printing, and navigation by mirroring. BMC Surg. 2023;23:351. doi: 10.1186/s12893-023-02268-0 DOI
14. Kotecha S, Ferro A, Harrison P, Fan K. Orbital reconstruction: a systematic review and meta-analysis evaluating the role of patient-specific implants. Oral Maxillofac Surg. 2023 Jun;27(2):213-226. 10.1007/s10006-022-01074-x.
15. Kallaverja E, Barca I, Ferragina F, Cristofaro MG. Classical Orbital Floor Post-Traumatic Reconstruction vs. Customized Reconstruction with the Support of "In-House" 3D-Printed Models: A Retrospective Study with an Analysis of Volumetric Measurement. Diagnostics 2024;14:1248. doi: 10.3390/diagnostics14121248. DOI

CONFLICT OF INTEREST

The Authors declare no conflict of interest

CORRESPONDING AUTHOR

Agnieszka Rolek
Private Dental Practice - Agnieszka Rolek,
Wroclaw, Poland
e-mail: aga.rolek@gmail.com

ORCID AND CONTRIBUTIONSHIP

Piotr Pławecki: 0000-0003-2550-8452 A B D F
Magdalena Jędrusik-Pawłowska: 0000-0002-8339-7618 B D E F
Agnieszka Rolek: 0009-0007-2880-2055 D E F
Agata Cieślik-Bielecka: 0000-0003-1111-2967 B D E F

A – Work concept and design, B – Data collection and analysis, C – Responsibility for statistical analysis, D – Writing the article, E – Critical review, F – Final approval of the article

RECEIVED: 10.05.2024
ACCEPTED: 05.07.2024

CASE STUDY

CONTENTS

Three cases of fatal postoperative thromboembolic complications in patients with liver cirrhosis and bleeding from esophageal varicose veins after COVID-19

Diana V. Rudyk, Mykola I. Tutchenko, Sergiy L. Chub, Mykola S. Besedinskyi
BOGOMOLETS NATIONAL MEDICAL UNIVERSITY, KYIV, UKRAINE

ABSTRACT

Coronavirus disease (COVID-19), which broke out in China and caused a devastating pandemic worldwide, is associated with a significantly increased risk of thrombotic complications, especially pulmonary embolism. During the COVID-19 pandemic, investigations have reported a high incidence of venous thromboembolic (VTE) events in hospitalized patients with COVID-19, often despite thromboprophylaxis. Current recommendations for thromboprophylaxis are based on randomized clinical trials, which usually exclude patients at a potentially high risk of hemorrhagic complications. This category includes patients with liver cirrhosis complicated by variceal bleeding, thrombocytopenia, and coagulopathy. We present three patients who suffered severe covid pneumonia and were hospitalized with acute variceal bleeding, who developed fatal thromboembolic complications in the postoperative period.

KEY WORDS: thrombosis, pulmonary embolism, thromboembolic complications, COVID associated thromboembolic complications

Wiad Lek. 2024;77(8):1627-1632. doi: 10.36740/WLek202408114 DOI

INTRODUCTION

Coronavirus disease (COVID-19), which broke out in China and caused a devastating pandemic worldwide, is associated with a significantly increased risk of thrombotic complications, especially pulmonary embolism [1]. During the COVID-19 pandemic, investigations have reported a high incidence of venous thromboembolic (VTE) events in hospitalized patients with COVID-19, often despite thromboprophylaxis [1-4].

Emerging evidence suggests that the coagulation function is significantly deranged during SARS-CoV-2 (COVID-19) infection and may predispose to arterial and venous thrombotic complications due to excessive inflammation, platelet activation, endothelial dysfunction and stasis [5].

However, as many researchers point out, the risk of hospital-associated VTE extends from the moment of admission and over the first 90 days after discharge from the hospital also in COVID-19 patients [6-9].

In this article, we would like to present the cases of 3 patients with cirrhosis and variceal bleeding who recently underwent Covid 19 and whose postoperative period was complicated by thrombosis or thromboembolic complications.

CASE REPORT

CASE REPORT 1

A 56-year-old women with autoimmune liver cirrhosis (Child-Pugh class A) and first massive bleeding from esophageal veins was referred by ambulance to the emergency department of Kyiv City Emergency Hospital. Her vital signs on admission were as follows: blood pressure, 80/40 mmHg; heart rate, 120 beats/min. The endoscopy revealed a dilated and tortuous veins in the low part of the esophagus with oozing blood, with "red sign", evidence of acute bleeding (Fig. 1).

It was known that three monts ago the patient was hospitalized with severe bilateral COVID-19 pneumonia and received LMWH at a therapeutic regimen. Severe COVID-19 disease was also identified when computed tomography of the chest reveals lung infiltrates >90%.

The patient's medical history of thromboembolic complications has not been reported in the past, but for the past twelve years she has been controlled for diabetes mellitus on insulin therapy, overweight and hypertention. Laboratory tests showed decreased hemoglobin (57 g/L), hematocrit (27.1%); leukocyte (4.6×10^9/L) and platelet (78×10^9/L) counts, total

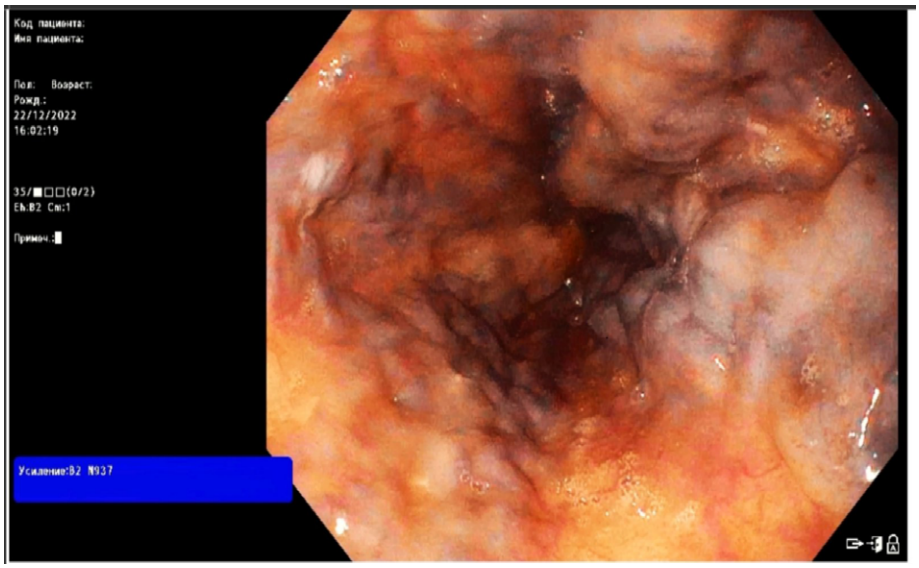

Fig. 1. Endoscopic examination of the upper gastrointestinal tract of a 56-year-old woman showed dilated and tortuous varices of the esophagus with red marks and blood leakage.

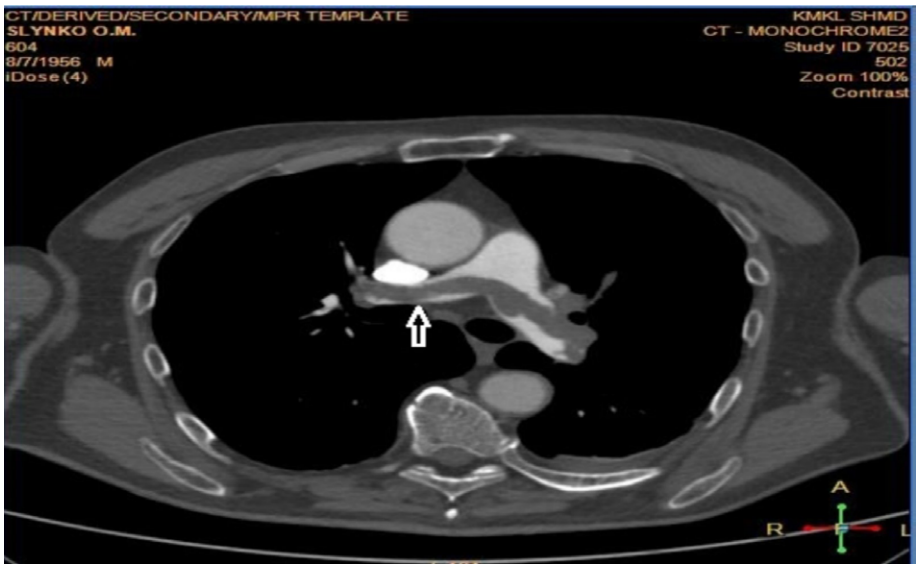

Fig. 2. A 56-year-old woman with autoimmune cirrhosis of the liver shows a massive pulmonary embolism on a contrast-enhanced computed tomography scan. The thrombus, which almost completely closes the pulmonary artery, is indicated by an arrow.

bilirubin (28.9mmol/L), and alanine aminotransaminase (67U/L); aspartate aminotransferase (39U/L), urea 11,6 mmol/L; creatinine (0.7 mkmol/L); glucose (9,1mkmol/L); sodium (144 mmol/L); potassium (4.8 mmol/L); total protein (62 g/L); serum albumin (29 g/L). Blood coagulation tests showed: increased prothrombin time (24.0seconds); activated partial thromboplastin time (30 sec); International Normalized Ratio (1.4). Serological markers for previous or current hepatitis B and C infection were negative. There was no previous history of alcohol abuse.

The patient was admitted to intensive care unit for preoperative preparation. The active bleeding was stopped by endoscopic ligation and administration of hemostatic agents. After stabilization of hemodynamic parameters, surgical intervention was performed, which consisted of devascularization of the upper part of the stomach, distal part of esophagus, followed by transection with a circular stapler. During the operation, the patient was transfused four units of packed erythrocytes and fresh-frozen-plasma. The patient was discharged on the tenth postoperative day in satisfactory condition. The next day after discharge, her condition suddenly deteriorated. The patient had difficulty breathing, chest pain, and an ambulance was immediately called. A contrast-enhanced computed tomography (CT) scan performed in the hospital confirmed the suspicion and revealed a massive pulmonary embolism (Fig. 2).

In the intensive care unit, the patient received cardiopulmonary support, anticoagulant therapy and unsuccessful thrombolysis, and unfortunately, the patient died.

Despite the patient's hypersplenism and the absence of hypercoagulability according to coagulation tests, we did not expect such a complication, which nevertheless led to a shift in the balance of our patient's haemostasis towards hypercoagulation and led to death.

CASE REPORT 2

A 40-year-old female patient with liver cirrhosis (Child-Pugh class B) was admitted to the emergency department with severe gastrointestinal bleeding, manifested by vomiting blood, loss of consciousness and melena. This was the fifth esophageal variceal bleeding in the past two years. Serological markers for previous or current hepatitis B and C infection were negative. There was no previous history of alcohol abuse also.

Fore months ago, the patient was treated for 3 weeks for severe bilateral COVID-19-associated pneumonia. Severe disease is also identified when computed tomography of the chest reveals lung infiltrates >45%. She did not receive anticoagulant therapy due to the high risk of rebleeding from esophageal varices.

Endoscopic evaluation with esophagogastroduodenoscopy revealed massively bleeding, grade III, lower esophageal varices. The active source of bleeding was stoped by the introduction of a Sengstaken-Blakemore tube and hemostatic therapy.

Physical examination revealed blood pressure 90/40 mmHg; pulse rate, 122 beats/min; pallor; melena. The liver function parameters were appropriate to patient with cirrosis and blood examination showed severe anemia. Hepatic enchephalopaty corresponded to grade I.

Laboratory tests showed decreased hemoglobin (60g/L), hematocrit (25.1%), leukocyte (15.6×10^9/L) and platelet (51×10^9/L) counts, alanine aminotransaminase (77 U/L); aspartate aminotransferase (69U/L), urea (4,3 mmol/L), creatinine (77 mkmol/L), glucose (6,9 mkmol/L), sodium (141 mmol/L), potassium (4.3 mmol/L), total protein (59 g/L), serum albumin (29 g/L), total bilirubin (68.9mmol/L). Blood coagulation tests showed: increased prothrombin time (25.0seconds), activated partial thromboplastin time (50 sec), International Normalized Ratio (1.56). Serological markers for previous or current hepatitis B and C infection were negative. After stabilization of vital signs, an operation was performed aimed at porto-azigal separation, which consisted in devascularization of the proximal part of stomach, distal part of esophagus, followed by transection of the esophagus with a circular stapler. During the operation, the patient was transfused several units of fresh-frozen-plasma.

The patient suddenly developed serious respiratory failure developed on the 7th day after operation, which manifested as a feeling of lack of air, shortness of breath and coughing. Patient was started on oxygen therapy, continued with antibiotic, intravenous hydration, anticoagulant therapy (Heparin), and supportive care. Despite the therapy, the clinical and laboratory picture deteriorated rapidly. Due to progressive respiratory failure and critical drop in oxygen saturation, the patient was intubated and mechanical ventilation was initiated. The patient died the next day with progressive multiorgan failure. An autopsy showed the presence of thrombotic mass in the branches of the pulmonary arteries with pulmonary infarctions associated with bilateral pneumonia and pleural effusion.

This case also demonstrates the need for further research and rethinking of the mechanisms of blood coagulation system imbalance in the post-COVID period, despite the presence of hypersplenism and the absence of obvious signs of hypercoagulation according to the patient's coagulogram and, probably, the need for thromboprophylaxis in the postoperative period.

CASE REPORT 3

A 72-year-old woman with a history of liver cirrhosis (Child-Pugh class B) presented to the emergency room with the first episode of massive bleeding from esophageal veins. Four weeks prior to admission she was treated with bilateral COVID associated pneumonia with lung damage exceeding 50% and was receiving anticoagulant therapy. The active bleeding was stopped by endoscopic ligation (Fig. 3) of varicose veins and hemostatic therapy, after which a porto-azigal disconnection operation was performed with devascularization of the proximal stomach and distal esophagus with reduction of splenic perfusion by ligation of the a.lienalis in the proximal part. On the eleven postoperative day she was discharged in satisfactory condition. Three weeks after discharge, the patient suddenly developed nausea, vomiting, distention and diffuse abdominal pain that had started without a clear trigger. The vital parameters at entry were as follows: temperature 38.5 ° C, blood pressure 110/60 mm HG, heart rate 89 beats per minute and oxygen saturation of 98% on room air. Blood analysis showed: hemoglobin (88 g/L), Hct (24.9%), leukocyte (34.6×10^9/L, 83.5% neutrophils) and platelet (95×10^9/L), total bilirubin (18.9mmol/L), ALT (8I U/L), AST (9IU/L), total protein (68 g/L), serum albumin (32.8g/L), urea (9,9 mmol/L), creatinine (119 mkmol/L), glucose (6.0 mmol/L), sodium (141 mmol/L), potassium (4.6 mmol/L). Blood coagulation tests showed: increased prothrombin time (35 sec), PTI 45%, activated partial thromboplastin time (31 sec).

Physical examination revealed diffuse abdominal pain, which worsened with deep palpation, and peritoneal symptom appeared. Ultrasonographic examination revealed thrombosis of the portal vein with spread to the branches and signs of intestinal obstruction (Fig. 4.,

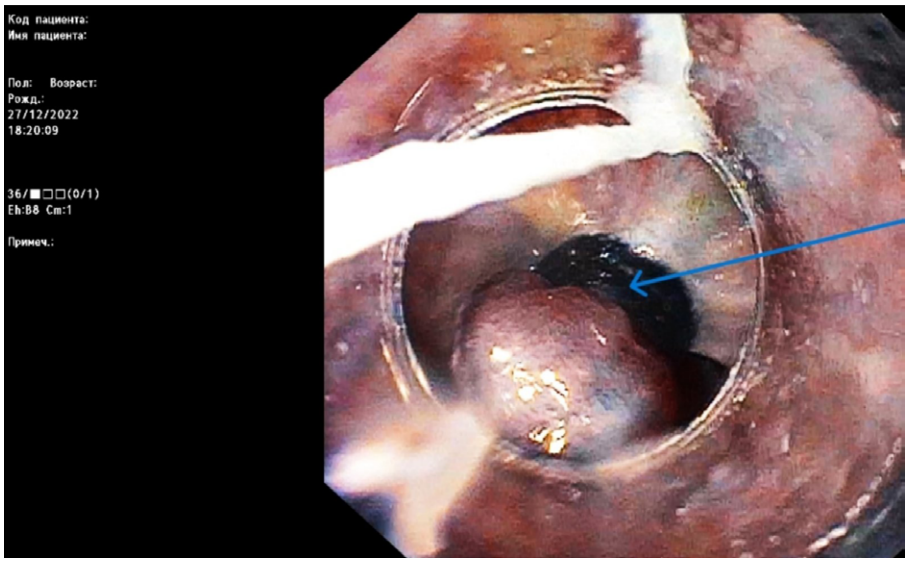

Fig. 3. Active bleeding was stopped by endoscopic ligation.

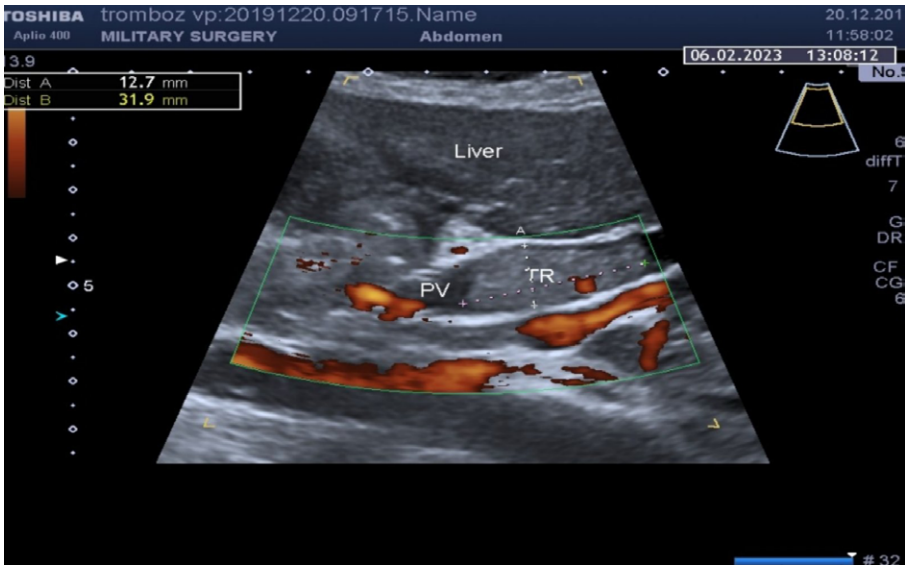

Fig. 4. Ultrasound Doppler examination of a 72-year-old woman with toxic cirrhosis reveals a thrombus in the portal vein that completely blocks the lumen of the vessel.

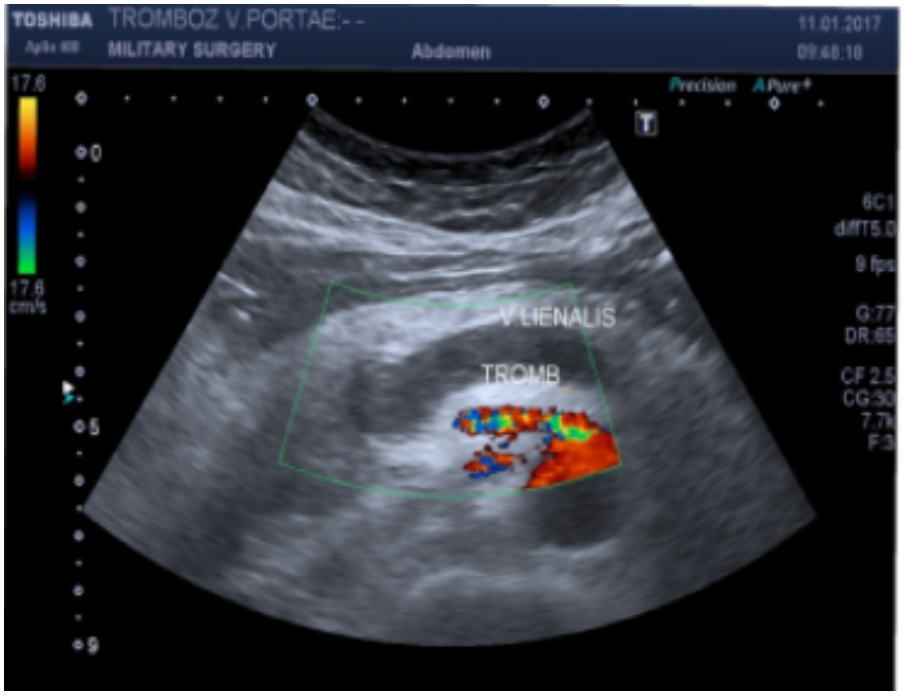

Fig. 5. Ultrasound examination of a 72-year-old woman with toxic cirrhosis reveals a thrombus in the portal vein, which spreads to the branches (splenic and superior mesenteric veins), which caused mesenteric thrombosis and intestinal necrosis.

Fig. 5.). The next step was laparoscopic revision, which revealed a necrotized ileal loop located 50 cm proximal to the ileocecal valve. An intestinal resection with entero-enteral anastomosis was performed. Recurrent retrombosis on the 9th day of the postoperative period and progression of liver failure led to the patient's death.

When analysing the three deaths in patients with cirrhosis, we noted that thrombotic complications occurred in all of these patients who had a recent history of severe covid pneumonia, despite the fact that 2 of these patients were receiving adequate anticoagulant therapy, which requires further investigation and special attention in patients with covid history.

The liver plays a central role in the regulation of homeostasis. By producing the majority of plasma proteins involved in hemostasis including pro– and anticoagulant factors, pro– and antifibrinolytic factors, and thrombopoietin [11]. It follows that liver diseases are commonly responsible for hemostasis abnormalities including decreased production of clotting factors, thrombocytopenia, platelet dysfunction, and increased circulating fibrinolytic activity. Such alterations in the hemostatic system were historically interpreted as indicators of bleeding risk in liver disease and patients were considered to be anticoagulated.

There are many lines of evidence which contradict this point of view. Not only are procoagulant pathways reduced in liver disease but also anticoagulant and fibrinolytic mechanisms are impaired. Moreover, low platelet count can be counterbalanced by increased platelet activity. Several clinical studies on the risk of bleeding and thrombosis suggest that liver disease is not simply a bleeding disorder, but also confirms that the hemostatic system in liver disease is rebalanced [11,14].

Bleeding from esophageal varices is a common complication in patients with liver cirrhosis. However, it has now been well established that this complication is unrelated to a defective hemostatic system [13]. Routine tests of hemostasis such as the prothrombin time (PT), activated partial thromboplastin time (APTT), and platelet count are frequently abnormal in these patients and these test results all indicate a hypocoagulable status [11]. However, standard coagulation tests do not fully reflect hemostatic disorders and do not accurately predict the risk of bleeding or thrombosis.

For a long time, thrombotic complications were traditionally considered rare events in patients with cirrhosis, but our observations have shown that thrombotic complications can paradoxically occur in the posthemorrhagic/postoperative period, especially in patients after covid pneumonia. Therefore, it is likely difficult to predict using laboratory tests or clinical scores which patient is more likely to tip towards a bleeding and which one is more likely to develop thrombosis. The clinical reality is that patients may present with bleeding and thrombosis simultaneously, and obviously management of such patients is a particularly difficult clinical challenge.

CONCLUSIONS

Rebalanced hemostasis in patients with liver disease is unreliable and may shift toward hemorrhage or thrombosis, depending on coexisting circumstantial risk factors.

Patients with liver cirrhosis and variceal bleeding with previous COVID-19 infection require special attention to prevent thromboembolic complications. However, in this category of patients, the use of anticoagulants requires caution and should be selected individually, taking into account the risks of thrombosis and rebleeding.

REFERENCES

1. Poor HD. Pulmonary Thrombosis and Thromboembolism in COVID-19. Chest. 2021;160(4):1471-1480. doi: 10.1016/j.chest.2021.06.016. DOI
2. Sastry S, Cuomo F, Muthusamy J. COVID-19 and thrombosis: The role of hemodynamics. Thromb Res. 2022;212:51-57. doi: 10.1016/j.thromres.2022.02.016. DOI
3. Roubinian NH, Dusendang JR, Mark DG et al. Incidence of 30-Day Venous Thromboembolism in Adults Tested for SARS-CoV-2 Infection in an Integrated Health Care System in Northern California. JAMA Intern Med. 2021;181(7):997-1000. doi: 10.1001/jamainternmed.2021.0488. DOI
4. Dutch COVID & Thrombosis Coalition; Kaptein FHJ, Stals MAM, et al. Incidence of thrombotic complications and overall survival in hospitalized patients with COVID-19 in the second and first wave. Thromb Res. 2021;199:143-148. doi: 10.1016/j.thromres.2020.12.019. DOI
5. Bikdeli B, Madhavan MV, Jimenez D et al. Global COVID-19 Thrombosis Collaborative Group, Endorsed by the ISTH, NATF, ESVM, and the IUA, Supported by the ESC Working Group on Pulmonary Circulation and Right Ventricular Function. COVID-19 and Thrombotic or Thromboembolic Disease: Implications for Prevention, Antithrombotic Therapy, and Follow-Up: JACC State-of-the-Art Review. J Am Coll Cardiol. 2020;75(23):2950-2973. doi: 10.1016/j.jacc.2020.04.031. DOI
6. Patell R, Bogue T, Koshy A et al. Postdischarge thrombosis and hemorrhage in patients with COVID-19. Blood. 2020;136(11):1342-1346. doi: 10.1182/blood.2020007938. DOI

7. Engelen MM, Vandenbriele C, Balthazar T et al. Venous Thromboembolism in Patients Discharged after COVID-19 Hospitalization. Semin Thromb Hemost. 2021;47(4):362-371. doi: 10.1055/s-0041-1727284. DOI
8. Rashidi F, Barco S, Kamangar F et al. Incidence of symptomatic venous thromboembolism following hospitalization for coronavirus disease 2019: Prospective results from a multi-center study. Thromb Res. 2021;198:135-138. doi: 10.1016/j.thromres.2020.12.001. DOI
9. DeWane MP, Davis KA, Schuster KM et al. Venous Thromboembolism-Related Readmission in Emergency General Surgery Patients: A Role for Prophylaxis on Discharge? J Am Coll Surg. 2018;226(6):1072-1077.e3. doi: 10.1016/j.jamcollsurg.2018.03.021. DOI
10. Lisman T, Porte RJ. Pathogenesis, prevention, and management of bleeding and thrombosis in patients with liver diseases. Res Pract Thromb Haemost. 2017;1(2):150-161. doi: 10.1002/rth2.12028. DOI
11. Lisman T, Porte RJ. Rebalanced hemostasis in patients with liver disease: evidence and clinical consequences. Blood. 2010;116(6):878-85. doi: 10.1182/blood-2010-02-261891. DOI
12. Kujovich JL. Coagulopathy in liver disease: a balancing act. Hematology Am Soc Hematol Educ Program. 2015;2015:243-9. doi: 10.1182/asheducation-2015.1.243. DOI
13. Garcia-Tsao G, Bosch J. Management of varices and variceal hemorrhage in cirrhosis. N Engl J Med. 2010;362(9):823-32. doi: 10.1056/NEJMra0901512. DOI
14. Shah NL, Intagliata NM, Northup PG et al. Procoagulant therapeutics in liver disease: a critique and clinical rationale. Nat Rev Gastroenterol Hepatol. 2014;11(11):675-82. doi: 10.1038/nrgastro.2014.121. DOI

CONFLICT OF INTEREST

The Authors declare no conflict of interest

CORRESPONDING AUTHOR

Diana V. Rudyk
Bogomolets National Medical University
13 T. Shevchenko Boulevard, 01601 Kyiv, Ukraine
e-mail: Dianavrudyk@ukr.net

ORCID AND CONTRIBUTIONSHIP

Diana V. Rudyk: 0000-0001-9736-3614 A B D E F
Mykola I. Tutchenko: 0000-0002-5050-6494 E F
Sergiy L. Chub: 0000-0001-6489-7345 A F
Mykola S. Besedinskyi: 0009-0009-8618-1458 A B

A – Work concept and design, B – Data collection and analysis, C – Responsibility for statistical analysis, D – Writing the article, E – Critical review, F – Final approval of the article

RECEIVED: 13.11.2023
ACCEPTED: 17.07.2024

CASE STUDY

CONTENTS

Complex mechanism of brugada phenocopy: moderate hyponatremia and right ventricular compression by liver metastatic tumor – case report

Waldemar Elikowski, Anna Strzelecka, Natalia Fertała, Magdalena Zawodna-Marszałek, Marcin Żytkiewicz
DEPARTMENT OF INTERNAL MEDICINE, JÓZEF STRUŚ HOSPITAL, POZNAŃ, POLAND

ABSTRACT

Brugada phenocopy (BrP) occurs in various clinical conditions and manifests as a Brugada-like ECG pattern with coved (type 1) or saddle-back (type 2) ST-segment elevation in the right precordial leads. Unlike Brugada syndrome (BrS), which is an inherited channelopathy, BrP is not associated with an increased risk of malignant arrhythmia. BrP has been reported in severe metabolic disturbances (significant hyponatremia, hypokalemia or hyperkalemia), mechanical heart compression, coronary artery disease, pulmonary embolism and myocarditis/pericarditis.

The authors described a case of a 69-year-old female whose Brugada-like ECG was atypically associated with only moderate hyponatremia (127 mmol/l). She was admitted due to a skin and subcutaneous tissue infection of the left shank and coexistent urinary tract infection (without a fever). She had the history of advanced melanoma with multiple liver metastases. Her cardiac history was negative, especially the patient has never suffered from ventricular arrhythmias. ECG on admission showed saddle-back ST-segment elevation in the right precordial leads; however, the patient did not report any chest pain. Troponin I level and left ventricular function in echocardiography were normal while regional longitudinal strain in RV apex was decreased and showed post-systolic shortening. The substernal view revealed compression of the right ventricle (RV) by liver metastatic tumor. ECG changes disappeared quickly during natrium chloride supplementation and did not recur during hospitalization. This case illustrates that even moderate hyponatremia may be a reversible cause of BrP when other predisposing conditions (e.g. heart compression by tumor) coexist.

KEY WORDS: Brugada syndrome, Brugada phenocopy, Brugada-like ECG pattern, hyponatremia, right ventricle compression, longitudinal strain

Wiad Lek. 2024;77(8):1633-1637. doi: 10.36740/WLek202408115 DOI

INTRODUCTION

Brugada phenocopy (BrP) occurs in various clinical conditions and manifests as a Brugada-like ECG pattern with coved (type 1) or saddle-back (type 2) ST-segment elevation in the right precordial leads [1,2]. Unlike Brugada syndrome (BrS), which is an inherited channelopathy, BrP is not associated with an increased risk of malignant arrhythmia [3,4]. Expert cardiologists suggest that BrP and BrS ECG patterns are visually identical and indistinguishable [5]. BrP has been reported in severe metabolic disturbances (significant hyponatremia, hypokalemia or hyperkalemia), mechanical heart compression, coronary artery disease, pulmonary embolism, and myocarditis/pericarditis [6,7]. Typically, Brugada-like ECG pattern has transient character, but when caused by mechanical heart compression (due to right ventricular outflow tract-RVOT tumor or pectus excavatum), usually persists until the target treatment is applied [7,8].

Differential diagnosis between BrS and BrP includes evaluation of the above-mentioned clinical conditions, history of life-threatening arrhythmias, provocative pharmacological tests with sodium channel blockers and genetic assessment [6]. However, serious health condition, advanced age, coexistence of multiple disorders and lack of arrhythmia symptoms as well as negative family history suggestive of BrS may indicate the omission of such algorithm [9].

AIM

The purpose of this paper is to show that Brugada phenocopy may have a complex mechanism related to underlying coexisting conditions whose expression would not be sufficient independently to provoke Brugada-like ECG.

CASE REPORT

A 69-year-old female was admitted due to a skin and subcutaneous tissue infection of the left shank, coexistent urinary tract infection (with high inflammatory markers levels, but without a fever), and transient renal function deterioration (creatinine concentration 216 µmol/l; normal up to 106 µmol/l) with moderate hyponatremia (sodium concentration 127 mmol/l; normal 135-145

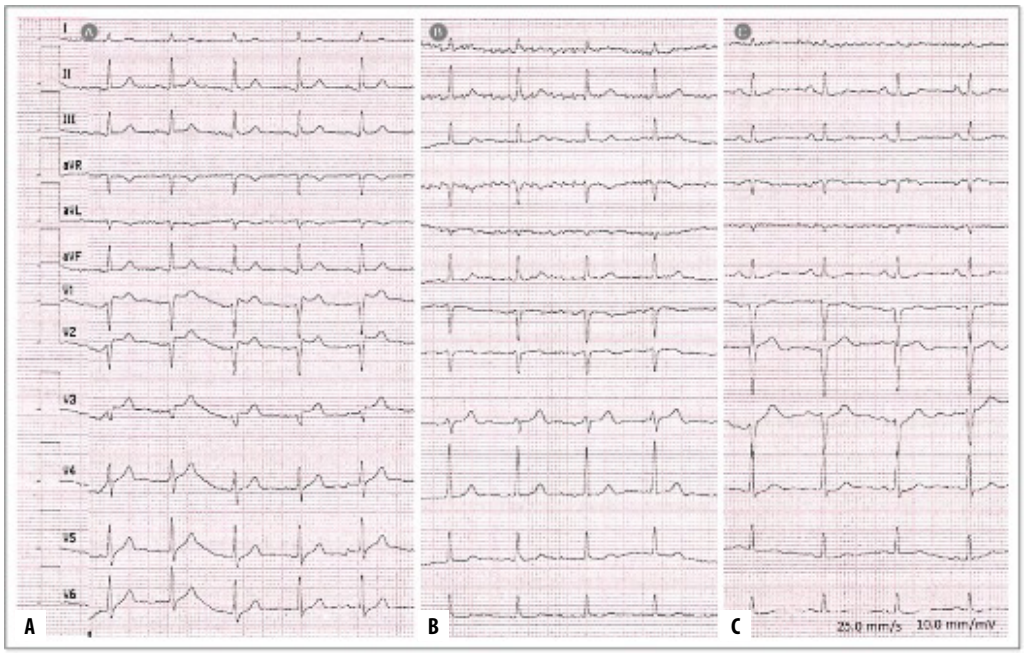

Fig.1. ECG: saddle-back ST-segment elevation in V1-3 on admission (A), disappearance of changes during sodium chloride supplementation (B), normal ST-segment in V1-3 from day 2 (C).

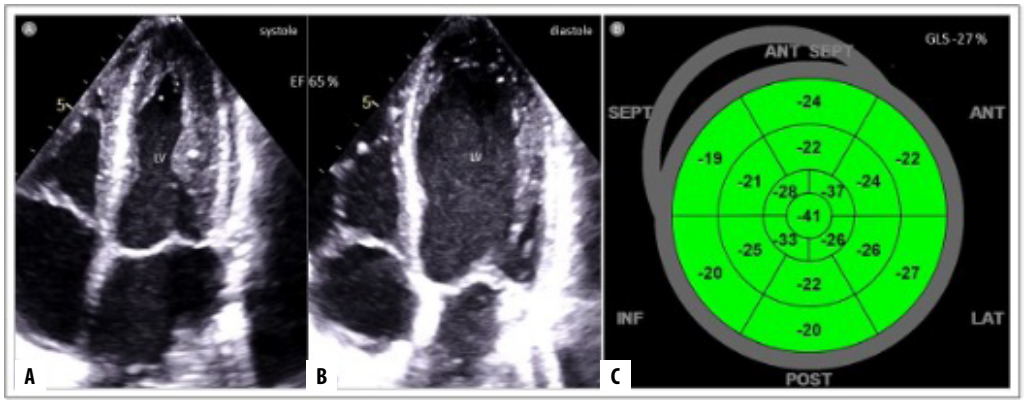

Fig.2. Two-dimensional echocardiography in apical four-chambers view: normal left ventricular function with ejection fraction (EF) 65% (A) and global longitudinal strain (GLS) -27% (B); see high regional LS in apical segments (C).

mmol/l). Potassium and phosphates were within the normal range. Patient's clinical status was determined by multi-morbidity, including advanced melanoma with multiple liver metastases and ovarian cancer. She was disqualified from chemotherapy. Her cardiac history was negative, especially she has never suffered from ventricular arrhythmias. Also, family history of cardiac arrhythmias, including sudden cardiac death, was negative.

ECG on admission showed saddle-back ST-segment elevation in the right precordial leads (fig.1A); however, the patient did not report any chest pain. Troponin I level and left ventricular function in echocardiography, evaluated by ejection fraction (EF) and global and regional longitudinal strain (GLS and RLS), were normal (fig.2A-B). Regional longitudinal strain of RV apex was decreased and showed post-systolic shortening, whereas in basal and midventricular segments RLS was hypernormal (fig.3). The substernal view revealed compression of the RV by liver metastases (fig.4), which was not visible in previously done abdominal computed tomography. ECG changes quickly disappeared during natrium chloride supplementation and did not recur during hospitalization (fig.1B-C). 24-hour ECG monitoring did not show any ventricular arrhythmia. After a few days, the patient was transferred to palliative care; she was discharged with normal renal function and normal inflammatory markers after appropriate treatment with antibiotics.

DISCUSSION

The main groups of BrP reported in the literature include: severe metabolic disturbances (significant hyponatremia, hypokalemia or hyperkalemia), mechanical heart compression, coronary artery disease, myocarditis/pericarditis and pulmonary embolism [7-10]. It is unclear why some patients present with BrP and some do not under the same environmental conditions [6].

Generally, metabolic disturbances, especially electrolyte abnormalities, account for approximately half of BrP cases reported in the literature (a hundred and so patients). On the other hand, BrP is diagnosed only in a

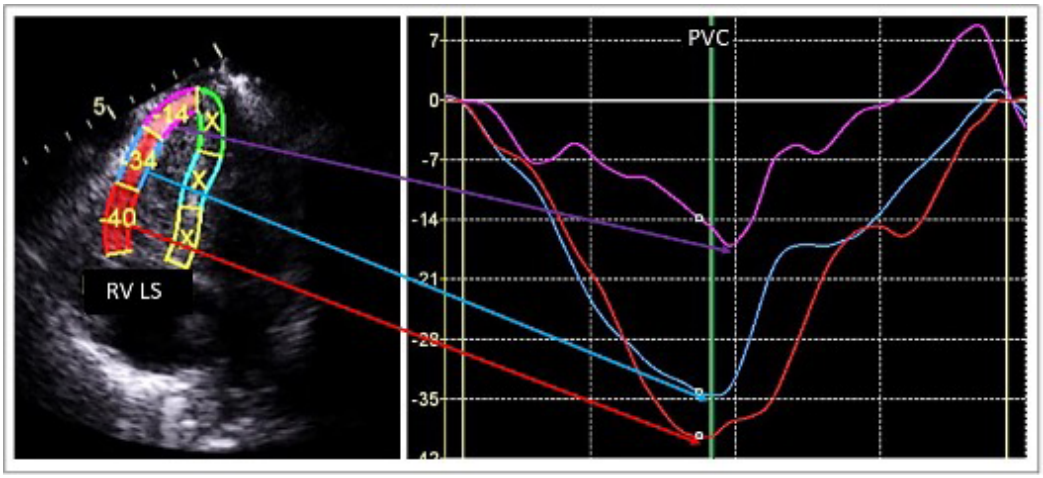

Fig.3. Regional longitudinal strain of the RV free wall: see decreased strain and post systolic shortening (in strain curves presentation) of the apical RV segment as well as hypernormal strain of basal and midventricular RV segments; RV - right ventricle, LS - longitudinal strain, PVC – pulmonary valve closure.

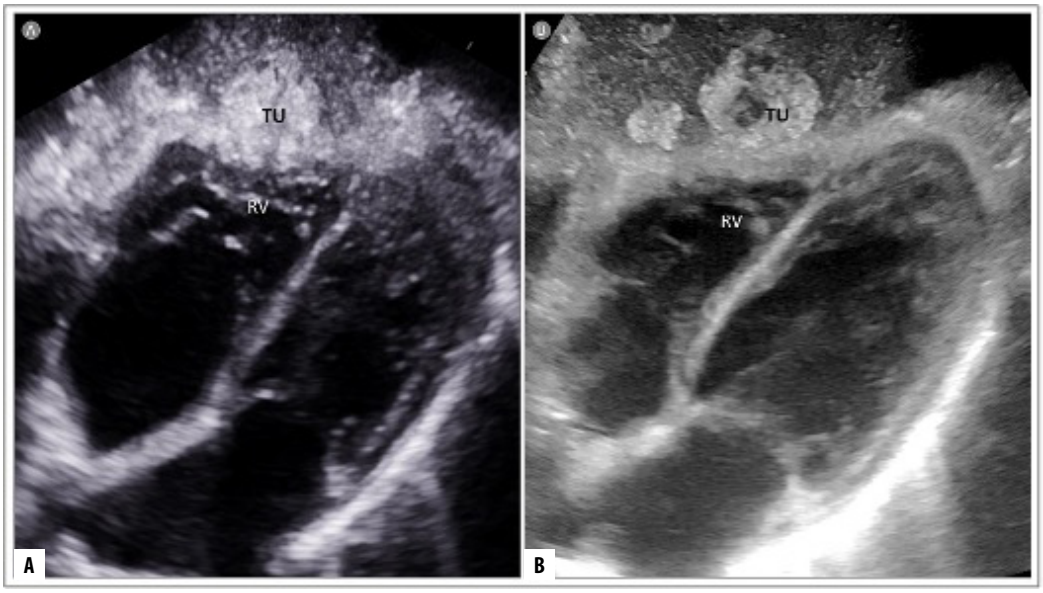

Fig.4. Right ventricle compression by liver metastatic tumor (Tu) - substernal echocardiographic view using cardiac sector probe (A) and convex probe (B).

fraction of population presenting with such abnormalities. Hyponatremia (sodium concentration of less than 135 mmol/l) is the most common electrolyte abnormality and is defined as mild (130-134 mmol/l), moderate (120-129 mmol/l) or severe (<120 mmol/l) [11,12]. The pathophysiology of Brugada-like ECG pattern may be explained by reduced inward sodium current in the RVOT epicardium and/or conduction delay which produce transmural gradient. Using longitudinal strain evaluation in the presented case, we demonstrated significant differences between reduced apical and increased basal RV RLS as well as strain dispersion related to post-systolic shortening in the RV apex. All cases of BrP and hyponatremia described so far were associated with severe sodium concentration decrease (sodium values close to 100-110 mmol/l**)** and presented with type 1 Brugada ECG pattern in most patients [10,13-15] Interestingly, in coexistent hyperkalemia, unique ECG with type 1 Brugada pattern in V1 and type 2 in V2 could be observed [16,17]. Hyponatremia, regardless of its etiology, may contribute to the development of Brugada-like ECG pattern; e.g. in: kidney injury [15], excessive fluids intake [10,13], dehydration during diuretics and antihypertensive drug use [14], dehydration caused by diarrhea and vomiting [13], syndrome of inappropriate antidiuretic hormone secretion (SIADH) [18], adrenal crisis [19], ketoacidosis [20,21]. In the last three examples other than hyponatremia, metabolic/endocrine factors were involved in modulating ECG pattern. It should be remembered, that hyponatremia can reveal BrS [22].

A review of 11 published cases of BP caused by tumor compression of the heart showed that 10 patients represented a type 1 Brugada ECG pattern and only one type 2 Brugada ECG pattern [8,23]. In all these patients, heart compression was associated with RVOT involvement, either by neoplastic (benign or malignant) tumor [23,24] or non-neoplastic (e.g. inflammatory or being hematoma) tumor [25,26] located in the anterior mediastinum, in the RV cavity or in the pericardium [8,24-26]. After appropriate treatment (surgery, radiotherapy, chemotherapy), clinical improvement was accompanied by ECG normalization [23,27]. Contrary to

above cases, in the presented one, echocardiography revealed RV apex compression by liver metastatic tumor. However, it should not be excluded that RVOT was infiltrated by cancer cells. The clinical course indicated that sole RV apex compression was not sufficient to generate Brugada-like ECG, whereas when only moderate hyponatremia additionally occurred, typical BrP could be observed.

CONCLUSIONS

This case illustrates that even moderate hyponatremia may be a reversible cause of BrP when other predisposing conditions (e.g. heart compression by tumor) coexist. The concomitance of underlying conditions in a patient with BrP should always be taken into account because different pathologies may have combined effect on ECG morphology.

REFERENCES

1. Baranchuk A, Nguyen T, Ryu MH et al. Brugada phenocopy: new terminology and proposed classification. Ann Noninvasive Electrocardiol. 2012;17:299-314. doi: 10.1111/j.1542-474X. 2012.00525.x. DOI
2. Anselm DD, Baranchuk A. Brugada phenocopy: redefinition and updated classification. Am J Cardiol. 2013;111:453. doi: 10.1016/j.amjcard.2012.09.005. DOI
3. Bayes de Luna A, Brugada J, Baranchuk A et al. Current electrocardiographic criteria for diagnosis of Brugada pattern: a consensus report. Journal of electrocardiology. 2012;45:433-442. doi: 10.1016/j.jelectrocard.2012.06.004. DOI
4. Brugada J, Campuzano O, Arbelo E et al. Present Status of Brugada Syndrome: JACC State-of-the-Art Review. J Am Coll Cardiol. 2018;72:1046-1059. doi: 10.1016/j.jacc.2018.06.037. 5. Gottschalk BH, Anselm DD, Brugada J et al. Expert cardiologists cannot distinguish between Brugada phenocopy and Brugada syndrome electrocardiogram patterns. Europace. 2016;18:1095-1100. doi: 10.1093/europace/euv278. DOI
6. Çinier G, Tse G, Baranchuk A. Brugada phenocopies: Current evidence, diagnostic algorithms and a perspective for the future. Turk Kardiyol Dern Ars. 2020;48:158-166. doi: 10.5543/ tkda.2020.06118. DOI
7. de Oliveira Neto NR, de Oliveira WS, Mastrocola F et al. Brugada phenocopy: Mechanisms, diagnosis, and implications. J Electrocardiol. 2019;55:45-50. doi: 10.1016/j.jelectrocard. 2019.04.017. DOI
8. Elikowski W, Fertała N, Zawodna-Marszałek M et al. Brugada-like ECG pattern and tumors involving right ventricular outflow tract - case series and literature review. Wiad Lek. 2023;76:452-457. doi: 10.36740/WLek202302130. DOI
9. Elikowski W, Łazowski S, Fertała N et al. Brugada phenocopy in pulmonary embolism - clinicopathological case study and literature review. Pol Merkur Lekarski. 2022;50(300):378-383.
10. Tamene A, Sattiraju S, Wang K et al. Brugada-like electrocardiography pattern induced by severe hyponatraemia. Europace. 2010;12:905-907. doi: 10.1093/europace/euq034. DOI
11. Adrogué HJ, Tucker BM, Madias NE. Diagnosis and Management of Hyponatremia: A Review. JAMA. 2022;328:280-291. doi: 10.1001/jama.2022.11176. DOI
12. Otterness K, Singer AJ, Thode HC Jr et al. Hyponatremia and hypernatremia in the emergency department: severity and outcomes. Clin Exp Emerg Med. 2023;10:172-180. doi: 10.15441/ceem.22.380. DOI
13. Agrawal Y, Aggarwal S, Kalavakunta JK et al. All that looks like "Brugada" is not "Brugada": Case series of Brugada phenocopy caused by hyponatremia. J Saudi Heart Assoc. 2016;28:274-277. doi: 10.1016/j.jsha.2016.02.003. DOI
14. Ramsaroop K, Seecheran R, Seecheran V et al. Suspected hyponatremia-induced Brugada phenocopy. Int Med Case Rep J. 2019;12:61-65. doi: 10.2147/IMCRJ.S200201. DOI
15. Yılmaz E, Özdemir F. Brugada Phenocopy Induced by Hypovolemic Hyponatremia. Cureus. 2023;15:e45667. doi: 10.7759/cureus.45667. DOI
16. Hunuk A, Hunuk B, Kusken O et al. Brugada Phenocopy Induced by Electrolyte Disorder: A Transient Electrocardiographic Sign. Ann Noninvasive Electrocardiol. 2016;21:429-432. doi: 10.1111/anec.12350. DOI
17. Amusina O, Mehta S, Nelson ME. Brugada phenocopy secondary to hyperkalemia and hyponatremia in primary adrenal insufficiency. J Am Coll Emerg Physicians Open. 2022;4:e12800. doi: 10.1002/emp2.12800. DOI
18. Rosyidi MA, Yogibuana V, Rizal A. Syncope and Brugada-Like ECG Pattern in a Patient with Syndrome of Inappropriate Antidiuretic Hormone Secretion (SIADH). Eur J Case Rep Intern Med. 2024;11:004510. doi: 10.12890/2024_004510. DOI
19. Dogan M, Ertem AG, Cimen T et al. Brugada-like ECG pattern induced by adrenal crisis. Herz. 2015;40:304-306. doi: 10.1007/s00059-013-3983-z. DOI
20. Kovacic JC, Kuchar DL. Brugada pattern electrocardiographic changes associated with profound electrolyte disturbance. Pacing Clin Electrophysiol. 2004;27:1020-1023. doi: 10.1111/j.1540-8159.2004.00579.x. DOI
21. Landa E, Sharifi S, Abraham J et al. Brugada Pattern Phenocopy Induced by Diabetic Ketoacidosis. Cureus. 2021;13:e15066. doi: 10.7759/cureus.15066. DOI

22. Rattanawong P, Senthong V. Hyponatremia induced Brugada syndrome mimicking ST segment elevation myocardial infarction. J Arrhythm. 2021;37:1377-1379. doi: 10.1002/joa3.12617. DOI
23. Asteriou C, Lazopoulos A, Giannoulis N et al. Brugada-like ECG pattern due to giant mediastinal lipoma. Hippokratia. 2013;17:368-369.
24. Tarín N, Farré J, Rubio JM et al. Brugada-like electrocardiographic pattern in a patient with a mediastinal tumor. Pacing Clin Electrophysiol. 1999;22:1264-1266. doi: 10.1111/j.1540-8159.1999.tb00613.x. DOI
25. Nakazato Y, Ohmura T, Shimada I et al. Brugada-like precordial ST elevation on ECG by anterior mediastinal infective mass lesion. Indian Pacing Electrophysiol J. 2003;3:184.
26. Tomcsányi J, Simor T, Papp L. Images in cardiology. Haemopericardium and Brugada-like ECG pattern in rheumatoid arthritis. Heart. 2002;87:234. doi: 10.1136/heart.87.3.234. DOI
27. Pérez-Riera AR, Barbosa Barros R, Daminello-Raimundo R et al. Brugada phenocopy caused by a compressive mediastinal tumor. Ann Noninvasive Electrocardiol. 2018;23:e12509. doi: 10.1111/anec.12509. DOI

CONFLICT OF INTEREST

The Authors declare no conflict of interest

CORRESPONDING AUTHOR

Waldemar Elikowski
Józef Struś Hospital
3 Szwajcarska st., Poznan, Poland
e-mail: welikowski@wp.pl

ORCID AND CONTRIBUTIONSHIP

Waldemar Elikowski: 0000-0003-4825-087X A B D E F
Anna Strzelecka: 0009-0009-2161-9746 A B D
Natalia Fertała: 0000-0001-9976-1667 A B D
Magdalena Zawodna-Marszałek: 0000-0002-6878-3860 A B D
Marcin Żytkiewicz: 0000-0002-0229-7093E E

A – Work concept and design, B – Data collection and analysis, C – Responsibility for statistical analysis, D – Writing the article, E – Critical review, F – Final approval of the article

RECEIVED: 08.07.2024
ACCEPTED: 07.08.2024

Jubileuszowy Kongres Polonii Medycznej

XXX-LECIE FEDERACJI POLONIJNYCH ORGANIZACJI MEDYCZNYCH

12-14.09.2024, Kraków

Medycyna – wyścig z czasem

W Komitecie Honorowym:

Minister Zdrowia

Minister Spraw Zagranicznych

Organizatorzy:

FEDERACJA POLONIJNYCH ORGANIZACJI MEDYCZNYCH

FUNDACJA POLONII MEDYCZNEJ

Partner Główny:

MAŁOPOLSKA

Partner Strategiczny:

Kraków

Partnerzy Naukowi:

UNIWERSYTET JAGIELLOŃSKI COLLEGIUM MEDICUM W KRAKOWIE

OKRĘGOWA IZBA LEKARSKA W KRAKOWIE

Partnerzy:

TZ

KOPALNIA SOLI WIELICZKA

DONUM CORDE CENTRUM REHABILITACJI I OPIEKI MEDYCZNEJ

Sponsor:

Dr Irena Eris

Biuro Organizacyjne:

Targi w Krakowie PCO DMC

Centrum Kongresowe ICE Kraków • kongrespoloniimedycznej.org